

**MATURATION AND AGING OF THE RETINA IN NORMAL AND NIGHT
BLIND ALBINO GUINEA PIGS: A STRUCTURAL AND FUNCTIONAL STUDY**

Julie Racine
Montreal Children's Hospital-Research Institute
Department of Neurology & Neurosurgery
McGill University, Montreal

July 2007

A thesis submitted to McGill University in partial fulfillment of the requirements of the
degree of Doctor of Philosophy.

© Julie Racine
2007



Library and
Archives Canada

Bibliothèque et
Archives Canada

Published Heritage
Branch

Direction du
Patrimoine de l'édition

395 Wellington Street
Ottawa ON K1A 0N4
Canada

395, rue Wellington
Ottawa ON K1A 0N4
Canada

Your file Votre référence
ISBN: 978-0-494-50982-1
Our file Notre référence
ISBN: 978-0-494-50982-1

NOTICE:

The author has granted a non-exclusive license allowing Library and Archives Canada to reproduce, publish, archive, preserve, conserve, communicate to the public by telecommunication or on the Internet, loan, distribute and sell theses worldwide, for commercial or non-commercial purposes, in microform, paper, electronic and/or any other formats.

The author retains copyright ownership and moral rights in this thesis. Neither the thesis nor substantial extracts from it may be printed or otherwise reproduced without the author's permission.

AVIS:

L'auteur a accordé une licence non exclusive permettant à la Bibliothèque et Archives Canada de reproduire, publier, archiver, sauvegarder, conserver, transmettre au public par télécommunication ou par l'Internet, prêter, distribuer et vendre des thèses partout dans le monde, à des fins commerciales ou autres, sur support microforme, papier, électronique et/ou autres formats.

L'auteur conserve la propriété du droit d'auteur et des droits moraux qui protègent cette thèse. Ni la thèse ni des extraits substantiels de celle-ci ne doivent être imprimés ou autrement reproduits sans son autorisation.

In compliance with the Canadian Privacy Act some supporting forms may have been removed from this thesis.

Conformément à la loi canadienne sur la protection de la vie privée, quelques formulaires secondaires ont été enlevés de cette thèse.

While these forms may be included in the document page count, their removal does not represent any loss of content from the thesis.

Bien que ces formulaires aient inclus dans la pagination, il n'y aura aucun contenu manquant.

■+■
Canada

Mieux vaut tard que jamais

TABLE OF CONTENTS

Preface: Part I	viii
1. Contribution of authors on co-authored papers	ix
1.1 Manuscript 1 (Chapter 2)	ix
1.2 Manuscript 2 (Chapter 3)	ix
1.3 Manuscript 3 (Chapter 4)	x
1.4 Manuscript 4 (Chapter 5)	xi
2. Signed waivers from the publishers for all published manuscripts	xii
2.1 Published manuscript 1 (Chapter 2)	xii
2.1.1 Identification of student	xii
2.1.2 Title and authors of manuscript	xii
2.1.3 Letter of authorization (Publisher)	xii
2.2 Published manuscript 2 (Chapter 3)	xiv
2.2.1 Identification of student	xiv
2.2.2 Title and authors of manuscript	xiv
2.2.3 Letter of authorization (Publisher)	xiv
2.3 Published manuscript 3 (Chapter 4)	xvi
2.3.1 Identification of student	xvi
2.3.2 Title and authors of manuscript	xvi
2.3.3 Letter of authorization (Publisher)	xvi
3. Signed waivers form co-authors of unpublished manuscripts	xviii
3.1 Unpublished manuscript 4 (Chapter 5)	xviii
3.1.1 Identification of student	xviii
3.1.2 Title and authors of manuscript	xviii
3.1.3 Declaration of co-authors	xviii
Preface: Part II	xix
1. Acknowledgements	xx
Preface: Part III	xxiii
1. Abstract	xxiv
2. Résumé	xxv
Chapter I: General Introduction	1
1. General Introduction	2
2. Guinea pigs	5
3. Retinal structure	8
3.1 Retinal cytoarchitecture	8
FIGURE 1: Schematic representation of the retinal structure	9
3.1.1 Retinal pigment epithelium (RPE)	10
3.1.2 Photoreceptor layer (PL)	10
3.1.3 Outer plexiform layer (OPL)	12
3.1.4 Inner nuclear layer (INL)	13
3.1.4.1 Horizontal cells (HC)	13

3.1.4.2 Bipolar cells (BC)	13
3.1.4.3 Amacrine cells (AC)	14
3.1.4.4 Muller cells (MC)	14
3.1.5 Inner plexiform layer (IPL)	15
3.1.6 Ganglion cell layer (GCL)	15
3.2 Retinal physiology	16
3.2.1 Phototransduction	16
3.2.2 Retinal ON- and OFF-pathways	18
FIGURE 2: ON- and OFF-retinal pathways of the retina	19
4. Retinal function	19
4.1 The electroretinogram (ERG)	19
FIGURE 3: Short flash ERG/OP recordings	21
FIGURE 4: Long flash ERG recording	22
4.2 Origin of the electroretinogram components	23
4.2.1 a-wave	23
4.2.2 b-wave	24
4.2.3 i-wave	25
4.2.4 c-wave	25
4.2.5 Oscillatory potentials (OPs)	26
4.2.6 Photopic negative response (PhNR)	27
4.2.7 d-wave	28
4.3 Stimulus-related characteristic of the ERG	29
4.3.1 Photopic intensity-response function of the ERG	29
4.3.2 Scotopic intensity-response function of the ERG	31
5. Retinal disorders	32
5.1 Retinitis pigmentosa (RP)	33
5.1.1 Description	33
5.1.2 Animal models of RP	35
5.2 Congenital stationary night blindness (CSNB)	35
5.2.1 History	35
5.2.1.1 CSNB with normal fundus	36
5.2.1.2 CSNB with abnormal fundus	37
5.2.2 Differences between complete and incomplete CSNB	37
5.2.3 Animal models of CSNB	38
TABLE 1: Known genes that produced human CSNB	40
6. Animal models in vision research	41
6.1 Naturally occurring animal models	42
TABLE 2: Naturally occurring animal models of ret. degenerations	43
6.2 Genetically manipulated animal models	44
7. General objectives	45
Chapter II: Manuscript 1	48
1. Preface to chapter II	49
2. Abstract	50
3. Introduction	50
4. Material and Methods	52

4.1 Animals	52
4.2 ERG recordings	53
4.3 Histology	55
5. Results	56
5.1 Maturation of the photopic ERG	56
5.2 Maturation of the scotopic ERG	57
5.3 Maturation of the retinal structure	60
6. Discussion	60
7. References	67
8. Figures and legends	74
Chapter III: Manuscript 2	84
1. Preface to chapter III	85
2. Abstract	86
3. Introduction	86
4. Material and Methods	87
4.1 Data analysis	89
5. Results	90
6. Discussion	94
7. References	97
8. Tables and legends	101
9. Figures and legends	102
Chapter IV: Manuscript 3	108
1. Preface to chapter IV	109
2. Abstract	110
3. Introduction	110
4. Material and Methods	112
5. Results	114
6. Discussion	120
7. References	124
8. Tables and legends	130
9. Figures and legends	133
Chapter V: Manuscript 4	137
1. Preface to chapter V	138
2. Abstract	139
3. Introduction	140
4. Material and Methods	141
4.1 Animals	141
4.2 Electroretinogram recordings	142
4.3 Retinal histology	144
4.4 Retinal immunohistochemistry	145
4.5 Data analysis	146

5. Results	146
5.1 Cone-mediated function	147
5.2 Rod and rod-cone mediated function	149
5.3 Retinal structure: light and electron microscopy	150
5.4 Retinal structure: Immunohistochemistry	152
6. Discussion	153
7. Acknowledgments	158
8. References	159
9. Figures and legends	164
Chapter VI: General Discussion and Conclusion	180
1. General discussion	181
1.1 Summary of findings	181
1.2 Maturation of the retinal structure and function in guinea pigs	183
TABLE 3: Significant maturational events (altricial VS precocial)	185
1.3 Aging of the retinal structure and function in guinea pigs	190
FIGURE 5: Normalized cone ERG VS scotopic ERG parameters	192
1.4 Albino versus pigmented animals	193
1.5 The night blind guinea pig	194
1.6 Understanding the negative morphology...	198
FIGURE 6: Scotopic ERG following 12h, 3h, 1h, and 30 min DA	200
FIGURE 7: Rod cone ERG following intravitreal injections	202
1.7 Novelty of the results	203
1.8 Future avenues	205
2. Conclusion	207
Chapter VII: References	208
1. References	209
Chapter VIII: Appendix	243
1. Permission to published manuscripts 1, 2 and 3 letters	244
2. Signed waiver from the publisher for published manuscripts 1, 2 and 3	247
3. Ethic certificates	251

PREFACE: PART I

1 Contribution of authors on co-authored papers.

1.1 Manuscript 1 (Chapter 2)

Racine J., Behn D., Lachapelle P. (2007) Structural and functional maturation of the retina of the albino Hartley guinea pig. Doc Ophthalmol, (Epub ahead of print).

As first author of this paper, I was responsible 1- for the design of the experiment, 2- the execution of the protocol, 3- analyzing the results and finally, 4- writing the paper.

In this first study, I performed all the ERG recordings as well as the retinal histology in both normal albino and night blind albino guinea pigs. I also analyzed all the data and wrote the manuscript. Dr Pierre Lachapelle helped in revising the manuscript. Darren Behn did not participate in any experimental procedures neither in writing the manuscript, but he was the master's student with Dr Lachapelle who discovered and tested the first night blind albino guinea pig.

1.2 Manuscript 2 (Chapter 3)

Racine J., Joly S., Rufiange M., Rosolen S., Casanova C., Lachapelle P. (2005) The photopic ERG of the albino guinea pig (*Cavia Porcellus*): A model of the human photopic ERG. Doc Ophthalmol, 110: 67-77.

As first author of this paper, I was responsible 1- for the design of the experiment, 2- the execution of the protocol, 3- analyzing the results and finally, 4- writing the paper.

In this second study, Marianne Rufiange performed the human ERG recordings while Sandrine Joly and I, together, performed the rat and mouse ERG recordings. On the other hand, I performed all the ERG recordings in guinea pigs as well as the intravitreal injection of pharmacological agents in guinea pigs eyes. I also analyzed all the data collected by Dr Rufiange, Dr Joly and myself, and then wrote the manuscript. Dr Serge Rosolen, Dr Christian Casanova and Dr Pierre Lachapelle helped revising it.

1.3 Manuscript 3 (Chapter 4)

Racine J., Behn D., Simard E., Lachapelle P. (2003) Spontaneous occurrence of a potentially night blinding disorder in guinea pigs. *Doc Ophthalmol*, 107: 59-69.

As first author of this paper, I was responsible 1- for the design of the experiment, 2- the execution of the protocol, 3- analyzing the results and finally, 4- writing the paper.

In this third study, I performed all the short and long flash ERG recordings in normal and night blind guinea pigs. I also analyzed all the data collected and wrote the manuscript. Dr Pierre Lachapelle helped in revising the manuscript. Darren Behn and Éric Simard did not participate in any experimental procedures neither in writing the manuscript, but were the first two to discover the night blind guinea pig in our population of albino guinea pigs.

1.4 Manuscript 4 (Chapter 5)

Racine J., Joly S., Lachapelle P. Maturation and aging of the retinal structure and function in the normal and the night blind albino guinea pigs. In preparation.

As first author of this paper, I was responsible 1- for the design of the experiment, 2- the execution of the protocol, 3- analyzing the results and finally, 4- writing the paper.

In this fourth study, I performed all the ERG recordings, light microscopy, electron microscopy and immunohistochemistry on normal and night blind albino guinea pigs. I also analyzed all the data and wrote the manuscript. Dr Sandrine Joly taught me the rudiments of histology. Dr Lachapelle helped in revising the manuscript.

2 Signed waivers from the publishers for all published manuscripts.

2.1 Published manuscript 1 (Chapter 2)

2.1.1 Identification of student:

Name: Julie Racine

Program: Neurological Sciences

Department: Neurology-Neurosurgery

University: McGill University

2.1.2 . Title and authors of manuscript:

Racine J., Behn D., Lachapelle P. (2007) Structural and functional maturation of the retina of the albino Hartley guinea pig. Doc Ophthalmol, (Epub ahead of print).

2.1.3 Letter of authorization (Publisher)

See appendix for the original authorization.

Dear Ms. Racine,

With reference to your request (copy herewith) to re-use material on which Springer controls the copyright, our permission is granted free of charge, on the following conditions:

1. It concerns original material which does not carry references to other sources,

2. If material in question appears with credit to another source, authorization from and reference to that source is required as well, and permission is also obtained from the author (address is given on the imprint page or with the article);

3. Allows you non-exclusive reproduction rights throughout the world,

4. Permission includes use in an electronic form, on the condition that content is:

4.1. Password protected,

4.2. At Intranet or

4.3. In CD-ROM/E-book;

5. Full credit (book/journal title, volume, year of publication, page, chapter/article title, name(s) of author(s), figure number(s), original copyright notice) is given to the publication in which the material was originally published by adding: With kind permission of Springer Science and Business Media.

Permission free of charge does not prejudice any rights we might have to charge for reproduction of our copyrighted material in the future.

With best regards,

Alice Essenpreis

Springer

Rights and Permissions

Tiergartenstrasse 17,

69121 Heidelberg GERMANY

FAX: +49 6221 487 8223

Alice.Essenpreis@springer.com

www.springeronline.com/rights

2.2 Published manuscript 2 (Chapter 3)

2.2.1 . Identification of student:

Name: Julie Racine

Program: Neurological Sciences

Department: Neurology-Neurosurgery

University: McGill University

2.2.2 Title and authors of manuscript:

Racine J., Joly S., Rufiange M., Rosolen S., Casanova C., Lachapelle P.
(2005) The photopic ERG of the albino guinea pig (*Cavia Porcellus*): A model of
the human photopic ERG. *Doc Ophthalmol*, 110: 67-77.

2.2.3 Letter of authorization (Publisher)

See appendix for the original authorization.

Dear Ms. Racine,

With reference to your request (copy herewith) to re-use material on which Springer controls the copyright, our permission is granted free of charge, on the following conditions:

1. It concerns original material which does not carry references to other sources,

2. If material in question appears with credit to another source, authorization from and reference to that source is required as well, and permission is also obtained from the author (address is given on the imprint page or with the article);

3. Allows you non-exclusive reproduction rights throughout the world,

4. Permission includes use in an electronic form, on the condition that content is:

4.1. Password protected,

4.2. At Intranet or

4.3. In CD-ROM/E-book;

5. Full credit (book/journal title, volume, year of publication, page, chapter/article title, name(s) of author(s), figure number(s), original copyright notice) is given to the publication in which the material was originally published by adding: With kind permission of Springer Science and Business Media.

Permission free of charge does not prejudice any rights we might have to charge for reproduction of our copyrighted material in the future.

With best regards,

Alice Essenpreis

Springer

Rights and Permissions

Tiergartenstrasse 17,

69121 Heidelberg GERMANY

FAX: +49 6221 487 8223

Alice.Essenpreis@springer.com

www.springeronline.com/rights

2.3 Published manuscript 3 (Chapter 4)

2.3.1 Identification of student:

Name: Julie Racine

Program: Neurological Sciences

Department: Neurology-Neurosurgery

University: McGill University

2.3.2 Title and authors of manuscript:

Racine J., Behn D., Simard E., Lachapelle P. (2003) Spontaneous occurrence of a potentially night blinding disorder in guinea pigs. *Doc Ophthalmol*, 107: 59-69.

2.3.3 Letter of authorization (Publisher)

See appendix for the original authorization.

Dear Ms. Racine,

With reference to your request (copy herewith) to re-use material on which Springer controls the copyright, our permission is granted free of charge, on the following conditions:

1. It concerns original material which does not carry references to other sources,
2. If material in question appears with credit to another source, authorization from and reference to that source is required as well, and permission is also obtained from the author (address is given on the imprint page or with the article);

3. Allows you non-exclusive reproduction rights throughout the world,

4. Permission includes use in an electronic form, on the condition that content is:

- 4.1. Password protected,
- 4.2. At Intranet or
- 4.3. In CD-ROM/E-book;

5. Full credit (book/journal title, volume, year of publication, page, chapter/article title, name(s) of author(s), figure number(s), original copyright notice) is given to the publication in which the material was originally published by adding: With kind permission of Springer Science and Business Media.

Permission free of charge does not prejudice any rights we might have to charge for reproduction of our copyrighted material in the future.

With best regards,

Alice Essenpreis
Springer
Rights and Permissions
Tiergartenstrasse 17,
69121 Heidelberg GERMANY
FAX: +49 6221 487 8223
Alice.Essenpreis@springer.com
www.springeronline.com/rights

3 Signed waivers from co-authors of unpublished manuscripts.

3.1 Unpublished manuscript 4 (Chapter 5)

3.1.1 Identification of student:

Name: Julie Racine

Program: Neurological Sciences

Department: Neurology-Neurosurgery

University: McGill University

3.1.2 Title and authors of manuscript:

Racine J., Joly S., Lachapelle P. Maturation and aging of the retinal structure and function in the normal and the night blind albino guinea pigs. Article in preparation.

3.1.3 Declaration of co-authors:

As a co-author on the above-mentioned paper, I accept that **Julie Racine** include the latter, as part of her doctorate thesis entitled: Maturation and aging of the retina in normal and night blind albino guinea pigs: A structural and functional study.

Sandrine Joly

Co-author

Signature

December 5th, 2007

Date

Pierre Lachapelle

Co-author

Signature

10 12 2007

Date

PREFACE: PART II

1 Acknowledgements

First and foremost, I would like to sincerely thank my thesis supervisor, Dr. Pierre Lachapelle, for his academic as well as financial support during the past few years (I stopped counting several years ago...). Dr Lachapelle's help, patience and encouragement towards the completion of this project were the key to my success. Not only did he share his knowledge in electrophysiology, but he also shared his time whenever I needed it (which was almost all the time!). Pierre was and will probably be the best thesis supervisor a student can ask for. By the way Pierre, if you thought you'd gotten rid of me, think twice... I'll be back...

Secondly, I would like to thank all the graduate students that were part of the laboratory while I was pursuing my degree. Special thanks go to Olga for teaching me all the basics in electrophysiology and teaching me how to survive in Pierre's laboratory! It took a long time Olga, but I finally managed to write papers *à la Pierre!* Special thanks also go to Marianne for sharing her clinical expertise with me. I really liked being your guinea pig and your calibration partner. A special thank you also goes to Allison, my ARVO bed partner, shopping girlfriend, drinking buddy and best friend. How many laughs did we share together about everything and nothing? Do you remember the jeans situation? The histology lamp accident? I hope you do, because I will remember all the good moments we spent together for the rest of my life. And please do not panic... I will always be around when you need me. I hope we will see each other on a regular basis. I would also like to thank Sandrine for her help and advice. She always knew everything. I hope you will always remember the recording session at the hospital! By the way don't forget you owe me this paper... I am looking forward to seeing you in Switzerland. I also have to thank Julie L. for her good advice throughout those years. Even though you were adopted by our lab for the journal club, I really enjoyed the time you spent in the lab. I will always remember the time when some guy filmed us doing VEPs! We had such a blast. I would also like to thank Catherine, for her peacefulness and her sense of humor. Even though

we did not spend much time working together (because you are on *garde partagée!*), I would like to say that you are a good friend. Finally, I would like to thank all the new girls in the lab for their support during my writing and also for their friendship. I would have liked to work with you all for a longer period, but at one point, I had to leave... It was a great pleasure working with you. I look forward to see you all soon.

My gratitude also goes to Éric Simard for his patience, friendship and his expertise in animal care. From the second to fourth floor, you were always there when I needed your help. Actually, without you I would probably still be waiting in the corridor in front of a locked door... I will sincerely miss you. Don't worry, I will come by sometimes to say BONJOUR!

I would also like to thank other people who were not with me on a day-to-day basis, but who made a difference in my work. Those thanks goes to 1- Jo-anne Trempe and all the members of her team in the audiovisual department for their advice and support during critical periods, 2- Claudine, Diane, Renée, for your kindness and support through these years at the eye clinic 3- Dr Robert Koenekoop and Dr John Little for your expertise in ophthalmology, 4- Dr Hakima Moukhles for her extreme patience and her expertise in histology, and finally, 5- a special thanks goes to Louise Pelletier for her kindness, help and patience. Even though her work duties at University of Montreal did not include helping a McGill student, she never hesitated to help me when it came to histology. You were always so nice; I hope I will be able to work with you again some day.

I also wish to extend my sincere thanks to the members of my advisory committee, Dr. Michelle McKerral, Dr. Sylvain Chemtob and to my mentors Dr Heather Durham (1999-2004) and Dr Edith Hamel (2004-2006).

My gratitude also goes to my family (Serge, Ginette, Isabelle and Pierre-Luc), for their support and love during this process. They always believed in me,

even when I thought I was not good enough to do a PhD. They were always there for me, and because of that they will always have a special place in my heart.

Furthermore, I would like to thank Mario and Mathieu, two extraordinary people that were there at certain points in my life, for supporting me during the difficult moments. You both had to endure the most difficult moments, and we know that there were a lot! I will always be grateful for your support and kindness.

Finally, I also would like to thank all my friends for believing in my writing capabilities... Without your help and support, I would probably still be writing the first page! Thank you for being there for me and believing in me.

On a less serious note, let's say that I will miss the journal clubs but not as much as the Friday wine and cheese lunches. I will also miss the McGill day, the Réseau vision meeting, ARVO and all the other meetings we were attending! By the way, that was a joke. I am also looking forward to going back at the Winterset to sleep with Allison (j'ai des visions!).

See you soon big balloon. J'ève les feutres!

PREFACE: PART III

1 Abstract

Most studies that examined the relationship between retinal structure and function did so on altricial animals; animals that are born with closed eyes and an immature retina. However, if one wishes to transpose results to humans, we must take into consideration the fact that the human infant is born with its eyes opened and mature retina (precocial). Also, while the human retina is composed of approximately 6% cones, the retinas of rats and mice (the most common models) are made of 1-3% cones. Hence, the guinea pig (*Cavia Porcellus*) offers an excellent alternative to the usual rodent models. It is born with its eyes open following 65 days of gestation. Guinea pigs are diurnal animals (unlike most rodents) and their retina is reported to include between 8-15 % cones. Compared to the usual rodent models (rats and mice), newborn guinea pigs are thus closer to human infants. Consequently, the purpose of this thesis was to investigate the maturation and aging of the retinal structure and function of the Hartley albino guinea pig in order to determine if they represent a better animal model of human retinal structure and function.

Following an accidental mating between a brother and a sister in our pedigree of albino guinea pigs, we discovered that one pup (out of four) was affected with a night blinding disorder as per ERG. Consequently, the second purpose of this thesis was also to examine the maturation and aging of the retinal structure and function of our night blind guinea pig colony in order to characterize this unique retinopathy.

In summary, our studies demonstrated that albino guinea pigs do represent a better animal model of the human retinal structure and function compared to the more frequently used altricial animals. We demonstrated that even if the retina of albino guinea pigs is adult-looking at birth, it undergoes retinal maturation of its structure and function albeit not to the same extent as in altricial animals like rats and mice. Additionally, our new and naturally occurring animal model of night blindness could represent a valid model to study the mechanisms involved in generating a functional retinal disorder such as those encountered in humans and to study the cone in absence of rod.

Résumé

La plupart des études décrites dans la littérature ont examiné la fonction et la structure rétinienne chez des animaux (ex : rats, souris, etc.) qui, à la naissance, ont un système visuel immature. Cependant, pour transposer ces résultats aux humains, il est important de prendre en compte que les nouveaux-nés naissent avec les yeux ouverts et avec un système visuel mature. Sans compter que les rétines humaines ont un pourcentage de cônes (6%) qui est largement supérieur au pourcentage de cônes contenus dans la rétine de rats (1-2%) et/ou de souris (2-3%). Dans cette optique, le cochon d'Inde offre une excellente alternative à l'utilisation de rongeurs tels la souris et le rat dans la recherche ophtalmique. En effet, le cochon d'Inde est un animal diurne qui, comme l'homme, naît avec les yeux ouverts et avec un système visuel dit mature à la naissance. De plus, le pourcentage de cônes (8-17%) est plus près de ce que l'on retrouve chez l'humain.

Les objectifs de mon étude étaient 1- Déterminer si la structure et la fonction de la rétine chez les cochons d'Inde subissent une maturation postnatale malgré le fait qu'ils naissent avec un système visuel dit mature; 2- Comparer la fonction rétinienne en condition photopique du cochon d'Inde à celle de l'homme, afin de déterminer s'il représente un meilleur modèle animal, comparativement aux souris et aux rats; 3- et finalement, caractériser la fonction ainsi que la structure de la rétine en fonction de l'âge chez notre modèle animal spontané d'héméralopie congénitale.

Les résultats obtenus nous laissent suggérer que la rétine de cochons d'Inde nouveaux-nés subit des changements significatifs au niveau de sa structure et de sa fonction en relation avec l'âge, et ce, même si ce dernier naît avec un système visuel mature. De plus, les résultats démontrent que les cobayes sont d'excellents modèles de la fonction rétinienne photopique de l'homme. Finalement, notre modèle animal d'héméralopie congénitale représente un modèle valide pour étudier les mécanismes pathophysiologiques de rétinopathies humaines. De plus, notre modèle nous offre l'opportunité d'étudier la fonction des cônes en l'absence de bâtonnets.

CHAPTER I: GENERAL INTRODUCTION

1 General Introduction

Altricial animals such as cats (Hamasaki 1985; Jakobson 1987), dogs (Gum 1973; Kirk 1973), rats (Braekevelt 1970; Kurihara 1977; El Azazi 1990, 1991), rabbits (Sanada 1962; Gorfinkel 1988, 1990) and mice (Bonaventure 1968; Gresh 2003), are born with an immature visual system and closed eyes, while precocial animals such as guinea pigs (Spira 1975), chickens (Ookawa 1971a, 1971b), macaques (Smelser 1974) and humans (Hollenberg 1972, 1973; Spira 1973) are born with a relatively more mature visual system and opened eyes.

The opening of the eyes in altricial animals varies between species (ie: rats: P14; rabbit P8; mice P13) but usually occurs during the second week of life (Bonaventure 1968; Braekevelt 1970; Gorfinkel 1990). At birth, the retina of altricial animals is usually composed of only two nuclear layers: 1- the inner nuclear layer, consisting of a row of well differentiated ganglion cells and 2- the outer nuclear layer which consists of undifferentiated neuroblastic cells (Weidman 1968; Gum 1973). The differentiation of the neuroblastics cells will continue after birth, and even beyond eye opening.

As a consequence of this retinal immaturity, an electroretinogram (ERG), which is the recording of the mass electrical activity of the retina in response to light stimulation, is flat at birth in altricial animals. The first ERG component recorded is usually a negative wave, which is observed for the first time at the opening of the eye (Bonaventure 1968; Fulton 1980; Gorfinkel 1988; Kirk 1973). The other components of the ERG (e.g.: b-wave and OPs) usually appear a few days later, so that by the end of the first month of life the retina is functionally mature (Braekevelt 1970, Bonaventure 1968; Jacobson 1987; Gorfinkel 1990).

Upon opening the eye, the entire retinal cell layer structure is present although cells are present in excessive numbers. In the presence of visual cues, the

retinas of altricial animal undergo maturational process (apoptosis) that will end with the refinement of the retina. These structural changes are also accompanied with functional changes.

On the other hand, the retina of precocial animals such as guinea pigs (Spira 1975), chickens (Ookawa 1971a, 1971b), macaques (Smelser 1974) and humans (Hollenberg 1972; 1973; Spira 1973) is well developed at birth since most of the retinal maturation occurs *in utero*, where synapse formation precedes the formation of the outer segment of photoreceptors. As opposed to altricial animals, in precocial animals an electroretinogram can be recorded at birth (Ookawa 1971 a, 1971b; Bui 1999). The electrical potential (ERG) can be recorded on neonatal precocial animals in response to light, it also has an adult-like morphology. The 'at birth' maturity of the retinal structure found at birth in precocial animals, probably explains the adult-like morphology measured by the electroretinogram.

The electroretinogram was proven to be a useful method of assessing the developmental status of the visual system in a wide variety of species. Although the ERG has been frequently used to explore the functional development and aging of mammalian retinas (Grün 1982), it has rarely been used to detect the earlier manifestations and subsequent development of retinal function in species that have functional vision at birth (precocial animals). In fact, most studies that examined the relationship between retinal structure and function were done on altricial rodents (ie: rats and mice).

Consequently, the purpose of this project was to compare the maturation of the retinal structure and function on a normal and night blind precocial animal model, namely the Hartley albino guinea pig.

In the first study, we examined the maturation of the retinal structure and function on normal Hartley albino guinea pigs. The results showed that despite its relative maturity at birth (compared to other rodents like rats and mice), the retina

of newborn albino guinea pigs undergoes significant postnatal maturation. That being the modification of its structure as well as its function, albeit not as extensively as what was previously documented for altricial animals. The cone-mediated ERG of albino Hartley guinea pigs shares several similarities with the human photopic ERG, as presented in the second study of this thesis. A finding that led me to believe that the albino guinea pig was a rodent model of the human cone-mediated ERG that is superior when compared to other rodents like rats and mice. During the course of our experiments, an accidental consanguineous mating between a brother and a sister occurred. From this union, four pups were born and only one yielded ERG abnormalities. The anomalies were: 1- absence of rod-mediated vision, 2- abnormal rod-cone mediated ERG morphology (photopic-like), 3- attenuated OFF-retinal response and 4- ON-post b-wave electronegativity as documented in the third study of this thesis. We believe that our results supported the supposition that our guinea pig is night blind, making it an interesting animal model to study the pathophysiological processes of a human-like retinal disorder. Selective breeding enabled us to produce more affected guinea pigs. In order to further our understanding of this retinal anomaly, in the fourth study, we investigated the maturation and aging of the retinal structure and function on the night-blind guinea pigs. Results revealed 1- an absence of rod-mediated vision from birth, 2- mixed rod-cone mediated ERG probably generated by cones, 3- near normal photopic responses, 4- absence of rod photoreceptors, 5- remnants of cone outer segments buried in the inner segment layer, 6- thinning of the outer nuclear layer, outer plexiform layer and the ganglion cell layer, 7- re-localization of rhodopsin in the outer nuclear layer with normal cone and synaptic immunoreactivity, and finally, 8- progression of the retinal anomaly with age. We concluded that this retinal disorder was inherited as an autosomal recessive trait and that the retinopathy was degenerative over time, where only cone photoreceptors were present in the retina. This model offers a unique opportunity to study cone function in the absence of rods.

In summary, the general purpose of this study was to investigate the maturation and aging of the retinal structure and function of the normal and night blind Hartley albino guinea pigs. The results will be presented in chapter 2, 3, 4 and 5. However, before presenting these results, I will introduce key elements that will help acquire a better understanding of the work that has been done.

2 Guinea pigs

Are guinea pigs rodents or not? Several studies have debated the taxonomy of the guinea pig. Although the traditional taxonomy classifies the guinea pig into the order Rodentia (Novacek 1992; Luckett 1993), the molecular phylogenetics has been challenging this view. The first attempt was made by Graur, Hide and Li in 1991, who suggested that the order Rodentia may not be monophyletic, and that the guinea pig-like rodents (caviomorpha) may be part of another group than the one formed by the rat-like rodents (myomorpha). More recently, D'Erchia (1996), also claimed that the guinea pig was not a rodent, since myomorphs appear to emerge before guinea pigs in their molecular phylogenetic tree. However, the monophyly of rodents is supported by numerous morphological characteristics (Novacek 1992; Luckett 1993) as well as several molecular studies (Martignetti 1993; Cao 1994; Frye 1995). Finally, Cao et al. (1997), in a letter to the editor, concluded that considering all the data available to date, one can only conclude that the evidence presented by D'Erchia et al., is weak to exclude the rodent monophyly hypothesis and that this hypothesis will remain as such. Since the paper presented by Cao et al. in 1997, no others challenged the concept of monophyly of the order Rodentia. Therefore, it is acceptable, for now, to say that guinea pigs are rodents.

The guinea pig (*Cavia porcellus*) has been so frequently used in scientific and medical investigations that its name, has entered in the English language as an informal descriptor for subjects that take part in any sort of experimentations. In

addition of being an animal subject for research purposes, the guinea pig is a frequent household pet and could also be occasional food source. In fact, the guinea pig is surely among the most familiar of the domesticated rodents within research purposes. Given the above, it is remarkable how little is known about several basic features of the visual system and vision in these animals.

However, reports of Spira (1975) helped us better understand the guinea pig's visual system. Guinea pigs' photoreceptor cells begin to form outer segment lamellae in the central retina between the 45th (E45) and 49th (E49) days of gestation (Spira 1975; Rees 1992; Loeliger 2005) (full term 68-69 days). Synaptic contacts between photoreceptors and second order neurons begin to be established at E49, while synapses between inner retinal neurons are formed at an even earlier stage in the inner plexiform layer (Spira 1975). The presence of substantial amounts of several neurotransmitters and their associated enzymes in retinal cells, which are located in their definitive adult position (Spira 1976; 1984; Cepko 1996), suggest that guinea pigs retinal synapses are functionally competent before birth.

In fact, in 1990, Huang et al. in their study on the development of the electroretinogram in guinea pigs, reported adult-like cone and rod-mediated electroretinograms from birth. These findings were also supported by the study presented by Bui et al. (1999) and Vingrys et al. (2001) who reported the maturation of the rod-mediated ERG and also by Racine et al. (2007; Epub ahead of print) who described the maturation and aging of the rod and cone-mediated ERG in these animals.

Like most mammals, the guinea pig's retina is rich in rods and contains typical mammalian rhodopsin with peak absorption at 497 nm. In fact, Granit (Granit 1944) described the guinea pig's retina as being populated only by rod photoreceptors. There has been considerable inconsistencies of opinion about the presence of cones in the guinea pig retina. However, O'Day in 1947, reported that

he had observed cones in the guinea pig's retina and concluded that they were not pure rods. Later on, Sjostrand (1965) conducted a detailed examination of the synaptic terminals of the guinea pig's photoreceptors and he differentiated two types of photoreceptors (rods and cones) in the guinea pig's eye.

The use of specific cone visual pigment antibodies, monoclonal antibodies that are specifically labeled blue-sensitive and green-red sensitive visual pigments, provided evidence that the guinea pig retina contained at least two different types of cone photoreceptor pigments which peaked at 429 nm and 529 nm (Jacob 1994; Röhlich 1994; Parry 2002). The presence of two classes of cones suggests a retinal basis for color discrimination and behavioral tests showed that guinea pigs have dichromatic color sensitivity with a spectral neutral point at about 480 nm (Jacob 1994; Röhlich 1994; Parry 2002).

Finally, it is also important to note that the retinas of most mammals, including humans, have their oxygen supply derived from both the choroidal circulation, which lies behind the retina, and the retinal circulation, which is distributed throughout the inner retina. There is however, in humans and macaques, an avascular region in their retina, which is the foveal avascular zone. In many species, the retinal vasculature is absent and the full thickness of the retina is supplied with oxygen by diffusion from the choriocapillaris, lying on the distal part of the retinal pigmented epithelium (RPE). Absence of an additional blood supply from vessels located in the retina is correlated with retinal thickness, avascularized retinae being around 60% thinner than those with retinal vessels (Chase 1982, Dreher 1992). In guinea pigs there is no retinal vasculature (Chase 1982; Cringle 1996; Yu 2001). In fact, in the avascular retina of guinea pigs, the deep retinal and inner capillaries are absent. Therefore, the guinea pig's inner retina survives in an essentially anoxic environment (Chase 1982; Cringle 1996; Yu 2001).

3 Retinal structure

The vertebrate retina is a highly organized structure consisting of alternate layers of cell bodies and synaptic processes (Dowling 1966; Neves 1999; Kolb 2003). A single common pathway, mediated by the axons of retinal ganglion cells, conveys visual information from the retina to the brain (Kolb 1994, 2003). The retina is the most important part of the eye, for it contains both the sensory neurons that are responsive to light and the neural circuits that are responsible for the first stages of image processing. Ramon y Cajal (1892), the renowned Spanish histologist, was the first modern neuroscientist to acknowledge that the retina was a true nervous centre. Dowling qualified it as the “approachable part of the brain” (Dowling 1987). Derived from the neuroectoderm, this complex tissue differentiates along a central to peripheral gradient (Johnson 1985). In humans, and most primates, the retina differentiates *in utero*. They are born with their eyes open and with a fully mature retina (Winkelman 1962; Shipley 1964). However, some animals, such as rats and mice, are born with their eyes closed and with a retina that is not entirely developed at birth. In those cases, the final maturation will take place after birth (Braekevelt 1970; Webster 1991; Weisse 1995).

3.1 Retinal cytoarchitecture

The retina lies at the back of the eye between the vascularized choroid and the vitreous humor (Dowling 1970; Johnson 1985; Kolb 2003). In humans and most primates, the retinal tissue is subdivided into three cellular layers and two synaptic layers. Starting from the retinal pigmented epithelium (RPE) to the vitreous humour, we find: 1- the photoreceptor layer (PL), which include the inner and outer segments (IS and OS respectively) of the photoreceptors and the outer nuclear layer (ONL), 2- the outer plexiform layer (OPL), 3- the inner nuclear layer (INL), 4- the inner plexiform layer (IPL) and 5- the ganglion cell layer (GCL) (Figure 1).

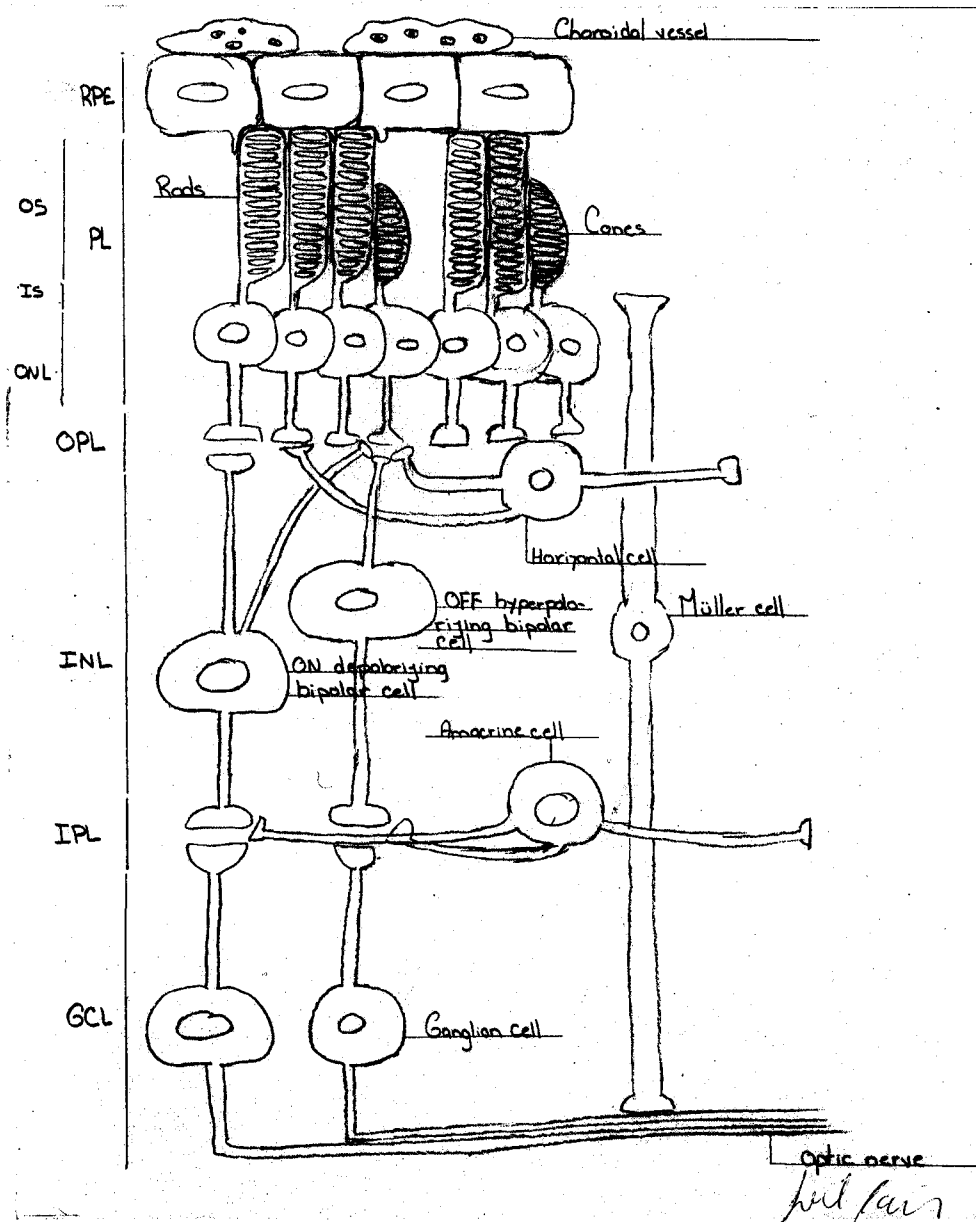


Figure 1: Schematic representation of the retinal structure. The retinal pigment epithelium (RPE), photoreceptor layer (PL), outer segments of the photoreceptors (OS), inner segments of the photoreceptors (IS), outer nuclear layer (ONL), outer plexiform layer (OPL), inner nuclear layer (INL), inner plexiform layer (IPL), ganglion cell layer (GCL), ON-depolarizing bipolar cells (ON-DBC), OFF-hyperpolarizing bipolar cell (OFF-HBC), Müller cells, horizontal cells, amacrine cells, rods, cones, choroidal vessels, optic nerve.

3.1.1 Retinal pigment epithelium (RPE)

The retinal pigment epithelium is not *per se* a part of the neural retina but is often indicated as such because of its crucial role in maintaining retinal function. The RPE contains a single layer of cubical epithelial cells. Their cells are regularly arranged as hexagonal tiles, which separates the photoreceptor outer segments from the choroid. Each eye contains an estimated 4 to 6 million RPE cells (Steinberg 1985; Strauss 2005). The apical surface of the RPE cells are folded to form the 5-7 μm long microvilli, which extends up to one third of the photoreceptor outer segment length. The RPE supports and maintains the functions of the photoreceptor's outer segments. The main functions of the RPE include: 1- Create a barrier between the choroidal circulation and the retina, 2- Transport ions, water and metabolites between the retina and the choroids. 3- Phagocytosis of the shed photoreceptor outer segments (Steinberg 1985; Rizzolo 1997; Strauss 2005; Bharti 2006).

3.1.2 Photoreceptor layer (PL)

The photoreceptor layer is subdivided into three sub-layers, namely: 1- The outer segment (OS) of the photoreceptors. 2- The inner segment (IS) of the photoreceptors. 3- The photoreceptor nuclei, which composes the outer nuclear layer (ONL). The outer segments of the photoreceptors contains all of the necessary components for the conversion of light into an electrical signal, whereas the inner segments of photoreceptors contains all of the necessary components for the metabolism of the cell (Baylor 1987).

Photoreceptors are highly specialized cells that convert light into a neural signal by a process called phototransduction (Baylor 1987; Chen 2005). The distal part of the photoreceptor is adapted for capturing the light and the proximal part is adapted to transmit the signal using glutamate as the neurotransmitter. Two main

types of photoreceptor cells exist, namely rods and cones. In humans, the approximate 120 million rods are responsible for vision in a dim environment, whereas about 5 million cones are responsible for vision under brighter illumination as well as color vision (Curcio 1990; 2001; Forrester 2002).

All human rods contain the same visual pigment (rhodopsin), whereas human cones contain three different visual pigments (opsins), which are sensitive to three different regions of the light spectrum. The opsins have their peak absorptions at 420 nm (blue), 531 nm (green) and 588 nm (red). These pigments also define the S-cones, M-cones and L-cones, respectively (Kolb 1991a; Kolb 2003).

It is suggested that cones were probably the first photoreceptor type to appear during evolution, while rods emerged later (Hollenberg 1972, 1973). This sequence of appearance of cones and rods is also evidenced during the embryonic development of the photoreceptors, where cones developed before rods (Hollenberg 1972, 1973).

Animal species have adapted their eyes and retinal design according to the environment in which they lived. In general, the non-mammal animals have very well developed cones as their photoreceptors of choice (Kolb 2001; Linberg 2001). However, most mammals have a predominance of rods in their retina. Cones are present in a lower number and are generally organized in a specialized area of the retina (Hollenberg 1972, 1973). Some mammals, like rats and mice, do not have specialized cone areas in their retinas, while others, like cats, dogs and rabbits, have an elongated horizontal strip (visual streak) predominantly composed of cones. The ultimate specialized area is achieved in some birds and primates and is called the fovea (Curcio 1990; Linberg 2001). The latter is the most essential part of the primate retinas since it is a specialized area for high-resolution vision. In the fovea, cone photoreceptors are concentrated at maximum density, between 98 000 and 324 000/mm², with the exclusion of rods, and arranged at their most efficient

packing density, which is in a hexagonal mosaic (Curcio 1990). Also important to note, this particular region of the retina is avascular (Provis 2000). Guinea pigs, on the other hand, do not have a fovea or a definite visual streak as seen in humans or rabbits, dogs and cats. However, guinea pigs have a temporal expansion that may represent the analogue of the area centralis, which is similar to the human fovea (Do-Nascimento 1991).

3.1.3 Outer plexiform layer (OPL)

The photoreceptor cells synapse with the bipolar and horizontal cells in the outer plexiform layer (OPL), where its most distal part is predominantly occupied by the axons of the photoreceptors. While their synaptic bodies, rod spherules and cone pedicles, occupy the middle of the OPL. Finally, dendrites of bipolar and horizontal cells occupy the inner most part of this plexiform layer (Dowling 1966; Kolb 1994; Rodieck 1998).

Processes from bipolar and horizontal cells invaginate into the rod spherules. The three components (one bipolar cell and two horizontal cells) form a structure called a triad. Cone pedicles, however, have an organization, which is different from that of rod spherules. In fact, the cone pedicle is larger than the rod spherule and allows a greater number of connections (Kolb 1994, 2003).

Also important to note, is that from each cone pedicle protrudes up to a dozen small lateral extensions, which extend to neighbouring rod spherules. In this situation, cones connect to rods through gap junctions. The significance of these contacts still remains debated (Kolb 1994, 2003).

3.1.4 Inner nuclear layer (INL)

The inner nuclear layer contains four types of cells: 1- The horizontal cells, 2- The bipolar cells, 3- The amacrine cells, and 4- The Müller cells. Horizontal cells are located in the distal part of the inner nuclear layer, whereas amacrine cells are located in the most proximal part of this layer. Bipolar and Müller cell nuclei, on the other hand, occupy the intermediate portion of this layer (Rodieck 1998; Kolb 2003).

3.1.4.1 Horizontal cells (HC)

Horizontal cells have long processes that extend exclusively in the outer plexiform layer. The mammalian retina has two types of horizontal cells. The HII cells to which only cone cells synapse and the HI cells that receives imputes from the cones and rods. In return, horizontal cells provide inhibitory feedback to photoreceptor cells or inhibitory feed forward to the bipolar cells through GABAergic neurotransmission (Rodieck 1998; Kolb 2003).

3.1.4.2 Bipolar cells (BC)

Bipolar cells carry the signal from the photoreceptors to the ganglion or amacrine cells. They are classified according to whether they contact rod or cone cells (Forrester 2002).

Only one variety of rod bipolar cell has been described in mammals and it is easily identified by its high content in protein kinase C (PKC) enzyme (Jindrova 1998). Cone bipolar cells, on the other hand, can be divided into 8-10 types according to their dendritic branching pattern, the number of cone cells contacted and the shape and stratification of their processes in the inner plexiform layer.

Both rod and cone bipolar cells use glutamate as their neurotransmitter. In general, rod photoreceptor cells will only connect to ON depolarizing bipolar cells (ON-DBC) through mGluR6 receptors, whereas cone photoreceptor cells will connect to either ON-DBC (mGluR6 receptors) or OFF hyperpolarizing bipolar cells (OFF-HBC) through AMPA-kainate receptors (Kolb 1994, 2003).

3.1.4.3 Amacrine cells (AC)

Most amacrine cells are located in the proximal part of the inner nuclear layer, but some can also be found in the ganglion cell layer. The latter are called displaced amacrine cells. Amacrine cells modulate signals in the inner plexiform layer. As many as 50 different types exist, but only a few have been well characterized. Neuroactive substances detected in amacrine cells include glycine, GABA, acetylcholine, serotonin, dopamine, and nitric oxide, but most amacrine cells are glycinergic (ie: AII amacrine cells) or GABAergic (ie: A17 amacrine cells) (Kolb 1994, 1997). One of the best-characterized glycinergic amacrine cells is the AII. The latter is an important part of the rod pathway, relaying signals from the rods to cone OFF-hyperpolarizing bipolar cells (Kolb 2003).

3.1.4.4 Müller cells (MC)

Müller cells are the main glial cells of the retina. They extend through the whole thickness of the neural retina, with their nuclei in the INL. In addition to the structural support of the retina, Müller cells regulate the extracellular environment of the retina by buffering the light-evoked variations of potassium (K^+) concentrations in the extracellular space. They also remove glutamate from the extracellular space, by active uptake (Newman 1996).

3.1.5 Inner plexiform layer (IPL)

The inner plexiform layer is where retinal bipolar, amacrine and ganglion cells form connections. Occasionally, however, displaced amacrine or ganglion cell bodies can also be found in this layer. It is subdivided into two sublamina (*a* and *b*), with sublamina *a* being the most distal and sublamina *b* the most proximal (Kolb 1994, 2001, 2003). The bipolar cells terminals and dendrites of amacrine and ganglion cells branch in either sublayer *a* or *b* of the inner plexiform layer. More specifically, rod bipolar cell terminals occupy sublamina *a* (ON layer), whereas those of cone bipolar cells reach sublayer *b* (OFF layer). Furthermore, the dendrites of the OFF-ganglion cells connect the cone bipolar cells in sublayer *b*, whereas the dendrites of the ON-ganglion cells connect either the rod or cone bipolar cells in sublamina *a*. The distribution of the ON and OFF ganglion cells in two different sublamina of the IPL demonstrates the anatomic basis of the two parallel channels (section 3.2.2) that exist in the retina. Finally, gap junctions are also common in the IPL, joining amacrine cells to bipolar cells (Kolb 1994, 2003; Sharpe 1999).

3.1.6 Ganglion cell layer (GCL)

Ganglion cells are the neurons that collect the information processed by the retina and send it to the visual centers of the brain. There are two major types of ganglion cell namely, the P (parasol) cells and the M (midget) cells (Isenmann 2003; Silveira 2004). The former cells (P cells), which are smaller in diameter, project to the parvocellular part of the lateral geniculate nuclei (LGN) and carry information regarding forms and color perception (Kolb 1991a, 1991b; Isenmann 2003). The M ganglion cells, on the other hand, which are of larger diameter, project to the magnocellular part of the LGN and respond to moving stimuli (Dacey 1999; Isenmann 2003).

Recently, another type of ganglion cell was described. These new cells are named the melanopsin-containing retinal ganglion cells. Studies report that the melanopsin ganglion cells run in parallel with the image forming visual system and are supposedly directly excitable by light and would have a role in synchronizing the circadian clock, controlling the pupil size and the melatonin release (Klein 1972; Lucas 2001; Hattar 2002; Berson 2003; Peirson 2006).

3.2 Retinal physiology

In vertebrate retinas there are two types of photoreceptors. Simply, there are the cones and the rods. The cones are responsible for day (or photopic) vision as well as for colour vision and have a high stimulation threshold. On the other hand, the rods are mostly responsible for night (or scotopic) vision and have a very low stimulation threshold, thus permitting the detection of very dim light (Dowling 1987).

3.2.1 Phototransduction

At low light levels, opsin bleaching triggers the phototransduction cascade within the photoreceptor outer segments. The transduction of a light photon into an electrical signal in rod photoreceptors is very well documented, but less is known about this process in cones.

Briefly, the absorption of light by the visual pigment in rod photoreceptors causes a change in the conformation of retinal, the light-absorbing molecule, going from the 11-*cis* configuration (non activated conformation) to an all-*trans* form. The conformational change occurs as a result of the breakdown of the visual pigment, in all-*trans* retinal and metaRII opsin (R*). The now active rhodopsin (R*), is able to bind to the G-protein transducin (Gt). In its normal inactivated

state, transducin binds a molecule of guanosine diphosphate (GDP) to one of its subunits (α subunit). When activated rhodopsin (R^*) encounters a molecule of transducin, GDP is exchanged for guanosine triphosphate (GTP), and the GTP carrying α subunit of transducin separates from the rest of the molecule, which is now activated (Gt^*). The molecule then binds cGMP phosphodiesterase (PDE) enzyme. The reduction in cGMP, causes the sodium and potassium channels to close, which causes the hyperpolarization of the photoreceptor membrane resulting in the decrease of glutamate neurotransmitter being released at the synaptic terminal (Tessier-Lavigne 2000; Arshavsky 2002). The phototransduction cascade stops when the activated rhodopsin is phosphorylated by the rhodopsin kinase (RK). This phosphorylation enables the arrestin protein (ARR) to bind the phosphorylated rhodopsin at the site where the activated rhodopsin (R^*) normally interacts with the G protein transducin (Gt). Blocking the site prevents further interaction with Gt and brings to an end the ability of rhodopsin to activate Gt. Moreover, arrestin promotes the separation of all-*trans* retinal from the rhodopsin. This is the final stage of the phototransduction cascade (Arshavsky 2002; Chen 2005).

The regeneration of the photopigments requires the conversion of the all-*trans* retinal to 11-*cis* retinal. This conformational change enables the retinal to recombine with the opsin. All but the recombination takes place in the retinal pigment epithelium, not in the photoreceptor. Proteins such as interstitial retinoid-binding protein (IRBP) are implicated in the translocation of the retinal from the outer segment of the photoreceptors to the RPE and from the RPE to the photoreceptors, and cellular retinoid-binding protein (CRALBP) is implicated in carrying the retinal within the RPE cells (Arshavsky 2002; Chen 2005).

The processes of activation, breakdown, and regeneration of cone pigments are probably similar to those encountered in the rods, but clearly much work needs to be done to better understand the phototransduction cascade in cones.

3.2.2 Retinal ON- and OFF-pathways

Anatomical and physiological studies of the mammalian retina have revealed two different visual pathways namely the ON- and OFF-retinal pathways. In general, the ON-pathway connects the rod and cone photoreceptors to the rod ON depolarizing bipolar cells or the cone ON depolarizing bipolar cells respectively, to the ON-ganglion cells. The OFF-pathway, on the other hand, only connects the cone photoreceptors to the OFF hyperpolarizing bipolar cells (OFF-HBC) and then to the OFF ganglion cells (figure 2).

More specifically, in dark-adapted state, three different means of transmitting the rod signal to the ganglion cells can be evidenced. One via rod ON bipolars, amacrine II cells, and ON/OFF cone bipolars, which is designed for the transmission of single photon absorption events (in scotopic condition); a second via rod-cone gap junctions, and ON/OFF cone bipolar cells, which is designed for the transmission of multiple photon absorption events at higher light levels (in mesopic condition); and a third which includes a direct coupling the rods to the OFF bipolars. More work needs to be done to better understand this third pathway (figure 2) (Kolb 1994; Sharpe 1999).

The cone pathway (photopic condition) is quite different. Cones make contact with two types of bipolar cells: cone ON-depolarizing bipolar cells and OFF-hyperpolarizing bipolar cells. While the ON-DBC are activated at the onset of a light stimulus, the OFF-HBC are activated at light offset. The ON bipolar cells synapse with ON-centre OFF-surround ganglion cells, whereas the OFF bipolar cells make contact with OFF-centre ON-surround ganglion cells. Finally, all ganglion cell axons will project to the lateral geniculate nuclei (LGN). The LGN will then send its projections to the visual cortex.

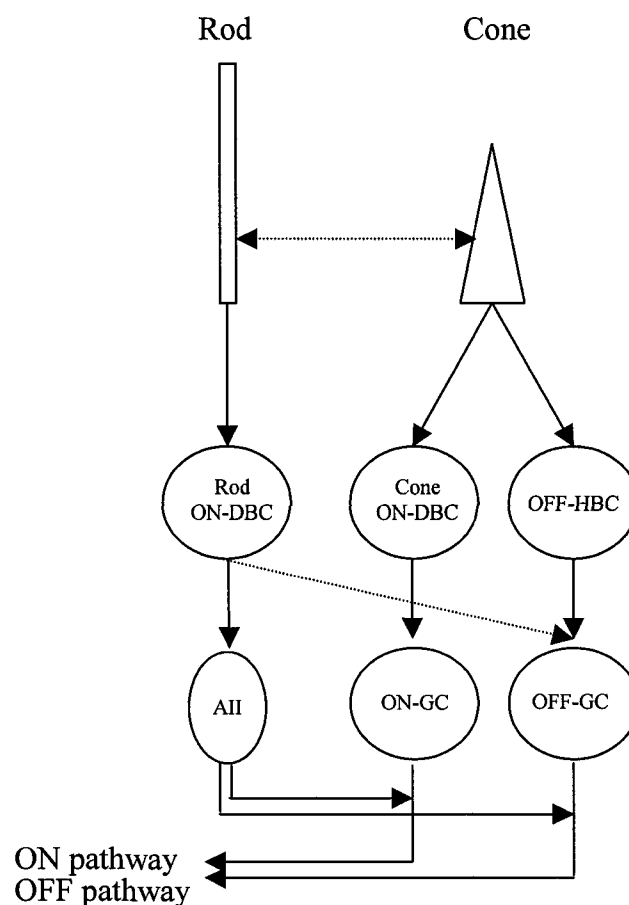


Figure 2: Vertical ON- and OFF-retinal pathways of the retina. ON depolarizing bipolar cells (ON-DBC), OFF hyperpolarizing bipolar cells (OFF-HBC), ON ganglion cells (ON-GC), OFF ganglion cells (OFF-GC), amacrine cell type II (AII). Solid lines: Common retinal pathways. Dash lines: Suggested retinal pathways for rod contribution to the OFF-retinal response.

4 Retinal function

4.1 The electroretinogram (ERG)

The electroretinogram (ERG) is the electrical signal produced by the retina in response to a flash of light. This biopotential, which reflects the summed

activity of a population of retinal cells, can be captured at the corneal surface of the eye. Unlike an ongoing electrical potential such as the electroencephalogram or the electrocardiogram, the ERG is an evoked potential and therefore must be triggered by a stimulus. Holmgren recorded the first electroretinogram in 1865 in frogs, but it was Deward in 1877, who first recorded this evoked potential in humans, making the ERG the first biopotential ever recorded from a man (Riggs 1986). As a general rule, the electroretinogram is recorded with preamplifiers that include at least the range of 0.3 to 300 hertz (Marmor 2004).

This low frequency signal, when evoked with a short duration stimuli (< 5 ms), as per the standard of the International Society of clinical Electrophysiology of Vision (ISCEV), shows an initial cornea-negative deflection, the a-wave, which is followed by a larger cornea-positive potential, the b-wave. These waves were named according to a nomenclature introduced by Einthoven & Jolly in 1908. Often seen on the ascending limb of the b-wave are a series of small wavelets (2 to 4) of high frequency (120–160 Hz), first described by Cobb & Morton (1954), but later named oscillatory potentials (OPs) by Yonemura & al (1962) (figure 3). The later, can also be recorded separately from the ERG, by changing the bandpass filters (75-100 to 300 hertz) (Marmor 2004).

Other waves, namely the d-wave, can also be recorded when the ERG is evoked with light stimuli of a longer duration (> 50 ms). In such conditions (long duration stimuli) a third wave appears, the d-wave (figure 4). From what is documented, when long duration stimuli are used, the terms ON- and OFF-response are used. The ON-potential, which include the a- and b-waves is evoked in response to the onset of the light stimulus, whereas the OFF- potential (d-wave) is evoked at the offset of the light stimulus. The later is characterized by a positive potential (Schiller 1992).

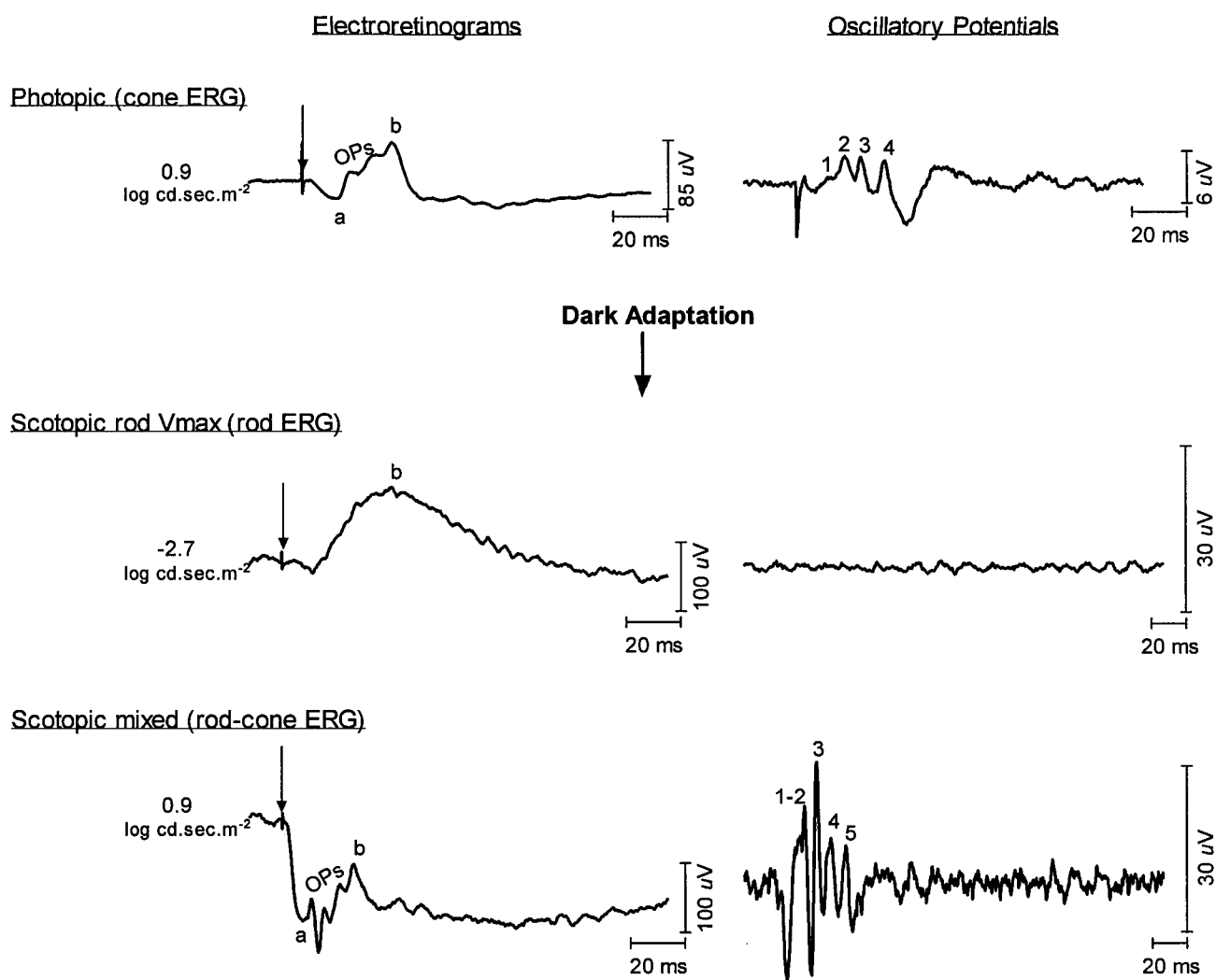


Figure 3: Example of a short flash ($20 \mu\text{s}$) cone (background: $30 \text{ cd}\cdot\text{m}^{-2}$; flash intensity: $0.9 \text{ log cd}\cdot\text{sec}\cdot\text{m}^{-2}$), rod (flash intensity: $-2.7 \text{ log cd}\cdot\text{sec}\cdot\text{m}^{-2}$) and rod-cone (flash intensity: $0.9 \text{ log cd}\cdot\text{sec}\cdot\text{m}^{-2}$) mediated ERG/OP waveforms, recorded in a Hartley albino guinea pig aged 15 days old. Vertical arrows identify flash onset, (a) a-wave, (b) b-wave, (1) OP_1 , (2) OP_2 , (3) OP_3 , (4) OP_4 , (OPs) Oscillatory potentials. Horizontal calibration: 20 ms. Electroretinogram vertical calibration: Cone: $85 \mu\text{V}$; Rod: $100 \mu\text{V}$; Rod-cone: $100 \mu\text{V}$. Oscillatory potentials vertical calibration: Cone: $6 \mu\text{V}$; Rod: $30 \mu\text{V}$; Rod-cone: $30 \mu\text{V}$.

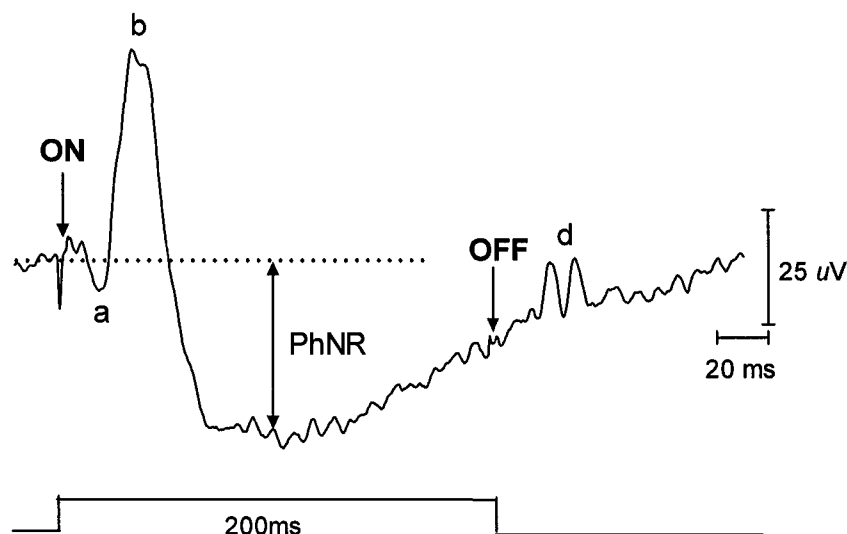


Figure 4: Example of a long flash (200 ms) cone (background: 15 cd.m^{-2} ; flash intensity: 125 cd.m^{-2}) mediated ERG waveform, recorded in a Hartley albino guinea pig aged 10 days old. Vertical arrows identify flash onset (ON) and offset (OFF), respectively. (a) a-wave, (b) b-wave, (PhNR) Photopic negative response, (d) d-wave. Horizontal calibration: 20 ms. Vertical Calibration: $25 \mu\text{V}$.

In 1933, Granit attempted, on a dark-adapted cat retina, to isolate the various components of the ERG in order to understand the origin of those waves. He showed that the ERG resulted from the summation of three independent processes namely P-I, P-II and P-III, which were later on shown to be at the origin of the c- b- and a-waves, respectively (Granit 1933). This study was the first to show that the ERG is a composite potential. This was later confirmed with the intra-retinal recording of the ERG with microelectrodes (Tomita 1950, Brown 1961).

In 1941, Riggs introduced a non-invasive contact lens, which provided a stable electrical connection with the cornea. Karpe in 1945, became the first researcher to clinically use the ERG as a diagnostic tool in a study which reported

that an extinguished response can be a characteristic of *Retinitis pigmentosa*. Furthermore, advancements in computer technology, which helped us with data acquisition and analysis, as well as the availability of more comfortable recording electrodes such as the DTL fibre electrode (Dawson 1979; Lachapelle 1993), have contributed to increase the clinical use of the ERG as a diagnostic tool.

4.2 Origin of the ERG components

In this section, I will discuss in more details the origin of the different components of the electroretinogram evoked by short and long flash stimuli.

4.2.1 a-wave

The a-wave is initiated at the level of the photoreceptors. It has long been associated with the hyperpolarization occurring in the photoreceptors following light stimulation (Brown 1968; Penn 1969; Heynen 1985). Recent models have proven this by demonstrating the quantitative correspondence between the electrical activity of the photoreceptors and the leading edge of the a-wave (Hood 1996). However, a recent report by Bush & Seiving in 1994, challenged this concept of a photoreceptor origin for the a-wave. They claimed that there was a large contribution of second-order neurons, the bipolar cells, to the genesis of the a-wave. Their hypothesis arose from the demonstration that intra-ocular administration of cis-2, 3-piperidine-dicarboxylic acid (PDA), which blocks synaptic transmission from the photoreceptors to the second order neurons, in monkey eyes significantly reduces the a-wave, suggesting a contribution of the second-order retinal neurons in the formation of the a-wave.

4.2.2 b-wave

The b-wave is the first and most prominent positive component of the ERG. Although it has been heavily studied, its origin still remains debated. Early investigation suggested the second-order retinal neurons, bipolar cells, as the probable site of the b-wave generation. In 1954, Noell and in 1968, Brown demonstrated that the ganglions cells and photoreceptors respectively, were not likely to be candidates in the genesis of the b-wave. Brown & Wiesel in 1961, with intra retinal recording, further supported this view by identifying the inner nuclear layer as the site where the b-wave reached its maximum amplitude. This idea was later challenged by Miller & Dowling (1970), who postulated the Müller cells, and not the second order neurons, as the site of origin of the b-wave. According to them, Müller cells depolarise when the extracellular concentration of potassium (K^+) is increased due to light-induced depolarization of second-order neurons [ON-depolarizing bipolar cells (ON-DBC)]. This current generated through the retina by Müller cells, called m-wave, is recorded at the cornea as the b-wave. This latter concept of the genesis of the b-wave has received substantial support from numerous studies (Dick 1978; Newman 1980, 1984).

A more recent concept, the push-pull model, proposed by Sieving et al. (1994) suggests that the bipolar cells interact in a “push” and “pull” manner in order to generate the b-wave. They proposed that the depolarizing bipolar cells (ON-DBC) are responsible for the initial “push” of the b-wave while the hyperpolarizing bipolar cells (OFF-HBC) and the Müller cells are responsible for the subsequent “pull” of the b-wave. The OFF-HBC and the Müller cells compete to sink the K^+ expelled by the ON-DBC and limit the amplitude of the b-wave. This “push”-“pull” concept is supported by the demonstration that intraocular injection of 2-amino-4-phosphonobutyric acid (L-AP-4), which blocs the synapses between the photoreceptors and the ON depolarizing bipolar cells, eliminates the b-wave from the ERG recording (Stockton 1989; Tian 1994; Hanitzsch 1996).

Xu & Karwoski (1994a, 1994b) further claimed that only the bipolar cells, and not the Müller cells, contributed to the genesis of the b-wave. Their studies showed that pharmacological removal of the buffer current of Müller cells [with barium (Ba^{++})] did not eliminate the b-wave from the ERG. Further investigations will be needed in order to clearly identify the precise origin of the b-wave.

4.2.3 i-wave

The i-wave of the electroretinogram is a positive potential, which follows the b-wave. This component can be evoked in photopic conditions and is probably the least studied wave of all the ERG components (Nagata 1963; Murayama 1992; Rousseau 1996; Rosolen 2004). Nagata in 1963, was the first to identify and name, this post b-wave component. He suggested that the i-wave reflects an OFF response to ERG evoked by brief flashes of light. More recent studies (Rousseau 1996) suggested that the i-wave would be generated at the level of the ganglion cells and/or the optic nerve. However, the origin of this post b-wave ERG component still remains debated.

4.2.4 c-wave

The c-wave of the electroretinogram is a slow positive potential that peaks several seconds following a light stimulus and is generated in response to neural activity by nonneuronal element of the retina (Steinberg 1970). In fact, the c-wave represents the decline in subretinal potassium, which is a consequence of the hyperpolarization of the apical membrane of the retinal pigment epithelium (Steinberg 1970, 1980, 1985). Noell in 1954, was probably the first to show that the c-wave of the vertebrate electroretinogram originate from the RPE. He reported that the c-wave disappeared in the rabbit retina after selectively poisoning of the RPE with sodium iodate. Later, Brown and Wiesel (1961) showed that the

c-wave of the cat's ERG reached maximum amplitude when the electrode was immediately adjacent to the pigment epithelium.

4.2.5 Oscillatory potentials (OPs)

The small oscillations seen on the ascending limb of the b-wave, named oscillatory potentials, were first identified by Cobb & Morton in 1954. Although much work has been done in trying to identify the origin of the OPs, the genesis of these wavelets still remains unclear. Several observations suggest that the OPs arise through retinal mechanisms, which are post-synaptic to the photoreceptors. Intra-retinal recordings have determined the inner retinal layer as the most probable site of origin of the OPs (Yonemura 1966; Ogden 1973; Wachtmeister 1978; Heynen 1985; Yanagida 1988). The horizontal cells were also eliminated as the cellular structure responsible for the OP genesis (Ogden 1973). Other investigations have eliminated the photoreceptors, the retinal ganglion cells and the Müller cells as probable OP generators (Brown 1968; Miller 1970; Ogden 1973). Intra-retinal recording in the mudpuppy eliminated the Müller cells as possible OP generators because the recordings did not produce an OP-like response (Miller 1970). Also following the administration of tetrodotoxin, which is known to block retinal ganglion cell action potentials, the OPs remained normal (Ogden 1973). Finally, Brown (1968) showed that the OPs and the b-wave were eliminated when the central retinal artery is occluded, thus demonstrating the dependence of the OP generators on retinal circulation, while the photoreceptors rely on choroidal circulation. The origin of the OPs is still debated and remains a determinant question in assessing the genesis of the ERG components. Although the intraretinal origin of the OPs remains to be identified, most studies to date suggest that they are generated by retinal cells different from those responsible for producing the a- and b-waves.

Studies of Yonemura (1962), Brunette (1970), and Speros (1981), revealed that the generation (formation) and maturation of the b-wave and the OPs are separated. This view is also supported by Hamasaki & Maguire (1985), which demonstrated that the formation of the b-wave preceded the formation of the OPs.

A slightly different picture was suggested by Lachapelle et al. in 1998 when he published comparisons between the photopic ERGs obtained from patients affected with congenital stationary night blindness (CSNB) or with cone dystrophy. In CSNB patients, the ERG morphology was described as a square shaped a-wave followed by a truncated b-wave. This characteristic ERG shape resulted from the absence of the initial segment of the rising phase of the b-wave and a complete abolition of OP₂ and OP₃ with relative preservation of OP₄. In the family affected with the cone disorder, the ERG morphology was also truncated, but this time it was the later part of the b-wave that was removed. This corresponds to the marked attenuation and delay of OP₄ and, to a lesser extent, of OP₃. Results obtained from these two pathologies would suggest that the OPs and the b-wave are intimately tied, where the OPs would represent the buildings blocks of the b-wave. Experimental evidence following intravitreal injection of iodoacetic acid (IAA), glycine and 2-amino-4-phosphonobutyric acid (APB) also support that claim (Matthews 1989; Lachapelle 1990; Guité 1990).

4.2.6 Photopic negative response (PhNR)

The photopic negative response (PhNR) is a slow negative potential that occurs following the ERG b-wave but prior to i-wave. It is particularly easy to see in responses to red flashes delivered against a blue background in monkeys, humans and cats (Viswanathan 1999, 2001). Several lines of experimental evidence indicate that the PhNR originates from the spiking activity of the retinal ganglion cells and their axons in these species (Colloto 2000; Viswanathan 2001). In fact, in monkeys and cats, the response is eliminated by the intravitreal

injection of tetrodotoxin (TTX), which blocks sodium-dependent action potentials that occur in all ganglion cells and some amacrine cells. Furthermore, in monkeys that developed laser induced glaucoma, a pathological condition that destroys ganglion cells, the PhNR is reduced or eliminated, strongly implicating ganglion cell spiking activity in the generation of the PhNR (Viswanathan 1999). In intraretinal microelectrode recordings in cats, local signals of the same time course as the PhNR were largest in and around the optic nerve head (Viswanathan 1999). The PhNR was also disrupted in cats by barium injections, indicating glial involvement in mediating the generation of the response (Viswanathan 2001). The PhNR holds promises for the clinical evaluation of retinal function in open angle glaucoma, since it is greatly reduced in patient affected with glaucoma.

4.2.7 d-wave

The d-wave of the electroretinogram is a positive going potential which is recorded at the termination of a light stimulus and is best recorded under photopic conditions with bandpass filters going from at least 0.3 to 300 hertz (Marmor 2004). The later is seen only when the ON- and OFF-phases of the ERG response are separated in time, by using light stimuli of a relatively long duration. Whereas the origin of the a- and b-waves, ON-components of the ERG, have been comprehensively studied, the d-wave has been studied less extensively. There is, however, some information on the origin of the d-wave.

Current source-density analysis suggest that the source of the d-wave is OFF-center bipolar cells (Karwoski 1996). Pharmacological studies in amphibian retinas (Stockton 1989; Gurevich 1993; Szikra 2001) and in primates (Sieving 1994) using selective blockers for ON-bipolar cell glutamate, metabotropic (mGluR6) receptors and OFF-bipolar cell AMPA/KA type receptors, have shown that the d-wave of the ERG depends entirely on AMPA/KA type synaptic transmission i.e. between photoreceptors and OFF-bipolar cells (OFF-HBC). A

more recent study by Ueno et al., in 2006, shows that the origin of the d-wave in the primate photopic ERG is very complex and the activities from several types of retinal neurons participate in the formation of the d-wave. The authors stipulated that not only the cone photoreceptors, but also postreceptoral components of the ON- and OFF-retinal pathways and the inner retinal neurons contribute to the genesis of the d-wave.

4.3 Stimulus-related characteristics of the ERG

The ERG is an evoked potential that can be initiated by a light stimulus and can be assessed in dark (scotopic) or light (photopic) conditions. The scotopic, dark-adapted, ERG, known as the rod or rod-cone mediated ERG depending on the intensity of the stimulus used, is the electrical response evoked in a retina previously adapted to a dark environment (Bayer 2001; Marmor 2004). Conversely, the photopic, light-adapted ERG or the cone ERG, is the biopotential produced by the retina previously adapted to a luminous environment. Different stimulus intensities can also be used to obtain an intensity-response function (Bayer 2001; Marmor 2004).

4.3.1 Photopic intensity-response function of the ERG

The photopic intensity-response function of the ERG can be obtained by using a wide range of stimulus intensities going from dim to bright. In a photopic environment, going for a dim to bright flash will bring upon the ERG an increase of the a-, b-, and i-waves amplitudes. In fact, the luminance-response function of the photopic electroretinogram b-wave was previously shown to adopt a unique shape where the amplitude of the b-wave first increases, then saturates briefly following which it decreases to reach a final plateau where the amplitude of the b-wave equals approximately that of the a-wave (Peachey 1992; Wali 1992, 1993;

Kondo 2000; Lachapelle 2001; Rufiange 2002, 2003, 2005). It was Wali & Leguire in 1992, who first named this phenomenon *photopic hill* to describe this unusual cone-mediated ERG function. More recently, Kondo et al. (2000) and Rufiange et al. (2002) reported that a *photopic hill*-like luminance response function could also be obtained with i-wave and OP₄ measurements.

Up to now, little is known about the retinal mechanisms at the origin of the phenomenon. However, in 2004, Ueno et al. proposed that the limitation of the cone b-wave V_{\max} could be governed by the same retinal mechanisms that were previously suggested to limit the amplitude of the cone ERG b-wave, namely the push-pull model (Sieving, 1994). The authors concluded that the *photopic hill* results mainly from two factors: 1- the amplitude reduction of the ON-component at higher intensities and 2- the delay in the positive peak of the OFF-component at higher intensities. Their results also indicated that the contribution from inner retinal neurons to the *photopic hill* is minor because at all stimulus intensities, both the implicit times and amplitude of the photopic b-wave, did not change much after tetrodotoxin (TTX; voltage-gated sodium channel blocker that prevent action potentials of ganglion cells) and N-methyl-D-aspartate (NMDA; suppresses synaptic transmission of the third order neurons) injections. Furthermore, the contribution of inhibitory feedback from the horizontal cells to the *photopic hill* is small, because the *photopic hill*, although somewhat reduced in amplitude in at least one animal, remained even with application of cis-2,3-piperidine dicarboxylic acid (PDA), a partial NMDA agonist which inhibits the transmission of the retinal signal from the cone and rod photoreceptors to the hyperpolarizing depolarizing bipolar cells (OFF-pathway).

In 2003, Rufiange et al. investigated if the use of pre-selected descriptors of key features of the *photopic hill* (ie: V_{\max} ¹, a_{\max} ², I_{\max} ³, K_a ⁴, K_d ⁵) could help

¹ Maximal b-wave amplitude.
² Amplitude of the a-wave at the V_{\max} intensity.
³ Flash intensity needed to generate the V_{\max} .

extract meaningful functional information that could potentially have some clinical relevance. The author concluded that the use of descriptors can be useful in documenting functional alterations in the retinal physiology triggered by a pathological process. In 2005, Rufiange et al. studies also revealed that the modulation of the human photopic ERG luminance-response function was dependent on the chromatic stimuli, where short wavelength stimulus triggered *photopic hill* was shifted to the left and where the long wavelength stimulus triggered *photopic hill* was shifted to the right with a decrease in the b-wave amplitude. The later results let us suggest that the human retina would be most sensitive to short wavelengths and less to long wavelengths.

4.3.2 Scotopic intensity-response function of the ERG

In scotopic condition, the intensity-response function is different from that seen in photopic condition. From dimmer to brighter flashes, the b-wave amplitude will increase as the intensity of the stimulus increases, until it reaches a plateau or the “first V_{\max} ” (Naka & Rushton 1966). In scotopic conditions, “first V_{\max} ” refers to the maximum amplitude of the b-wave generated by the rods. A further increase in flash intensity will, at this point, increase the amplitude of the b-wave until it reaches a second plateau, “second V_{\max} ”. At the highest intensities, both rod and cone pathways contribute to the genesis of the ERG, whereas before the first rod V_{\max} only the rod pathway contributed. However, unlike the light-adapted ERG intensity response function that shows a decrease in amplitude of the b-wave beyond V_{\max} , the dark-adapted ERG intensity-response reaches a plateau and then increases again, to create the second limb of the curve (Peachey 1989). This sigmoidal function describes the relationship of the rod b-wave potential to stimuli intensity (Naka & Rushton 1966).

⁴ Intensity of stimulation that will generate a b-wave half the amplitude of V_{\max} on the ascending portion of the *photopic hill*.

⁵ Intensity of stimulation that will generate a b-wave half the amplitude of V_{\max} on the descending portion of the *photopic hill*.

5 Retinal disorders

Human retinopathies are classified based on a number of criteria, such as fundus appearance, behavioral responses to visual stimuli and electroretinographic responses (Berson 1993; Nowak 1996; Besch 2003; Del Piore 2006; Hartong 2006). These non-invasive methods are relatively precise and enable the ophthalmologist to classify the different human retinopathies in an accurate way. The two major classes of retinal degeneration in North America are *Retinitis Pigmentosa* (RP) and aged macular degenerations (AMD) (Nowak 1996; Besch 2003; Del Piore 2006; Hartong 2006). As a general rule, the above-mentioned retinal anomalies, which specifically affect the outer retina, most specifically the photoreceptor cells, lead to complete (RP) or partial blindness (AMD) as their end-result. These retinopathies are known to arise from multiple defects of the visual cycle. The functional categories can be separated as follows: Retinal degenerations that affect 1-phototransduction, 2- the visual cycle, 3- the structure, 4- the transport, 5- the development, 6- the pigmentation, 7- the metabolism or 8- the synaptic transmission. In general, defects that fall into these categories lead to retinopathies such as *Retinitis Pigmentosa*, Congenital stationary night blindness, rod-cone dystrophies, Lebers congenital amarois (LCA) or Stargardt disease, to name a few (Chader 2002; Fauser 2002; Delyfer 2004).

In the literature, the classification of the retinal disorders is based on several criteria such as the retinal topographic distribution, the disease, the age at onset, the progression, the symptoms and the inheritance pattern (Chader 2002; Fauser 2002; Delyfer 2004; Hartong 2006). The distribution of the anomalies in the retina can help us determine if the anomalies are localized or diffuse. In fact, the pattern of distribution provides important clues to the disease process. The age at onset of the retinopathies provides information on the retinopathy. They may be present at birth (congenial), developed during the first decade (infantile), during the second decade (juvenile) during the third decade (adult) or at later age (Haim

1992). The progression of the retinopathy is also important. The retinal disorders are either stationary or degenerative. In fact, the retinopathy will show no signs of changes with time in the case of stationary retinopathies (ie: congenital stationary night blindness) but will progress in the case of progressive retinopathies (ie: *retinitis pigmentosa*). The symptoms are also the basis of distinguishing if, for example, it is a night blinding disorder or a color vision defect. The mode of inheritance is also very important in separating a number of retinal diseases whose clinical appearance might be identical but whose progression varies greatly according to inheritance pattern. The mode of inheritance depends if the gene implicated is located on the autosomal or the sexual chromosome. The Mendelian inheritance modes described in the literature are 1- the autosomal dominant, 2- autosomal recessive and 3- the X-linked mode of inheritance.

The following sections (4 and 5) will describe two types of retinal disorder which are either progressive (*Retinitis Pigmentosa*) or stationary (CSNB).

5.1 Retinitis pigmentosa (RP)

5.1.1 Description

Retinitis pigmentosa (RP) is the leading cause of inherited blindness in the developed countries and occurs approximately in 1 in 3000 individuals worldwide (Phelan 2000; Dejneka 2003; Delyfer 2004). RP is a heterogeneous group of inherited retinal degenerative diseases, characterized by the progressive death of rod and subsequently cone photoreceptors (Berson 1993; Hartong 2006). Most mutations affect the rods selectively and, through an unknown pathway, cause the rod cells to die by apoptosis (Chang 1993; Portera-Cailliau 1994; Travis 1998). Cones, on the other hand, are rarely directly affected by the identified mutations,

and yet, in many cases they degenerate secondary to rods, which accounts, with time, for loss of central vision and complete blindness (Berson 1993).

In typical cases, the rods are the predominantly affected photoreceptor cells (Hartong 2006). This generates a number of clinical symptoms including night blindness and bilateral symmetric loss of the peripheral visual fields. However, there is usually relative preservation of central vision. With progression, cone photoreceptor cells are also affected and day vision along with central visual acuity decrease.

In RP patients, the rod-cone disorder initially reveals alterations of the scotopic ERG and then of the photopic ERG. By the end stages of RP, the ERG responses are almost completely extinguished (Hartong 2006).

The age of onset of RP can vary from infancy to adulthood (Haim 1992). The age at which symptoms become clinically apparent is correlated with the mechanism of inheritance which can be: X-linked (5-15%), autosomal recessive (50-60%) or autosomal dominant (30-40%) (Bunker 1984; Grondahl 1987; Berson 1993; Hartong 2006). In general, the onset of the retinopathy is earlier in X-linked RP and later in autosomal dominant RP (Berson 1993; Phelan 2000).

In summary, a typical RP patient will present atrophy and pigment changes to the retina and retinal pigment epithelium, attenuation of the retinal vasculature, and changes to the optic nerve head during the course of the disease. Affected individuals first experience defective dark adaptation (night blindness), followed by constriction of the visual field and, eventually, loss of central visual acuity.

5.1.2 Animal models of RP

Many animal models of RP are available and have led to a better understanding of the disease. The archetypes being the rodless mouse (Keeler 1924), the RCS rats (Bourne 1938; Dowling 1962) and the retinal degeneration slow (*rds*) mouse models (Van Nie 1978). These animal models made possible the development of therapeutic strategies aimed at curing the specific genetic disorder (gene therapy), slowing down or even stopping the process of photoreceptor degeneration (growth factors or calcium blockers applications, vitamin supplementation), preserving the cones implicated in the central visual function (identification of endogenous cone viability factors) or even replacing the lost cells (transplantation, use of stem or precursors cells). Still, many obstacles will need to be overcome before most of these strategies can be applied to humans.

Up to now, there is a tremendous amount of animal models for the human disease *retinitis pigmentosa*. Since the description of the *rd* mouse by Keeler in 1924, many other *rd* mice have been described. A review by Chan in 2002, revealed the naturally occurring retinal degeneration in multiple *rd* mice. The candidate genes for RP are now outlined and grouped into functional categories. These categories include the following genes: *RHO*, *PDE6A*, *PDE6B*, *CNGA1*, *SAG*, *RPE65*, *RLBP1*, *ABCA4*, *RGR*, *RDS*, *ROM1*, *PROML1*, *NRL*, *CRX*, *RP1*, *RP2*, *RPGR*, *CRB1*, and *TULP1* (RetNet: www.sph.uth.tmc.edu/Retnet/disease.htm).

5.2 Congenital Stationary Night Blindness (CSNB)

5.2.1 History

Congenital Stationary Night Blindness (CSNB) was first reported by Cunier in 1838 when he described a seven-generation family in France with poor

night vision but exhibiting normal visual functions in all other respects. Genealogies and pedigrees were described throughout the world and, in time, a number of separate entities were described, all of which had in common a loss of darkness adaptation or a markedly prolonged darkness adaptation capacity. This congenital (i.e. appearing at birth) visual disorder can now be classified in two dominant groups: the first being CSNB with normal eye fundi, and the second being CSNB with abnormal fundi.

5.2.1.1 CSNB with normal fundus

Electroretinograms in CSNB patients essentially show two patterns with very characteristic features. The Riggs type, less frequent, presents attenuated a- and b-waves in both photopic and scotopic conditions (Riggs 1954). The Shubert-Bornschein type, more frequent, can be recognized by a severely reduced rod related activity and a negative ERG to bright flash stimuli delivered in scotopic condition (Shubert & Bornschein 1952). Several years later, Miyake et al. (1986) distinguished two forms of the Shubert- Bornschein type. They used the term complete and incomplete to describe these two varieties of the Shubert-Bornschein type CSNB. This distinction between the complete and incomplete types was based on the rod function, evaluated by routine dark adaptometry and rod-mediated ERG. Complete CSNB (cCSNB) lacks rod function, while incomplete CSNB (iCSNB) shows some residual rod function on the scotopic ERG (Miyake 1986; Takahashi 1987; Khouri 1988). Furthermore, cCSNB does not show any abnormalities in photopic condition, while the iCSNB shows an impaired cone ERG, the a- and b-waves being almost abolished (Miyake 1986, 1987). These differences confirm that these two types are different clinical entities. In 1998, the α -1-subunit of L-type voltage-gated calcium channel gene (CACNA1F) was identified as the mutated gene in X-linked incomplete CSNB and in 2000, NYX gene mutation was identified to cause X-linked complete CSNB (Bech-Hansen 1998; Push 2000; Gregg 2003).

5.2.1.2 CSNB with abnormal fundus

In the second group, three forms of CSNB can be described. The first one is the Oguchi's disease, which is characterized by a peculiar grey-white discoloration of the retina (Wilder 1953; Miyake 1996). The second form, Fundus Albipunctatus, is characterized by multiple small white spots in the retina, an absence of visual field changes and normal retinal vessels (Miyake 1992; Flynn 1999). Finally the third form is the fleck retina of Kandori, which is characterized by yellowish flecks that are larger, more irregular, and fewer in number than those seen in typical Fundus Albipunctatus (Kandori 1966, 1972). The latter forms are less frequent than those in group 1 (CSNB with normal fundus), and are described less extensively.

5.2.2 Differences between complete and incomplete CSNB

CSNB was described as a set of inherited (autosomal recessive, autosomal dominant, X-linked recessive), non-progressive retinal conditions in which the rod pathway is primarily affected; resulting in an elevation of the darkness adaptation threshold and night blindness (Schubert & Bornschein 1952, Riggs 1954, Auerbach 1969; Ripps 1982; Young 1986; Keunen 1988). In general, the Schubert-Bornschein type of CSNB is characterized by a negative electroretinogram: that is, the amplitude of the a-wave is larger than that of the b-wave (Miyake 1986). The darkness adaptation curve in incomplete CSNB is present although the final threshold is elevated by 1 to 1.5 log units, whereas in complete CSNB the threshold is elevated by 3%. In pure scotopic conditions, the rod mediated ERGs are subnormal (25 % of normal) in iCSNB and absent in cCSNB (Tremblay 1995). The mixed electroretinogram (rod-cone mediated ERG) are of negative morphology in both complete and incomplete CSNB. However, cCSNB patients revealed an absence of recordable oscillatory potentials, whereas with incomplete patients the

oscillatory potentials (OPs), often the ERG, are more frequently recordable (Tremblay 1995). In photopic condition, the ERGs are normal to subnormal in complete CSNB patients and present in absence of the early oscillatory potentials (OP₂, OP₃), while in incomplete CSNB patients the ERG is very small (delayed a-wave and barely recordable b-wave) with no recordable oscillatory potentials (Lachapelle 1983; Miyake 1986; Tremblay 1995). The visual acuity as well as the visual field in both forms are moderately affected (Miyake 1986). The refractive errors range, in iCSNB, from mild myopia to hyperopia, in contrast with cCSNB where patients have high to moderate myopia. In both forms the fundus appearance is essentially normal. In general, the macula is normal and good foveal reflex is observed. Some patients can also show signs of nystagmus and/or exotropia (Ripps 1982, Miyake 1986).

The malfunction of this retinopathy in humans arises at the level of the second order neurons, more specifically at the level of the ON-depolarizing bipolar cells (Alexander 1992; Quigley 1996). Clinical studies, animal studies and molecular genetics suggest that complete CSNB has a complete defect of the ON depolarizing bipolar cell synapses in both rod and cone visual pathways, leaving the OFF-pathway intact. On the other hand, incomplete CSNB has an incomplete defect of the ON and OFF bipolar cells synapses in the rod and cone visual pathway (Miyake 1987; Peachey 1990).

5.2.3 Animal models of CSNB

In research, few animal models of Congenital Stationary Night Blindness exist in comparison with other retinal diseases, like RP, where a lot of transgenic animals are used. Up to now three animal models of this human retinopathy have been used namely; a mouse model, a horse model and finally a dog model.

Witzel et al. in 1978 were the first group to work with an animal model of CSNB (Shubert-Bornschein type). They studied the nyctalopic Appaloosa horse where both scotopic and photopic retinal functions seemed to be affected. In scotopic condition, no rod-mediated responses were recorded, while in mixed condition only an a-wave was obtained. In photopic conditions, the morphology of the waves were normal but of smaller amplitudes. A couple of years later, Narfström et al. (1989) worked with a naturally occurring, autosomal recessive, Briard dog model of nyctalopia in which scotopic a- and b-waves were severely affected and only present at a photopic level. Pardue et al. (1998) also worked with a naturally occurring x-linked recessive model of CSNB, but in the mouse. This model was of particular interest because ERG responses never developed a b-wave (nob mouse). Only an a-wave could be seen in scotopic and/or photopic conditions and, consequently, the morphology of the waveforms were of negative shape. More recently we developed, through the selective breeding of guinea pigs, a new and naturally occurring animal model of CSNB (Racine 2003). In the course of an experiment, the accidental mating of a brother and sister occurred. Of the four guinea pigs born from this union, one yielded abnormal ERG recordings when compared to other guinea pigs. Unlike the responses normally seen in the guinea pig under scotopic mixed conditions, the ERG yielded a photopic-like waveform. Finally, even more recently, another animal model of CSNB was described. Zhang et al. (2003) described a potential spontaneous model of X-linked congenital stationary night blindness in a rat model, the key features of which were reduced rod and cone b-waves amplitude. In scotopic environment, maximal responses evoked by bright flashes in affected animals presented a selectively affected b-wave, a normal a-wave amplitude and in cone-mediated ERG. The b-wave were significantly reduced in amplitude along with delayed b-wave peak time. These different animal models did help us in identifying the genes responsible for the retinopathy in humans and helped us understanding the origin of the retinal anomaly.

Up to now, the catalogs of the currently known genes and loci responsible for the genes responsible for CSNB are available on RetNet: (www.sph.uth.tmc.edu/Retnet/disease.htm). In summary, most of the genes suggested to cause CSNB are located in the photoreceptor area. The first gene identified was the RHO gene, encoding for the rhodopsin protein (Dryja 1993). The second gene discovered was the PDE6 β gene, encoding for the phosphodiesterase β protein (Gal 1994). Then in 1995 and 1997, Fuchs et al. and Yamamoto et al. reported an anomaly on the SAG and RHOK genes, respectively. Both mutations lead to an impairment of the arrestin and the rhodopsin kinase proteins. The year after, Dryja found an anomaly on the GNAT1 gene that was encoding for the transducin α -subunit protein (Dryja 1996). Then in 1998 and 2000, Bech-Hansen et al. and Pusch et al. discovered the CACNA1F and NYX genes. The later genes affect the L-type voltage gated calcium channel and the nyctalopin protein to form properly (Table 1).

Phenotypes	Inheritance patterns	Genes	Proteins	References
CSNB	AD	RHO	Rhodopsin	Dryja 1993
CSNB	AD	PDE6B	Phosphodiesterase- β	Gal 1994
Oguchi disease	AR	RHOK	Rhodopsin Kinase	Yamamoto 1997
Oguchi disease	AR	SAG	Arrestin	Fuchs 1995
CSNB	AD	GNAT1	Transducin α -subunit	Dryja 1996
iCSNB	XL	CACNA1F	L-voltage-gated calcium channel α -subunit	Bech-Hansen 1998
cCSNB	XL	NYX	Nyctalopin	Pusch 2000

Table 1: Known genes that produced human Congenital Stationary Night Blindness (CSNB). The inheritance patterns and proteins implicated in this retinopathy are also mentioned. AD: Autosomal dominant; AR: Autosomal recessive; XL: X-linked.

Human retinopathies fall into two general categories, namely degenerative or stationary. In order to better understand the pathophysiological anomalies that govern stationary or degenerative human retinal disorders, several animal models are used and reported in the literature. The later are either naturally occurring or genetically engineered animal model. In the following chapter, I will briefly review the most important animal models of human retinopathies.

6 Animal models in vision research

Inherited retinal degenerations such as *retinitis pigmentosa* and age macular degenerations are common causes of blindness in North America (Nowak 1996; Besch 2003; Del Piore 2006; Hartong 2006). Recent advances in molecular genetics have lead to the mapping of more than 130 loci and cloning of more than 70 genes (Delyfer 2004; Chang 2005). However the mechanisms of most of the retinal degenerations are still unknown, hence a suitable treatment for most of these diseases has yet to be found. For that reason, animal models are very important to understand the pathophysiological mechanisms of the retinal degenerations and to help develop suitable treatments. In the literature, two types of animal models are described, namely the naturally occurring animal models of retinal degenerations and the genetically engineered animal models of retinal degenerations.

In both cases, rodents (mice in particular) are the most widely used animal model (Chader 2002; Chang 2002, 2005; Fauser 2002; Delyfer 2004, Dalke 2005). In gene therapy, mice are most popular models since transgenic technology is far more advanced in this model. Another advantage is the rapid progression of the disease process, which is measured in weeks as opposed to years in humans. Although mouse models are a good tool to investigate retinal disorders, one should keep in mind that the mouse retina is different form the human retina, particularly with respect to the proportion of cones in their retina (only 1-3% of

the photoreceptors), the distribution of the photoreceptor cells and that mice are nocturnal animals. Furthermore, mouse retina does not exhibit cone-rich area like the human fovea. Finally, while three cone pigments are present in the human retina, mice express only two distinct pigments with maximum absorption at 350 and 510 nm (Lyubassky 1999).

6.1 Naturally occurring animal models

The spontaneous animal models have been catalogued and maintained for decades. The fruit fly has been a key animal model for pinpointing mutated genes that can lead to retinal degeneration (Pak 1995). At the vertebrate level, zebra fish (Brockerhoff 1995) and chicken (Semple-Rowland 2000) are also good animal models to understand naturally occurring retinal degenerations. One of the first spontaneously occurring mammal models of retinal degeneration were the rodless mouse (rd), originally described by Keeler in 1924, followed by the Royal College of Surgeon (RCS) rats (Bourne 1938; Dowling 1962) and the retinal degeneration slow (rds) mouse (Van Nie 1978).

The rd mice, the RCS rats and the rds mice are now known to carry out defects in 1- the beta-subunit of the rod phosphodiesterase, 2- in the Mertk gene and in 3- the Prph2 gene, respectively (Dejneka 2003). They are important models to study the autosomal recessive retinal degeneration known as *Retinitis pigmentosa*. More recently, a naturally occurring rat model of X-linked cone dysfunction (Gu 2003) and one rat model of x-linked CSNB (Zhang 2003) were added to the list of naturally occurring animal models. Other spontaneous animal models of retinal disorders exist in the literature and are described at table 2.

A study by Chang et al. in 2002 at the Jackson Laboratory reported using ophthalmology, electroretinography and histology mice, affected with disorders involving all aspects of the eye namely the lid, the cornea, the iris, the lens and the

retina; resulting in corneal disorders, cataracts, glaucoma and retinal degenerations. In this survey, they identified sixteen naturally occurring mouse mutants that manifested degeneration of photoreceptors in the retina with preservation of all other retinal cell types.

Animals	Animal models	Genes	Human diseases	References
Mice	rd1	PDE6B	AR retinitis pigmentosa	Bowed 1990
	rds	RDS/periferin	AD retinitis pigmentosa	Travis 1989
	nob	NYX	X-Linked CSNB	Candille 1999
	A review by Chang B. et al. (2002) provides detail information on sixteen other rd mice model of retinal degeneration			
Rats	RCS	Mertk	AR Retinitis pigmentosa	D'Cruz 2000
	---	NA	X-Linked CSNB	Zang 2003
Cats	rdy	NA	AD retinitis pigmentosa	Barnett 1985
	Prcd	NA	AR retinitis pigmentosa	Narfström 1983
Dogs	Rcd1	PDE6B	AR retinitis pigmentosa	Suber 1993; Ray 1996
	Rcd3	PDEx	AR retinitis pigmentosa	Petersen-Jones 1999
	Erd	NA	AR retinitis pigmentosa	Acland 1999
	RPE65	RPE65	CSNB, Leber's congenital amaurosis	Narfstrom 1989; Aguirre 1998
	Prcd	NA	Retinitis pigmentosa	Acland 1998
	XLPRA	NA	Retinitis pigmentosa	Zeiss 1999
	cd	NA	Achromatopsia	Aguirre 1975; Gropp 1996
Chicken	rd	NA	Leber's congenital amaurosis	Ulshafer 1984, 1985; Semple-Rowland 1998
Guinea pig	---	NA	CSNB	Racine 2003

Table 2: Summary table of naturally occurring animal models of retinal degenerations. AD: Autosomal dominant, AR: Autosomal recessive, NA: not available.

Furthermore, in the literature, larger animal models are also described. Several canine and cat models of inherited retinal degenerations have been identified. Aguirre and co-workers have identified and characterized several forms of canine retinal degeneration (Aguirre 1975, 1998, 1999). These are mostly autosomal recessive conditions, although an X-linked model has been characterized (Aguirre 1998). The defect in the Irish setter (Suber 1993; Aguirre 1999) is particularly interesting since it exhibits the same defect in the cyclic GMP phosphodiesterase beta subunit gene observed in the rd mouse and in some human families with recessive RP. This gives the opportunity of studying faithful models of human retinal degeneration disease both in small and larger animals.

Finally, significant progress has been made over the last few years in constructing bioengineered animal models that mimic human retinopathies.

6.2 Genetically manipulated animal models

The use of knock-out, knock-in, chimeras and transgenic mice was also instrumental in advancing our understanding of retinal development and diseases. In fact, an important finding using animal models has been that photoreceptor cell death occurs by apoptosis in many different models with various underlying gene defects (Chang 1993, Portera-Cailliau 1994). Although this does not tell us anything about the mechanism of the different retinal diseases, it has important therapeutic implications as this final common pathway might be blocked.

Many examples of genetically engineered animals are now described in the literature, where nearly 90 % of the mutations are induced in mouse models. However, other animal models such as rats, dogs, cats, chickens and pigs are also represented in this category (Petters 1997; Pardue 1998; Chader 2002). In 2002, Fauser et al. overviewed all of the broad variety of genetic animal models for

retinal degenerations. They reviewed more than 80 genetic animal models for retinal degenerations and they grouped them into functional categories. The categories were as follows: anomalies that affect the 1- phototransduction cascade, 2- the visual cycle, 3- the structure, 4- the transport of protein in the OS, 5- the pigmentation, 6- the development, 7- the metabolisms, 8- the brain, 9- the cell cycle, 10- the synaptic transmission or 11- the apoptosis of the retinal cells.

The well-established methods for generating transgenic animals will produce many additional models in the following years. The main goal will be to understand the function of the disease genes in the process of retinal degenerations. The rapid progress gives hope that we can give a treatment within the coming years.

7 General Objectives

As previously mentioned in section 1 of the introduction, most studies that have examined the retinal structure and retinal function did so in altricial animals, which are born with closed eyelids and with a very immature visual system. On the other hand, only few studies reported the retinal changes, function and structure simultaneously, that occur in precocial animals such as the guinea pig.

The general purpose of my research was to study the maturation and aging of the retinal structure and function of the normal and night blind Hartley albino guinea pigs. We wanted to determine if, even with its at birth relative retinal maturity, the retina of guinea pigs undergoes maturation and to determine if, in fact, normal albino guinea pigs represent a better animal model, as opposed to other rodents, to study the human maturation and aging of the visual system. Furthermore, we wanted to examine if our night blind guinea pigs represent a valid model to study the mechanisms involved in generating functional retinal disorder such as those encountered in humans.

1- In the first study, I examined if, despite the at-birth mature retina of guinea pigs, there was some postnatal maturation of the retinal structure and function similar to that reported for altricial animals. Results revealed that guinea pigs are born with nearly adult-like ERG waveforms where the photopic ERGs reached their peak amplitudes earlier (P5) than scotopic ERGs (P10-P15). However, the amplitude of the cone ERG was significantly more enhanced in the first few days of life when compared to rod-mediated ERG, suggesting that guinea pigs are essentially born with a mature rod function. These ERG changes were also accompanied by subtle age-dependent cytoarchitectural reorganization of the retinal tissue that was most pronounced at the level of the ONL, OPL and GCL.

2- In the second study, I compared the human and guinea pig's retinal function in order to determine if the albino guinea pig could represent a good animal model of human cone-mediated ERG. Results revealed that the morphology of the photopic ERG of guinea pigs, its amplitude as well as its timing, were nearly identical to those of the human subjects obtained under similar conditions. At low intensity of stimulation, a small but noticeable a-wave as well as a b-wave are recorded from both human and guinea pig subjects. As the intensity of the flash increases, a larger a-wave as well as OPs are added to the ERG waveform. Further increments in the intensity of the stimulus increase the amplitude of the b-wave to a maximum voltage (V_{max}) at approximately $0.90 \log \text{cd}\cdot\text{sec}\cdot\text{m}^{-2}$ and then decrease it progressively with the brightest stimuli. At V_{max} , humans and guinea pigs share a similar b/a wave ratio as well as a similar relative amplitude of individual OPs. Similarly, like in humans, the cone b-wave of the guinea pig is followed by an i-wave. The above similarities between cone-mediated ERG between guinea pigs and humans led us to suggest that the guinea pig is a superior rodent model to study the human cone-mediated ERG.

3- In the third study, I documented the retinal function of a night blinding disorder that occurred spontaneously in our colony of guinea pigs. The key

features of the anomaly were 1- severe impairment of the scotopic (rod-mediated) ERG a- and b-waves as witnessed with the elevated threshold as well as an abnormal, photopic-like, response evoked by the brighter flashes; 2- elevated threshold for scotopic OPs to intensities well within the photopic range and 3- significantly attenuated OFF-ERG retinal responses and ON- ERG post b-wave electronegativity. We concluded that even though the functional anomalies found in our colony of guinea pigs are not exactly similar to the human CSNB, our animal model could represent a good model to study the pathophysiological processes of a human-like night blinding retinal disorder.

4-Finally, in the fourth study, I compared the maturation and aging of the retinal structure and function of our night blind and normal guinea pigs in order to better understand the pathophysiology of this interesting retinal anomaly. Key features were: 1- non recordable rod-mediated vision from birth, 2- scotopic responses evoked by bright flashes most probably generated by cones; 3- near normal photopic responses; 4- no histological evidence of rod photoreceptors, 5- remnant cone outer segments, 6- thinning of the outer nuclear, outer plexiform and ganglion cell layers of the retina with age, 7- re-localization of rhodopsin in the ONL, 8- normal cone and synaptic immunoreactivity and finally, 9- slight evidence of progression (larger than normal decrease of ERG components amplitude) with age. Results led us to suggest that the anomaly was inherited as an autosomal recessive trait and that the retinopathy was most likely degenerative. Finally, our model offers the opportunity to study cone function in the absence of functional rod photoreceptors.

CHAPTER II: MANUSCRIPT 1

Racine J., Behn D., Lachapelle P. (2007) Structural and functional maturation of the retina of the albino Hartley guinea pig. Doc Ophthalmol, (Epub ahead of print).

1 Preface to chapter II

Up to now, only few studies of the retinal structure and/or retinal function have been conducted using the albino guinea pig as the animal model. Therefore, little is known about the postnatal structural and functional maturation of its retina. The albino guinea pigs, like humans, are precocial animals meaning that most of the retinal maturation occurs *in utero*. In order to address the above, we investigated the postnatal maturation of the retina of albino guinea pigs (up to P75) in order to determine if, despite this at-birth mature retina, there was some postnatal maturation of the retinal structure and function similar to that seen in altricial animals.

2 Abstract

Purpose: Altricial animals, such as rats and mice, are born with their eyes closed, compared to precocial animals, such as guinea pigs and humans, which have their eyes opened at birth. The purpose of this study was to investigate if the retina of guinea pigs (precocial animal) is subjected to a postnatal maturation process similar to that previously reported for rodents. **Methods:** Photopic and scotopic electroretinograms (ERG) and retinal histology were obtained from albino guinea pigs aged P1 to P75. **Results:** Photopic ERG responses reached maximal amplitudes at P5 (a- and b-waves), that is 5 days (b-wave) to 10 days (a-wave) earlier than scotopic responses. However, the postnatal gain in b-wave amplitude was significantly ($p < 0.05$) more important for the cone ($73.38 \pm 4.4\%$) signal than for the rod ($15.23 \pm 3.96\%$), suggesting that the rod function is more mature at birth. Similarly, the short latency photopic oscillatory potential (ie: OP₂) reached its maximal value 5 days (P10) earlier than its scotopic equivalent (P15), while the long latency OPs (ie: OP₃, OP₄), reached their maximal values nearly 20 days sooner in scotopic condition. Finally retinal histology revealed a thinning of the retina with age, the latter being most pronounced at the level of the ganglion cell layer (GCL). **Conclusion:** Our results thus confirm that despite its relative maturity at birth (compared to rodents), the retina of newborn albino guinea pigs undergoes significant postnatal maturation modifying its structure as well as its function, albeit not as extensive as that previously documented for altricial animals.

3 Introduction

Most studies that examined the postnatal development of the retina did so in animals, such as cats^{1,2}, dogs^{3,4}, rats^{5,6,7,8}, rabbits^{9,10,11} and mice^{12,13} that are born with an immature visual system and closed eyes (altricial animals). In altricial

animals, the opening of the eyes varies with species (ie: rats: P14; rabbit P8; mice P13) but usually occurs during the second week of life^{8,9,13}. At birth, the retina of altricial animals is usually composed of only two nuclear layers: the inner layer consisting of a row of well differentiated ganglion cells and the outer layer which is formed of undifferentiated neuroblastic cells^{3,14}. This is in sharp contrast with the adult-like retinal cytoarchitecture of newly born precocial animals such as guinea pigs¹⁵, chickens^{16,17}, macaques¹⁸ and humans^{19,20,21}. As a consequence of this retinal immaturity, an electroretinogram (ERG) cannot be recorded at birth from altricial animals. As a rule, the first ERG component recorded is usually a negative wave, which is observed for the first time at the opening of the eye^{4,10,13,22}. The other components of the ERG (e.g.: b-wave and OPs) usually appear a few days later, so that by the end of the first month of life or so, the retina is functionally mature^{2,8,9,13}. In their study on the functional development of the kitten's retina, Hamasaki et al. (1985)¹ showed that it proceeded in three distinct steps, where the first step was characterized by the gradual appearance of the b-wave and the oscillatory potentials (OPs), followed by (second step) a rapid growth in amplitude of the all the ERG components (a- b-waves, OPs) and finally (third step) a slow differentiation of the properties of the retina that spread over several months. Gorfinkel et al. (1988)¹⁰, in their study of the postnatal maturation of the rabbit ERG also reported that the a-wave was the only component recorded at the opening of the eyes (P8) and was followed a few days later by the b-wave and OPs. A similar sequence of event was also reported for newborn rats, albeit delayed by nearly a week since, in the latter, eye opening occurs at P14^{8,14}.

Contrasting with the above well-documented postnatal maturation of the retinal structure and function, to our knowledge only a few studies provided evidence suggesting an equivalent staging of functional (and presumably structural) maturation of the retina in precocial animals, such as lambs^{23,24}, chickens^{16,17}, monkeys¹⁸ and humans²⁵⁻²⁹. As a rule, the retina of precocial animals is well developed at birth since most of the retinal maturation occurs *in utero*, where the synapse formation precedes the formation of the outer segment of

photoreceptors. This explains why an ERG of adult-like morphology is readily recorded at birth^{27,30,31}. However, is this to say that precocial retinas do not demonstrate a postnatal maturation of their structure and function?

In order to address the above, we investigated the postnatal maturation of the retina of albino guinea pigs (up to P75) in order to determine, with the electroretinogram (photopic and scotopic) and retinal histology, whether it showed a significant postnatal maturation process. Our results indicate that both the retinal structure and function (scotopic and photopic) change over time; albeit not to the same extent as that previously demonstrated with altricial animal models. Finally, our results are also in accord, at least with respect to the age at which the maximal amplitude of a-, b-waves and OPs are reached, with the previously reported data on the development of the scotopic receptor³² (a-wave) and postreceptoral³³ (b-wave) retinal function (ERG) of the albino (Dunkin-Hartley) and pigmented (English-Shorthair) guinea pigs taking place from P1 to P60.

4 Material and Methods

4.1 Animals

A total of 50 albinos Hartley Guinea pigs (*Cavia porcellus*, Charles River, St-Constant, Québec) aged between 1 to 75 days old were included in this study, where 20 guinea pigs were followed from P1 to P75 to study the maturation of the electroretinogram only and another 30 (P1: n=5; P5 (n=5); P10 (n=5); P15 (n=5); P30 (n=5); P75 (n=5) were used for histological and electrophysiological purposes. Throughout the study, the guinea pigs were housed in our animal care facility where the luminous environment (12-hours light/dark cycle) was kept at 30 cd.m⁻² (measured at cage level) and the temperature maintained at 23°C. This light intensity was far below that shown to produce retinal degeneration in albino

rodents³⁴. The experimental protocol was reviewed and approved by the McGill University-Montreal Children's Hospital Research Institute animal care committee.

4.2 ERG recordings

Prior to the recording of the electroretinograms, the guinea pigs were dark adapted for a period of 12 hours. Then, under dim red light illumination, their pupils were dilated with drops of 1% cyclopentolate hydrochloride following which they were anesthetized with an intramuscular injection of a mixture of ketamine (85 mg/kg) and xylazine (5 mg/kg). The guinea pigs were then placed in a recording box (ganzfeld-like) of our own design³⁵, which also housed the flash stimulator and background light. Throughout the recording session the temperature inside the recording box remained at 28°C.

A DTL fiber electrode (27/7 X-Static silver coated conductive nylon yarn: Sauquoit Industries, Scranton, PA, USA) was positioned on the surface of the cornea and held in place with a moisturizing solution (2 % methylcellulose: Gonioscopic solution, Alcon Laboratories, Texas, USA). Reference (Grass E5 disc electrode, Grass Instruments, Quincy, MA, USA) and ground (Grass E2 subdermal electrode) electrodes were placed in the mouth and subcutaneously in the neck respectively. Following the preparation of the animal, an extra 10 minutes of dark adaptation was added before the beginning the experiment.

Broadband electroretinograms (bandwidth: 1-1000 Hz, 10 000 X, Grass P511K pre-amplifier) and oscillatory potentials (bandwidth: 100-1000 Hz, 50 000 X, Grass P511K pre-amplifier) were averaged simultaneously using the Biopac MP 100 Acknowledge system (Biopac MP 100 WS, BIOPAC System Inc., Goleta, CA, USA). Scotopic responses were evoked to flashes of white light (Grass PS 22 Photostimulator, Grass Instruments, Quincy, MA, USA), spanning

over a 6-log unit range (in 0.3 log unit increments) with a maximal intensity of 0.6 log cd.sec.m⁻² in energy. Three (3) to five (5) responses were averaged depending on the stimulus intensity used to produce the response. In order to avoid the conditioning flash effect previously reported to affect dark-adapted OPs^{36,37}, an inter-stimulus interval (ISI) of 9.60 seconds was used for all scotopic recordings. Following the recording of the scotopic ERGs, a background light of 30 cd.m⁻² was turned on. After a period of 20 minutes of light adaptation, cone-mediated ERGs (average of 20 flashes; ISI: 0.96 seconds) were evoked to flashes of white light of 0.9 log cd.sec.m⁻².

ERG components were measured according to a method previously described³⁸. Briefly, the amplitude of the a-wave was measured from baseline at flash onset to the first negative trough and the amplitude of the b-wave was measured from the most negative trough to the peak of the b-wave. However, while in most instances the most negative trough did correspond to the peak of the a-wave, scotopic responses evoked to the brightest flashes generated a short latency OP whose trough culminated below the a-wave (see figure 4). We have arbitrarily decided to include this component in the measurement of the b-wave, a choice that explains that while we are illustrating scotopic ERG responses with negative morphologies, the amplitude measurements we report (figures 4-7) always present the resulting responses with b-wave amplitudes larger than a-wave amplitudes. Peak times were measured from the flash onset to respective peaks. Scotopic luminance-response function curves were also obtained from our data from which V_{\max} was calculated. The latter (V_{\max}), which represents the maximal (pure) rod ERG response, is defined as the ERG signal where a clear a-wave is first noticed³⁹. Oscillatory potentials were also measured. OP₁₋₂ was measured from baseline to peak, while the amplitudes of the remaining OPs were measured from preceding trough to peak. Their amplitudes were also summated (SOP= OP₁₋₂+OP₃+OP₄) to yield the photopic and scotopic (mixed rod-cone) SOPs values. Again, OP peak times were also measured from flash onset to individual peaks.

4.3 Histology

Retinal histology was performed on guinea pigs aged 1, 5, 10, 15, 30 and 75 days old. At the end of the ERG recording session, the animals were euthanized with carbon dioxide inhalation and eyes were excised and immersed three hours in 3.5% glutaraldehyde for fixation. Lenses were removed and the eyes were kept in glutaraldehyde solution (3.5%) for another 12 hours. The following day, the anterior segment of each eye was removed and the retina, still attached to the choroids, was cut into sections (central retina) of 2mm wide by 4 mm long using the optic nerve as the reference. The retinal sections were immersed in a solution of osmium (OsO_4) 4% with 0.1 M phosphate buffer for one hour and then rinsed in the 0.1 M phosphate buffer. Sections were then gradually dehydrated in ethanol baths going from 50 to 100% in 5 steps and finally in propylene oxide for 10 minutes. Retinal sections were embedded in resin (Durcupan® ACM Fluka epoxy resin kit, Sigma-Aldrich, Canada) and stored at 58°C for 48 hours. Once polymerization was completed, the retinas were cut (Leica EM UC6 microtome, Leica microsystem, USA) in ultra thin sections of 0,7 μm . Cuts were made perpendicularly to the retina by orienting the blocks until achieving sections longitudinal to the photoreceptors. Retinal sections were mounted on slides and stained with toluidine blue. Pictures were taken with a Zeiss microscope (Zeiss Axiophot, Zeiss microscope, Germany: 40X) attached to a digital camera (RR slider spot, Diagnostics instruments inc., Germany). Thickness of the different retinal layers was determined with a calibrated grating inserted in the ocular of the microscope.

Finally, all values are reported as mean \pm 1 standard deviation (SD). Statistical significance was determined using a one factor ANOVA for related (repeated measures) samples. A Tukey's honestly significant difference analysis was performed as the pairwise comparison test ($p < 0.05$).

5 Results

5.1 Maturation of the photopic ERG

During the course of maturation (from postnatal day 1 to 75), all the ERG components, including the OPs, rapidly increased in amplitude to a maximal value and then slowly decreased until P75, while the peak times accelerated from P1 to P75 (figures 1, 2, 3). More specifically, the amplitude of the a-wave increased significantly ($p < 0.05$) from P1 ($17.37 \pm 7.00 \mu\text{V}$) to P5 ($31.03 \pm 5.90 \mu\text{V}$) and then gradually decreased to reach at P75 a value ($18.95 \pm 3.55 \mu\text{V}$) not significantly ($p > 0.05$) different from that measured at P1 (figures 1a, 1c, 2a). In contrast, its peak time remained stable from birth ($13.77 \pm 1.27 \text{ ms}$) to P35 (13.10 ± 2.10 ; $p > 0.05$) where it gradually accelerated until adulthood (P75: $10.95 \pm 1.5 \text{ ms}$; $p < 0.05$) (figures 1a, 1c, 3a). Similarly, the amplitude of the b-wave increased from P1 ($64.30 \pm 15.69 \mu\text{V}$) to P5 ($113.45 \pm 20.97 \mu\text{V}$; $p < 0.05$) following which it decreased significantly ($p < 0.05$) to $74.06 \pm 18.75 \mu\text{V}$ at P15 and remained stable until P75 ($71.35 \pm 12.62 \mu\text{V}$; $p > 0.05$). Of interest, the amplitude of the b-wave reached at P75 is not significantly ($p > 0.05$) different from that measured at P1 (figures 1a, 1c, 2a), while, the peak time of the b-wave at P75 ($31.92 \pm 1.48 \text{ ms}$) is significantly ($p < 0.05$) faster than that measures at P1 ($35.90 \pm 0.71 \text{ ms}$) (figures 1a, 1c, 3a).

Retinal maturation also modified the amplitudes and peak times of the oscillatory potentials, as evidenced with the SOPs variable (figures 1b, 1d, 2b, 3b). Analysis of individual OPs revealed that from birth to adulthood the amplitude of OP₂ increased rapidly from P1 to P10 ($6.10 \pm 1.82 \mu\text{V}$; $11.60 \pm 1.64 \mu\text{V}$; $p < 0.05$) (figures 1b, 1d, 2b). This was followed by a significant ($p < 0.05$) decrease in amplitude until P20 ($7.40 \pm 1.21 \mu\text{V}$). Finally, from P20 to P30, the amplitude of

OP₂ increased significantly ($p < 0.05$) to reach $10.11 \pm 1.41 \mu\text{V}$ and remained at this level until P75 ($10.14 \pm 2.64 \mu\text{V}$; $p > 0.05$), the age of the oldest guinea pigs included in this study (figures 1b, 1d, 2b). Compared to OP₂, OP₃ and OP₄ adopted a slightly different maturation pattern. The amplitude of OP₃ grew almost linearly from $3.02 \pm 1.15 \mu\text{V}$ (P1) to a maximum of $6.21 \pm 1.32 \mu\text{V}$ ($p < 0.05$) at P35 (figures 1b, 1d, 2b) and remained at that level until adulthood (P75: $6.15 \pm 1.01 \mu\text{V}$; $p > 0.05$). Similarly, the amplitude of OP₄ also increased significantly ($p < 0.05$) from $3.47 \pm 1.31 \mu\text{V}$ (P1) to $5.12 \pm 1.85 \mu\text{V}$ reached at P35 and remained at this value until P75 ($4.62 \pm 1.46 \mu\text{V}$; $p > 0.05$) (figures 1b, 1d, 2b). Thus, irrespective of the age of the guinea pigs, OP₂ was always the largest OP followed by OP₃ and then OP₄. OP₂ was also that which showed the most prominent amplitude change with age.

As indicated earlier, retinal maturation also modified the peak times of the OPs. As a rule, the timing of all the OPs (OP₂, OP₃, OP₄) accelerated by nearly 5 msec with age [$20.40 \pm 0.84 \text{ ms}$ (P1) to $15.95 \pm 0.98 \text{ ms}$ (P75) ($p < 0.05$) for OP₂; $26.77 \pm 1.14 \text{ ms}$ (P1) to $22.99 \pm 0.98 \text{ ms}$ (P75) ($p < 0.05$) for OP₃; $35.45 \pm 1.37 \text{ ms}$ (P1) to $29.46 \pm 0.99 \text{ ms}$ (P75) ($p < 0.05$) for OP₄] (figures 1b, 1d, 3b).

5.2 Maturation of the scotopic ERG

Scotopic electroretinograms recorded from guinea pigs are very different from those recorded from other rodents, especially the ERGs evoked to the brightest flashes^{32,33,38,40} which present with a negative (e.g. a-wave larger than b-wave) morphology (figure 4). This is best illustrated at figure 4, where a representative scotopic ERG intensity-response function is shown, at figure 5 where the group data is reported and at figure 6, where the maturation of ERGs is illustrated with responses evoked to key intensities namely: the rod Vmax (-2.4

log cd.sec.m⁻²), the intensity where the ERG become of negative morphology (-0.9 log cd.sec.m⁻²) and the intensity where the ERG is of fully negative shape. In responses to the dimmer flashes of light, the scotopic ERG is essentially formed of a b-wave, the amplitude of which increasing regularly with progressively brighter flashes to reach a maximal amplitude (V_{max}), usually attained at a flash intensity between -2.4 and -2.7 log cd.sec.m⁻² (figures 4, 5b). Brighter flashes will gradually yield the typical negative ERG waveform (approximately -0.9 log cd.sec.m⁻²) with a well-developed a-wave and a b-wave whose amplitude never crosses the baseline. It is also at that intensity that the three major OPs (OP₁₋₂, OP₃, OP₄), seen as small oscillations on the ascending limb of the b-wave, are reproducibly recorded for the first time. Finally, at the brightest scotopic intensity (0.6 log cd.sec.m⁻²) we used, the ERGs retained their negative morphologies with four oscillatory potentials (OP₁, OP₂, OP₃, OP₄) now observed on the rising phase of the b-wave as well as in the filtered version of the ERG (figures 4, 6a-6d). At figure 6 are illustrated representative ERGs (from 2 normal guinea pigs) evoked to key stimulus intensities showing that, irrespective of age, the typical morphology of the scotopic ERG is retained, albeit the increasing prominence of the OPs with age as we will see later.

Irrespective of age, the a-wave was first identified in responses evoked to the -2.4 log cd.sec.m⁻² flash, compared to -4.8 log cd.sec.m⁻² for the b-wave. Figure 5 shows that the amplitude of the a-wave grows almost linearly from -2.4 to 0.6 log cd.sec.m⁻², without showing significant age related differences. The latter luminance-response function curve is strikingly different from that obtained with b-wave measurements as shown in figure 5b. First, irrespective of stimulus intensity, the b-wave reached its maximal amplitude at P10 and its lowest at P75 (figure 5b). Secondly, irrespective of age, the intensity response function of the scotopic b-wave adopted a unique behavior with an initial increase in amplitude from threshold to rod V_{max} reached between -2.4 and -2.7 log cd.sec.m⁻² followed by a gradual decline to reach a minimal amplitude at intensity -1.2 log cd.sec.m⁻². The b-wave then resumed its gradual growth in amplitude with brighter flashes.

Similar to what we reported above for the photopic responses, individual components of the scotopic ERG did not mature at the same rate. This is best exemplified at figures 7 and 8 where we present the maturation curves derived from the amplitude and peak time measurements of the rod V_{max} (scotopic b-wave), the mixed (rod-cone mediated) a- and b-waves and corresponding OPs. As exemplified in figure 7a, the amplitude of the rod V_{max} increased from $86.52 \pm 15.43 \mu\text{V}$ at P1 to a maximum of $96.21 \pm 11.60 \mu\text{V}$ ($p > 0.05$) at P10 following which there was a gradual decrease to reach $79.50 \pm 15.51 \mu\text{V}$ ($p < 0.05$) at P75. This age-dependent amplitude change was accompanied by an abrupt speeding of the peak time of the (V_{max}) b-wave from P1 to P10 (76.24 ± 3.01 ms to 54.57 ± 3.30 ms; $p < 0.05$) which then stabilized (53.99 ± 3.15 ms; $p > 0.05$) until P75 (figure 8a). Similarly, the amplitude of the mixed (rod-cone mediated) a-wave ($p > 0.05$) increased from $100.95 \pm 12.32 \mu\text{V}$ (P1) to a maximum of $117.23 \pm 26.49 \mu\text{V}$ (P15) followed by a gradual decline to $90.02 \pm 16.96 \mu\text{V}$ ($p < 0.05$) measured at P75. In comparison, the amplitude of the mixed (rod-cone mediated) b-wave increased from $114.52 \pm 17.62 \mu\text{V}$ (P1) to a maximum of $135.82 \pm 14.42 \mu\text{V}$ ($p < 0.05$) at P10 followed by a biphasic reduction with an initial rapid phase to $111.21 \pm 10.59 \mu\text{V}$ ($p < 0.05$) at P20 and a subsequent slower phase to $99.49 \pm 11.56 \mu\text{V}$ ($p > 0.05$) measured at P75 (figure 7a). In comparison, age-dependent peak time changes were more linear. From P1 to P75, the timing of the mixed (rod-cone mediated) a-wave progressively shortened from 12.68 ± 1.09 ms to 10.99 ± 2.10 ms ($p < 0.05$) while that of the mixed (rod-cone mediated) b-wave shortened from 43.17 ± 2.94 ms (P1) to 39.59 ± 1.27 ms (P75) ($p < 0.05$) (figure 8a).

The scotopic oscillatory potentials also demonstrated maturational changes in amplitude and timing as illustrated at figures 7 and 8. The effect of maturation on the ERG a-wave, b-wave and OPs are also compared in the tracings shown at figure 6, where relatively immature OPs (compared to a- and b-waves) are recorded at P1. Further analysis revealed that the short latency OP_{1-2} and OP_3

reached maximal amplitude at P15 (OP₁₋₂: $26.92 \pm 6.36 \mu\text{V}$; OP₃: $35.84 \pm 8.52 \mu\text{V}$) that is 5 days later than OP₄ ($12.78 \pm 4.40 \mu\text{V}$ at P10) (figure 7b). Of interest, irrespective of age, OP₃ was always the largest of all OPs. Similarly the timing of OP₁₋₂, OP₃ and OP₄ decreased regularly from P1 to P75 [from $18.03 \pm 1.84 \text{ ms}$ to $14.99 \pm 2.35 \text{ ms}$ ($p < 0.05$) for OP₁₋₂; from $25.90 \pm 1.06 \text{ ms}$ to $21.86 \pm 2.65 \text{ ms}$ ($p < 0.05$) for OP₃ and from $34.48 \pm 1.94 \text{ ms}$ to $30.48 \pm 2.99 \text{ ms}$ ($p < 0.05$) for OP₄] (figure 8b).

5.3 Maturation of the retinal structure

Maturation of the retinal function was also accompanied by a significant age-dependent thinning of the retina as shown at figures 9 and 10. From P1 to P75, the outer nuclear layer (ONL) lost more than 22% in thickness (P1: $32.17 \pm 2.43 \mu\text{m}$; P75: $25.21 \pm 1.37 \mu\text{m}$; $p < 0.05$) compared to more than 40% for the GCL (P1: $24.02 \pm 3.64 \mu\text{m}$; P75: $14.03 \pm 1.46 \mu\text{m}$; $p < 0.05$), 24% for the outer plexiform layer (OPL) (P1: $6.43 \pm 0.83 \mu\text{m}$; P75: $4.86 \pm 0.95 \mu\text{m}$; $p < 0.05$), 20% for the inner nuclear layer (INL) (P1: $25.58 \pm 0.93 \mu\text{m}$; P75: $20.35 \pm 2.26 \mu\text{m}$; $p < 0.05$) and 7.5% for the inner plexiform layer (IPL) (P1: $26.79 \pm 2.00 \mu\text{m}$; P75: $24.79 \pm 0.64 \mu\text{m}$; $p < 0.05$). In contrast, during the same period of time, the outer and inner segment of the photoreceptors lengthened by more 20% (P1: $11.25 \pm 1.20 \mu\text{m}$; P75: $14.31 \pm 1.67 \mu\text{m}$; $p < 0.05$) and 18% (P1: $10.89 \pm 1.03 \mu\text{m}$; P75: $13.13 \pm 1.30 \mu\text{m}$; $p < 0.05$) respectively, while there was no significant changes observed for the retinal pigment epithelium (P1: $5.54 \pm 0.64 \mu\text{m}$; P75: $5.14 \pm 0.59 \mu\text{m}$; $p > 0.05$).

6 Discussion

Like all other precocial animals described in the literature, guinea pigs are also born with nearly adult-like photopic and scotopic ERGs and that irrespective

of the component considered. Furthermore, while components of the photopic (cone-mediated) electroretinograms reached their peak amplitudes earlier than scotopic (rod-mediated) ERGs, the cone ERG gained significantly more amplitude in the few days that followed birth when compared to rod ERG, suggesting that guinea pigs are essentially born with a nearly mature rod function. Finally, these ERG changes were also accompanied by subtle, but significant, age-dependent cytoarchitectural reorganization of the retinal tissue affecting nearly all layers. It is worth mentioning, as previously shown by Bui et al. (1999), that the age-related changes in retinal structure and function we report were not the result of the concomitant increase in size of the eye as a result of the normal growth of the guinea pigs. Our results thus suggest that despite its precocial (born with eyes open) nature, the retina of the albino guinea pig does undergo significant postnatal maturation of its structure and function, albeit not to the same extent as that previously documented for altricial animals such as rodents^{5,6,7,8,12,13}. To the best of our knowledge, this study is the first that compared the maturation of the entire retinal structure (cellular and plexiform layers) and function (scotopic and photopic ERG a- and b-waves and individual OPs) in the same cohort of guinea pigs.

Our results are in accord with previous studies reporting the postnatal maturation of retinal function in other precocial animals, such as human^{25,26,27,28,29,41}, primates¹⁸, lamb²³, sheep²⁴, chicken^{16,17} and guinea pigs^{32,33}, where the neural differentiation and establishment of synaptic connections within the retina occur mostly *in utero*^{15,18,42,43,44}, explaining the almost adult-like ERG at birth^{16,17,24,25,27,32,33,44}. This is however in sharp contrast with reports demonstrating a significant maturation of the retinal signal in altricial animals, such as rodents^{8,45,46}, rabbits^{9,10,11,47}, cats^{1,2} and dogs^{3,4} where a significant maturation of the retina takes place after birth and the first ERG manifestation is usually obtained at eye opening (normally during the second week of life). However, notwithstanding the fact that guinea pigs are born with an ERG response of adult-like morphology^{32,33,44,48}, all its components (e.g. a- and b-waves

and OPs) do nonetheless show age-dependent amplitude and peak time changes suggestive of a maturation process, albeit not as marked as in altricial animals. Bui et al. (1999) and Vingry et al. (2001) also reported that although guinea pigs had scotopic ERGs of adult like morphology at birth, there was nonetheless significant postnatal maturation of the P3, P2 and OP components. Their study also revealed that the maturation of the a-wave (P3) peaked at around P12 compared to P10-P12 for P2 and the OPs, values that are quite similar to ours. Of interest, in photopic responses, the a-wave along with the late OPs (e.g.: OP₃, OP₄) only demonstrated small amplitude changes with time compared to the more pronounced amplitude changes noted for the b-wave and the short latency OP₂ (figure 2). The latter might support the claim of a different retinal origin for the early and late OPs⁴⁹⁻⁵⁴. Our results are in line with previous studies also reporting a postnatal maturation of the photopic ERG in human infants^{26,27,29,41}. Given our previous demonstration⁵⁵ of significant morphological and functional similarities between the photopic ERGs of guinea pigs and human, our results could also suggest that, compared to other rodents such as rats or mice, the newborn guinea pigs could represent a better animal model to study the normal postnatal retinal maturation in the human infant.

Scotopic ERGs obtained from guinea pigs are different from those observed in other species, including rodents. While in altricial animals, progressively brighter flashes will generate ERG responses of increasing amplitudes, in guinea pigs, this quasi-linear relationship could only be observed in responses evoked to the dimmer flashes of the intensity-response function (figures 4, 5b). In fact, with brighter flashes the scotopic ERG of the guinea pig became negative and that irrespective of age (figure 5b) giving to the resulting intensity-response curves an unexpected biphasic presentation. Vingry et al (2001) also reported a similar two-limbed scotopic intensity-response function in guinea pigs and suggested that it could reflect the rod-cone interactions in the guinea pig's retina. To our knowledge such a negative morphology, previously reported by others as representative of the guinea pigs scotopic ERGs^{32,33}, has never before

been documented as the normal feature of other animal species. It is well documented that some form of human retinal disorders, mostly involving the rod pathway, will generate at brighter flash intensities scotopic ERGs with negative morphologies⁵⁶⁻⁶².

Our results further revealed that the photopic a- and b-waves reached their peak amplitudes earlier (ie: a-wave: 10 days faster; b-wave: 5 days faster) than the corresponding scotopic ERG waves. This is in accord with Spira (1975)¹⁵ who reported that during the initial stages of retinal development *in utero*, the cones developed faster than the rods in the guinea pig. Of interest however the postnatal gain in amplitude was significantly larger for cones compared to rod responses, suggesting that guinea pigs are born with a more mature rod signal. The latter contrast with recent results suggesting that human infants are born with a peripheral cone function relatively more mature than rod⁴¹. Similarly, when considered as a whole (SOPs variable), photopic OPs reached their peak amplitude between P10 and P15 compared to P15 for the scotopic OPs. However, as reported above for the b-wave, the gain in amplitude for the cone SOPs (approximately 40% between P1 and P15) is significantly larger than that measured for the rod SOPs (approximately 22% between P1 and P15), pointing again to a more mature rod function at birth. A similar rod-cone maturational discrepancy was also shown in other species. For example, El Azasi and Wachtmeister (1990)⁶ also reported that scotopic OPs in rats appeared to mature earlier than photopic OPs. Similarly, Jacobson and Ikeda (1987)² reported that the implicit time of the rod generated b-wave in cats reached adult values between the 6 and 7 weeks of life, compared to 11-12 weeks for the cone b-wave. The morphology of the rod and cone b-waves, however, reached maturity (adult like) simultaneously (ie: 4.5 weeks). A slightly different picture is seen in the rabbit retina where the photopic b-wave matures one week faster than the scotopic b-wave^{9,10}.

In the method section, we indicate that we only controlled the temperature of the animal's environment, not that of the animal per se. Could this have biased

our results? For example, Kong and Gouras⁶³ reported a significant 60% drop in b-wave amplitudes (maximal ERG response from 1000 uV to 400 uV) when the body temperature of a mouse was progressively cooled from 37 to 30°C, representing a rate of decline of nearly 100 uV/°C, a value slightly larger than the 30% decline (estimated from their figure 5: 650 uV at 37 °C to 450 uV at 30 °C) in ERG amplitude reported by Mizota and Adachi-Usami⁶⁴ using a similar approach and same animal model. We also examined the effect of temperature on the ERG⁵². In our study, the eyeball of a rabbit was wrapped with a cooling tube filled with running water at 18°C. After more than 10 minutes of direct contact between the cold tubing and the sclera, the amplitude of the ERG a- and b-waves were reduced to 67% and 90% of control respectively.

Given that the present study involves gradually larger animals, one would intuitively expect younger (and thus of smaller body mass) animals to be more prone to a cooling effect compared to older (and thus of a larger body mass) ones. Consequently, should there have been a temperature contribution to our results; the ERG of young guinea pigs should be of lower voltages compared to that of older guinea pigs. Recordings on the first day were generally low and had longer peak times than those in more mature animals. However, there was no consistent trend as animals become larger. For example, for the photopic ERG the largest ERGs (a- and b-waves) were obtained from 5 day old specimens and the amplitude of the b-wave at P1 is not significantly different from that measured at P30 or beyond. As indicated in the method section, our recording system³⁵ is quite different from that used elsewhere; the animal being literally housed in a small (light-proof and almost air-tight) ganzfeld (L: 60 cm, W: 50 cm, H: 22 cm) and not in an open environment, something that would definitely accelerated body heat exchange. The animals lie on their side facing the light source (background and flash). The distance separating the light source from the animal is 10 cm (in our most recent version the floor height can be adjusted mechanically to meet this requirement). At this distance the background light provides a radiating source of heat (during photopic recordings) that effectively maintains the

ambient temperature at 28 °C and therefore most probably efficiently replace a heating pad; a claim that we tested by comparing, for one hour, the variation in rectal temperature (measured with a Cole Parmer thermistor thermometer model 8402-10) of anesthetized guinea pigs placed in room air or inside our recording box. Results showed a decline in rectal temperature of 2.1 °C after one hour (1.1 °C after the first 20 minutes) at room air compared to 0.6 °C (0 °C after the first 20 minutes) when the guinea pig was kept inside our recording device, suggesting that our recording apparatus did limit body heat loss. We also examine if the 0.6 °C drop in body temperature had a measurable impact on the amplitude of the photopic ERG. Data analysis revealed a 16% variation in b-wave amplitude (3% after 40 minutes) throughout the 60 minutes recording. The largest b-wave amplitude was measured after 10 minutes of anesthesia and the lowest one after 60 minutes. Interestingly, a similar variation in b-wave amplitude was also noted when the guinea pig was kept warm (at 37 °C) with a heating pad (Harvard Apparatus, Homeothermic Blanket System). However, this time the largest amplitude was measured after 60 minutes of anesthesia and the lowest one after 20 minutes.

It is important to note here that our ERG protocol starts with the scotopic ERG; the guinea pigs having been dark-adapted overnight. The scotopic recording takes approximately 15 minutes following which the background light is opened. The photopic portion of our protocol takes approximately 25 minutes or so since we allow 20 minutes of light adaptation prior to the recording of the cone ERG in order to avoid the light adaptation phenomena. Therefore, for most of the recording procedure, the animal will benefit from the radiating source of heat provided by the background light. Consequently, gradual body heat loss was probably not a problem in our experiments.

Maturation of the retinal function in guinea pigs was also accompanied by a significant modification of the cytoarchitecture of the retina. Changes included an increase in length of the inner and outer segments of the photoreceptors along

with a thinning of all the other cellular layers, which was most significant for the ganglion cell layer; changes similar to those recently reported by Loeliger and Rees (2004)⁶⁵. The age-dependent thinning of the INL, where the alleged generators of the b-wave (e.g. bipolar cells) are found, would therefore explain the concomitant attenuation of the b-wave of the ERG and corresponding OPs with maturation. Similarly, given that maturation also reduced the thickness of the GCL, it would not be surprising to find an equivalent attenuation in the amplitude of the visual evoked potential (VEP) as the guinea pig aged. In their study on the maturation of the guinea pigs, Loeliger and Rees (2005)⁶⁵ also demonstrated an age-dependent thinning of the nuclear layers as a result of the lateral expansion of the retina that was accompanied by the lengthening of photoreceptor segments.

In summary, although guinea pigs are born with a mature visual system, retinal structure and function will undergo significant modification as the newborn ages. However, these age-dependent changes are closer in magnitude to what is reported for humans or primates compared to what is reported for animals born with a more immature visual system such as rodents (mice and rats). Given that the ERG of albino guinea pigs, especially the photopic ERG, was also previously shown to share features common to the human cone ERG⁵⁵, we believe that it should be considered as a valid alternative whenever an animal model of the human ERG is considered.

7 References

1. Hamasaki DI, Maguire GW (1985) Physiological development of the kitten's retina: An ERG study. *Vision Res* 25: 1537-1543.
2. Jacobson SG, Ikeda H, Ruddock K (1987) Cone-mediated retinal function in cats during development. *Doc Ophthalmol* 65: 7-14.
3. Gum GG, Gelatt KN, Samuelson DA (1973) Maturation of the retina of the canine neonate as determined by electroretinography and histology. *Am J Vet Res* 45: 1166-1171.
4. Kirk GR, Boyer SF (1973) Maturation of the electroretinogram in the dog. *Exp Neurol* 38: 252-264.
5. El Azazi M, Wachtmeister L (1991) The postnatal development of the oscillatory potentials of the electroretinogram II: photopic characteristics. *Acta Ophthalmol* 69: 6-10.
6. El Azazi M, Wachtmeister L (1990) The postnatal development of the oscillatory potentials of the electroretinogram: Basic characteristics. *Acta Ophthalmol* 68: 401-409.
7. Kurihara H (1977) Developmental process of ERG of the albino rat. *Jpn J Ophthalmol* 81: 1313-1320.
8. Braekevelt C, Hollenberg M (1970) The development of the retina of the albino rat. *Am J Anat* 127: 281-302.
9. Gorfinkel J, Lachapelle P (1990) Maturation of the photopic b-wave and oscillatory potentials of the electroretinogram in the neonatal rabbit. *Can J Ophthalmol* 25: 138-144.

10. Gorfinkel J, Lachapelle P, Molotchikoff S (1988) Maturation of the electroretinogram of the neonatal rabbit. *Doc Ophthalmol* 69: 237-245.
11. Sanada T (1962) Study on the ERG on suckling rabbits. Report I. Development of the ERG (in dark adaptation). *Jpn J Ophthalmol* 66: 1430-1436.
12. Gresh J, Goletz PW, Crouch RK, Rohrer B (2003) Structure-function analysis of rods and cones in juvenile, adult, and age C57BL/6 and Balb/c mice. *Vis Neurosci* 20: 211-220.
13. Bonaventure N, Karli P (1968) Maturation des potentiels ERG et évoqués visuels chez la souris. *C R Soc Biol (Paris)* 161: 553-555.
14. Weidman TA, Kuwabara T (1968) Postnatal development of the rat retina. *Arch Ophthalmol* 79: 470-484.
15. Spira AW (1975) In utero development and maturation of the retina of a non-primate mammal: a light and electron microscopic study of the guinea pig. *Anat Embryol* 14: 279-300.
16. Ookawa T (1971a) The onset and development of the chick electroretinogram: the a- and b-waves. *Poult Sci* 50: 601-608.
17. Ookawa T (1971b) Further studies on the ontogenetic development of the chick electroretinogram. *Poult Sci* 50: 1185-1190.
18. Smelser GK, Ozanics V, Fayborn M, Sagun D (1974) Retinal synaptogenesis in the primate. *Invest Ophthalmol Vis Sci* 13: 340-361.
19. Spira AW, Hollenberg MJ (1973) Human retinal development: Ultrastructure of the inner retinal layers. *Dev Biol* 31: 1-21.

20. Hollenberg JJ, Spira AW (1973) Human retinal development: Ultrastructure of the outer retina. *Am J Anat* 137: 357-386.
21. Hollenberg JJ, Spira AW (1972) Early development of the human retina. *Can J Ophthalmol* 7: 472-491.
22. Fulton AB, Graves AL (1980) Background adaptation in developing rat retina: An electroretinographic study. *Vision Res* 20: 819-826.
23. Woods JR, Parisi V, Coppes V, Brooks DE (1983) Maturation sequence of the visual system: Serial measurements of visual evoked potential and electroretinogram in the healthy neonatal lamb. *J Obstet Gynecol* 145: 738-743.
24. Knave B, Moller A, Persson HE (1972) A component analysis of the electroretinogram. *Vision Res* 12: 1669-1684.
25. Horsten GPM., Winkelman JE (1960) Development of the ERG in relation to histological differentiation of the retina in man and animals. *Arch Ophthalmol* 63: 232-242.
26. Mets MB, Smith VC, Pokorny J, Pass A (1995) Postnatal retinal development as measured by the electroretinogram in premature infants. *Doc Ophthalmol* 90: 111-127.
27. Rodriguez-Saez E, Otero-Costas J, Moreno-Montanes J, Relova JL (1993) Electroretinographic changes during childhood and adolescence. *Eur J Ophthalmol* 3: 6-12.
28. Breton ME, Quinn GE, Schuller AW (1995) Development of electroretinogram and rod phototransduction response in human infants. *Invest Ophthalmol Vis Sci* 36: 1588-1602.

29. Westall CA, Panton CM, Levin AV (1996) Time courses for maturation of electroretinogram responses from infancy to adulthood. *Doc Ophthalmol* 96: 355-379.
30. Hamilton R, Dudgeon J, Gradnam MS, Mactier H (2005) Development of the electroretinogram between 30 and 50 weeks after conception. *Early Hum Dev* 81: 461-464.
31. Breceelj J (2003) From immature to mature pattern ERG and VEP. *Doc Ophthalmol* 107: 215-224.
32. Bui BV, Vingrys AJ (1999) Development of receptor responses in pigmented and albino guinea pigs (*Cavia porcellus*). *Doc Ophthalmol* 99: 151-170.
33. Vingrys AJ, Bui BV (2001) Development of postreceptor function in pigmented and albino guinea pigs. *Vis Neurosci* 18: 605-613.
34. Semple-Roland S, Dawson W (1987) Retinal cyclic light damage threshold for albino rats. *Lab ani Sci* 37: 289-298.
35. Lachapelle P, Blain L (1990a) A new speculum electrode for electroretinography. *J Neurosci Methods* 32: 245-249.
36. Lachapelle P, Benoit J, Clain L, Guité P, Roy M (1990b) The oscillatory potentials in response to stimuli of photopic intensities delivered in dark adaptation: an explanation of the conditioning effect. *Vision Res* 30: 503-513.
37. Peachey N, Alexander R, Fishman G (1987a) Rod and cone system contribution to oscillatory potentials: an explanation for the conditioning effect. *Vision Res* 27: 859-866.

38. Racine J, Behn D, Simard E, Lachapelle P (2003) Spontaneous occurrence of a potentially night blinding disorder in guinea pigs. *Doc Ophthalmol* 107: 59-69.
39. Hébert M, Lachapelle P, Dumont M (1996) Reproducibility of electroretinograms recorded with DTL electrodes. *Doc Ophthalmol* 91:333-42.
40. Jutras S, et al. *IOVS* 1997; 38: ARVO Abstract S884.
41. Hansen RM, Fulton AB (2005) Development of the cone ERG in infants. *Invest Ophthalmol Vis Sci* 46: 3458-3462.
42. Winkelman J, Horsten G (1962) The ERG of premature and full term born infants during their first days of life. *Ophthalmologica* 143: 92-101.
43. Shipley T, Anton M (1964) The human electroretinogram in the first day of life. *J Ped* 65: 733-739.
44. Huang J, Wyse J, Spira A (1990) Ontogenesis of the electroretinogram in a precocial mammal, the guinea pig (*Cavia Porcellus*). *Comp Biochem Physiol* 95A: 149-155.
45. Webster MJ, Rowe MH (1991) Disruption of developmental timing in the albino rat retina. *J Comp Neurol* 307: 160-174.
46. Weisse I (1995) Changes in the aging rat retina. *Ophthalmic Res* 27: 154-163.
47. Stone J, Egan M, Rapaport DH (1985) The site of commencement of retinal maturation in the rabbit. *Vision Res* 25: 309-317.
48. Legein C, Van Hof M (1970) The effect of light deprivation on the electroretinogram of the guinea pig. *Pflugers Arch Gen Physiol* 318: 1-6.

49. Kojima M, Zrenner E (1978) Off-components in response to brief light flashes in the oscillatory potential of the human electroretinogram. *Graefe Archiv Ophthalmol* 206: 107-120.
50. King-Smith PE., Loffing DH, Jones R (1986) Rod and cone ERGs and their oscillatory potentials. *Invest Ophthalmol Vis Sci* 27: 270-273.
51. Lachapelle P (1990c) A possible contribution of the optic nerve to the photopic oscillatory potentials. *Clin Vision Sci* 5: 421-426.
52. Lachapelle P, Benoit J, Guité P (1996) The effect of in vivo retinal cooling on the electroretinogram of the rabbit. *Vision Res* 36: 339-344.
53. Lachapelle P, Little JM, Polomeno RC (1983) The photopic electroretinogram in congenital stationary night blindness with myopia. *Invest Ophthalmol Vis Sci* 24: 442-450.
54. Lachapelle P, Rousseau S, McKerral M, Benoit J, Polomeno RC, Koenekoop RK, Little JM (1998) Evidence supportive of a functional discrimination between photopic oscillatory potentials as revealed with cone and rod mediated retinopathies. *Doc Ophthalmol* 95: 35-54.
55. Racine J, Joly S, Rufiange M, Rosolen S, Lachapelle P (2005) The photopic ERG of the albino guinea pig (*Cavia porcellus*): A model of the human photopic ERG. *Doc Ophthalmol* 110: 67-77.
56. Miyake Y, Horiguchi M, Suzuki S, Kondo M, Tanikawa A (1996) Electrophysiological findings in patients with Oguchi's disease. *Jpn J Ophthalmol* 40: 511-519.

57. Miyake Y, Yagasaki K, Horiguchi M (1986) Congenital stationary night blindness with negative electroretinogram. *Arch Ophthalmol* 104: 1013-1020.
58. Peachey NS, Fishman GA, Kilbride PE, Alexander KR, Keehan KM, Derlacki DJ (1990) A form of congenital stationary night blindness with apparent defect of rod phototransduction. *Invest Ophthalmol Visl Sci* 31: 237-246.
59. Peachey NS, Fishman GA, Derlacki DJ, Brigell M (1987b) Psychophysical and electroretinographic findings in X-linked juvenile retinoschisis. *Arch Ophthalmol* 105: 513-516.
60. Berson EL, Lessel S (1988) Paraneoplastic night blindness with malignant melanoma. *Am J Ophthalmol* 106: 307-311.
61. Tremblay F, Laroche RG, Becker I (1995) The electroretinographic diagnosis of the incomplete form of congenital stationary night blindness. *Vision Res* 35: 2383-2393.
62. Kimura A, Nemoto H, Nishimiya J, Yuasa T, Hiroko Y (2004) Spinocerebellar degeneration with negative electroretinogram: dysfunction of the bipolar cells. *Doc Ophthalmol* 108: 241-247.
63. Kong J, Gouras P. (2003) The effect of body temperature on murine electroretinogram. *Doc Ophthalmol* 106: 239-242.
64. Mizota A, Adachi-Usami E. (2002) Effect of body temperature on electroretinogram of mice. *Invest Ophthalmol Vis Sci* 43: 3754-3757.
65. Loeliger M, Rees S (2005) Immunocytochemical development of the guinea pig retina. *Exp Eye Res* 80:1-13.

8 Figures and legends

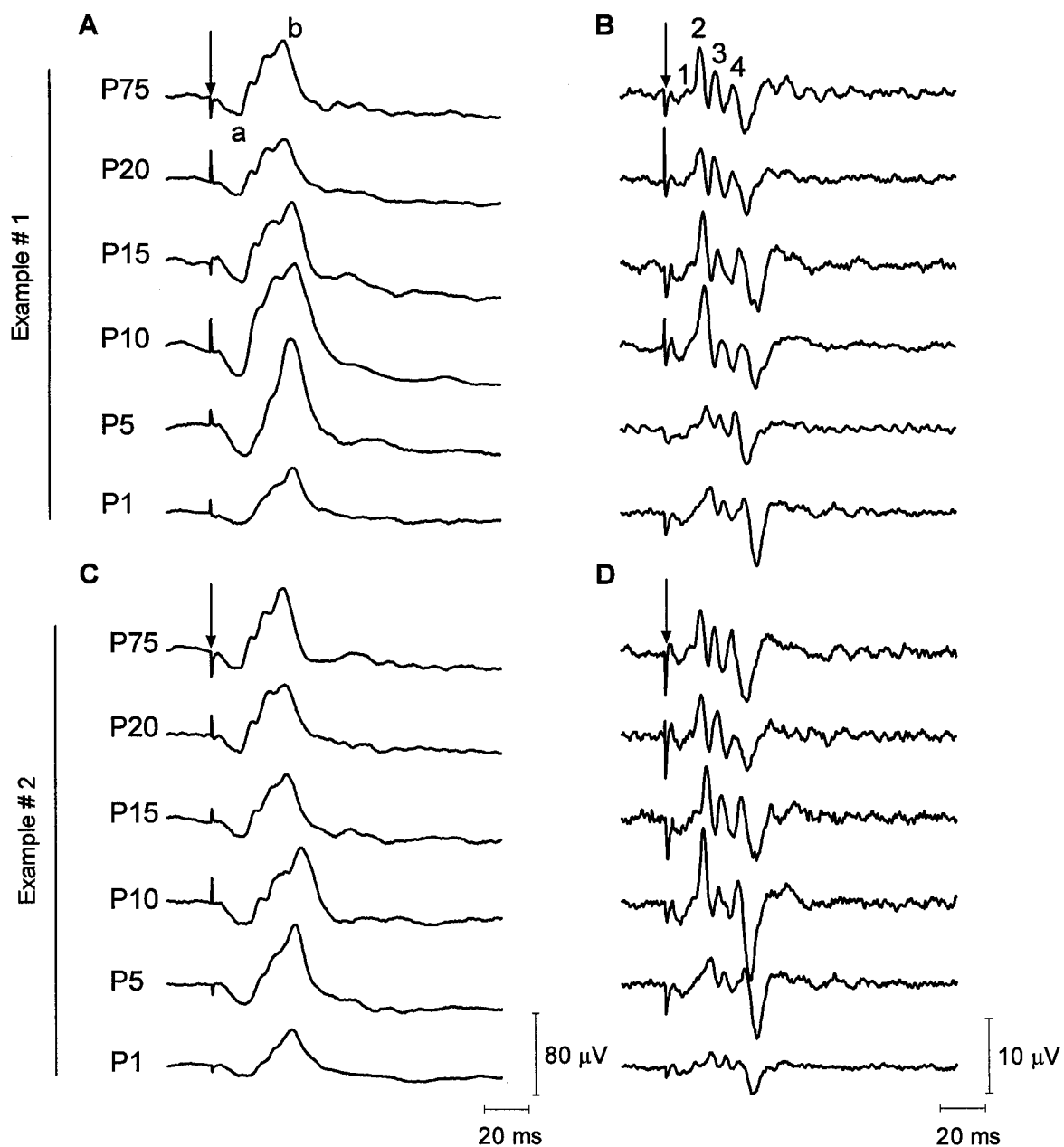


Figure 1: Representative photopic electroretinograms (A, C) and oscillatory potentials (B, D) (background: 30 cd.m^{-2} ; flash intensity: $0.9 \text{ log cd.sec.m}^{-2}$; average of 20 flashes at ISI of 0.96 seconds) obtained from two normal albino guinea pigs as they aged (P1, P5, P10, P15, P20 and P75). Vertical arrows identify flash onset, (a) a-wave, (b) b-wave, (1) OP_1 , (2) OP_2 , (3) OP_3 , (4) OP_4 . Horizontal calibration: 20 msec. Vertical calibration: ERG (A, C): $80 \mu\text{V}$; OP (B, D): $10 \mu\text{V}$.

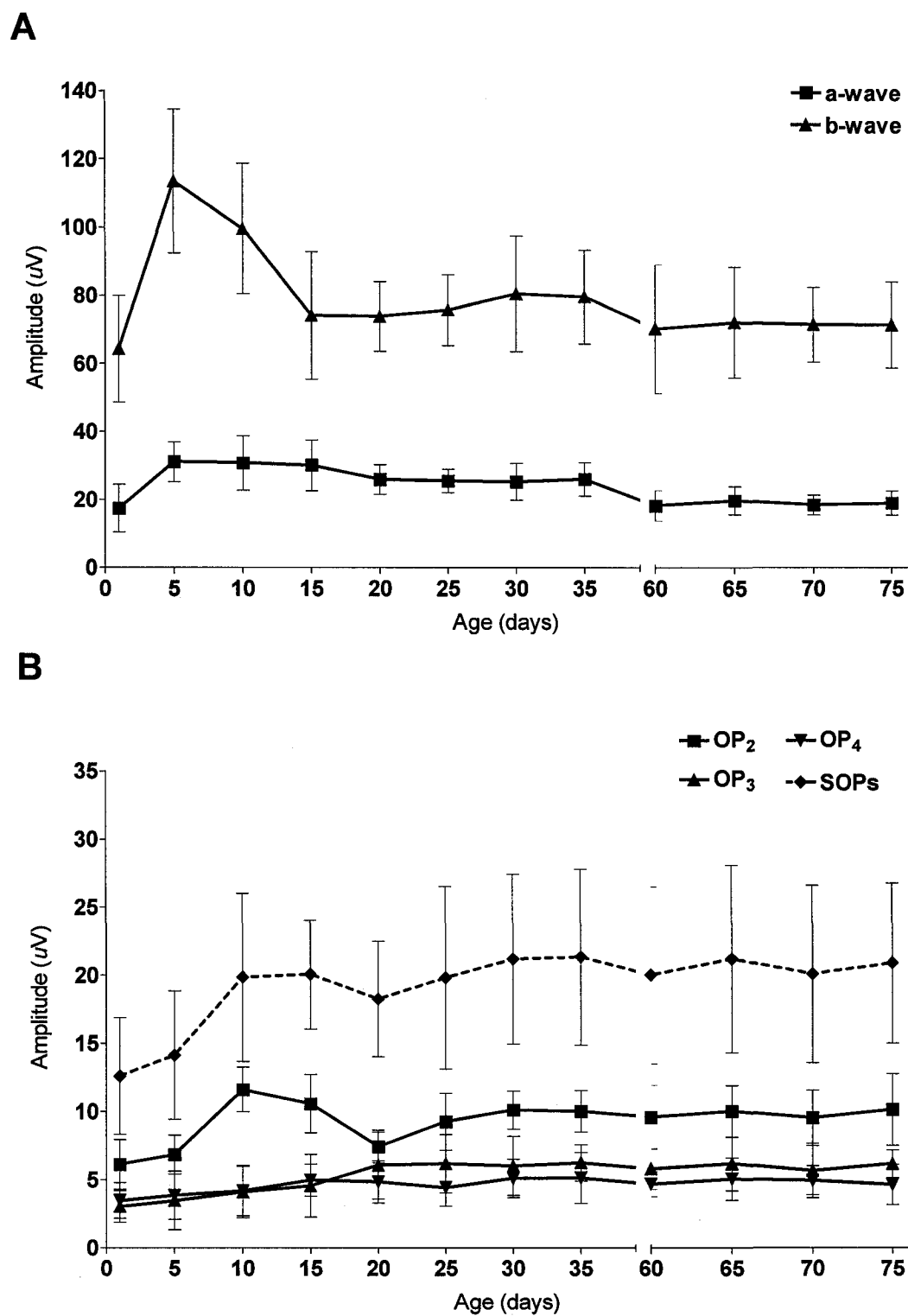


Figure 2: Photopic ERG (flash intensity: $0.9 \log \text{cd} \cdot \text{sec} \cdot \text{m}^{-2}$; background: $30 \text{ cd} \cdot \text{m}^{-2}$) [A] a-wave, b-wave, [B] OP₂, OP₃, OP₄ and SOP amplitude changes as a function of age (P1-P75 n=20). Each data point represents the mean amplitude (A) in μV or peak time (B) in msec \pm 1 S.D.

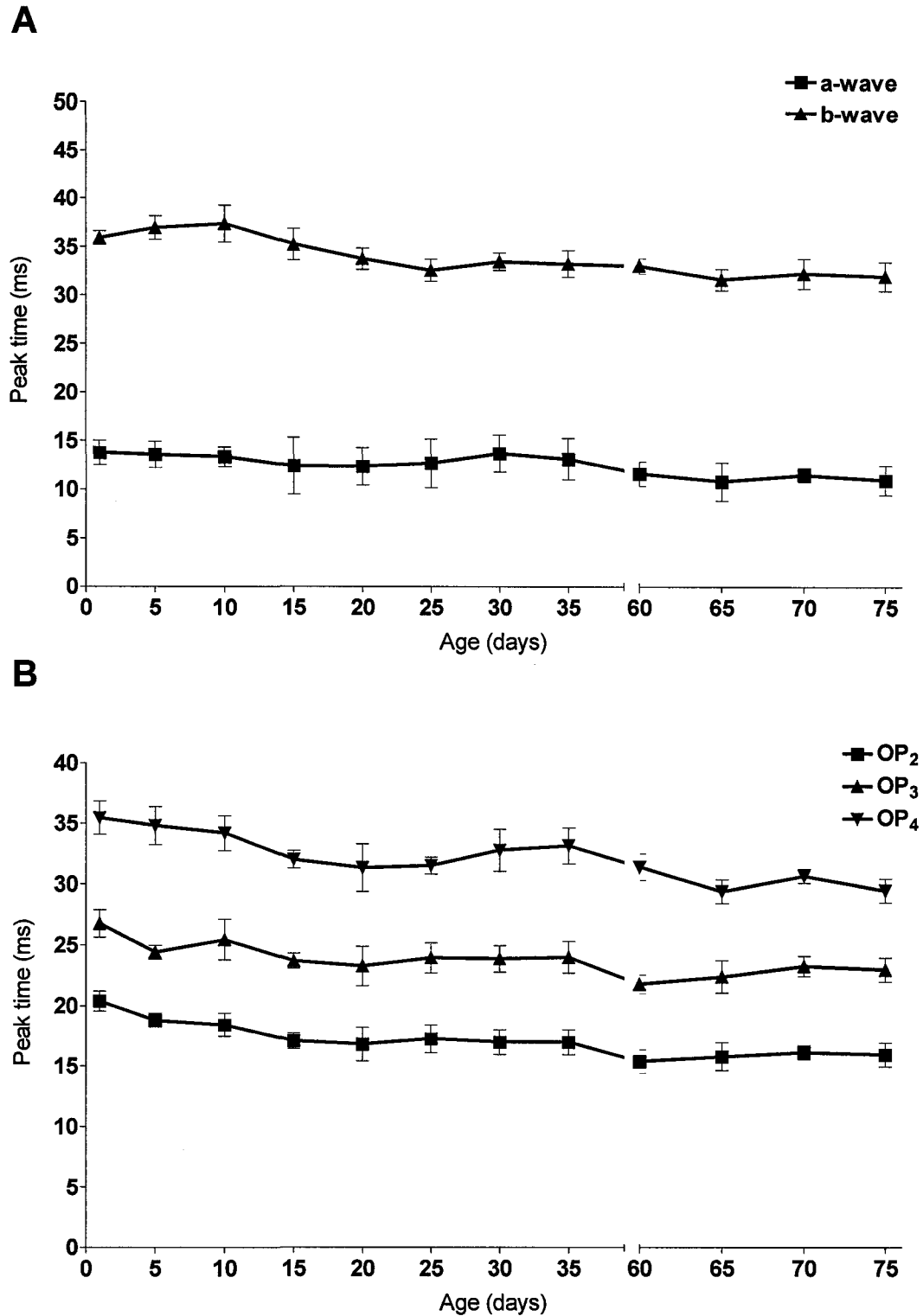


Figure 3: Photopic ERG (flash intensity: $0.9 \log \text{cd} \cdot \text{sec} \cdot \text{m}^{-2}$; background: $30 \text{ cd} \cdot \text{m}^{-2}$) [A] a-wave, b-wave, [B] OP₂, OP₃ and OP₄ peak time changes as a function of age (P1-P75 n=20). Each data point represents the mean amplitude (A) in μV or peak time (B) in msec ± 1 S.D.

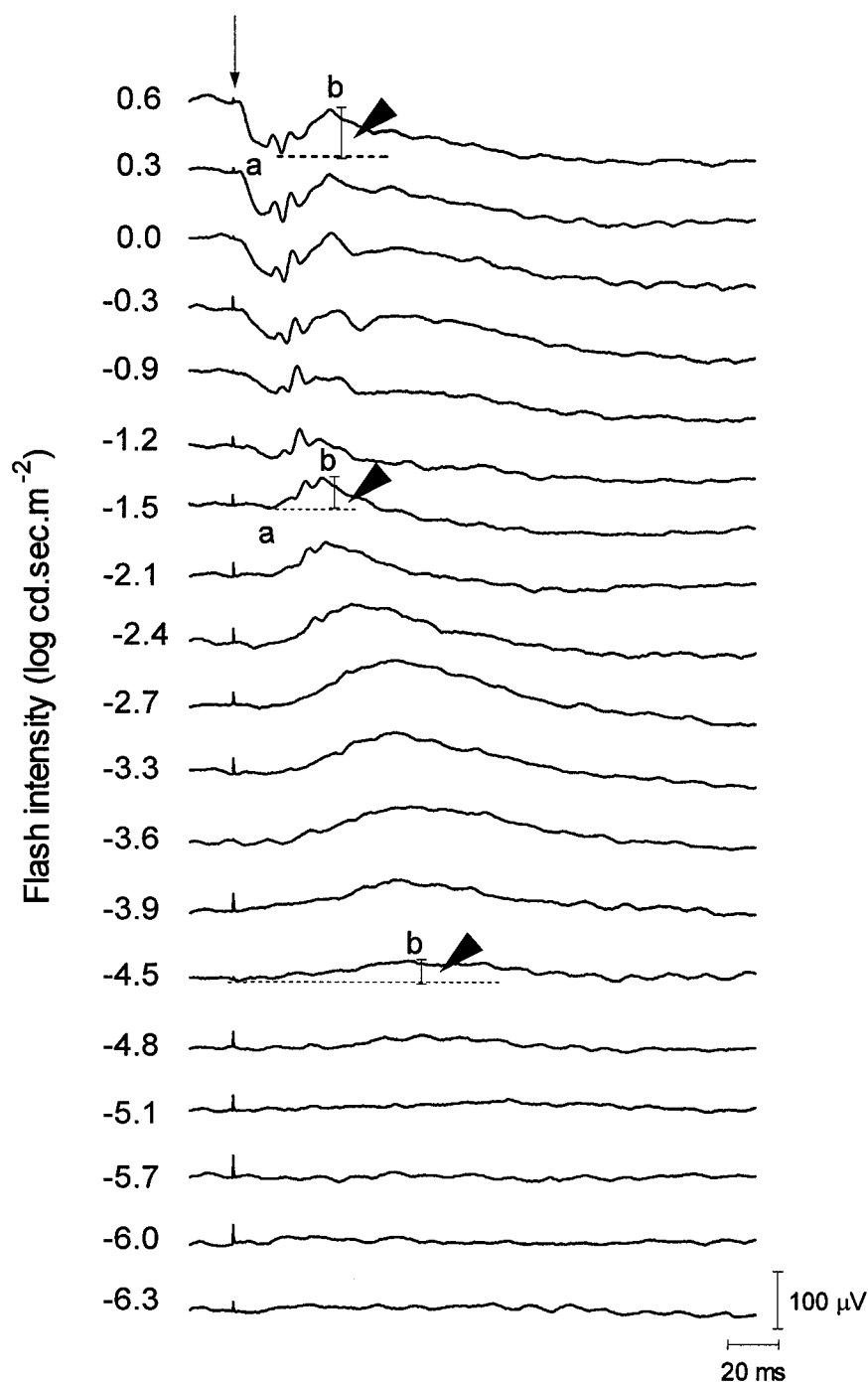
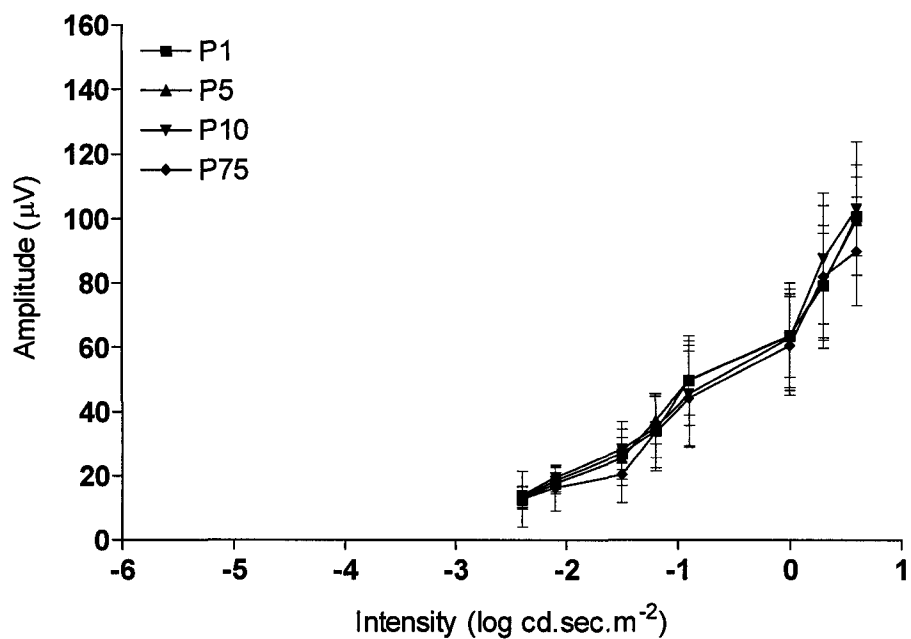


Figure 4: Scotopic ERG intensity-response series (flash intensity range from -6.3 to 0.6 log cd.sec.m⁻² as indicated at left of each tracing) obtained from a normal adult albino guinea pig age 10 days old. Vertical arrows identify flash onset, (a) a-wave, (b) b-wave. As indicated in the method, the amplitude (arrowhead) of the b-wave is always measured from the most negative trough to the peak of the b-wave. Horizontal calibration: 20 msec. Vertical calibration: 100 μ V.

A



B

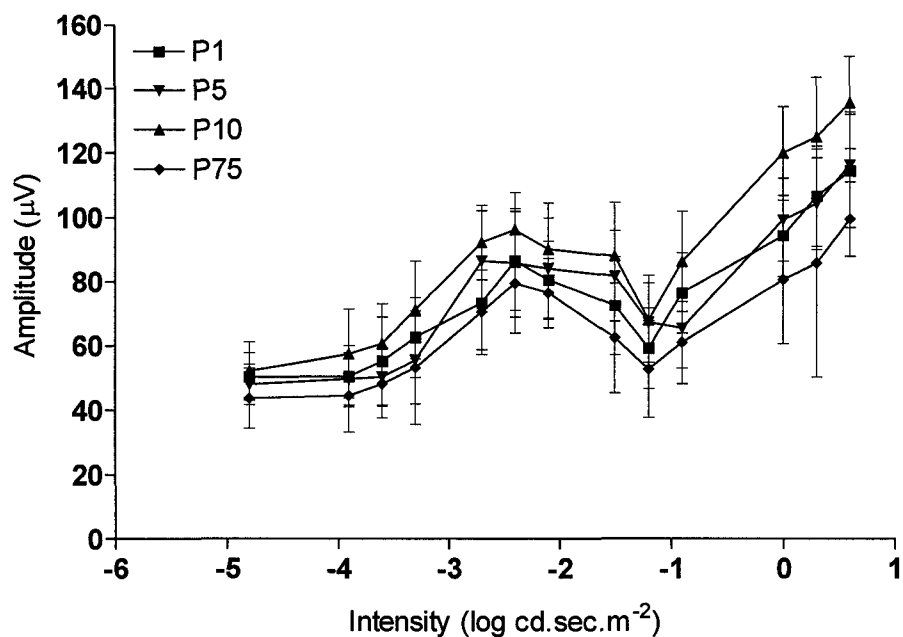


Figure 5: Scotopic (A) a- wave and (B) b-wave intensity (abscissa in $\log \text{cd}\cdot\text{sec}\cdot\text{m}^{-2}$) response (ordinate in μVolts) function obtained from normal albino guinea pigs aged 1 ($n=20$), 5 ($n=20$), 10 ($n=20$), and 75 ($n=20$) days old. Each data point represents the mean amplitude in $\mu\text{V} \pm 1 \text{ S.D.}$

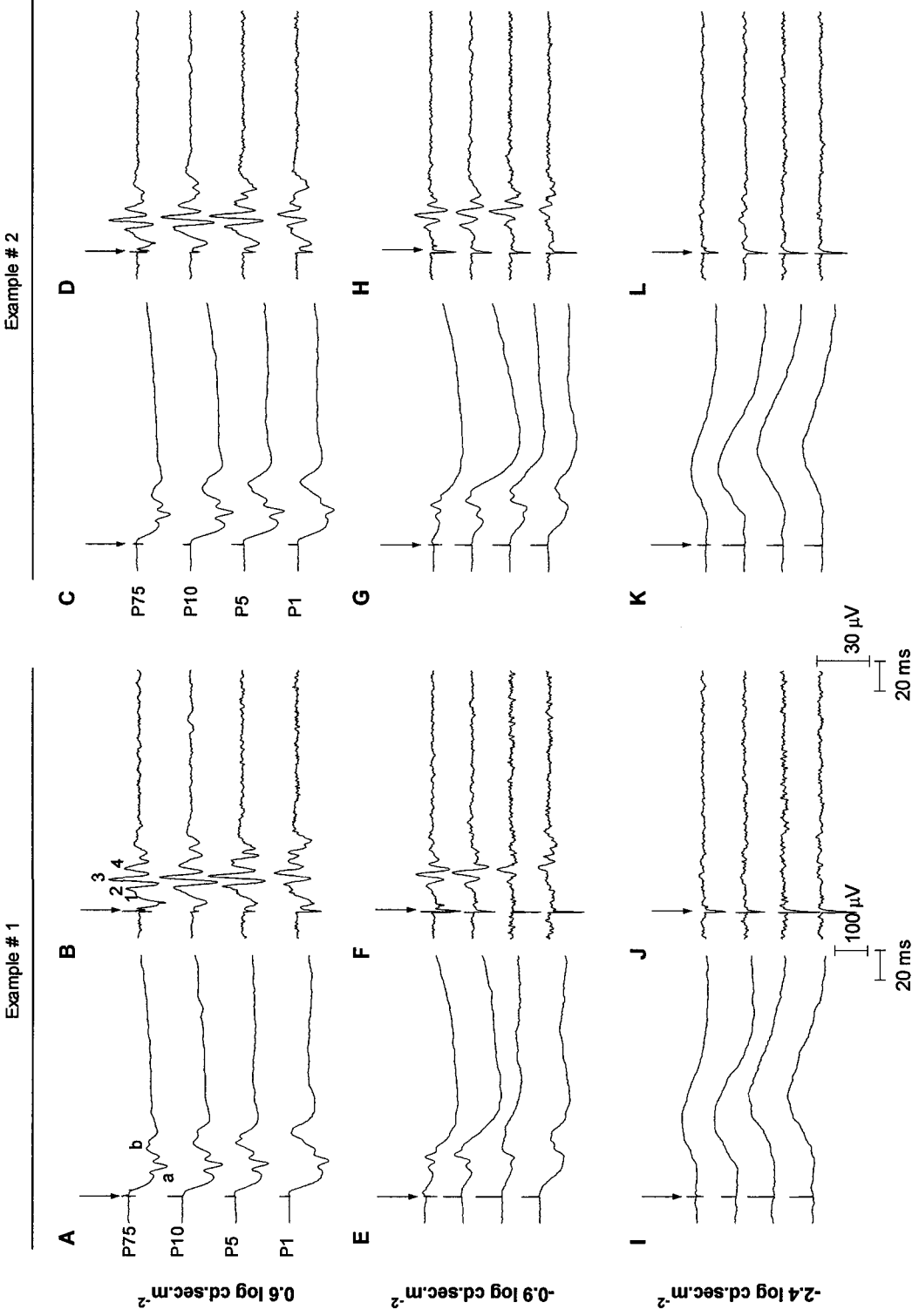


Figure 6: The effect of maturation (P1, P5, P10 and P75) on representative ERG and corresponding OP responses obtained from two different guinea pigs. Responses illustrated were taken around rod V_{max} ($-2.4 \log \text{cd}\cdot\text{sec}\cdot\text{m}^{-2}$, bottom 4 tracings), at inversion (from a positive to a negative morphology) of the b-wave (usually around $-0.9 \log \text{cd}\cdot\text{sec}\cdot\text{m}^{-2}$, middle 4 tracings) and at maximal intensity (mixed rod-cone ERG at $0.6 \log \text{cd}\cdot\text{sec}\cdot\text{m}^{-2}$, top 4 tracings). Vertical arrows identify flash onset, (a) a-wave, (b) b-wave, (1) OP₁, (2) OP₂, (3) OP₃, (4) OP₄. Horizontal calibration: 20 msec. Vertical calibration: ERG: 100 μV ; OP: 30 μV .

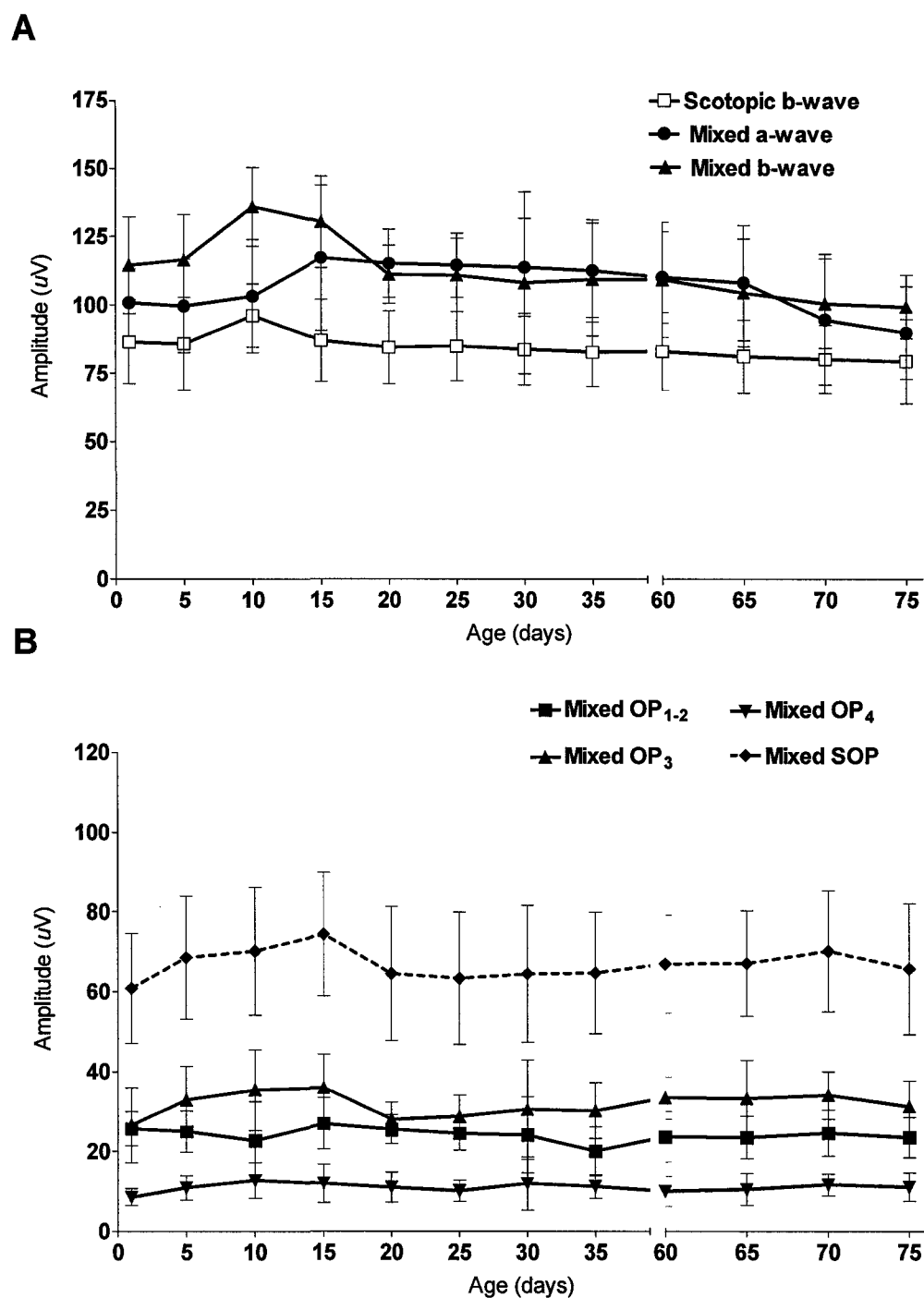


Figure 7: Scotopic ERG [A] rod-mediated b-wave (scotopic b-wave; $-2.4 \log \text{cd}\cdot\text{sec}\cdot\text{m}^{-2}$), rod-cone mediated a- and b-waves (mixed a- and b-waves; $0.6 \log \text{cd}\cdot\text{sec}\cdot\text{m}^{-2}$), and [B] rod-cone mediated OP₁₋₂, OP₃, OP₄ and SOP (mixed OPs; $0.6 \log \text{cd}\cdot\text{sec}\cdot\text{m}^{-2}$) amplitude changes as a function of age age (P1-P75 n=20). Each data point represents the mean amplitude in $\mu\text{V} \pm 1 \text{ S.D.}$

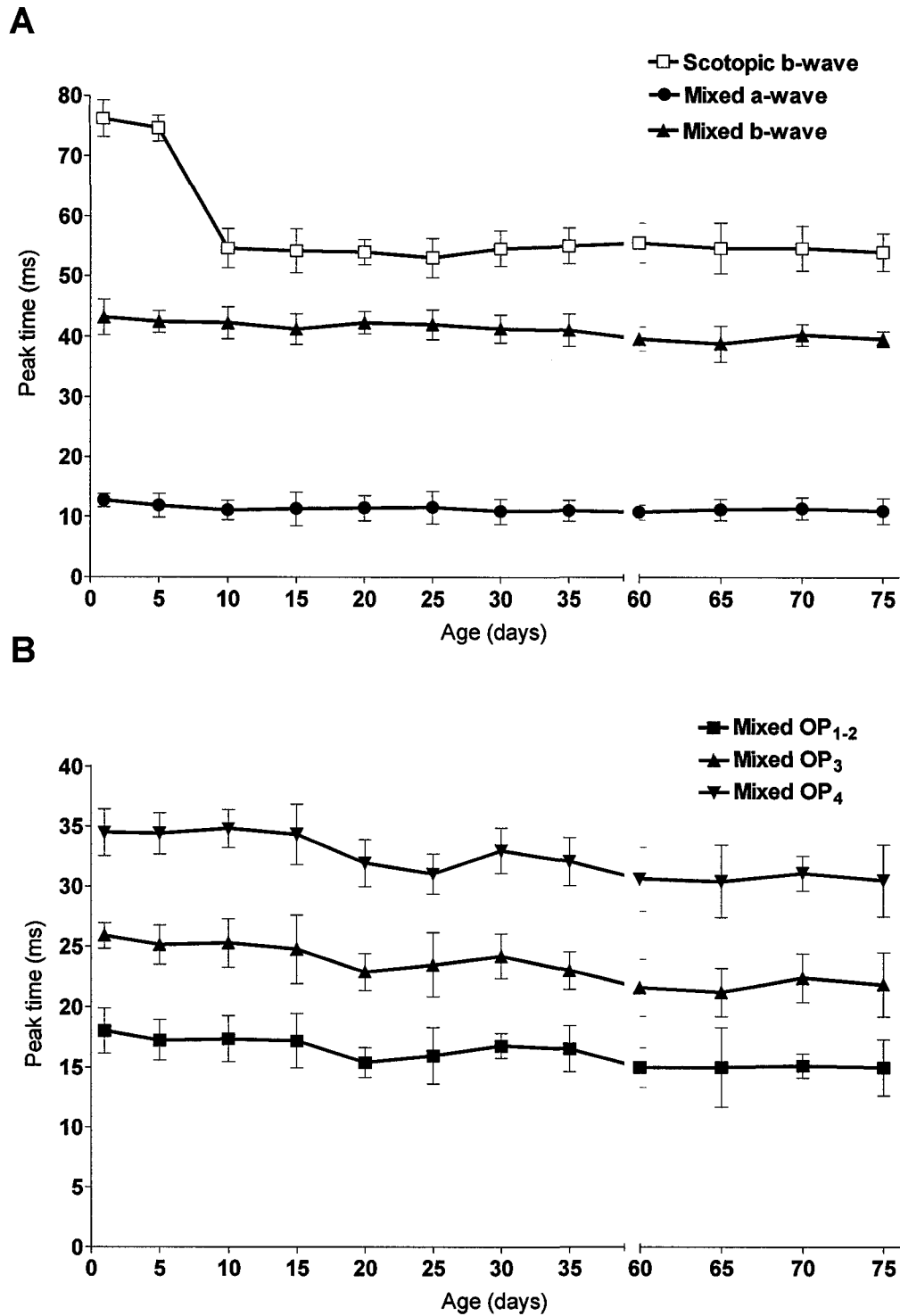


Figure 8: Scotopic [A] rod-mediated b-wave (scotopic b-wave; $-2.4 \log \text{cd}\cdot\text{sec}\cdot\text{m}^{-2}$), rod-cone mediated a- and b-waves (mixed a- and b-waves; $0.6 \log \text{cd}\cdot\text{sec}\cdot\text{m}^{-2}$), and [B] rod-cone mediated OP₁₋₂, OP₃ and OP₄ (mixed OPs; $0.6 \log \text{cd}\cdot\text{sec}\cdot\text{m}^{-2}$) peak time changes as a function of age age (P1-P75 n=20). Each data point represents the mean peak time in msec \pm 1 S.D.

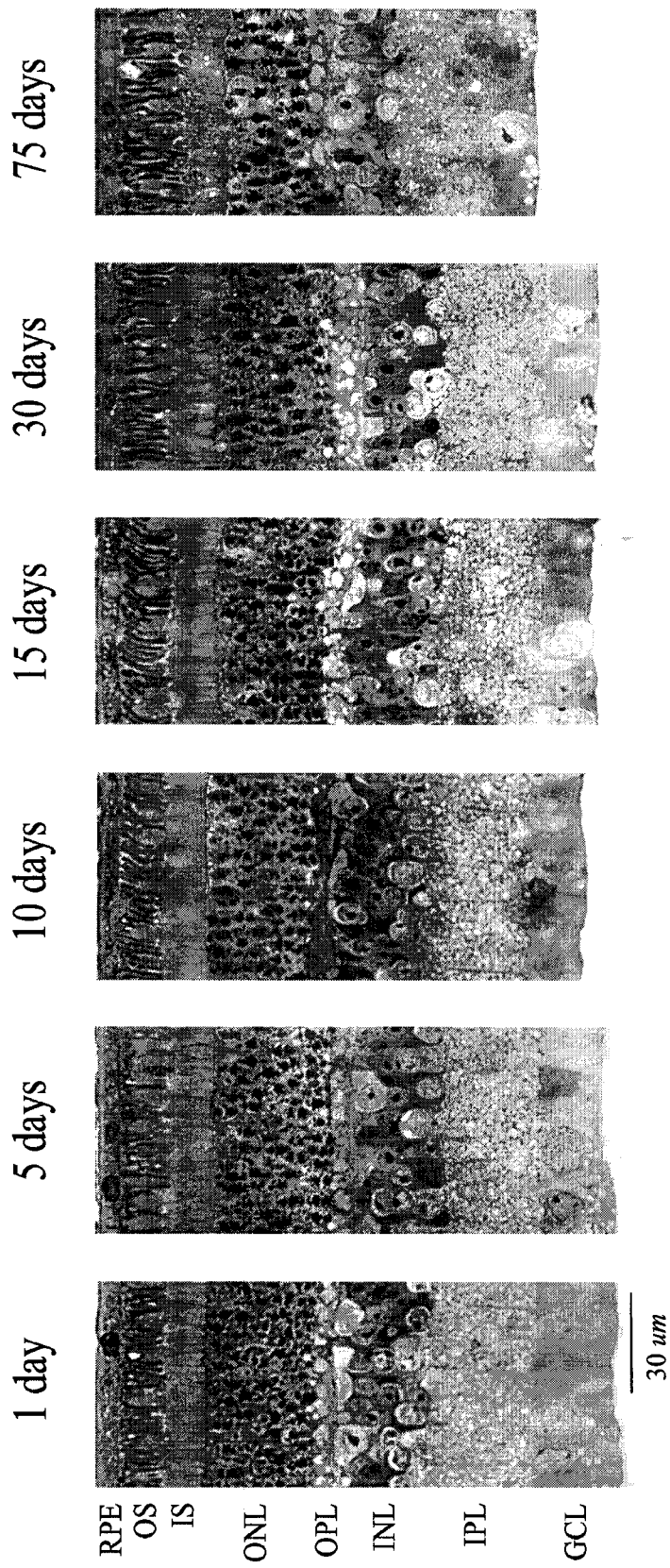


Figure 9: Representative sections of the guinea pig retina obtained at P1 (n=5), P5 (n=5), P10 (n=5), P15 (n=5), P30 (n=5) and P75 (n=5). RPE: retinal pigmented epithelium, OS: outer segment of the photoreceptors, IS: inner segment of the photoreceptors, ONL: outer nuclear layer, OPL: outer plexiform layer, INL: inner nuclear layer, IPL: inner plexiform layer, GCL: ganglion cell layer. Horizontal calibration: 30 μ m

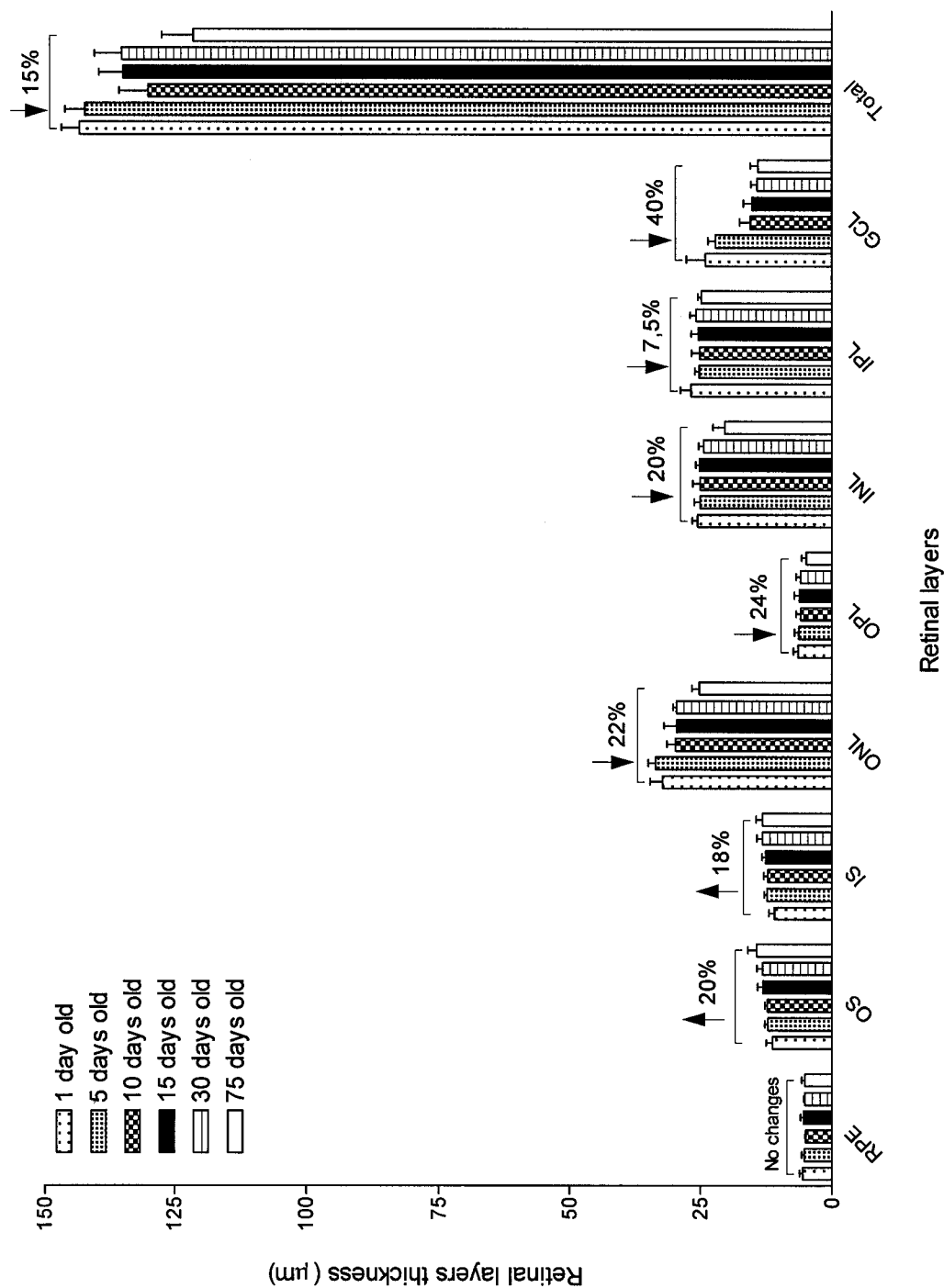


Figure 10: The effect of maturation on the structure of the different layers of the retina (n=5 per age group). RPE: retinal pigmented epithelium, OS: outer segment of the photoreceptors, IS: inner segment of the photoreceptors, ONL: outer nuclear layer, OPL: outer plexiform layer, INL: inner nuclear layer, IPL: inner plexiform layer, GCL: ganglion cell layer. Each bar represents the mean retinal thickness in $\mu\text{m} \pm 1 \text{ S.D.}$

CHAPTER III: MANUSCRIPT 2

Racine J., Joly S., Rufiange M., Rosolen S., Casanova C., Lachapelle P. (2005) The photopic ERG of the albino guinea pig (*Cavia Porcellus*): A model of the human photopic ERG. Doc Ophthalmol, 110: 67-77.

1 Preface to chapter III

Most studies that reported the relationship between retinal structure and function did so in altricial animals (eg: rats, mice), that is animals that are born with their eyes closed and with immature visual system. However, if one wishes to transpose results to humans, we must take into consideration the fact that the human infant is born with its eyes open (precocial). Also while the human retina is composed of approximately 6% cones, the retinas of rats and mice (the most common models) are made of 1-3% cones. The guinea pig (*Cavia Porcellus*) offers an excellent alternative to the usual rodent models. It is born with its eyes open following a 65 days gestation. Guinea pigs are diurnal animals (unlike most rodents) and their retina is reported to include between 8-15 % cones. Compared to the usual rodent models (rats and mice), newborn guinea pigs are thus closer to human infants and therefore could represent a better animal model of human retinal structure and function.

The general purpose of this first paper was to study the retinal function of the Hartley albino guinea pigs in order to determine if the in fact they represent a better animal model than rats and mice to study the human photopic ERG.

2 Abstract

Altricial rodents such as rats and mice are probably the most widely used animal model in the electroretinogram (ERG) literature. However, while the scotopic responses of these rodents share obvious similarities with that of humans, their photopic electroretinograms are strikingly different. For instance, the photopic ERGs of rats and mice include, when measurable, a minimal a-wave, while the b-wave is of much larger amplitude than that of humans. The purpose of this study is to present the albino guinea pig which is like human, a precocial animal, as a better rodent model of the human photopic ERG. In order to investigate the above, photopic electroretinograms and oscillatory potentials, obtained from guinea pigs and human subjects, were compared. Furthermore, in a subset of animals we injected, intravitreally, selective blockers of the ON- (L-2-amino-4-phosphonobutyric acid: L-AP-4; 10mM) or OFF- (kynurenic acid: KYN; 50mM) retinal pathways in order to mimic similar retinal disorders found in human. Based on our results, we believe that, compared to rats and mice, the photopic (cone-mediated) ERG of the guinea pig clearly represents a superior rodent model of the human photopic ERG.

3 Introduction

Of all the animal models used in experimental electroretinography today, altricial rodents (mice and rats) are probably the most widely used. Interestingly however, while the scotopic responses of these rodents are similar to that of humans, their photopic ERGs are strikingly different. For instance, the photopic ERG of rats and mice do not include an a-wave while the b-wave is of much larger amplitude than that of humans [1-4]. The retinal potentials (ERGs and OPs) are also delayed compared to humans [1-4]. In a study recently published by our group [5], we compared the photopic ERG responses obtained under similar

recording condition from a variety of species, including human. The purpose of this study was to examine if the i-wave, the post-b-wave positivity seen in the human photopic ERG was a feature common to all photopic ERGs, irrespective of species. Our study revealed that except for rats and mice, the i-wave appeared to be characteristics of the photopic ERG of the species selected. This study also drew our attention on the similarity in waveforms between the photopic ERG of guinea pigs and human. Interestingly, unlike rats and mice which are born with their eyes closed (altricial animals), guinea pigs are born with their eyes open (precocial) [6-9]. Furthermore, rats and mice are nocturnal animals and their retina is composed of 1.5% [10] and 3% [11] cones, respectively. In comparison the proportion of cones in the retina of the diurnal guinea pig varies between 8-17% depending on the area sampled. The latter value is much closer to the 6% or so reported for human subjects [12]. Consequently, the purpose of our study was to further explore the photopic ERG similarities shared between guinea pigs and humans in order to determine if the photopic ERG of guinea pigs could not, compared to rats and mice, represent a superior rodent model of the human photopic ERG. Our results would suggest that it does.

4 Material and Methods

Animal experimentation was conducted in accordance with the ARVO statement on the use of animals in Ophthalmic and Vision Research and performed following a protocol reviewed and approved by the McGill University-Montreal Children's Hospital Research Institute animal care committee. Adult albino Hartley guinea pigs (*Cavia porcellus*, $n = 19$) purchased from a commercial breeder (Charles River, St-Constant, Quebec) were used in this study. Data was compared to that obtained from Sprague Dawley ($n = 5$) rats (Charles River, St-Constant, Quebec), Balb/C ($n = 5$) mice (Charles River, St-Constant, Quebec) as well as human subjects ($n = 30$; data from previously published study [13]) tested under identical recording conditions. Throughout the study the guinea pigs, rats,

and mice were maintained in a cyclic environment of 12 hours light/dark cycle and the room was kept at a temperature of 22-23°C. The ambient room illumination (at cage level) varied between 25-30 cd.m⁻².

Prior to the ERG testing, the animal subjects (i.e. guinea pigs, rats and mice) were anaesthetized with an intramuscular injection of a mixture of ketamine (85 mg/kg) and xylazine (5 mg/kg), following which the pupils were dilated with drops of 1% cyclopentolate hydrochloride (Alcon, Texas, USA). ERG responses were recorded with DTL fibre electrodes (27/7 X-Static silver coated conductive nylon yarn, Sauquoit Industries, Scranton, PA, USA) positioned on the cornea and maintained in place with drops of 2 % methylcellulose (Gonioscopic solution, Alcon Laboratories, Texas, USA). Reference (Grass E5 disc electrode, Grass Instruments, Quincy, MA, USA) and ground (Grass E2 subdermal electrode, Grass Instruments, Quincy, MA, USA) electrodes were placed in the mouth and subcutaneously in the neck, respectively. Human ERGs were recorded similarly. Briefly, the ERGs were recorded from both eyes simultaneously, also with a DTL fibre electrode positioned into the conjunctival bag. Ground (Grass E5 disc electrode, Grass Instruments, Quincy, MA, USA) and reference (Grass E5 disc electrode, Grass Instruments, Quincy, MA, USA) electrodes were placed on the forehead and external canthi, respectively. All recordings were obtained with fully dilated pupils (1% cyclopentolate hydrochloride, Alcon, Texas, USA).

Guinea pigs, rats, mice and human subjects were then placed in front of a ganzfeld (30 cm in diameter) following which they were adapted to a rod desensitizing background of 30 cd.m⁻² for 10 minutes in order to normalize the state of retinal adaptation prior to testing. The stimuli consisted of flashes of white light of intensities ranging between -0.62 to 2.84 log cd.sec.m⁻² that were presented against the same rod desensitizing background of 30 cd.m⁻² and at an interstimulus interval of 1.5 seconds. Broadband electroretinograms (bandwidth: 0.3-500 Hz; 10 000X) and oscillatory potentials (bandwidth: 100-500 Hz; 50 000X) were recorded simultaneously with the use of the LKC UTAS-E-3000

(LKC Systems Inc., Gaithersburg, MD, USA). Background luminance and flash intensities were calibrated with a research radiometer (IL 1700; International Light, Newburyport, MS, USA). Unless otherwise indicated all tracings represent an average of ten responses and included a prestimulus baseline of 20 milliseconds (msec).

To further our comparison of human and guinea pig's retinal responses, we also created pathological photopic ERGs that mimicked human-like retinal disorders. To do so, intravitreal injections of L-2-amino-4-phosphonobutyric acid (L-AP-4; Sigma-Aldrich, Canada; n=6 guinea pigs) and Kynurenic acid (KYN; Sigma-Aldrich, Canada; n=6 guinea pigs) were performed on adult guinea pigs. The pharmacological agents were diluted in sterile water and the pH was adjusted to 7.4. The injection (50 μ l of either L-AP-4 or KYN) was delivered through the pars plana of the superior pole of the eye with a 45-degree angle using an Hamilton syringe (Hamilton company, Reno, Nevada) with a 30 gauge, 0.5 inch needle. After the injection the needle was held in place in the vitreous for approximately 1 minute prior to withdrawal. The latter waiting period enables us to avoid fluid leakage from the site of penetration into the subconjunctival space. The retinal concentrations of L-AP-4 and KYN were calculated to be 10 mM and 50 mM, respectively assuming a complete mixing of the pharmacological agent within the guinea pig's vitreous. Previous experiments (unpublished data) showed that maximal effect on the ERG responses were typically observed 2 hours and 3-5 days following injection for L-AP-4 and KYN respectively.

4.1 Data analysis

Analysis of the ERG waveforms was performed as recommended [14]. The amplitude of the a-wave was measured from pre-stimulus baseline to the first negative trough or when a flash artifact was recorded, the amplitude of the a-wave was measured from the onset of a-wave descent (ie: bottom baseline as illustrated at figure 2) to the first negative trough. The amplitude of the b-wave was

measured from the trough of the a-wave to the most positive peak of the response. The amplitude of each OP was measured individually from the preceding trough to the peak of the OP under evaluation, except for OP₁, which was measured from the preceding baseline (first 20 msec of recording) to its peak. All peak times were measured from flash onset to peak. Statistical significance was determined with student t-test ($p < 0.05$) for independent samples.

5 Results

At figure 1 are compared representative photopic ERGs intensity response curves obtained, under identical recording conditions, from a normal human subject, a guinea pig, a rat and a mouse. It is interesting to note that while rat and mouse ERGs differ substantially in composition (a-wave present or not), morphology (more prominent OPs in the mouse ERG), time course (peak time of b-wave and interpeak intervals of OPs) and relative amplitude (larger signals in murine responses compared to the guinea pig) from that of human, those recorded from the guinea pig are remarkably similar. The most obvious similarity lies in the presence of a well delineated a-wave, a feature not seen in murine ERGs, resulting, at Vmax (human and guinea pig), in a b-/a-wave ratio of 2.58 ± 0.6 , a value not significantly different ($p > 0.05$) to that measured in human (2.47 ± 0.6). Similarly and as previously reported [5], like in human, the cone b-wave of the guinea pig is followed by an i-wave, again a feature not seen in murine responses. Of interest, while the amplitude of the b-waves of guinea pigs and humans are of a comparable range, that of our murine subjects are markedly larger (almost double the size as per figure 1).

As illustrated at figure 1, the morphology and time course of the photopic electroretinogram of human and guinea pigs are very similar. This is further exemplified at figure 2, where the photopic ERG (A, C) and OPs (B, D) luminance-response function of a representative human (A, B) and a guinea pig

(C, D) subject are compared. At low intensity of stimulation (bottom tracings) a small but noticeable a-wave as well as a b-wave are recorded from both human and guinea pig subjects. As the intensity of the flash increases, a larger a-wave as well as OPs (on the ascending limb of the b-wave) are added to the basic ERG waveform. Further increments in the intensity of the stimulus increase the amplitude of the b-wave to a maximum voltage (V_{\max}) at approximately $0.90 \log \text{ cd}\cdot\text{sec}\cdot\text{m}^{-2}$ and then decrease it progressively with the brightest stimuli. Of interest, for the same intensity of stimulation, the amplitude of the ERG is usually larger in guinea pigs compared to human. The latter is best visualized at figure 2. The intensity response function of the human and guinea pigs OPs are also comparable. In both species, OP_2 is the oscillatory potential with the lowest threshold (figure 2 B, D) to which OP_3 and OP_4 are added with progressively brighter flashes and in the same orderly sequence in both species. Similarly, use of the brighter flashes (approximately $> 1.40 \log \text{ cd}\cdot\text{sec}\cdot\text{m}^{-2}$ at figure 2 B, D) will cause a split of OP_4 into OP_{4a} and OP_{4b} . Of interest however, while in human ERGs the amplitude of OP_{4a} and OP_{4b} will decrease regularly in response to stimuli beyond the b-wave V_{\max} , in guinea pigs the same OPs (OP_{4a} more than OP_{4b}) retained relatively larger amplitudes. As a consequence of the above, the peak time of the brighter ($> 1.90 \log \text{ cd}\cdot\text{sec}\cdot\text{m}^{-2}$) flash b-wave is determined by OP_3 in the human ERG (see tracing: $2.84 \log \text{ cd}\cdot\text{sec}\cdot\text{m}^{-2}$) and OP_{4a} or OP_{4b} in the guinea pig ERG. It is this unique behavior of the long latency OPs that best distinguishes human from guinea pigs photopic ERGs. The latter difference cannot be better illustrated than with the luminance response function curves shown at figure 3, where ERG luminance-amplitude (A, B) and peak time (C, D) response function curves obtained from human (A, C) and guinea pig (B, D) subjects are presented. As previously reported elsewhere [13, 15, 16], compared to the near linearity of the human a-wave luminance-response function curve that of the human cone b-wave adopts a unique shape. In the initial phase, the amplitude of the cone b-wave increases, almost linearly, as the intensity of the flash augments to reach a plateau (between 0.39 and $0.64 \log \text{ cd}\cdot\text{sec}\cdot\text{m}^{-2}$) at a maximal amplitude (V_{\max}) of $85.07 \pm 21.10 \mu\text{V}$ (figure 3A). A further increase in flash

intensity will then cause a gradual reduction in the amplitude of the b-wave. The term photopic hill was previously coined to describe the unique shape of the human cone b-wave luminance-response function [15, 17].

This unique feature of the human cone b-wave luminance-response function is not as readily obvious with guinea pig responses. If the amplitude of the cone b-wave of guinea pigs is measured at the maximal height of the b-wave (i.e.: at the peak of wave 4a as in figure 2 C) then we cannot reproduce a human-like photopic hill, the amplitude of the b-wave remaining at a plateau of approximately 100 μV for responses evoked to intensities $\geq 0.64 \log \text{cd}\cdot\text{sec}\cdot\text{m}^{-2}$. However, if the amplitude of the guinea pig's photopic b-wave evoked to flashes brighter than $0.90 \log \text{cd}\cdot\text{sec}\cdot\text{m}^{-2}$ (b-wave V_{max} as per figure 3 B) are measured at the peak of wave 3, as done with the human response, then a photopic hill similar to that of human is observed (figure 3 B, dash line). It would thus appear that it is the gradual destruction of the long latency OPs, from the human photopic ERG that yields the photopic hill phenomenon. Since long latency OPs are, in guinea pigs, more resistant to brighter flashes this would explain why this phenomenon is not as readily observed in the latter species. Similarly, the intensity-response function of the human and guinea pig a-wave also differs significantly. While in humans the amplitude of the a-wave grows almost linearly with flash intensity (figure 3 A) in guinea pigs, the a-wave reaches a maximal value of $57.80 \pm 15.44 \mu\text{V}$ at $1.4 \log \text{cd}\cdot\text{sec}\cdot\text{m}^{-2}$ and then decreases with further increments of the flash intensity.

In a previous study [18] we challenged the arbitrary nature of the ISCEV ERG standard flash (SF), which defines the intensity rather than the ERG response itself. Instead, we presented evidences in support of a standard based on a typical ERG waveform; an approach we believed was more physiological. Given that most of the ISCEV ERG standard responses are photopic in nature; our suggested standard ERG waveform was also photopic. It was defined as the photopic ERG response where OP_4 reached its maximal amplitude. ERG and OP waveforms

representing the latter are illustrated at figure 4, while amplitude and peak time data are given at table 1. In human, this standard photopic ERG waveform is typically evoked to a flash of $0.64 \text{ log cd}\cdot\text{sec}\cdot\text{m}^{-2}$, that is an intensity yielding a response found at the top of the photopic hill (figure 3 A). The resulting human waveform has the following characteristics: 1- a a/b wave ratio of 0.42 ± 0.10 and, 2- relative amplitude of individual OPs of $24.06 \pm 5.62 \%$ (OP_{1-2}), $30.99 \pm 5.60 \%$ (OP_3) and $44.96 \pm 8.34 \%$ (OP_4) as per data in table 1. As exemplified at figure 4, a similar waveform can also be evoked from our guinea pigs. The guinea pig standard photopic ERG waveform, which is evoked to a flash of $0.90 \text{ log cd}\cdot\text{sec}\cdot\text{m}^{-2}$, has the following characteristics: 1- an a/b wave ratio of 0.36 ± 0.05 , and 2- relative amplitude of individual OPs of $34.77 \pm 5.30 \%$ (OP_{1-2}), $27.34 \pm 7.09 \%$ (OP_3) and $37.89 \pm 4.69 \%$ (OP_4) (table 1). Despite minor differences, the morphologies of the ERG and OP responses recorded from the humans and guinea pigs are strikingly similar. Similarly, the timing of the ERG and OP components are, on average, 1-2 msec slower in guinea pig responses (table 1). As a result of this delayed retinal response, the frequency domain of the OPs in the guinea pig is slightly lower than that of human as shown at figure 5. Fast Fourier Transform (FFT) of human OP responses reveals three major power peaks at $39.86 \pm 0.24 \text{ Hz}$, $70.43 \pm 7.14 \text{ Hz}$ and $140.00 \pm 5.00 \text{ Hz}$, compared to $31.67 \pm 2.58 \text{ Hz}$, $61.67 \pm 7.53 \text{ Hz}$ and $104.17 \pm 9.17 \text{ Hz}$ for the guinea pig response.

Results presented at figures 4, 5 and table 1 suggest that the human and guinea pig standard photopic response are of equivalent waveforms in terms of a/b wave ratio, OP composition, timing and frequency domain. Are they however generated through equivalent retinal channels? To examine this issue, we compared selected human pathological ERGs with those obtained from guinea pigs that were subjected to pharmacological manipulations in order to mimic the human retinal disorder. The human retinal disorders we selected were: Congenital Stationary Night Blindness (CSNB) and a form of cone dystrophy (CD) that we have recently reported [19]. There are several reports suggesting that CSNB results from an anomaly of the ON-retinal pathway (presumably at the synapse

between the photoreceptors and the ON depolarizing bipolar cells: ON-DBC) [20]. Similarly, our CD patients most probably suffer from an anomaly along the OFF-retinal pathway, presumably at the level of the OFF hyperpolarizing bipolar cells (OFF-HBC) [20]. At figure 6 are illustrated representative standard photopic ERGs and OPs from a CSNB (C: dotted tracings) and a CD (D: dotted tracings) patients and compared to responses obtained from a normal subject (solid tracings). As previously reported, the most important feature of these pathological recordings is the absence of OP₂ and OP₃ from the CSNB tracing and of OP₄ from the CD tracing [19].

In order to mimic, in guinea pigs, malfunction of the ON- and OFF-retinal pathways, intravitreal injection of L-AP-4 (ON-retinal pathway blocker) and KYN (OFF-retinal pathway blocker) were preformed. As exemplified at figure 6, L-AP-4 completely abolished OP₂ and OP₃ from the guinea pig's responses, leaving only an OP₄ of near normal amplitude. The resulting OP response is almost identical in morphology to that of our CSNB patient (figure 6 C). Similarly, an intravitreal injection of KYN reduced the amplitude of OP₄ and slightly delayed OP₃ while OP₂ remained basically unchanged. Aging the resulting OP response is almost of the same morphology as that recorded from our CD patient (figure 6 D).

6 Discussion

The purpose of this study was to present the albino guinea pig as a superior rodent model of the human photopic (cone-mediated) ERG. Our results clearly show that the photopic ERG and OPs of human, and guinea pigs are comparable in several ways, a conclusion in accord with that of Lei who compared the ERGs of guinea pigs, primates and rats [21]. This cannot be better exemplified than when their respective "standard" ISCEV photopic responses (figures 4, 5 and table 1) as well as with the luminance response function of the b-wave (figure 1, 2) and OPs (figure 2) are compared. Similarly, intravitreal injections of blockers of the

ON- and OFF-retinal pathways remarkably mimicked human retinopathies known to have specific ON- or OFF-retinal pathways anomalies (figure 6). There are however some differences. For instance, while the a-wave of the human photopic ERG appears to grow linearly as the intensity increases (at least within the intensity range we used), that of the guinea pig photopic ERG increased to a maximum amplitude reached at intensity $1.40 \log \text{ cd}\cdot\text{sec}\cdot\text{m}^{-2}$ and decreased afterwards. The latter difference in photopic a-wave amplitude between human and guinea pigs might reflect the known differences in cone type and cone sensitivity between the two groups. As previously published [21-24] guinea pigs are dichromate whereas human are trichromate, which implies that guinea pigs lack one type of cone when compared to human. In fact guinea pigs lack the long wavelength (L-type) type cones, while the sensitivity of the guinea pigs S-type cones (429 nm) and M-types cones (529 nm) are similar to human (430 nm, 531 nm, respectively). Furthermore, the timing of the different ERG components are slightly delayed in guinea pigs compared to human (see figures 1, 2, 3 and table 1), but faster than in mice and rats [4]. Finally, the guinea pig's OP_4 appears to be more resistant than its human counterpart to the high intensities of stimulation as witnessed at figure 2 (B, D). However, notwithstanding these minor differences, compared to mice and rats, the photopic ERG of the guinea pig does represent a superior model of human photopic ERG and should therefore be considered as the rodent model of choice in experiments where the photopic system is targeted, such as in drug development for instances, a view in accord with that of Lei who presented the guinea pig's ERG as the best substitute of the primate photopic ERG [21].

Added to these photopic ERG similarities, human and guinea pigs also share other common features. For instance, unlike most other altricial animal models used, such as rats, mice, cats, rabbits and dogs to name a few, that are born with their eyes closed and their retina undeveloped [6, 7, 25-28], guinea pigs, like human, are precocial animals, meaning that they are born with their eyes opened and with an adult-like retina [8]. The gestational period is also longer in guinea

pigs, 68-69 days, compared to 21 days in other rodents such as rats and mice [8]. Similarly to human, there is a substantial growth of rod outer segments which occurs during gestation and an extensive maturation of the plexiform layers is observed before the development of the outer segment of the photoreceptor is complete [8]. Furthermore, guinea pigs, like human, are diurnal animals and their retina contains approximately 8-17% cones [29] compared to approximately 6% in human [12] while rats and mice have 1-2 % [10] and 3 % [11], respectively.

It is also of interest to note that while there is a high degree of morphological as well as physiological similarity between human and guinea pigs photopic signals, their scotopic responses are very dissimilar. In response to stimuli of photopic intensity range, the scotopic ERGs of guinea pigs are of a negative morphology (i.e. a-wave significantly larger than the b-wave) almost of the Schubert-Bornschein type [9, 30-33]. The fact that their photopic responses are almost identical while their scotopic ERG responses differ significantly suggest that there is minimal, if any, interference between the two pathways when tested with the ERG protocol used in the present study. The latter is further exemplified with the results published in a recent study from our group where we presented a guinea pig model of a retinal disorder that shared some similarities with human CSNB [33]. The results we presented did reveal a completely abolished rod-mediated function with maintaining of a normal cone function as seen in some forms of human CSNB. The latter gives even more support to our contention that guinea pigs are an excellent animal model of the human photopic ERG.

To date, few studies of the retinal function (ERG or otherwise) have been conducted using the albino guinea pig as the animal model. We hope that the results presented here will be convincing enough to generate new interests in this excellent animal model of human photopic (cone-mediated) retinal function.

7 References

1. Nixon PJ., Bui BV., Armitage JA., Vingrys AJ. The contribution of cone responses to rat electroretinogram. *Clin Exp Ophthalmol* 2001; 29: 193-196.
2. Xu L., Ball SL., Alexander KR., Peachey NS. Pharmacological analysis of the rat cone electroretinogram. *Vis Neurosci* 2003; 20: 297-306.
3. Gresh J., Goletz PW., Crouch RK., Rohrer B. Structure-function analysis of rods and cones in juvenile, adult, and age C57BL/6 and Balb/c mice. *Vis Neurosci* 2003; 20: 211-220.
4. Dembinska O., Rojas LM., Chemtob S., Lachapelle P. Evidence for a brief period of enhanced oxygen susceptibility in the rat model of oxygen-induced retinopathy. *Invest. Ophthalmol. Vis. Sci.* 2002; 43: 2481-2490.
5. Rosolen SG., Rigaudiere F., Legargasson J-F., Chalier C., Rufiange M., Racine J., Joly S., Lachapelle P. Comparing the photopic ERG i-wave in different species. *Vet Ophthalmol* 2004; 7: 189-192.
6. Weidman TA., Kuwabara T. Postnatal development of the rat retina. *Arch Ophthalmol* 1968; 79: 470-484.
7. Weidman TA., Kuwabara T. Development of the rat retina. *Invest Ophthalmol Vis Sci* 1969; 8: 60-69.
8. Spira AW. In utero development and maturation of the retina of a non-primate mammal: a light and electron microscopic study of the guinea pig. *Anat Embryol* 1975; 14: 279-300.

9. Bui BV., Vingrys AJ. Development of receptor responses in pigmented and albino guinea pigs (*Cavia porcellus*). *Doc Ophthalmol* 1999; 151-170.
10. LaVail MM, Sidman M, Rausin R, Sidman RL. Discrimination of light intensity by rats with inherited retinal degeneration: a behavioural and cytological study. *Vis Res* 1974; 14: 693-702.
11. Carter-Dawson LD., LaVail MM. Rods and cones in the mouse retina. 1- Structural analysis using light and electron microscopy. *J Comp Neurol* 1979; 1888: 245-262.
12. Curcio CA., Sloan KR., Kalina R.E., Hendrickson A.E. Human photoreceptor topography. *J Comp Neurol* 1990; 292: 497-523.
13. Rufiange R., Dassa J., Dembinska O., Koenekoop RK., Little JM., Polomeno RC., Dumont M, Chemtob S., Lachapelle P. The photopic ERG luminance-response function (photopic hill): method of analysis and clinical application. *Vis Res* 2003; 43: 1405-1412.
14. Marmor MF., Zrenner E. Standard for clinical electroretinography (1999 update). *Doc Ophthalmol* 1998; 97: 143-156.
15. Wali N., Leguire LE. The photopic Hill: A new phenomenon of the light adapted electroretinogram. *Doc Ophthalmol* 1992; 80: 335-345.
16. Rufiange M., Rousseau S., Dembinska O., Lachapelle P. Cone-dominated ERG luminance-response function: the Photopic Hill revisited. *Doc Ophthalmol* 2002; 104: 248-248.
17. Wali N., Leguire LE. Fundus pigmentation and the electroretinographic luminance-response function. *Doc Ophthalmol* 1993; 84: 61-69.

18. Lachapelle P., Ruffange M., Dembinska O. A physiological basis for definition of the ISCEV ERG standard flash (SF) based on the photopic hill. *Doc Ophthalmol* 2001; 102: 157-162.
19. Lachapelle P, Rousseau S., McKerral M., Benoit J., Polomeno RC., Koenekoop RK., Little JM. Evidence supportive of a functional discrimination between photopic oscillatory potentials as revealed with cone and rod mediated retinopathies. *Doc Ophthalmol* 1998; 95: 35-54.
20. Sieving PA, Murayama K, Naarendorp F. Push-pull model of the primate photopic electroretinogram: A role for hyperpolarizing neurons in shaping the b-wave. *Vis Neurosci* 1994; 11: 519-532.
21. Lei B. The ERG of guinea pig (*Cavia Porcellus*): comparison with I-type monkey and E-type rat. *Doc Ophthalmol* 2003; 106: 243-249.
22. Parry J.W.L., Bowmaker J.K. Visual pigment coexpression in guinea pig cones: a microspectrophotometric study. *Invest Ophthalmol Vis Sci* 2002; 43: 1662-1665.
23. Jacobs G.H., Degan II J.F. Spectral sensitivity, photopigments, and color vision in the guinea pig (*Cavia porcellus*). *Behav Neurosci* 1994; 108: 339-1004.
24. Röhlich P., van Veen Th. Szél A. Two different visual pigments in one retinal cone cell. *Neuron* 1994; 13: 1159-1166.
25. Donovan A. The postnatal development of the cat retina. *Exp Eye Res* 1966; 5: 249-259.
26. Braekevelt CR., Hollenberg MJ. The development of the retina of the albino rat. *Am J Anat* 1970; 127: 281-302.

27. Vogel M. Postnatal development of the cat's retina. *Adv Anat Embryol Cell Biol* 1978; 54: 1-56.
28. Fulton AB., Graves AL. Background adaptation in developing rat retina: an electroretinographic study. *Vis Res* 1980; 20: 819-826.
29. Peichl L., Gonzalez-Suriano J. Morphological types of horizontal cells in rodent retinae : A comparison of rat, mouse, gerbil, and guinea pig. *Vis Neurosci* 1994; 11: 501-517.
30. Jutras S, Doke A, Chemtob S, Casanova C, Lachapelle P. Negative scotopic ERGs in Guinea pigs. *Invest Ophthalmol Vis Sci* (abstract) 1997; 38: S884.
31. Bui BV, Sinclair AJ, Vingrys AJ. Electroretinograms of albino and pigmented guinea pigs (*Cavia porcellus*). *Aust N Z J Ophthalmol* (abstract) 1998; 26: S98.
32. Bui BV, Weisinger HS, Sinclair AJ, Vingrys AJ. Comparison of guinea pig electroretinograms measured with bipolar corneal and unipolar intravitreal electrodes. *Doc Ophthalmol* 1998; 95: 15-34.
33. Racine J., Behn D., Simard E., Lachapelle P. Spontaneous occurrence of a potentially night blinding disorder in guinea pigs. *Doc Ophthalmol* 2003; 107: 59-69.

8 Tables and legends

	a-wave		b-wave		OP ₁₋₂		OP ₃		OP ₄	
	Amplitude (μV)	Peak time (ms)								
Human	35.00 \pm 7.22	14.13 \pm 0.80	85.07 \pm 21.18	34.58 \pm 1.28	12.89 \pm 0.64	16.58 \pm 0.09	17.30 \pm 1.37	23.80 \pm 0.11	25.35 \pm 1.76	32.84 \pm 0.35
Guinea pigs	39.87 \pm 11.53	14.29 \pm 1.43	111.30 \pm 30.14	36.45 \pm 1.48	22.77 \pm 4.27	17.36 \pm 0.83	18.03 \pm 6.15	25.16 \pm 1.37	25.22 \pm 6.47	34.88 \pm 1.55

Table 1: Summary table of the photopic (background: 30 $\text{cd}\cdot\text{m}^{-2}$) ERG a-wave, b-wave, OP₁₋₂, OP₃ and OP₄ amplitudes (μV) and peak time (ms) in human (flash intensity: 0.64 $\log \text{cd}\cdot\text{sec}\cdot\text{m}^{-2}$) and guinea pigs (flash intensity: 0.9 $\log \text{cd}\cdot\text{sec}\cdot\text{m}^{-2}$). Each data represents the mean \pm 1S.D.

9 Figures and legends

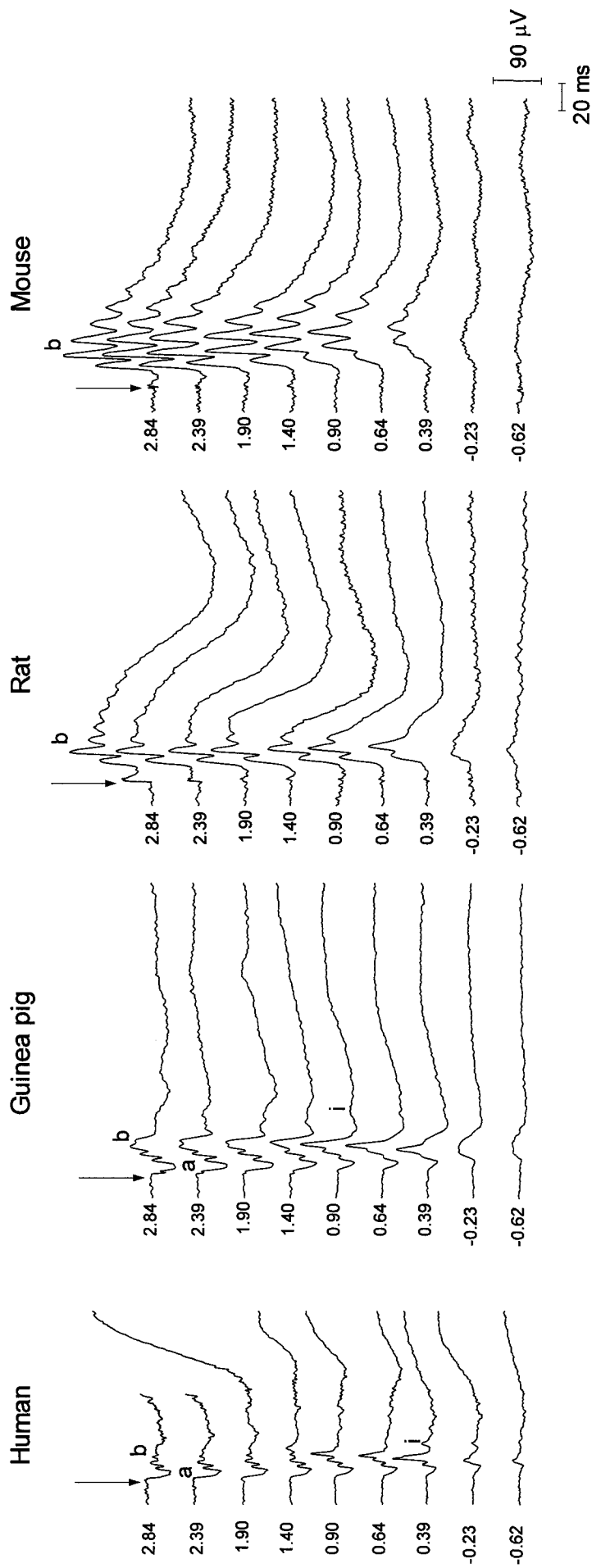


Figure 1: Representative photopic (stimulus intensity: $-0.62 \log \text{cd}\cdot\text{sec}\cdot\text{m}^{-2}$ to $2.84 \log \text{cd}\cdot\text{sec}\cdot\text{m}^{-2}$; background: $30 \text{ cd}\cdot\text{m}^{-2}$) electroretinograms luminance-response function recorded from a human, a guinea pig, a rat and a mouse. Vertical arrows identify flash onset, (a) a-wave, (b) b-wave, (i) i-wave. Horizontal calibration: 20 ms. Vertical calibration: 90 μV .

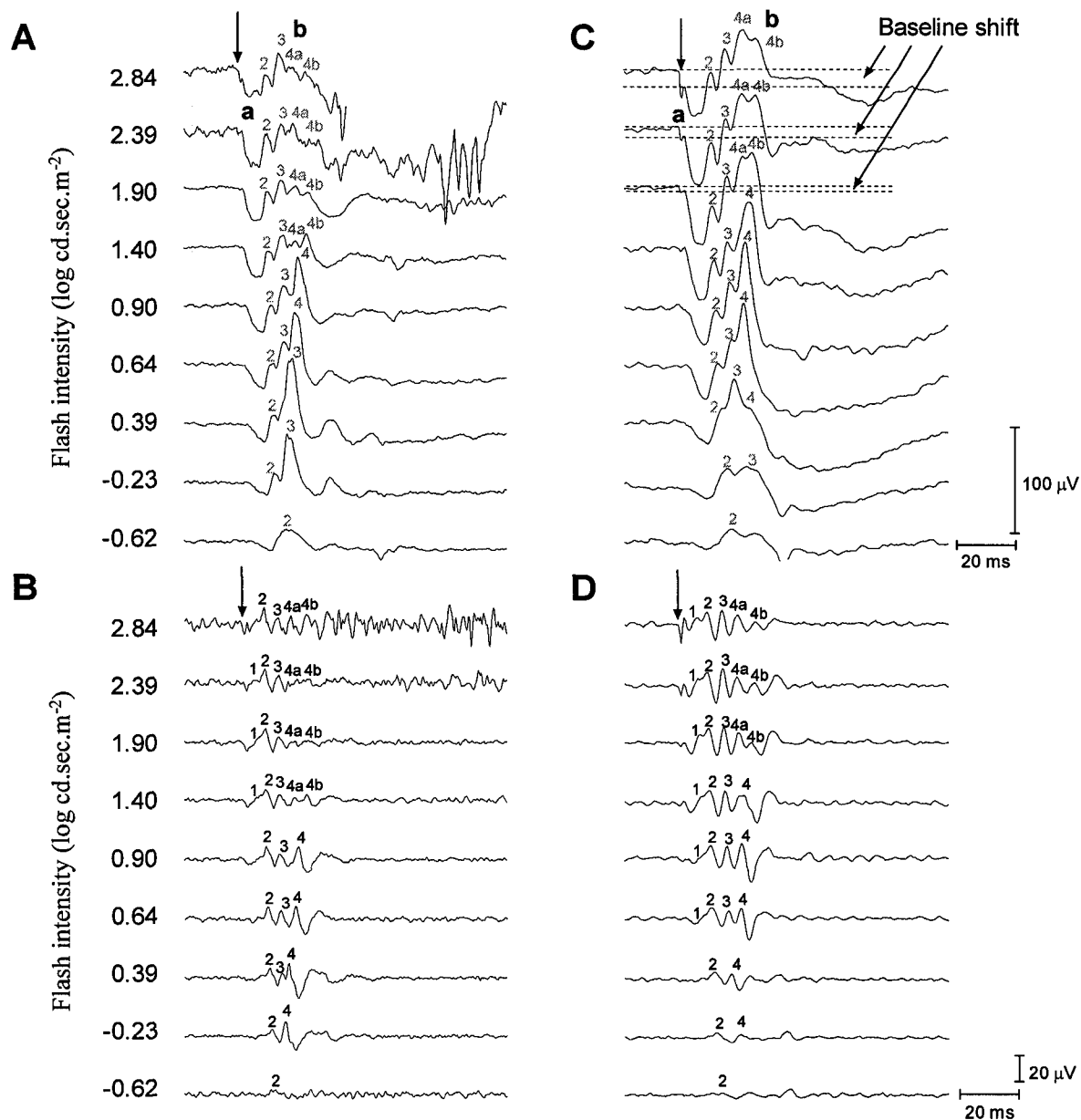


Figure 2: Representative photopic (stimulus intensity range from -0.62 to 2.84 log cd.sec.m⁻² as indicated at left of each tracing; background: 30 cd.m⁻²) ERGs (A, C) and OPs (B, D) luminance-response function recorded from a human (A, B) and a guinea pig (C, D). Vertical arrows identify flash onset, (a) a-wave, (b) b-wave, (1) OP₁, (2) OP₂, (3) OP₃, (4a) OP_{4a}, (4b) OP_{4b}. Horizontal calibration: 20 ms. Vertical calibration: 100 μV (ERG); 20 μV (OP).

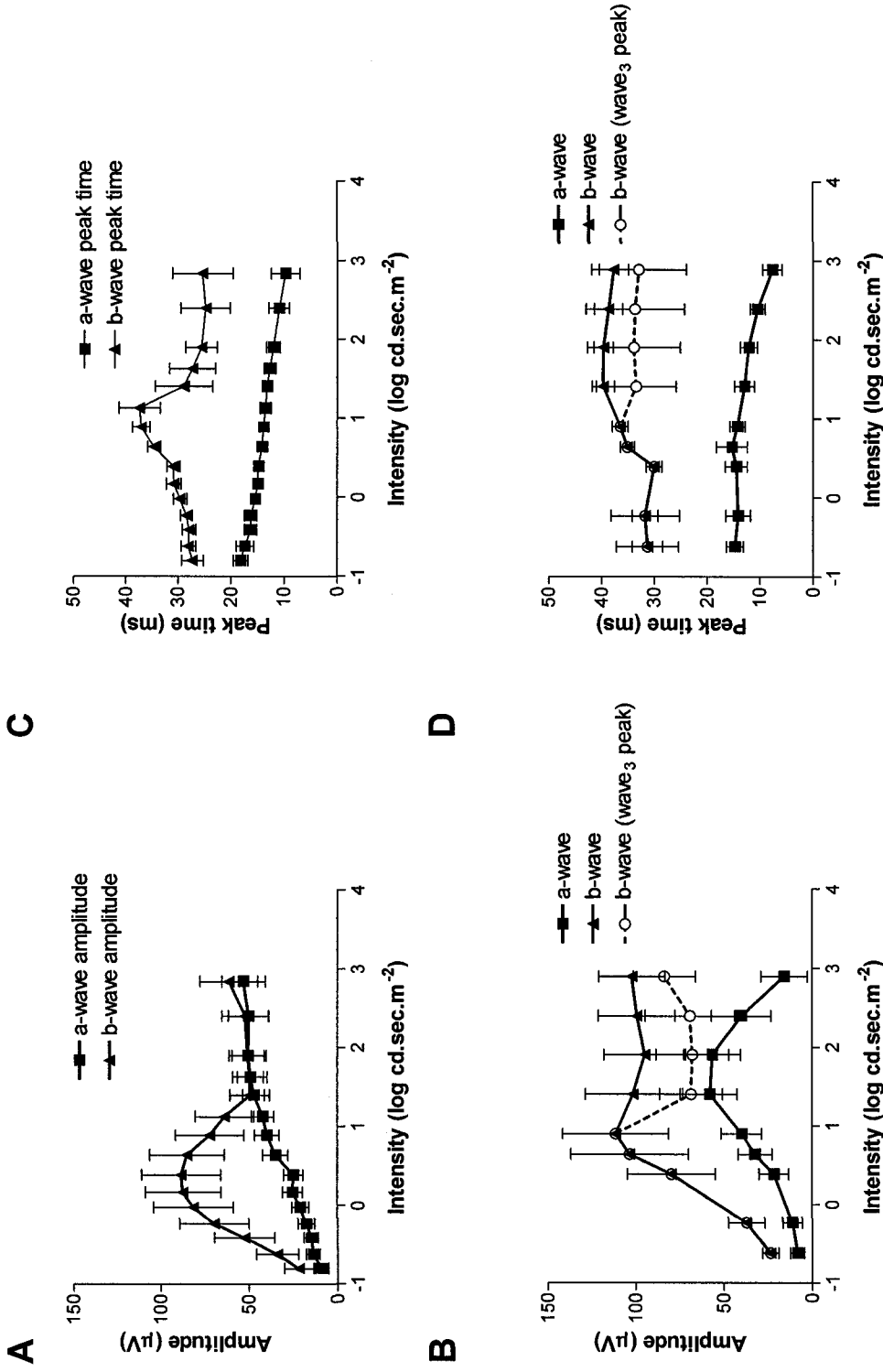


Figure 3: Photopic (background: $30 \text{ cd} \cdot \text{m}^{-2}$) ERG luminance response curves [amplitude (A, B), peak time (C, D)] for the a-wave (■), the b-wave (▲), and b-wave measured at wave 3 peak for the guinea pig (○) obtained from human (A, C) and guinea pigs (B, D). Each data point represents the mean ± 1 S.D. The ordinate represents the amplitude (μV) (A, B) or the peak time (ms) (C, D) while the abscissa represents the intensity of the flash ($\log \text{cd} \cdot \text{sec} \cdot \text{m}^{-2}$).

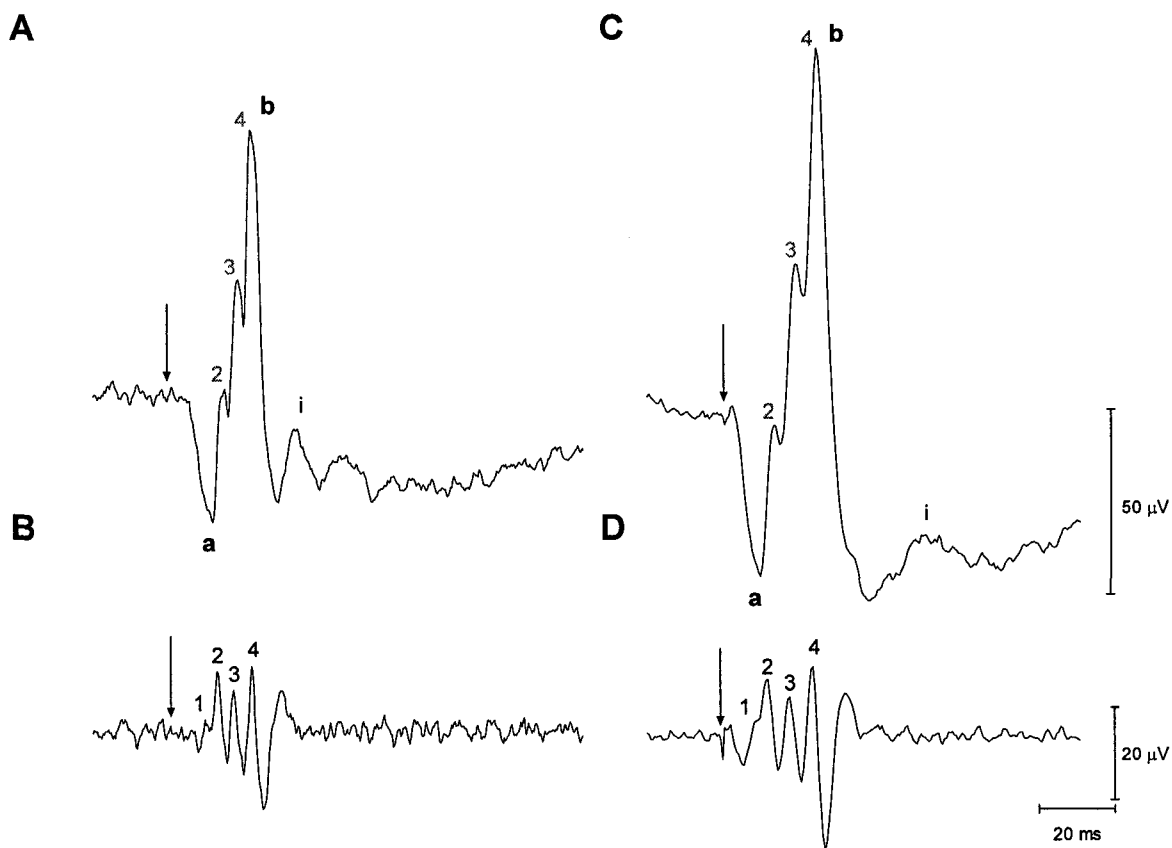


Figure 4: Photopic electroretinograms (A, C) and oscillatory potentials (B, D) recorded from a human (stimulus intensity: $0.64 \log \text{cd} \cdot \text{sec} \cdot \text{m}^{-2}$; background: $30 \text{cd} \cdot \text{m}^{-2}$: (A, B)) and a guinea pig (stimulus intensity: $0.90 \log \text{cd} \cdot \text{sec} \cdot \text{m}^{-2}$; background: $30 \text{cd} \cdot \text{m}^{-2}$: (C, D)). Vertical arrows identify flash onset, (a) a-wave, (b) b-wave, (i) i-wave, (1) OP₁, (2) OP₂, (3) OP₃, (4) OP₄. Horizontal calibration: 20 ms. Vertical calibration: 50 μV (ERG); 20 μV (OP).

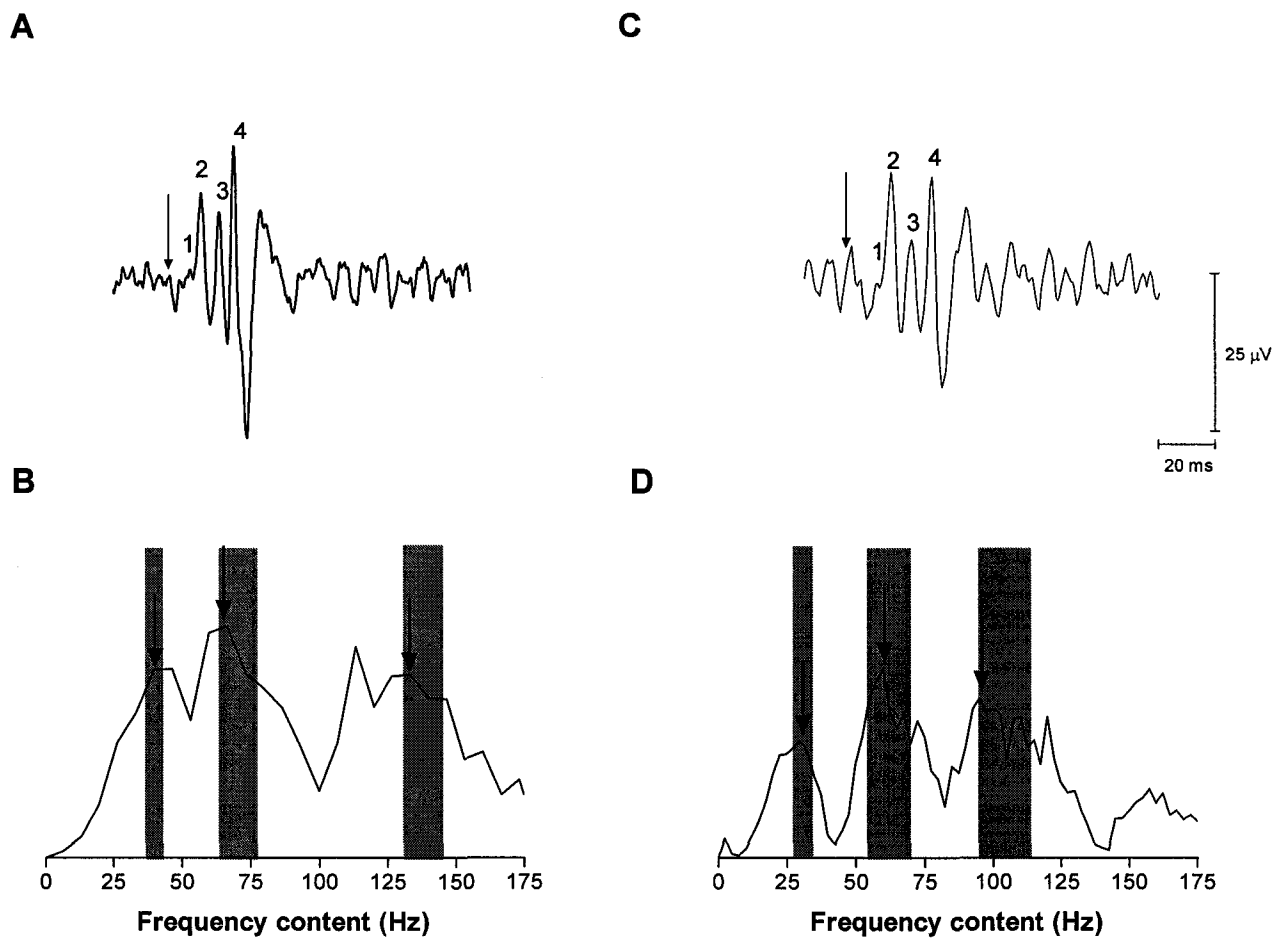


Figure 5: Representative photopic (background: 30 cd.m^{-2}) oscillatory potentials (A, C) recorded from a human (flash intensity: $0.64 \text{ log cd.sec.m}^{-2}$: (A)) and a guinea pig (flash intensity: $0.90 \text{ log cd.sec.m}^{-2}$: (C)). Fast-Fourier transforms (B, D) were obtained from the photopic oscillatory potentials represented in panel A and C. Vertical arrows identify flash onset, (1) OP₁, (2) OP₂, (3) OP₃, (4) OP₄. Horizontal calibration: 20 ms. Vertical calibration: $25 \mu\text{V}$ (OP).

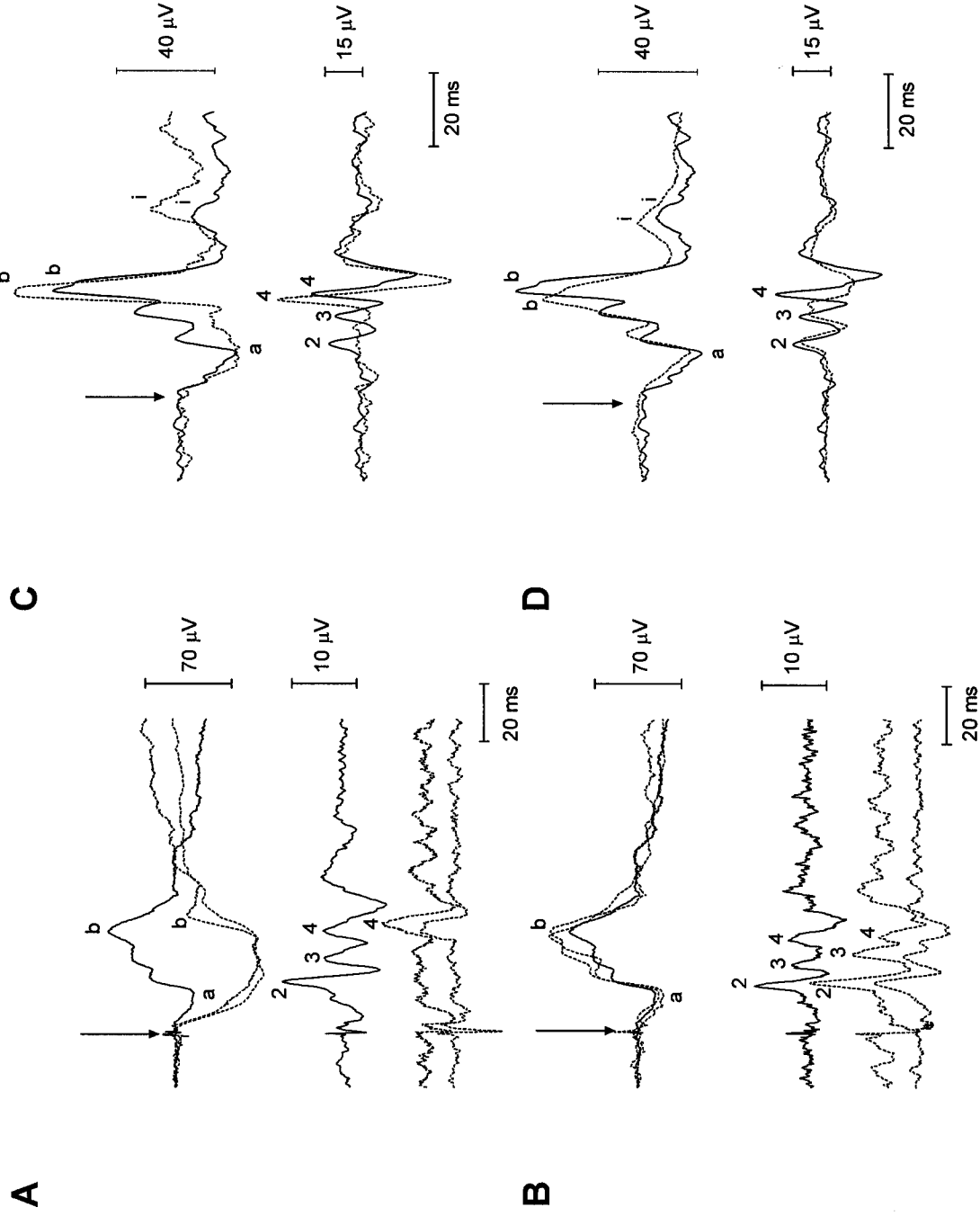


Figure 6: Representative photopic (solid lines; background: 30 cd.m^{-2}) ERGs and OPs recorded from guinea pigs (flash intensity: $0.9 \text{ log cd.sec.m}^{-2}$; A, B) following intravitreal injection (dashed lines) of L-AP-4 (A) and KYN (B). Results are compared to ERG recorded from human subjects (flash intensity: $0.64 \text{ log cd.sec.m}^{-2}$; C, D), affected with either CSNB with myopia (C) or cone dystrophy (D). Vertical arrows identify flash onset, (a) a-wave, (b) b-wave, (i) i-wave, (j) j-wave, (2) OP₂, (3) OP₃, (4) OP₄. Horizontal calibration: 20 ms. Vertical calibration: $70 \text{ } \mu\text{V}$ (ERG); $10 \text{ } \mu\text{V}$ (OP) [A, B]; $40 \text{ } \mu\text{V}$ (ERG); $15 \text{ } \mu\text{V}$ (OP) [C, D].

CHAPTER IV: MANUSCRIPT 3

Racine J., Behn D., Simard E., Lachapelle P. (2003) Spontaneous occurrence of a potentially night blinding disorder in guinea pigs. *Doc Ophthalmol*, 107: 59-69.

1 Preface to chapter IV

During the course of our experiments, an accidental mating between a brother and a sister (albino guinea pigs) occurred. From this union, four guinea pig pups were born and one of them yielded abnormal ERG recordings suggestive of a rod disorder.

Since only few spontaneous animal model of retinal disorders are described in the literature, in this third study, we document the functional retinal anomalies found in this naturally occurring animal model hoping that it will help us better understand the pathophysiological processes involved in this retinopathy.

2 Abstract

Several hereditary retinal disorders such as retinitis pigmentosa (RP) and Congenital Stationary Night Blindness (CSNB) compromise, sometimes exclusively, the activity of the rod pathway. Unfortunately, there are few animal models of these disorders that could help us better understand the pathophysiological processes involved. The purpose of this report is to present a pedigree of guinea pigs where, as a result of a consanguineous mating and subsequent selective breeding, we developed a new and naturally occurring animal model of a rod disorder. Analysis of the retinal function with the electroretinogram reveals that the threshold for rod-mediated electroretinograms (ERGs) is significantly increased by more than 2 log-units compared to that of normal guinea pigs. Furthermore, in response to a suprathreshold stimulus, also delivered under scotopic condition, which yield a mixed cone-rod response in normal guinea pigs, the ERG waveform in our mutant guinea pigs is almost identical (amplitude and timing of a- and b-waves) to that evoked in photopic condition. The above would thus suggest either a structural (abnormal development or absence) or a functional deficiency of the rod photoreceptors. We believe that our pedigree possibly represents a new animal model of a night blinding disorder, and that this condition is inherited as an autosomal recessive trait in the guinea pig population.

3 Introduction

Several retinal disorders share night blindness as their initial symptom. However, while in some conditions, nyctalopia will remain the only symptom the patient will ever complain of, in several others, vision will progressively deteriorate to include day vision impairment as well. For example, Congenital

Stationary Night Blindness (CSNB) is described as a set of inherited, non-progressive retinal conditions in which the rod pathway is primarily affected resulting in an elevation of the dark-adapted threshold [1,2,3,4]. CSNB can be inherited either as an autosomal recessive, autosomal dominant, or x-linked trait [5]. In human, several subtypes may be distinguished on the basis of measurements of retinal function, namely: CSNB with normal fundi and CSNB with abnormal fundi. The former includes the Schubert-Bornschein type, the Riggs type as well as the Nougaret type whereas the latter includes the Oguchi's disease and Fundus albipunctatus [1].

The Riggs and Nougaret types of CSNB present attenuated a- and b-waves in both photopic and scotopic conditions. The Riggs type is less frequent and no clear mode of inheritance has been identified. The Nougaret type on the other hand is more frequent and is inherited as an autosomal dominant trait [5]. The Schubert-Bornschein type of CSNB is characterized by an absence of the dark-adapted, bright-flash ERG b-wave and by a unique negative shape electroretinogram (ERG) due to a normal a-wave amplitude and a suppressed b-wave [5]. Based on the evaluation of the rod ERG and the dark adaptation period, two major groups can be distinguished in the Schubert-Bornschein type. The complete type is characterized with an absence of rod-mediated function and a normal cone-mediated function while the incomplete type demonstrate a rod-ERG impairment accompanied with an anomaly of the cone function [5,6,7].

In the present study we report a naturally occurring guinea pig model of what we believe could be, based on the analysis of the rod- and cone-mediated ERGs, a form of night blindness. Although it remains to be determined if the phenotype (and genotype) of our guinea pig is homologous to a human form of a night blinding disorder, results suggest that this new animal model could represent a valid model to study the pathophysiological processes which are involved in generating a functional retinal disorder such as those encountered in humans.

4 Material and Methods

A total of 42 Hartley albino guinea pigs (*Cavia porcellus*) were included in this study out of which 31 were found to be normal and 11 night blind as determined by ERG. All animals were kept in a cyclic environment of 12 hours of light (30 cd.m^{-2}) and 12 hours of dark. Results presented in this study were obtained from young animals aged 10 days old since unlike rats and mice, guinea pigs are born with their eye open and a nearly mature retina. Prior to ERG measurements, guinea pigs were anaesthetised under dim red light with an intramuscular injection of a mixture of ketamine (85 mg/kg) and xylazine (5 mg/kg). The animals had their pupils dilated with drops of 1% cyclopentolate hydrochloride after which they were placed in a ganzfeld-like box of our design in which the temperature remained at 23 degrees throughout the recording period. [8-10]. ERGs were recorded with a DTL electrode (27/7 X-Static silver coated conductive nylon yarn : Sauquoit Industries, Scranton, PA, USA) with reference (Grass E5 disc electrode, Grass Instruments, Quincy, MA, USA) and ground (Grass E2 subdermal electrode, Grass Instruments, Quincy, MA, USA) electrodes placed in the mouth and subcutaneously in the neck, respectively. This study was conducted in accord with the ARVO statement on the use of animals in research and performed following a protocol reviewed and approved by the McGill University-Montreal Children's Hospital Animal Care Committee.

Scotopic, full-field, flash ERGs were recorded following a period (overnight) of dark adaptation to which an extra five minutes of dark adaptation was added following the instrumentation of the animals. The responses were generated with flashes of white light (Grass PS 22 photostimulator, Grass Instruments, Quincy, MA, USA; flash duration: 20 μsec .) spanning over a 6 log-unit range. The intensity of the flash was increased in steps of 0.3 log unit (maximum intensity: $0.6 \text{ log cd.sec.m}^{-2}$). For each intensity, averages of 2 responses were collected at an inter-stimulus interval of 10 seconds. Immediately

after the scotopic recording, the photopic background light (30 cd.m^{-2}) was opened and cone-mediated ERGs were recorded following exposure for 20 minutes to this background. Two intensities of flashes (0.6 and $0.9 \text{ log cd.sec.m}^{-2}$) were used and presented against this photopic background. Averages of 10 responses (interstimulus interval: 1.024 seconds) were obtained.

In order to further document the functional anomaly of this retinal condition, ERGs evoked to flashes of a longer duration were also obtained with the use of a stimulator previously described [11]. These photopic ERGs were generated in response to flashes of white light (Halogen lamp; 12Volts, 100 Watts) of 125 cd.m^{-2} in energy delivered against a background of 15 cd.m^{-2} . The duration of the stimulus was extended to 200 msec. with the use of an electromagnetic shutter (Uniblitz electronic shutter, Vincent Associates, Rochester, NY) and averages of 20 responses (interstimulus interval: 1.024 seconds) were taken.

Broadband electroretinograms (bandwidth: 0.3-1000 Hz; 10000X) and oscillatory potentials (bandwidth: 100-1000 Hz; 50000X) were recorded simultaneously with the use of the Acknowledge data acquisition system (Biopac MP 100 WS, BIOPAC System Inc., Goleta, Ca, USA) and all ERG responses included a 20 msec baseline recording prior to the onset of the stimulus. Analysis of the ERG waveform was performed as recommended [12]. The amplitude of the a-wave was measured from baseline to the first negative trough, while the amplitude of the b-wave was measured from the trough of the a-wave to the most positive peak of the response. Scotopic luminance-response function curves were obtained by plotting the amplitude of the b-wave against the intensity of the flash stimulus used to evoke the response. From that curve, the V_{max} value was defined as the amplitude of the b-wave measured in the ERG where a clear a-wave could be observed for the first time (e.g. a-wave threshold). The amplitude of each OP was measured from the preceding trough to peak. Only the first three major OPs (e.g.: OP₂, OP₃, OP₄) of responses evoked to the highest photopic and scotopic

intensities (e.g. 0.9 and 0.6 log cd.sec.m⁻², respectively) were considered. Their amplitudes were summated to yield the photopic and scotopic sum of OPs variable (e.g. SOPs= OP₂ + OP₃ + OP₄). It should be noted that since OP₁ was often difficult to identify accurately, we opted to include it in the measurement of OP₂. Consequently, the amplitude of OP₂ always reflected the portion of the signal comprised between the first negative trough that followed the onset of the stimulus and the peak of OP₂. In responses produced to flashes of longer duration, ON and OFF components were evaluated separately. The amplitude of the a- and b-waves of the ON-ERG were measured as described above. Following the ON-ERG b-wave, the signal rapidly returned to a value significantly below the baseline. This component of the response, identified as the post b-wave electronegativity (n), was measured from the baseline to the peak of this negative segment. Similarly, the OFF stimulus generated a series of small oscillations, the amplitude of which, measured from the preceding trough to peak, were summated to represent the OFF-ERG response. Statistical analysis, which compared the data obtained from the night blind guinea pig with that of normal guinea pigs, was performed using a Student t-test for independent samples (p<0.05).

5 Results

Figure 1 illustrates the pedigree of our guinea pig colony where, as a result of a consanguineous mating (II-1 and II-2) one of the four siblings, a male (III-4), presented with an ERG anomaly suggestive of a rod defect. To date, as a result of selective breeding, we have been able to reproduce this electrophysiological phenotype another 10 times. Pedigree analysis further reveals that out of the 11 affected, 9 were males and 2 were females and that the mode of inheritance is most probably autosomal recessive.

The electroretinographic anomalies that characterize the retinal disorder of our guinea pigs are best illustrated with the scotopic luminance-response function

shown in figure 2. As previously reported elsewhere [13-16] the normal morphology of the guinea pig's electroretinogram is unique especially that evoked to bright flashes delivered in fully dark-adapted condition. As illustrated in figure 2, with progressively brighter flashes, there is an initial increase in the amplitude of the slow rod-mediated b-wave (threshold at $-4.5 \log \text{ cd. sec. m}^{-2}$) up to a maximum amplitude, reached in response to the $-2.4 \log \text{ cd. sec. m}^{-2}$ stimulus, following which the amplitude of the b-wave gradually reduces while the OPs become a more prominent feature of the response (tracings -1.5 to $-0.9 \log \text{ cd. sec. m}^{-2}$). Further increases in the intensity of the stimulus, generate ERG responses where the a-wave contribution is progressively more important. At maximal intensity (tracing $0.6 \log \text{ cd. sec. m}^{-2}$), the amplitude of the a-wave exceeds that of the b-wave resulting in an ERG waveform of negative morphology, a feature previously reported elsewhere [13,16,17]. The unusual morphology of the scotopic bright flash ERG (mixed rod-cone) differs from the photopic signal produced in response to the same stimulus where, as seen in figure 2 (bottom two tracings) the morphology is no longer negative and in fact closely resembles that of human ERGs obtained under the same conditions.

In night blind animals, a scotopic b-wave is first noticed in response to a flash of $-2.1 \log \text{ cd. sec. m}^{-2}$, that is a value more than 2.4 log-units brighter than the normal scotopic threshold and in fact beyond the normal scotopic V_{\max} ($-2.4 \log \text{ cd. sec. m}^{-2}$). As shown in table 1, the amplitude of the rod V_{\max} ($35.90 \pm 8.5 \mu\text{V}$) which is evoked in response to a flash of $-1.2 \log \text{ cd. sec. m}^{-2}$ in night blind guinea pigs is significantly reduced ($p < 0.05$) compared to normal ($91.52 \pm 28.5 \mu\text{V}$). Furthermore, unlike the normal guinea pigs where a further increase in the intensity of the flash causes an initial reduction in the amplitude of the b-wave, the scotopic ERG b-wave of our night blind guinea pigs continues to grow as the stimulus becomes brighter. The latter b-wave increase is not, unlike in normal guinea pigs, accompanied by a marked enhancement of the a-wave contribution. At maximal intensity, the amplitudes of the a-wave in night blind guinea pigs ($24.5 \pm 9.7 \mu\text{V}$) is significantly ($p < 0.05$: table 1) reduced compared to normal

($113.28 \pm 50.7 \mu\text{V}$), while the b-wave amplitude (night blind: $126.7 \pm 20.1 \mu\text{V}$; normal: $139.3 \pm 34.3 \mu\text{V}$; $p > 0.05$: table 1) does not significantly differ from normal. Finally while the timing of the mixed (rod-cone) a- and b-wave peaks are not different ($p > 0.05$) from normal, that of the rod V_{max} is significantly shorter ($p < 0.05$; table 1) in night blind ($41.30 \pm 1.8 \text{ msec}$) compared to normal ($54.57 \pm 4.7 \text{ msec}$).

The above ERG differences between the normal and night blind guinea pigs contrast with the findings obtained in photopic conditions where they both yield nearly equivalent ERG waveforms of similar morphologies, amplitudes and timings. The only two differences noted are a significant reduction in the amplitude of the a-wave ($15.09 \pm 8.5 \mu\text{V}$ compared to $25.73 \pm 5.9 \mu\text{V}$; $p < 0.05$, table 1) and a significant increase in the timing of the b-wave ($40.57 \pm 2.7 \text{ msec}$ compared to $37.26 \pm 2.6 \text{ msec}$; $p < 0.05$, table 1) affecting the ERG of night blind guinea pigs. Furthermore, it is of interest to note that while the amplitudes (a- and b-waves), timings and morphologies of the bright flash photopic and scotopic ERGs are significantly different from each other in normal, they are almost identical in responses obtained from night blind guinea pigs (figure 2 and table 1). The latter would suggest that at maximal intensity the scotopic ERG recorded from our night blind guinea pigs is generated solely through the activation of the cone pathway.

In figure 3 are compared the scotopic luminance-response function (closed symbols) obtained from all our normal and night blind guinea pigs. These values are also compared to the photopic responses evoked to the brightest flashes (open symbols). In normal guinea pigs, the amplitude of the a-wave grows regularly and quite significantly as the intensity of the stimulus increases. Analysis of the data shown in figure 3 reveals that the a-wave increases from $12.70 \pm 7.0 \mu\text{volts}$ ($-2.4 \log \text{ cd}\cdot\text{sec}\cdot\text{m}^{-2}$ stimulus) to $113.28 \pm 50.7 \mu\text{volts}$ ($0.6 \log \text{ cd}\cdot\text{sec}\cdot\text{m}^{-2}$ stimulus), representing an overall increase of almost 850 times ($p < 0.05$). In comparison, the amplitude of the a-wave of our night blind guinea pigs grows from $13.46 \pm 6.37 \mu\text{volts}$ ($-1.2 \log \text{ cd}\cdot\text{sec}\cdot\text{m}^{-2}$ stimulus) to $24.5 \pm 9.6 \mu\text{volts}$ ($0.6 \log \text{ cd}\cdot\text{sec}\cdot\text{m}^{-2}$

stimulus) representing a smaller, but nonetheless significant 82% increase ($p < 0.05$). Clearly, compared to our normal population, the increase in a-wave amplitude brought with brighter flashes is significantly less ($p < 0.05$) pronounced in night blind guinea pigs. In fact, irrespective of the intensity of the flash used, the amplitude of the scotopic a-wave is always significantly smaller in responses recorded from our night blind guinea pigs ($p < 0.05$, figure 3). Furthermore, in normal, the increase in a-wave amplitude during dark-adaptation (compare photopic and scotopic a-wave amplitudes in table 1: $>300\%$ gain; $p < 0.05$) is significantly larger ($p < 0.05$) than the non-significant 60% increase (table 1; $p > 0.05$) measured for our night blind guinea pigs. This finding further exemplifies the similarities shared between the photopic and scotopic ERGs of our night blind guinea pigs, a feature never observed in normal.

Figure 3 also compares the luminance-response functions that describe the scotopic b-waves of the normal and night blind guinea pigs. In normal, the amplitude of the rod b-wave first increases to a maximum (rod V_{\max} : 91.52 ± 28.5 μ volts; table 1) in response to a flash of $-2.4 \log \text{cd}\cdot\text{sec}\cdot\text{m}^{-2}$ in intensity, following which it decreases steadily to reach, in response to a stimulus of $-1.2 \log \text{cd}\cdot\text{sec}\cdot\text{m}^{-2}$ an amplitude of 55 ± 26.9 μ volts, a value not significantly different ($p > 0.05$) from the 52.1 ± 13.2 μ volts measured for rod b-waves evoked to dimmer ($-4.5 \log \text{cd}\cdot\text{sec}\cdot\text{m}^{-2}$) flashes. The amplitude of the b-wave then increases almost linearly to a maximum value of 139.3 ± 34.3 μ volts reached in response to a $0.6 \log \text{cd}\cdot\text{sec}\cdot\text{m}^{-2}$ stimulus. At that point, as shown in table 1, the amplitude of the scotopic b-wave is significantly different from that of the a-wave ($p < 0.05$, table 1), thus further exemplifying the fact that, in guinea pigs, the normal morphology of the scotopic mixed (rod-cone) ERG is negative and that the a-wave is the major contributor to this response. The above contrasts with the data obtained from our night blind guinea pigs, where the amplitude of the b-wave grows monotonically from 23.7 ± 6.8 μ volts (measured in response to a $-2.1 \log \text{cd}\cdot\text{sec}\cdot\text{m}^{-2}$ flash) to a maximum of 126.7 ± 20.2 μ volts (measured in response to a $0.6 \log \text{cd}\cdot\text{sec}\cdot\text{m}^{-2}$ flash). Comparing the intensity-response curves further show that for intensities

below $-1.2 \log \text{cd}\cdot\text{sec}\cdot\text{m}^{-2}$ the amplitude of the b-wave of the normal guinea pig is significantly larger ($p < 0.05$) than that of the night blind guinea pig (figure 3b). However, in response to brighter flashes, their amplitudes are not significantly different from each other ($p > 0.05$). Once again, it is of interest to note that while in normal guinea pigs there is a small but significant 40% increase in b-wave amplitude with dark adaptation (compare photopic and scotopic mixed b-wave amplitudes; $p < 0.05$; table 1) in night blind guinea pigs the amplitudes remain basically the same ($p > 0.05$, table 1). The latter finding further stresses the abnormally high similarity between the scotopic and photopic responses in our night blind guinea pigs.

As illustrated in figure 4, the oscillatory potentials (OPs) were also severely affected in our night blind guinea pigs. In normal guinea pigs, the short latency scotopic OPs (e.g. OP₂ and OP₃) are initially observed in response to the $-2.1 \log \text{cd}\cdot\text{sec}\cdot\text{m}^{-2}$ stimulus. With increasing intensities, OPs of longer latencies are added to this threshold response. In contrast, in our night blind guinea pigs, an ill-defined scotopic OP₂ is first seen in response to the $-1.2 \log \text{cd}\cdot\text{sec}\cdot\text{m}^{-2}$ stimulus. Increasing the intensity of the stimulus will add another two to three OPs of longer latencies to the original one. Furthermore, in normals, OP₃ is the most prominent oscillatory potential of the dark-adapted response; a feature most obvious in responses evoked to the dimmest flashes (such as tracing -1.2). In contrast, OP₂ is the most prominent oscillatory potential of the dark-adapted responses of our night blind guinea pigs, especially in signals evoked to dimmer stimuli (such as tracing -0.3). The above differences result in a significant reduction in the amplitude of the scotopic SOP variable of our night blind guinea pigs (normal: $82.17 \pm 19.4 \mu\text{V}$, night blind: $14.33 \pm 8.9 \mu\text{V}$; $p < 0.05$, table 1). There is also a significant ($p < 0.05$, table 1) shortening of the interpeak intervals in the scotopic OP response of the night blind guinea pigs ($7.68 \pm 0.4 \text{ msec}$) compared to normal ($8.81 \pm 0.5 \text{ msec}$). In contrast, in photopic recordings, the SOP variable is significantly larger ($p < 0.05$, table 1) in responses evoked from the night blind guinea pigs ($21.76 \pm 5.7 \mu\text{V}$) compared to normal ($13.37 \pm 6.6 \mu\text{V}$), while the interpeak intervals are not significantly affected.

This study also examined the ERG responses evoked to flashes of longer duration. Examples of the tracings obtained in normal and night blind guinea pigs are shown in figure 5, while amplitude and peak time measurements of the different components are reported in table 2. Analysis of the ON-response included the a- and b-waves evoked at the onset of the flash as well as the post b-wave electronegativity (identified n in tracings 3) while analysis of the OFF-response only included the measurement of the OFF oscillations. As seen in figure 5 (and table 2), the amplitude of the ON a- and b-waves of the night blind guinea pigs (a: $9.4 \pm 2.9 \mu\text{V}$, b: $46.4 \pm 9.0 \mu\text{V}$) are not significantly different ($p > 0.05$) from normal (a: $10.3 \pm 1.9 \mu\text{V}$, b: $53.6 \pm 20.5 \mu\text{V}$). In contrast, the two signals differ significantly in peak times. In responses obtained from night blind guinea pigs, the timing of the a- and b-waves ($21.9 \pm 1.5 \text{ msec}$; $49.4 \pm 2.0 \text{ msec}$ respectively) are significantly prolonged compared to normal ($20.2 \pm 0.6 \text{ msec}$; $36.3 \pm 1.3 \text{ msec}$ respectively). Also, in responses obtained from our night blind guinea pigs (see figure 5, tracings 3) the slope (estimated with the dA/dT measure: table 2) of the descending segment of the ON b-wave is significantly less steep ($0.84 \pm 0.1 \mu\text{V/msec}$) compared to the normal value ($2.1 \pm 0.2 \mu\text{V/msec}$). Similarly, the amplitude of the post b-wave electronegativity (table 2) is significantly reduced in responses obtained from our night blind guinea pigs (normal: $32.8 \pm 11.7 \mu\text{V}$; night blind: $2.1 \pm 2.7 \mu\text{V}$; $p < 0.05$, table 2). Finally, the amplitude of the OFF component is also significantly attenuated in responses obtained from our night blind guinea pigs. While in normal guinea pigs, two to three rapid oscillations are seen (figure 5), in night blind only one broad oscillation is observed. This results in a significant attenuation of the OFF response amplitude ($p < 0.05$, table 2) in night blind guinea pigs ($8.8 \pm 5.2 \mu\text{V}$) compared to normal ones ($32.7 \pm 15.8 \mu\text{V}$), the latter resulting in a significant increase in the ON/OFF amplitude ratio in responses obtained from night blind guinea pigs (table 2).

6 Discussion

Results presented in this report support the claim that our guinea pigs suffer from a retinal anomaly whose key features are: (1) severe impairment of the scotopic (rod-mediated) ERG a- and b-waves as witnessed by the elevated thresholds as well as an abnormal, photopic-like, responses evoked to the brighter flashes; (2) elevated threshold for scotopic OPs to intensities well within the photopic range; (3) significantly attenuated OFF-ERG responses and ON-ERG post b-wave electronegativity. Data obtained with the short flash would suggest that the pathophysiological process is almost entirely limited to impairment of the rod pathway, although there is a significant enhancement of the photopic SOPs noted in our abnormal guinea pigs. This added to the ON-ERG anomalies reported could suggest that there is, although relatively minimal, also some repercussions in the cone pathway. Consequently, based on the above we suggest that our mutant guinea pigs are affected with a retinal disorder impairing primarily the normal functioning of the rod pathway, thus raising the possibility that our diseased guinea pigs might be night blind. Furthermore, this retinopathy initially occurred spontaneously as a result of a consanguineous mating of two guinea pigs purchased from a commercial supplier, suggesting that this phenotype would be transmitted as an autosomal recessive trait, a claim, which could be supported with our pedigree (figure 1).

The availability of naturally occurring animal models of retinal disorders that primarily affect the rod function such as *rd* (*retinal degeneration*) or *rds* (*retinal degeneration slow*) mice [18,19], are of the utmost importance in order to increase our understanding of the pathophysiological mechanisms at the origin of debilitating retinopathies such retinitis pigmentosa (RP). However, while in the above models the condition will rapidly deteriorates to impair the cone function as well [9,20], preliminary results would suggest that the retinopathy of our guinea pigs is limited to an anomaly of the rod function only [21,22]. Consequently, our

findings would suggest that our guinea pigs are affected with a form of congenital night blindness. Unfortunately, to date our understanding of the pathophysiological process at the origin of night blinding disorders such as congenital stationary night blindness (CSNB) is somewhat limited due to the rarity of this retinopathy in humans combined with the scarcity of animal models replicating this retinal malfunction, especially in animals whose retinas approach that of humans. In that respect our guinea pig model is interesting since unlike rats and mice, guinea pigs behave more like diurnal animals. Also, while the retinas of rats and mice include approximately 1.5% [23] and 3% [24] cones, respectively, that of guinea pigs is composed of 8 to 17% of cones depending on retinal location [25].

To our knowledge, of all the animal models of spontaneously occurring retinopathies published to date, none presented a retinal disorder with no evidence of a rod-mediated function and where the bright flash scotopic and photopic ERGs are almost indistinguishable from each other, that is ERG features suggesting that only the cones are functional [26-30]. Clearly the photopic ERGs of our abnormal guinea pigs suggest a near normal cone-mediated retinal function, a claim well supported with the waveforms shown in figure 2 and the data reported in table 1. The similarity between photopic and scotopic bright flash ERGs of our night blind guinea pigs is even more striking when one takes into consideration the unusual morphology of the bright flash scotopic ERG which characterizes the normal waveform. Bright flash scotopic ERGs of similar, photopic-like, shape were previously shown to characterize the rhodopsin knockout mice, an animal model that was presented as an all-cone-retina [31,32]. A similar ERG phenotype (e.g. normal cone ERG and cone-like ERG in scotopic conditions) was also shown to characterize mice with a deletion in the RPE65 gene [33]. However, recent evidence would suggest that in the latter model, the ERG is not mediated by cones but rather most probably by rod system [34]. Similarly the transgenic rod transducin alpha-subunit mice ($\text{tr}\alpha^{-/-}$) did not produced rod-driven responses while the cone-driven components were normal [35,36]. The high degree of

similarity between the bright flash scotopic and photopic ERGs in our night blind guinea pigs is further supported with our findings that while, in normal, the amplitude of the scotopic a-wave is about 5 times larger than the photopic one, in our night blind guinea pigs there is basically no amplitude differences between the photopic and scotopic a-waves; a finding which would suggest an absence of rod photoreceptor response. However, only histological studies (including immunohistochemical analysis) will confirm if the ERG anomaly of our night blind guinea pigs result from an absence (structural or functional) of rods in their retina.

Analysis of the oscillatory potentials (OPs) also revealed interesting functional anomalies with our night blind guinea pigs. While in scotopic condition all OPs were smaller than normal, the photopic SOPs of our night blind guinea pigs were significantly larger than normal. Combining the latter finding with our observation of a slightly (but not significantly) larger amplitude for the short flash photopic b-wave as well as a significantly smoother descending limb of the photopic b-wave (smaller than normal dA/dT) would suggest, according to Sieving's PUSH-PULL concept of ERG b-wave genesis [37,38], a weaker PULL effect. In that respect, it is interesting to note that, in the human form of Congenital Stationary Night Blindness (type 1 CSNB), previous studies have shown that the anomaly resulted from a malfunction of the ON- retinal pathway, most probably at the synapse between the photoreceptors and the ON-depolarizing bipolar cells (ON-DBC) [37,39,40] while anomalies of the OFF-retinal pathway were suggested to characterize cone-related retinopathies [37]. Analysis of the ON-OFF ERG in type 1 CSNB indicates an almost exclusive anomaly of the ON ERG response [11,38], a feature which is not demonstrated in our guinea pigs. In fact if anything the OFF-ERG is markedly more affected compared to the ON-ERG, a finding that would suggest, according to Sieving's Push-Pull concept of ERG wave genesis, a retinal anomaly affecting the OFF-hyperpolarizing bipolar cells [37]. There was however an interesting anomaly of the ON-ERG response, namely the significant reduction in amplitude of the post

b-wave electronegativity. This ERG component, often referred to as the photopic negative response (PhNR) is said to arise at the level of the inner retina, as a consequence of spiking activity of the retinal ganglion cells [41-43]. However, it is not possible at this point to speculate if the abnormal PhNR should be interpreted as reflecting a direct or an indirect involvement of the retinal ganglion cells.

In summary, even though the functional retinal anomalies found in our guinea pig model of night blindness are not totally similar to human CSNB, our animal model could be a potential model to study the pathophysiological processes of the human like retinal disorder. Also of interest, our abnormal guinea pigs offer a unique opportunity to study cone function in the absence of functioning rods. However, in order to better understand the functional and structural anomalies that characterize our night blind guinea pigs, we need to ascertain its stationary nature with a longitudinal study as well investigate the structural anomaly (ies) with histology and immunohistochemistry.

7 References

1. Carr R E. Congenital stationary night blindness. In Heckenlively, J.R. & Arden, G.B. (Eds). Principles and practice of clinical electrophysiology of vision 1991:713-725.
2. Ripps H. Night blindness revised: From man to molecules. Invest Ophthalmol Vis Sci 1982; 23: 588 – 611.
3. Auerbach E, Godel V, Rowe H. An electrophysiological and psychophysical study of two forms of congenital night blindness. Invest Ophthalmol Vis Sci 1969; 8: 32.
4. Riggs LA. Electroretinography in cases of night blindness. Am J Ophthalmol 1954; 38: 70.
5. Miyake Y, Yagasaki K, Horiguchi M, Kawase Y, Kanda T. Congenital stationary night blindness with negative electroretinogram: a new classification. Arch Ophthalmol 1986; 104: 1013 – 1020.
6. Heckenlively JR, Martin DA, Rosenbaum AL. Loss of ERG oscillatory potentials, optic atrophy, and dysplasia in CSNB. Am J Ophthalmol 1983; 96: 525.
7. Lachapelle P, Little JM, Polomeno RC. The photopic electroretinogram in congenital stationary night blindness with myopia. Invest Ophthalmol Vis Sci 1983; 24: 442-450.
8. Dembinska O, Rojas LM, Varma DR, Chemtob S, Lachapelle P. Graded contribution of retinal maturation to the development of oxygen-induced retinopathy in rats. Invest Ophthalmol Vis Sci 2001; 42: 1111-1118.

9. Cayouette M, Behn D, Sendtner M, Lachapelle P, Gravel C. Intraocular gene transfer of ciliary neurotrophic factor prevents death and increases responsiveness of rod photoreceptors in the retinal degeneration slow mouse. *J Neurosci* 1998; 18: 9282-9293.
10. Lachapelle P, Blain L. A new speculum electrode for electroretinography. *J Neurosci* 1990; 32: 245-249.
11. Quigley M, Roy M-S, Barsoum-Homsy M, Chevrette L, Jacob J-L, Milot J. ON and OFF-responses in the photopic electroretinogram in complete-type congenital stationary night blindness. *Doc Ophthalmol* 1996; 92: 159-165.
12. Marmor MF. Standard for clinical electroretinography (1999 update). *Doc Ophthalmol* 1998; 97: 143-156.
13. Bui BV, Vingrys AJ. Development of receptor responses in pigmented and albino Guinea pigs (*Cavia porcellus*). *Doc Ophthalmol* 1999; 99: 151-170.
14. Bui BV, Weisinger HS, Sinclair AJ, Vingrys AJ. Comparison of guinea pig electroretinograms measured with bipolar corneal and unipolar intravitreal electrodes. *Doc Ophthalmol* 1998; 95: 15-34.
15. Bui BV, Sinclair AJ, Vingrys AJ. Electroretinograms of albino and pigmented guinea pigs (*Cavia porcellus*). *Aust N Z J Ophthalmol* (abstract) 1998; 26: S98.
16. Jutras S, Doke A, Chemtob S, Casanova C, Lachapelle P. Negative scotopic ERGs in Guinea pigs. *Invest Ophthalmol Vis Sci* (abstract) 1997; 38: S884.
17. Dassa J, Behn D, Casanova C, Lachapelle P. Maturation of the oscillatory potentials gradually shapes the unique morphology of the Guinea pig's electroretinogram. *Invest Ophthalmol Vis Sci* (abstract) 1998; 39: S132.

18. Farber DB. From mice to men: the cyclic GMP phosphodiesterase gene in vision and disease. *Invest Ophthalmol Vis Sci* 1995; 36: 263-275.
19. Molday RS. Peripherin/rds and rom-1: Molecular properties and role in photoreceptor cell degeneration. *Prog Ret Eye Res* 1994; 13: 271-299.
20. Chang B, Hawes NL, Hurd RE, Davisson MT, Nusinowitz S, Heckenlively JR. Retinal degeneration mutants in the mouse. *Vis Res* 2002; 42 : 517-527.
21. Racine J, Simard E, Gravel C, Casanova C , Lachapelle P. Spontaneous occurrence of complete and incomplete night blindness in a pedigree of guinea_pigs. *Invest Ophthalmol Vis Sci* (abstract) 2001; 42: B289.
22. Racine J, Gorgos A, Simard E, Lachapelle P. ON-OFF contribution to the photopic ERG of the night blind Guinea pig. *Invest Ophthalmol Vis Sci* (abstract) 2000; 41: B655.
23. LaVail MM, , Sidman M, Rausin R, Sidman RL. Discrimination of light intensity by rats with inherited retinal degeneration: a behavioral and cytological study. *Vis Res* 1974; 14:693-702.
24. Carter-Dawson L.D., LaVail M.M. Rods and cones in the mouse retina. 1- Structural analysis using light and electron microscopy. *J Comp Neurol* 1979; 1888: 245-262.
25. Szél À, Röhlich P. Two cone types of rat retina detected by anti-visual pigment antibodies. *Exp Eye Res* 1992; 55: 47-52.
26. Witzel, DA, Smith, EL, Wilson, RD, Aguirre, GD. Congenital stationary night blindness: an animal model. *Invest Ophthalmol Vis Sci* 1978; 17: 788 –795.
27. Narfstrom, K, Weigstad, A, Nilsson, SE. The Briard dog: a new animal model of congenital stationary night blindness. *Brit J Ophthalmol* 1989; 73: 750 –756.

28. Pardue MT, McCall MA, La Vail MM, Gregg RG, Peachey NS. A naturally occurring mouse model of X-linked congenital stationary night blindness. *Invest Ophthalmol Vis Sci* 1998; 39: 2443 – 2449.
29. Candille SI, Pardue MT, McCall MA, Peachey NS, Gregg RG. Localization of the mouse nob (no b-wave) gene to the centromeric region of the X chromosome. *Invest Ophthalmol Vis Sci* 1999; 40: 2748-2751.
30. Mukhopadhyay S, Candille S, Pardue MT, Ball SL, Peachey NS, McCall MA, Gregg RG. Physical mapping of the mouse X chromosome region containing the mouse nob gene. *Invest Ophthalmol Vis Sci* (abstract) 2000; 41: S 202.
31. Jaissle GB, May A, Reinhard J, Kohler K, Fauser S, Lütjen-Drecoll E, Zrenner E, Seeliger MW. Evaluation of the rhodopsin knockout mouse as a model of pure cone function. *Invest Ophthalmol Vis Sci* 2001; 42: 506-513.
32. Toda K, Bush RA, Humphries P, Sieving PA. The electroretinogram of the rhodopsin knockout mouse. *Vis Neurosci* 1999; 16: 391-398.
33. Redmond TM, Yu S, Lee E, Bok D, Hamasaki D, Chen N, Goletz P, Ma JX, Crouch RK, Pfeifer K. Rpe65 is necessary for production of 11-cis-vitamin A in the retinal visual cycle. *Nat Genet* 1998; 20: 344-351.
34. Seeliger MW, Grimm C, Stahlberg F, Friedburg C, Jaissle G, Zrenner E, Guo H, Reme CE, Humphries P, Hofmann F, Biel M, Fariss RN, Redmond TM, Wenzel A. New views on RPE65 deficiency: the rod system is the source of vision in a mouse model of Leber congenital amaurosis. *Nat Genet* 2001; 29: 70-74.

35. Dryja TP, Hahn LB, Reboul T, Arnaud B. Missense mutation in the gene encoding the alpha subunit of rod transducin in the Nougaret form of congenital stationary night blindness. *Nat Genet* 1996; 13: 358-360.
36. Calvert PD, Krasnoperova NV, Lyubarsky AL, Isayama T, Nicolo M, Kosaras B, Wong G, Gannon KS, Margolskee RF, Sidman RL, Pugh EN, Makino CL, Lem J. Phototransduction in transgenic mice after targeted deletion of the rod transducin alpha-subunit. *Proc Natl Acad Sci* 2000; 97: 13913-13918.
37. Sieving PA, Murayama K, Naarendorp F. Push-pull model of the primate photopic electroretinogram: A role for hyperpolarizing neurons in shaping the b-wave. *Vis Neurosci* 1994; 11: 519-532.
38. Sieving PA. Photopic ON- and OFF- pathway abnormalities in retinal dystrophies. *Trans Am Ophthalmol Soc* 1993; 91: 701-773.
39. Lachapelle P, Rousseau S, McKerral M, Benoit J, Polomeno RC, Koenekoop RK, Little JM. Evidence supportive of a functional discrimination between photopic oscillatory potentials as revealed with cone and rod mediated retinopathies. *Doc Ophthalmol* 1998; 95: 35-54.
40. Houchin KW, Purple RL, Wirtschafter JD. X-linked congenital stationary night blindness and depolarizing bipolar system dysfunction. *Invest Ophthalmol Vis Sci* (abstract) 1991; 32: B-1229.
41. Viswanathan S, Frishman LJ, Robson JG, Walters JW. The photopic negative response of the flash electroretinogram in primary open angle glaucoma. *Invest Ophthalmol Vis Sci* 2001; 42: 514-522.

42. Viswanathan S, Frishman LJ, Robson JG, Harwerth RS, Smith III EL. The photopic negative response of the macaque electroretinogram: Reduction by experimental glaucoma. *Invest Ophthalmol Vis Sci* 1999; 40: 1124-1136.

43. Colotto A, Falsini B, Salgarello T, Iarossi G, Galan AE, Scullica L. Photopic negative response of the human ERG: Losses associated with glaucomatous damage. *Invest Ophthalmol Vis Sci* 2000; 41: 2205-2211.

8 Tables and legends

	Normal		Night blind	
	Amplitude (μV)	Peak time (ms)	Amplitude (μV)	Peak time (ms)
Photopic a-wave	25,73 \pm 5,9 n=8	13,33 \pm 1,0 n=11	15,09 \pm 8,5 n=7 *	13,13 \pm 0,9 n=7
Photopic b-wave	97,23 \pm 26,1 n=12	37,26 \pm 2,6 n=11	105,33 \pm 41,5 n=7	40,57 \pm 2,7 n=7 *
Photopic SOP	13,37 \pm 6,6 n=11	7,88 \pm 0,4 n=11	21,76 \pm 5,7 n=7 *	8,04 \pm 0,8 n=7
Scotopic mixed a-wave	113,28 \pm 50,7 n=9	12,09 \pm 1,6 n=9	24,5 \pm 9,7 n=7 *	13,06 \pm 1,1 n=7
Scotopic mixed b-wave	139,3 \pm 34,3 n=9	42,25 \pm 6,7 n=9	126,7 \pm 20,1 n=7	43,71 \pm 1,3 n=7
Rod Vmax	91,52 \pm 28,5 n=9	54,57 \pm 4,7 n=9	35,9 \pm 8,5 n=7*	41,3 \pm 1,8 n=7*
Scotopic SOP	82,17 \pm 19,4 n=7	8,81 \pm 0,5 n=7	14,33 \pm 8,9 n=7 *	7,68 \pm 0,4 n=7 *

Table 1: Summary of amplitude and peak time measurements of short flash photopic and scotopic ERG parameters. All measurements were obtained from normal and night blind guinea pigs aged 10 days. Rod V_{max} was obtained at $-2.4 \log \text{cd} \cdot \text{sec} \cdot \text{m}^{-2}$ in normal and at $-1.2 \log \text{cd} \cdot \text{sec} \cdot \text{m}^{-2}$ in night blind. SOP= sum of all oscillatory potentials. SOP peak time represents mean interpeak interval time between $(OP_2-OP_3) + (OP_3-OP_4) / 2$.

* Significantly ($p < 0.05$) different from normal.

		Normal (n=10)	Night blind (n=6)
a-wave	Amplitude (μV)	10,3 \pm 1,9	9,4 \pm 2,9
	Peak time (ms)	20,2 \pm 0,6	21,9 \pm 1,5 *
b-wave	Amplitude (μV)	53,6 \pm 20,5	46,4 \pm 9,0
	Peak time (ms)	36,3 \pm 1,3	49,4 \pm 2,0 *
Electronegativity (μV)		32,8 \pm 11,7	2,1 \pm 2,7 *
dA/dT ($\mu V/ms$)		2,1 \pm 0,2	0,84 \pm 0,1 *
OFF-response amplitude (μV)		32,7 \pm 15,8	8,8 \pm 5,2 *
ON/OFF ratio		1.73 \pm 0,54	6.54 \pm 2.8 *

Table 2: Summary of amplitude measurements and peak time of long flash ERG. Measurements were obtained from normal (n=10) and night blind (n=6) guinea pigs aged 3 months. * Significantly ($p < 0.05$) different from normal.

9 Figures and legends

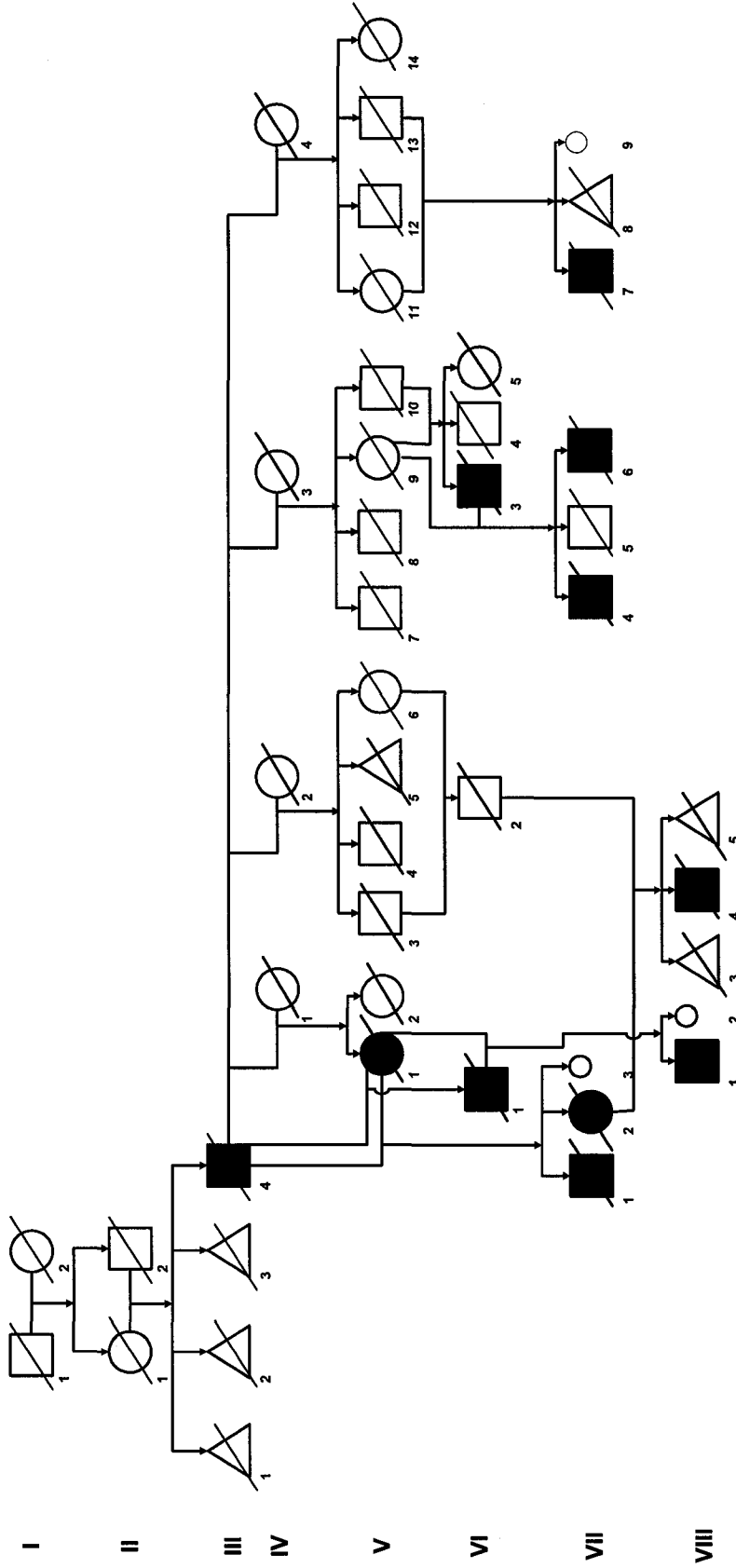


Figure 1: Pedigree of our night blind guinea pigs. O-Normal female, □-Normal male, ●-Affected guinea pigs, △-Euthanized before sex identification, O-Still born, ∅-Dead.

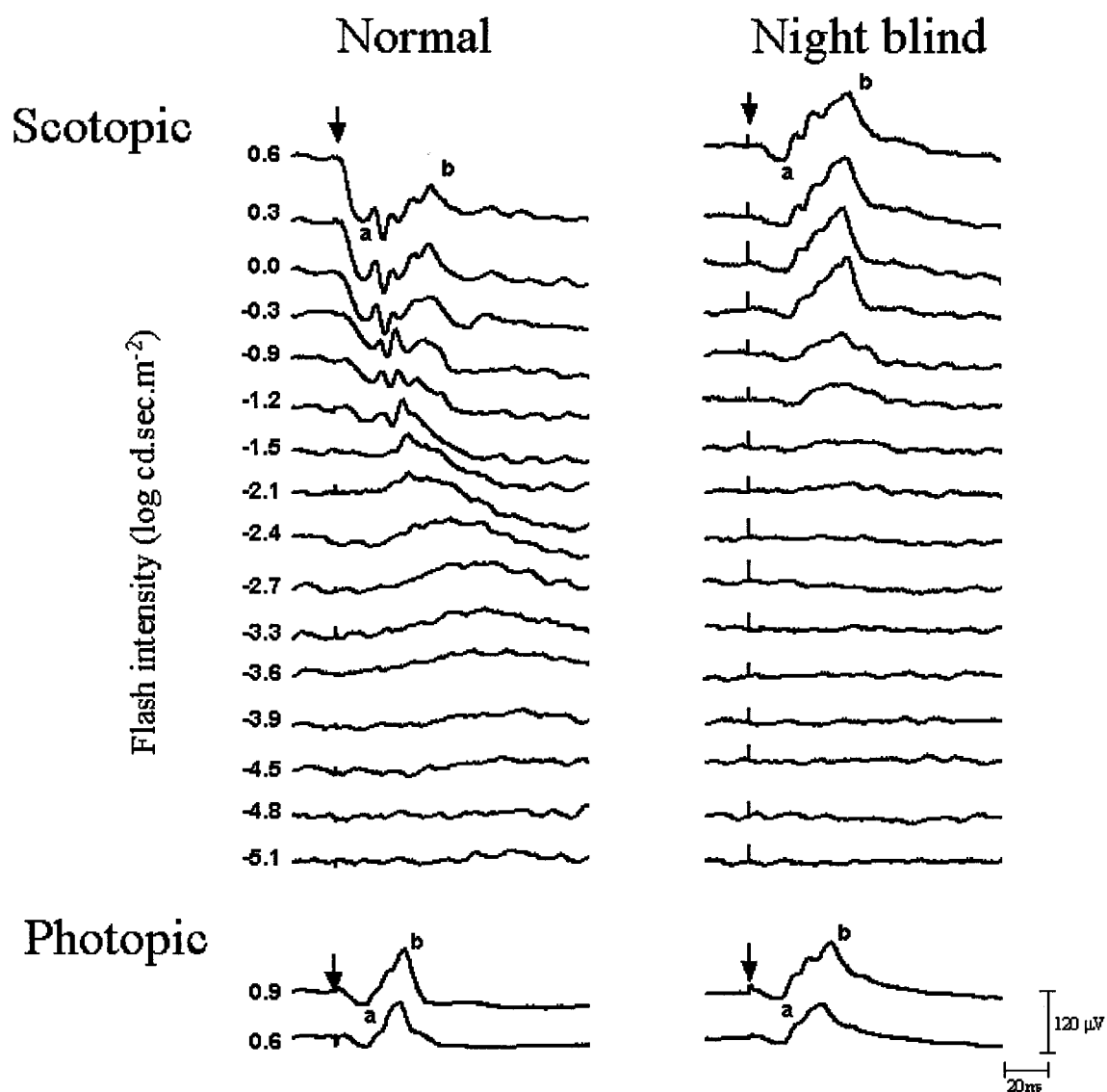


Figure 2: Short flash (20 μs) scotopic (stimulus intensity range from -5.1 to $0.6 \log \text{cd} \cdot \text{sec} \cdot \text{m}^{-2}$ as indicated at left of each tracing) and photopic (stimulus intensity: 0.6 and $0.9 \log \text{cd} \cdot \text{sec} \cdot \text{m}^{-2}$ as shown at left of each tracing) ERGs recorded from a normal (V-3) and a night blind (VI-1) guinea pig aged 10 days. Vertical arrows identify flash onset, a= a-wave, b= b-wave. Horizontal calibration: 20 ms. Vertical calibration: 120 μV .

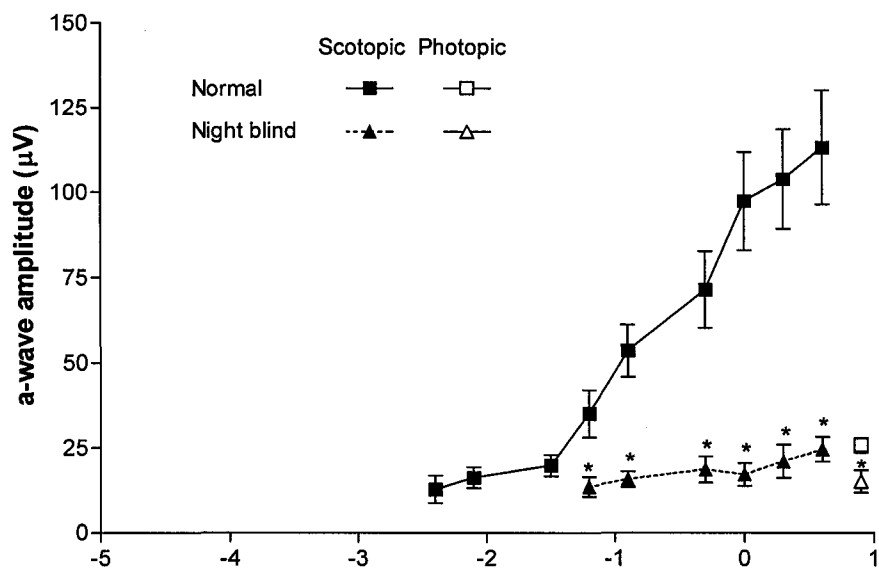
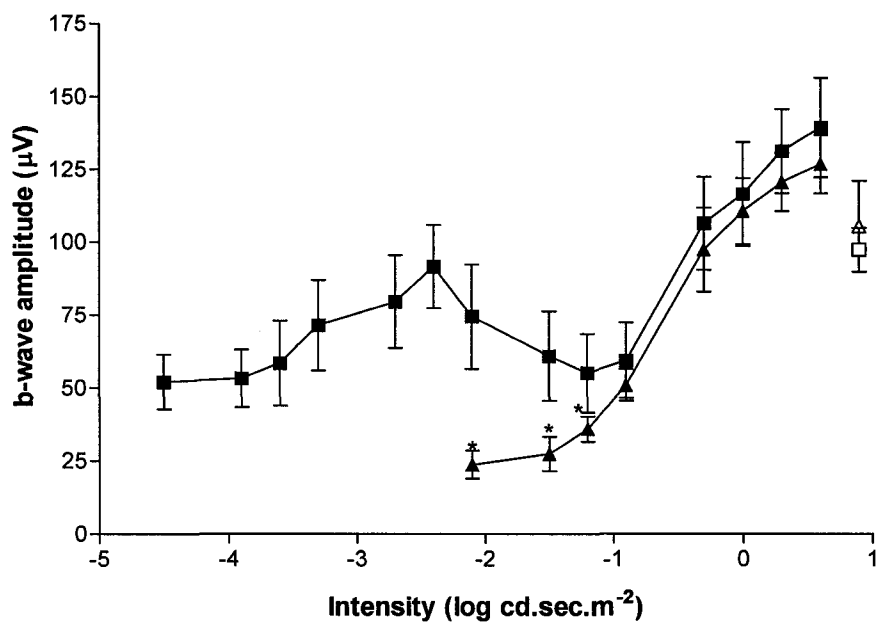
A**B**

Figure 3: Scotopic a- and b-waves (figure A and B respectively) intensity response functions obtained from normal (n=9; square data points) and night blind (n=7; triangle data points) guinea pigs aged 10 days. Filled and open symbols represent scotopic and photopic values respectively. * Significantly (p < 0.05) different from normal.

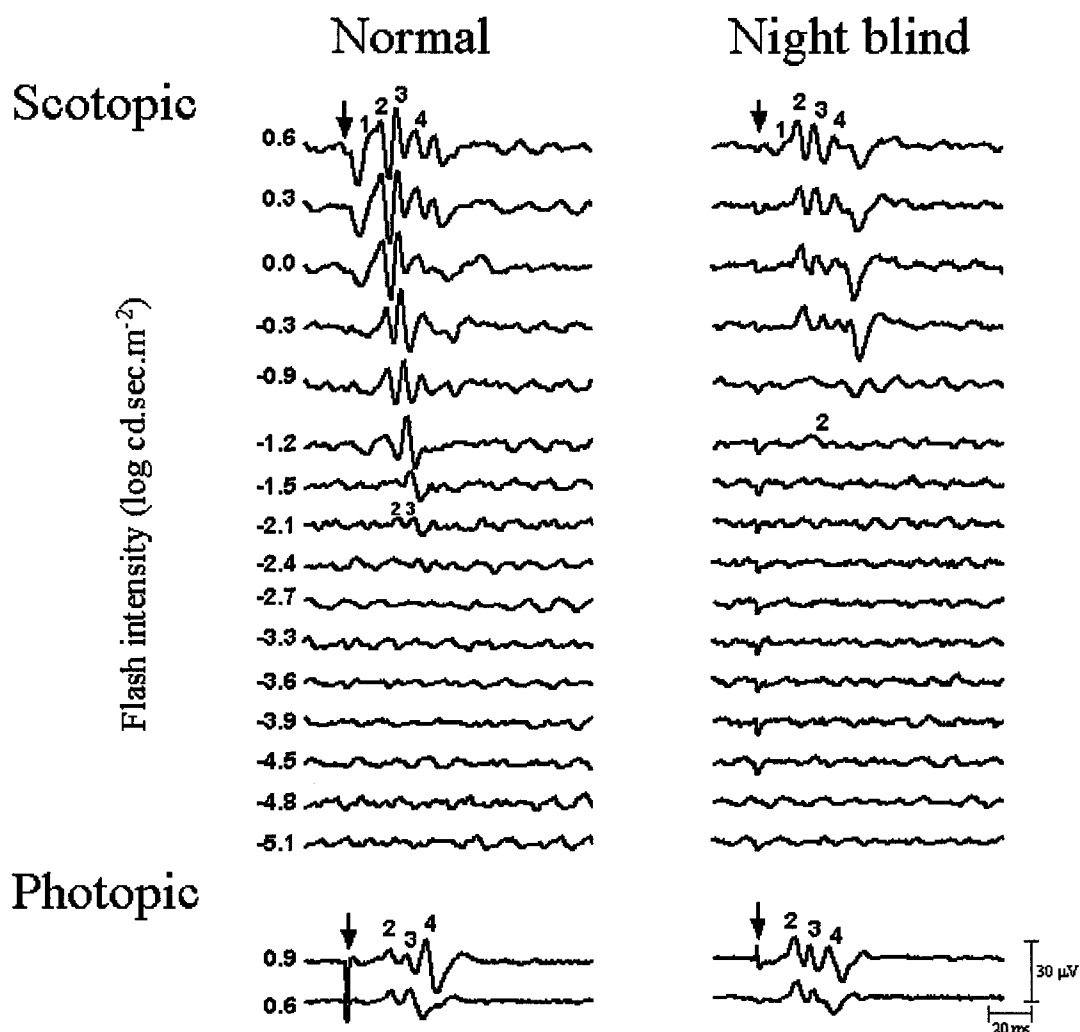


Figure 4: Short flash (20 μ s) scotopic (stimulus intensity range from -5.1 to 0.6 log cd.sec.m⁻² as indicated at left of each tracing) and photopic (stimulus intensity: 0.6 and 0.9 log cd.sec.m⁻² as shown at left of each tracing) OPs recorded from a normal (V-3) and a night blind (VI-1) guinea pig aged 10 days. Vertical arrows identify flash onset, 1,2,3,4= OP₁, OP₂, OP₃, OP₄. Horizontal calibration: 20 ms. Vertical calibration: 30 μ V.

Normal Night blind

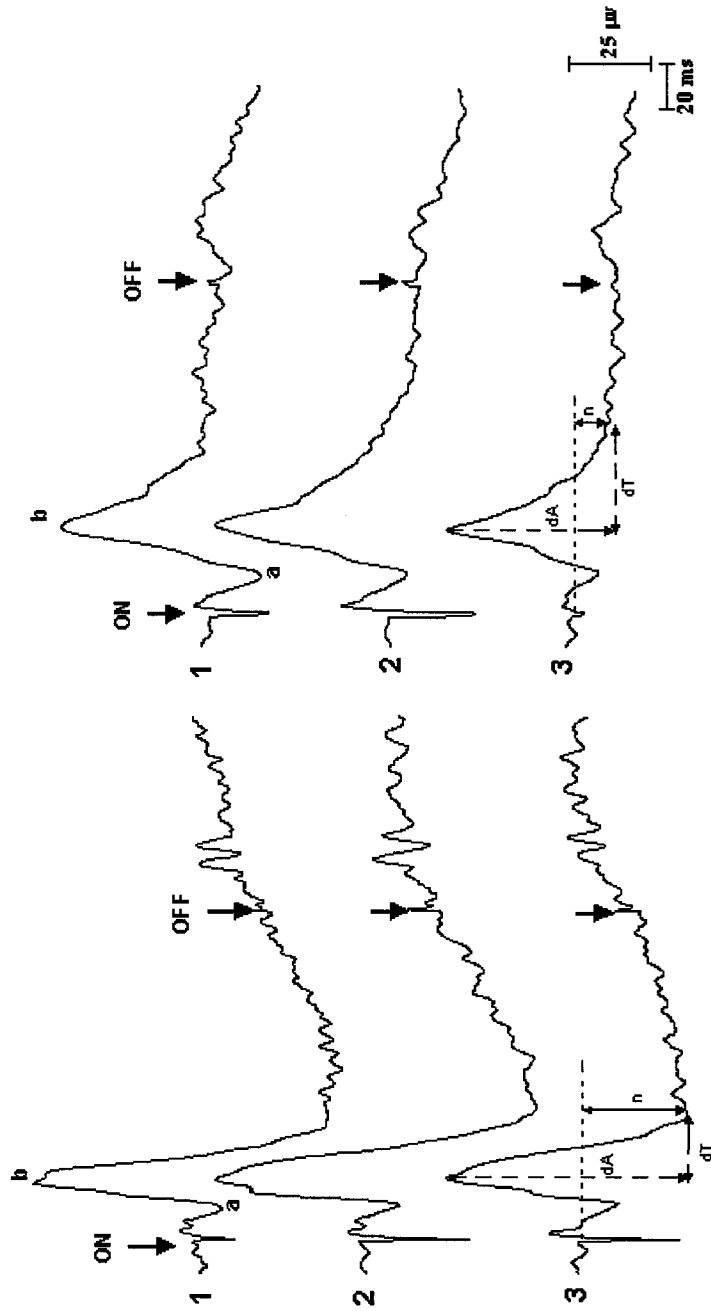


Figure 5: Long flash (duration: 200 msec) photopic (stimulus intensity: 125 cd.m^{-2} , background light: 15 cd.m^{-2}) ERGs recorded from normal (left column, $n=3$) and night blind (right column, $n=3$) guinea pigs aged 3 months. Vertical arrows identify flash onset (ON) and offset (OFF) respectively. a= a-wave, b= b-wave, n= post b-wave electronegativity, dA= amplitude of the descending limb of the b-wave, dT= duration in time of the b-wave descent. Horizontal calibration: 20 ms. Vertical calibration: $25 \text{ } \mu\text{V}$.

CHAPTER V: MANUSCRIPT 4

Racine J., Joly S., Lachapelle P. Maturation and aging of the retinal structure and function in the normal and the night blind albino guinea pigs. Article in preparation.

1 Preface to chapter V

In our previous study (chapter 4), we reported a new and naturally occurring guinea pig model of night blindness. However, our study only compared results in 10 day old animals. In order to further define the phenotype described in the previous chapter, we examined the maturation and aging of the retinal structure (light histology, electron microscopy, immunohistochemistry) and function (electroretinogram) of our guinea pig model. The aim is to determine if our night blind guinea pigs are affected with a stationary or degenerative retinopathy and also to identify the structural origin of this unique retinopathy.

2 Abstract

Purpose: We have previously reported a naturally occurring retinal disorder in a population of albino Hartley guinea pigs, where the affected guinea pigs present a defect of the rod-mediated vision. The purpose of the present study was, first, to investigate with a long-term follow-up study if our guinea pigs were affected with a stationary or degenerative retinopathy, and second to identify the retinal origin of this unique disorder. **Methods:** Scotopic (rod and rod-cone mediated) and photopic (cone mediated) flash ERG/OP were recorded from normal and mutant guinea pigs aged between P1 and P450. Retinal histology at P5, P150 and P450 and immunohistochemistry at P30, P150 and P450 were also obtained from mutants and normal guinea pigs. **Results:** Irrespective of age, the scotopic ERG of mutant guinea pigs could only be evoked by flashes of photopic intensity range and the resulting waveforms were of photopic morphology. Interestingly, the amplitude of the cone and the rod-cone mediated a-waves were always of smaller amplitude in mutants than in normal, but this difference tended to decrease with age. In contrast, the b-wave was of larger than normal amplitude in photopic ERGs obtained prior to age 25 and prior to age 10 for scotopic mixed ERGs. Light microscopy revealed, in mutants, an absence of the outer segment layer (OSL) along with a reduction in the thickness of the outer nuclear layer (ONL). Electron microscopy also disclosed the presence of cone outer segments (OS) that were buried in the inner segment layer; while no rod OS could be evidenced. Immunohistochemistry also revealed 1- the presence of rhodopsin, although unexpectedly concentrated in the ONL, 2- the presence of both cone opsins and 3- normal synaptophysin immunoreactivity. **Conclusion:** Our results suggest that our mutants are affected with a retinal disorder characterized with: 1- a non recordable rod-mediated vision from birth, 2- a rod-cone mediated response most probably generated by cones, 3- a near normal photopic response, 4- no evidence of rod photoreceptors OS, 5- remnant cone outer segments, 6- a thinning of the retina, 7- re-localization of rhodopsin in the ONL, 8- a normal cone and

synaptic immunoreactivity and finally, 9- evidence of progression with age. Correspondence with a human-like retinal disorder remains to be established.

3 Introduction

Disorders affecting the retina can be very devastating as vision loss is irreversible and frequently severe. The availability of transgenic and naturally occurring animal models of retinal dystrophies has helped us reach deeper insights in the pathophysiology of human retinal disorders such as *retinitis pigmentosa* (RP), congenital stationary night blindness (CSNB) and macular degeneration, to name a few (Narfström 1989; Travis 1989; Chang 1993; Portera-Cailliau 1994; Pak 1995; Petters 1997; Pardue 1998; Candille 1999; D'Cruz 2000; Chader 2002; Zhang 2003; Edward 2007). Several animal models have arisen from spontaneous mutations, while others have been induced by genetic manipulations. During the last 20 years or so, more than 70 different genes responsible for hereditary retinal degeneration have been cloned, out of which 52 genes have been mapped (Besch 2003, RetNet <http://www.sph.uth.tmc.edu/Retnet/>). On the other hand, during the same period, the number of spontaneously occurring animal models of retinal disorders has not increased as rapidly. Even though naturally occurring animal models are not as numerous as genetically engineered ones, both groups helped us expand our knowledge of basic retinal biology and, consequently, unravel the mysteries surrounding the pathophysiological mechanisms of retinal diseases.

Thus, the purpose of the present study was to conduct a longitudinal study to examine the structural (retinal histology and retinal immunohistochemistry) and functional (rod, rod-cone and cone-mediated electroretinograms) consequences of a rod mediated retinopathy that affected our colony of guinea pigs. In 2003, our group presented a new and naturally occurring animal model of a presumably night blinding disorder in a population of Hartley albino guinea pigs (Racine 2003). Based on the results obtained, we suggested that the mutant guinea pigs

were born with a retinal disorder, impairing primarily the normal functioning of rod mediated vision, thus raising the possibility that our guinea pigs might be night blind. However, our study only reported on 10 days old guinea pigs. Therefore, in order to better understand the functional and structural anomalies that characterize our night blind guinea pigs, we conducted long term follow up studies to determine if our guinea pigs were affected with a stationary or a degenerative retinal disorder, as well as identify the origin of this unique retinal disorder. Our results suggest that the retinopathy, which is inherited as an autosomal recessive trait, is most likely degenerative. In our mutant guinea pigs, no rod-mediated vision could be recordable from birth due to a lack of rod photoreceptor outer segments. Furthermore, the rod-cone mediated responses are most probably generated by cone photoreceptors alone, since the morphology of the latter is almost identical to that of the photopic ERG recorded in normal or mutant guinea pigs. Finally, with age, a significant thinning of the entire retina is observed in mutants when compared to normal.

4 Material and Methods

4.1 Animals

In the present study, normal and mutant Hartley albino guinea pigs aged from 1 to 450 days old were tested. Retinal function was assessed with the help of standard flash electroretinography, whereas retinal structure was assessed with light microscopy, electron microscopy and immunohistochemistry. During the entire study, the animals were maintained in our animal care facility, in an environment with a 12 hours light-dark cycle. The in-cage illumination was maintained at approximately 30 cd.m^{-2} and the room temperature was set at approximately 23 degree Celsius. The study was performed in accordance with the ARVO statement on the use of animals in Ophthalmic and Vision Research and

performed following a protocol reviewed and approved by the McGill University-Montreal Children's Hospital Research Institute animal care committee.

4.2 Electroretinogram recordings

Electroretinograms (ERG) were recorded every 5 days from birth to P30 and then monthly until P450. The electroretinograms were recorded in scotopic (rod and rod-cone mediated) and photopic (cone-mediated) conditions. Following overnight darkness adaptation and under dim red light illumination, anesthesia was obtained with an intra-muscular injection of a mixture of ketamine (85 mg/kg) and xylazine (5 mg/kg). Animals also had their pupils dilated with 2 drops of 1% cyclopentolate hydrochloride. The guinea pigs were then placed in a modified recording box (ganzfeld-like) of our own design, which also housed the flash stimulator and background light (Lachapelle 1990a). Throughout the recording session, the temperature inside the recording box remained at 28 degree Celsius. A DTL fiber electrode (27/7 X-Static silver coated conductive nylon yarn: Sauquoit Industries, Scranton, PA, USA) was positioned on the surface of the cornea in order to record the electroretinograms. The DTL fiber was kept moist with one drop of tear gel (Novartis Ophthalmics, Mississauga, Ontario, Canada). Reference (Grass E5 disc electrode, Grass Instruments, Quincy, MA, USA) and ground (Grass E2 subdermal electrode) electrodes were placed in the mouth and subcutaneously in the neck, respectively. Following animal preparation an extra 10 minutes of dark adaptation was added prior to the beginning of the recording session.

Electroretinograms (bandwidth: 1-1000 Hz, 10 000 X, Grass P511K pre-amplifier) and oscillatory potentials (bandwidth: 100-1000 Hz, 50 000 X, Grass P511K pre-amplifier) were recorded simultaneously throughout the study using the Biopac MP 100 Acknowledge system (Biopac MP 100 WS, BIOPAC System Inc., Goleta, CA, USA). First, scotopic ERGs and OPs were evoked by flashes of

white light (Grass PS 22 Photostimulator, Grass Instruments, Quincy, MA, USA), spanning over a 6-log unit range (0.3 log unit increments) with a maximal intensity of 0.6 log cd.sec.m⁻² in energy. Averages of three (3) to five (5) responses were taken depending on the stimulus intensity used to produce the response. In order to avoid the conditioning flash effect previously reported to affect dark-adapted OPs (Peachey 1987; Lachapelle 1990b), an inter-stimulus interval (ISI) of 9.6 seconds was used for all scotopic recordings.

Following the scotopic recordings, a background light of 30 cd.m⁻² was turned on. After 20 minutes of light adaptation to this steady background, photopic (cone mediated) ERGs and OPs were evoked to flashes of white light (Grass PS 22 Photostimulator, Grass Instruments, Quincy, MA, USA) with a flash intensity of 0.9 log cd.sec.m⁻² and an ISI of 0.96 seconds. An average of 20 responses were obtained for cone-mediated recordings.

Analysis of ERG and OP waves was performed, as previously described (Racine 2003, 2007). Briefly, the amplitude of the a-wave was measured from the baseline of the first negative trough while that of the b-wave was measured from the most negative trough to the most positive peak of the ERG. However, while in most instances the most negative trough did correspond to the peak of the a-wave, scotopic responses evoked to the brightest flashes generated a short latency OP, whose trough culminated below the a-wave. We have arbitrarily decided to include this component in the measurement of the b-wave, a choice that explains that, while we are illustrating scotopic ERG responses with negative morphologies, the amplitude measurements we report always present the resulting responses with b-wave amplitudes larger than a-wave amplitudes. The amplitude of each OPs was measured from the preceding trough to peak. The amplitude of all OPs was also summated (SOP= OP₂+OP₃+OP₄+OP_N) to yield the photopic (PSOP) and scotopic (SSOP) SOP values. All peak times were measured from the flash onset to the peak of each component.

4.3 Retinal histology

Retinal histology was performed on normal and mutant albino Hartley guinea pigs aged 5, 150 and 450 days. Once the ERG recordings were completed, the animals were euthanized with carbon dioxide inhalation. The left eyes were removed and prepared for histology whereas the right eyes were removed and prepared for immunohistochemistry (see next paragraph). The former were fixed with a three-hour immersion in a 3.5% glutaraldehyde solution. Lenses were then removed and the enucleated eyes were kept in glutaraldehyde solution (3.5%) for another 3 hours. The anterior segment was then removed and the retina, still attached to the choroid was cut into sectors 2mm wide by 4 mm long using the optic nerve as a reference point. Retinal sections were immersed in osmium (OsO_4) 4% and 0.1 M phosphate buffer for one hour following which they were rinsed in 0.1 M phosphate buffer. The sections were then dehydrated in progressive ethanol baths going from 50% to a 100% (5 steps). A final dehydration was performed in propylene oxide for 10 minutes, following which the retinal sections were embedded in resin (Durcupan® ACM Fluka epoxy resin kit, Sigma-Aldrich, Canada) and stored for 48 hours in a heat chamber kept at 58 degrees Celsius. Once polymerized, the retinas were cut (Leica EM UC6, Leica microsystem, USA) in ultra thin sections of 0,7 μm (6 mm histo-glass knives; Pelco International, California) for light histology and 150 nm (diamond knife; Diatome, Biel Switzerland) for electron microscopy. Sections were made perpendicularly to the retina by orienting the blocks until sections longitudinal to the photoreceptors were obtained. For light histology, retinal sections were mounted on slides and stained with toluidine blue. Photographs were obtained with a Zeiss microscope (Zeiss Axiophot, Zeiss microscope, Germany: 40X) attached to a digital camera (RR slider spot, Diagnostics instruments inc., Germany). The thickness of the different retinal layers was determined with a calibrated grating inserted in the ocular of the microscope. As for electron microscopy, sections were contrasted with 2% uranyl acetate and photographs

were taken with a JEOL JEM-100S transmission electron microscope operating at 80 kV.

4.4 Retinal immunohistochemistry

Retinal immunohistochemistry was performed on normal and mutant albino Hartley guinea pigs aged 30, 150 and 450 days. As previously mentioned, right eyecups were kept to perform immunohistochemistry. After enucleation, the eyes were fixed in a solution of paraformaldehyde 4% for three hours. Lenses were then removed and the eyes were kept in paraformaldehyde solution (4%) for another three hours. The eyes were then transferred in a 15% sucrose solution for 2 hours, and afterwards in a 30% sucrose solution overnight at 4 degree Celsius. Finally, the eyes were placed in an embedding mold (Marivac, St-Laurent, Québec, Canada) previously filled with OCT (optimal cutting temperature) compound (Tissue-Tek, Marivac, St-Laurent, Québec, Canada) and frozen by immersion of the whole in 2-methyl butane/liquid nitrogen. The molds were then stored in a freezer kept at -80°C .

The frozen eyes were cut in 14 μm thick sections with a cryostat (CM 3050S, Leica microsystem, Ontario, Canada) and mounted on polylysine-coated slides. Sections were incubated in 3% normal goat serum, 0.3% triton X-100 and in phosphate-buffered saline 0.1M for one hour at room temperature to block non-specific binding sites. Each primary antibody (see next paragraph for more details) was added in 3% normal goat serum and 0.3% triton X-100 and incubated overnight at 4 degrees. Sections were then incubated in the dark and at room temperature for 1 hour with the appropriate secondary antibody (see next paragraph for more details), washed in phosphate buffered saline 0.1M and mounted on microscope slides using an antifade reagent (Slowfade, Invitrogen, Burlington, Ontario, Canada).

The primary antibodies used were: the mouse anti-rhodopsin monoclonal antibody (MAB5316, Chemicon International, Temecula, California), the rabbit anti-opsin, blue polyclonal antibody, (AB5407, Cemicon International, Temecula, California), the rabbit anti-opsin, red-green polyclonal antibody (AB5405, Chemicon International, Temecula, California) and the synaptophysine mouse monoclonal antibody (VP-S285, Invitrogen, Burlington, Ontario, Canada). Secondary antibodies (Invitrogen, Burlington, Ontario, Canada) used were: the Alexa Fluor 488 goat anti-mouse (used for anti-rhodopsin and anti-opsins) and the Alexa Fluor 594 goat anti-mouse (used for synaptophysin).

Photo micrographs were taken with a Zeiss microscope (Zeiss Axiophot, Zeiss microscope, Germany: 40X) attached to a digital camera (RR slider spot, Diagnostics instruments inc., Germany).

4.5 Data analysis

In order to compare values obtained between normal and night blind guinea pigs according to age, a two-way analysis of variance (two-way ANOVA) for dependant values was performed ($p < 0.05$).

5 Results

The pedigree of our population of night blind guinea pigs, which is presented at figure 1, shows that the first affected guinea pig (III-4) was born following a consanguineous mating between a brother (II-2) and a sister (II-1). Since then, we have been able to reproduce (through selective mating), this phenotype another 80 times over 15 generations. Out of the 81 affected guinea pigs, 35 were males, 43 were females and another 3 were euthanized prior to sex identification. Based on the pedigree, the mode of inheritance of this unique retinopathy is most probably autosomal recessive.

5.1 Cone-mediated function

Representative photopic electroretinograms and oscillatory potentials recorded from normal and mutant guinea pigs at selected postnatal ages (indicated on top of the figure) are shown at figures 2 and 3, respectively. A further analysis of the amplitudes and peak times of the ERG (a- and b-waves) and OPs (OP₂, OP₃, OP₄) are reported in figures 4 and 5, respectively. As a rule, in both normal and night blind guinea pigs, the amplitudes of the ERG a- and b-wave increased from birth [normal (a-wave: $17.37 \pm 7.00 \mu\text{V}$; b-wave: $64.30 \pm 15.69 \mu\text{V}$); night blind: (a-wave: $16.95 \pm 4.99 \mu\text{V}$; b-wave $81.45 \pm 10.61 \mu\text{V}$)] to P5, where they reach their maximum value [normal (a-wave: $31.03 \pm 5.90 \mu\text{V}$; b-wave: $113.45 \pm 20.98 \mu\text{V}$); night blind: (a-wave: $19.46 \pm 5.79 \mu\text{V}$; b-wave $128.37 \pm 18.98 \mu\text{V}$)]. From P5, the amplitudes decreased steadily until the guinea pigs reached 450 days old [normal (a-wave: $11.55 \pm 3.61 \mu\text{V}$; b-wave: $50.15 \pm 17.04 \mu\text{V}$); night blind: (a-wave: $6.98 \pm 3.18 \mu\text{V}$; b-wave $25.45 \pm 13.18 \mu\text{V}$)], the oldest age at which results were obtained. Irrespective of the age of the guinea pig, the amplitude of the a-wave in night blind animals was always of smaller amplitude, but not always significantly different, than that of normal (figure 4). In contrast, from P1 to P25, the amplitude of the b-wave was slightly, but not significantly ($\rho > 0.05$), larger in night blind guinea pigs whereas the reverse was observed after P25 (figure 4).

The peak times of the a- and the b-waves on the other hand, changed differently between the two groups. While in normal there was a trend for the peak time of the a-wave to shorten with age [P1: $13.77 \pm 1.27 \text{ ms}$; P450: $10.90 \pm 1.41 \text{ ms}$; $\rho < 0.05$], in night blind individuals it lengthened [P1: $12.50 \pm 1.70 \text{ ms}$; P450: $15.6 \pm 2.55 \text{ ms}$; $\rho < 0.05$]. Similarly, in normal guinea pigs the timing of the b-wave shortened [P1: $35.90 \pm 0.71 \text{ ms}$; P450: $31.60 \pm 1.52 \text{ ms}$; $\rho < 0.05$] with age, while in night blind, it remained stable [P1: $39.30 \pm 2.25 \text{ ms}$; P450: $38.90 \pm 4.10 \text{ ms}$; $\rho > 0.05$]. It is important to note that, at most age intervals, the peak time of

the b-wave in night blind animals was always significantly slower than normal (figure 5).

The oscillatory potentials also showed differences between normal and night blind guinea pigs (figure 4, 5). From birth, all oscillatory potentials increased in amplitude to reach a maximal value [(OP₂: normal: $11.6 \pm 1.64 \mu\text{V}$, night blind: $10.92 \pm 3.87 \mu\text{V}$); (OP₃: normal: $6.21 \pm 1.32 \mu\text{V}$, night blind: $4.49 \pm 1.45 \mu\text{V}$); (OP₄: normal: $5.12 \pm 1.85 \mu\text{V}$, night blind: $8.41 \pm 1.40 \mu\text{V}$)] and then decreased with age. Of interest, the OPs of night blind guinea pigs reached their maximal value (OP₂: P5; OP₃: P10; OP₄:P10) earlier than normal guinea pigs (OP₂: P10; OP₃: P35; OP₄:P35), suggesting a faster maturation process in night blind guinea pigs. Furthermore, while from P5 the amplitudes of OP₂ and OP₃ are always significantly smaller in night blind guinea pigs ($\rho < 0.05$), that of OP₄ is slightly, but not significantly ($\rho > 0.05$) larger in night blind animals in responses recorded from birth to approximately P240 (figure 4). Analysis of group data also reveals that, in our mutants, OP₃ is completely abolished after age P120, while in normal guinea pigs it remains present to the end (P450). This feature is clearly evidenced at figure 4. Finally, the peak times of the OP also showed a different maturation pattern when normal and night blind guinea pigs were compared (figure 5). In normal, the peak times of OP₂ [P1: $20.4 \pm 0.84 \text{ ms}$; P450: $16.2 \pm 0.45 \text{ ms}$; $\rho < 0.05$], OP₃ [P1: $26.77 \pm 1.44 \text{ ms}$; P450: $22.98 \pm 0.99 \text{ ms}$; $\rho < 0.05$] and OP₄ [P1: $35.45 \pm 1.38 \text{ ms}$; P450: $30.2 \pm 1.86 \text{ ms}$; $\rho < 0.05$] shortened with age, whereas in night blind guinea pigs it lengthened {OP₂ [P1: $18.00 \pm 1.28 \text{ ms}$; P450: $21.8 \pm 1.85 \text{ ms}$; $\rho < 0.05$], OP₃ [P1: $24.6 \pm 1.98 \text{ ms}$; P450: $27.4 \pm 2.15 \text{ ms}$; $\rho < 0.05$]}, except for OP₄ [P1: $32.4 \pm 1.85 \text{ ms}$; P450: $31.8 \pm 1.13 \text{ ms}$; $\rho > 0.05$] whose peak time remained unchanged throughout the 450 days.

5.2 Rod and rod-cone mediated function

Figures 2 and 3 also illustrate representative rod and rod-cone mediated ERGs and oscillatory potentials recorded from aging (age indicated on top of the figure) normal and night blind guinea pigs. Independently of age, no rod-mediated responses could be recorded from our mutants. However, when the intensity of stimulation used ($0.6 \log \text{ cd}\cdot\text{sec}\cdot\text{m}^{-2}$) was sufficient to elicit a contribution of both rod and cone pathways, an ERG was recorded in our night blind guinea pigs. While, as previously documented, mixed rod-cone responses are of a negative morphology in normal guinea pigs (Racine 2003), it is not in our night blind guinea pigs.

In fact, the ERGs of night blind guinea pigs are of photopic-like morphology, suggesting that only the cone photoreceptors or the cone pathway participate to the genesis of this response. In normal and night blind specimens the a-wave reached maximal amplitude at P15 (normal: $117.23 \pm 26.49 \mu\text{V}$; night blind: $25.23 \pm 8.32 \mu\text{V}$) compared to P5 ($149.19 \pm 20.75 \mu\text{V}$) and P10 ($135.82 \pm 14.42 \mu\text{V}$) for the b-wave of night blind and normal guinea pigs, respectively (figure 6). The amplitude of both the a- and the b-waves then decreased until P450. Irrespective of age, the amplitude of the a-wave was always smallest ($p < 0.05$) in night blind guinea pigs; while that of the b-wave was larger than normal in night blind animals younger than P10 and smaller than normal afterward (figure 6).

Similar to what was reported for the photopic responses, the peak times of both the a- and b-waves shortened with age in normal [(a wave: P1: 12.69 ± 1.09 ms; P450: 11.7 ± 1.99 ms; $\rho > 0.05$) (b-wave: P1: 43.17 ± 2.94 ms; P450: 37.1 ± 3.02 ms; $\rho < 0.05$)] and increased with age in night blind guinea pigs [(a-wave: P1: 10.10 ± 2.14 ms; P450: 15.8 ± 2.55 ms; $\rho < 0.05$) (b-wave: P1: 45.5 ± 2.12 ms; P450: 44.0 ± 3.98 ms; $\rho > 0.05$)] (figure 7).

Finally, from birth, all scotopic oscillatory potentials increased in amplitude to reach a maximal value [(OP₂: normal: $26.93 \pm 6.36 \mu\text{V}$, night blind: $10.84 \pm 3.33 \mu\text{V}$); (OP₃: normal: $35.84 \pm 8.52 \mu\text{V}$, night blind: $10.98 \pm 3.74 \mu\text{V}$); (OP₄: normal: $12.78 \pm 4.40 \mu\text{V}$, night blind: $8.81 \pm 2.37 \mu\text{V}$)] and then decreased with age (figure 3, 6). Of interest, the oscillatory potentials of the night blind guinea pig reached their maximal amplitude (OP₂: P5; OP₃:P5; OP₄: P5) earlier than normal guinea pigs (OP₂: P15; OP₃: P15; OP₄: P10). Furthermore, the rod-cone mediated oscillatory potentials (OP₂, OP₃, OP₄) were always of significantly larger amplitude ($\rho < 0.05$) in normal than in night blind guinea pigs, contrasting with photopic recordings where, in young animals, the OPs were of larger amplitude in night blind compared to normal (figure 6). Finally, the OP peak times also matured differently between normal and night blind guinea pigs (figure 7). In normal, the peak times of OP₂ [P1: $18.03 \pm 1.85 \text{ ms}$; P450: $15.2 \pm 1.57 \text{ ms}$; $\rho < 0.05$], OP₃ [P1: $25.9 \pm 1.06 \text{ ms}$; P450: $21.08 \pm 1.67 \text{ ms}$; $\rho < 0.05$] and OP₄ [P1: $34.48 \pm 1.94 \text{ ms}$; P450: $29.5 \pm 1.42 \text{ ms}$; $\rho < 0.05$] shortened with age, whereas in night blind guinea pigs it lengthened {OP₂ [P1: $17.50 \pm 1.27 \text{ ms}$; P450: $18.1 \pm 1.55 \text{ ms}$; $\rho > 0.05$], OP₃ [P1: $24.1 \pm 2.99 \text{ ms}$; P450: $26.4 \pm 1.49 \text{ ms}$; $\rho < 0.05$], OP₄ [P1: $32.8 \pm 1.28 \text{ ms}$; P450: $33.6 \pm 3.01 \text{ ms}$; $\rho > 0.05$]}.

5.3 Retinal structure: Light and electron microscopy

Photomicrographs of retinal sections (increasing magnification from 8a to 8c), obtained from normal and night blind guinea pigs aged P5, P150 and P450, are shown at figure 8. The most striking feature that distinguishes normal from night blind guinea pigs is the fact that, in the latter, there is no evidence of well defined photoreceptor outer segments as seen at lower magnification (8a). A higher magnification (8b) examination of the outer layers of the retina suggests the presence of remnant OS of photoreceptors that are located in the inner segment layer (ISL) (figure 8b arrows), a finding that is confirmed with the evidence of a

lamellar structure at electron microscopy (8c). However, these lamellar structures were localized at the level of the inner segment layer (ISL) and they were reduced in quantity compared to normal. Given our ERG findings, which suggest that only cones contribute to the response (scotopic or photopic conditions), we believed that these are cone OS.

At P5, the retina of our mutant guinea pigs also demonstrates a significantly reduced outer nuclear layer (ONL) (normal: $35.63 \pm 1.33 \mu\text{m}$; night blind: $25.03 \pm 0.96 \mu\text{m}$; $\rho < 0.05$) (figure 8, 9). While in normal the ONL measures up to 6 nuclei thick, it is reduced to 4 nuclei in mutants. Interestingly, our results also showed a significantly thicker inner segment layer (normal: $14.98 \pm 1.44 \mu\text{m}$; night blind: $19.09 \pm 2.30 \mu\text{m}$; $\rho < 0.05$), inner nuclear layer (INL) (normal: $29.92 \pm 0.33 \mu\text{m}$; night blind: $37.85 \pm 4.91 \mu\text{m}$; $\rho < 0.05$), inner plexiform layer (IPL) (normal: $28.20 \pm 1.66 \mu\text{m}$; night blind: $37.65 \pm 5.57 \mu\text{m}$; $\rho < 0.05$) and ganglion cell layer (GCL) (normal: $22.13 \pm 1.33 \mu\text{m}$; night blind: $26.46 \pm 2.34 \mu\text{m}$; $\rho < 0.05$) which lead to an overall retinal thickness slightly larger in mutant compared to normal guinea pigs (figure 8, 9). No significant changes were observed in the retinal pigment epithelium (RPE) (normal: $5.00 \pm 0.22 \mu\text{m}$; night blind: $5.32 \pm 0.31 \mu\text{m}$; $\rho > 0.05$) and the outer plexiform layer (OPL) (normal: $6.33 \pm 1.55 \mu\text{m}$; night blind: $6.26 \pm 0.92 \mu\text{m}$; $\rho > 0.05$) (figure 8, 9).

At P150, the retinal structure of our mutant guinea pigs still revealed significant differences when compared to normal retinas (figure 8, 9). Similarly to what was observed at P5, the ONL thickness in our mutant guinea pigs ($15.39 \pm 1.55 \mu\text{m}$) was significantly reduced when compared to age match controls ($24.87 \pm 1.31 \mu\text{m}$; $\rho < 0.05$). The IS as well as the GCL in our mutant (IS: $16.78 \pm 0.75 \mu\text{m}$; GCL: $25.81 \pm 2.56 \mu\text{m}$; $\rho < 0.05$) were also significantly thicker than normal (IS: $14.40 \pm 1.07 \mu\text{m}$; GCL: $21.63 \pm 0.92 \mu\text{m}$; $\rho < 0.05$) in P150 animals. However, in contrast with results obtained at P5, the INL and the IPL of night

blind guinea pigs (INL: $23.57 \pm 2.44 \mu\text{m}$; IPL: $27.19 \pm 1.90 \mu\text{m}$) age P150, were no longer different ($p > 0.05$) from age matched normal (INL: $20.71 \pm 0.76 \mu\text{m}$; IPL: $24.63 \pm 0.97 \mu\text{m}$) (figure 8, 9). Notwithstanding the above, since there is no outer segment layer, there was a significant reduction of the total retinal thickness in P150 day old mutants ($118.82 \pm 4.74 \mu\text{m}$) compared to normal ($133.30 \pm 3.27 \mu\text{m}$) (figure 8, 9). At P450, only the ONL (normal: $25.18 \pm 2.15 \mu\text{m}$; night blind: $14.53 \pm 4.53 \mu\text{m}$) was significantly thinner in our mutants, resulting in a significantly ($p < 0.05$) thinner retina in our mutants ($104.65 \pm 9.25 \mu\text{m}$) compared to controls ($130.03 \pm 7.17 \mu\text{m}$). Finally, we noted the presence of loss of cellular bodies in the inner segment layer in our P150 and P450 days old mutants, a finding which was never observed in age and that matched controls (figure 8a).

5.4 Retinal structure: Immunohistochemistry

Immunohistochemistry was performed on normal and night blind guinea pigs aged P30, P150 and P450. Antibodies against cone opsins, rhodopsin and retinal synapses were used in order to better document the pathophysiological mechanisms at the origin of the retinopathy affecting our mutant guinea pigs. Furthermore, in order to better appreciate which retinal cell layers were labeled with our antibodies; we also double stained our slides with a nuclear and chromosome counter stain: propidium iodide. In order to better identify the photoreceptor origin of the lamellar structures found in the ISL with electron microscopy, immunoreactivity against cone opsins (blue cones and red-green cones) and rhodopsin was performed. Our results revealed that, similarly to the normal guinea pig, mutants showed immunoreactivity to both cone opsins (figures 10, 11), where the staining was located at the level of the ISL, a finding which is not surprising, given that the cone OS of our mutants were allegedly found in this layer as demonstrated by electron microscopy (figure 8c). Of interest, however, the immuno-fluorescence for both cone opsins was of a different shape when

normal and night blind guinea pigs are compared, being of a rectangular shape in normal compared to a round shape in night blind guinea pigs. This gives support to our electron microscopy results, which showed that the morphology of the cone OS in mutants were of a round morphology compared to a rectangular shape in normal (figure 8c). Our results also revealed a higher proportion of blue cones compared to the red-green cones in the retina of normal and night blind guinea pigs. On the other hand, despite the absence of rod mediated ERGs in our mutants, immunohistochemistry did reveal the presence of rhodopsin, albeit at the ONL level instead of the OSL level as would be in normal guinea pigs (figure 13). More specifically, the rhodopsin staining was located on the peri-nuclear side of photoreceptor cells. Finally, given that both pre-and post-synaptic components of the ERG were affected in our mutant animals, we examined if synaptic connectivity was also hampered. Analysis performed at ages P30, P150 and P45, did not reveal significant differences in labeling and localization (OPL, IPL) of synaptophysin between the two animal models (figure 12).

6 Discussion

In a previous study, our group described (Racine 2003) a colony of mutant guinea pigs affected with a retinal disorder presenting with : 1- a complete abolition of the rod-mediated function, 2- an abnormal scotopic mixed, rod-cone mediated, electroretinograms with photopic-like morphologies, 3- an elevated threshold for the rod-cone mediated oscillatory potentials to intensities well within the photopic range, 4- a significant attenuation of the OFF-retinal response and 5- a significant reduction of the ON-ERG post b-wave electronegativity.

In addition to the above functional anomalies, results presented in the present study enabled us to further characterize, in the newborn as well as in the aging guinea pigs, the functional anomalies and localize the retinal origin of this disorder. The retinopathy of our mutant guinea pig is thus characterized as

follows: 1- inherited as an autosomal recessive trait, as revealed by our pedigree, 2- no histological evidence of rod photoreceptor outer segments, 3- remnant of cone outer segments, which are misplaced in the inner segment layer, 4- thinning of the retinal outer nuclear layer, 5- re-localization of the rhodopsin pigment in the outer nuclear layer, 6- normal cone immunoreactivity, 7- normal synaptic immunoreactivity, and finally, 8- evidence of degeneration of the retinal structure and function with age.

One very interesting feature of the retinal function in our mutant guinea pigs is that their scotopic ERGs elicited to bright flashes are not of negative shape like in normal, but instead are of positive morphology. Of interest, these positive rod-cone mediated ERGs in our mutants are similar to the cone-mediated ERGs recorded in the same animal. The overall amplitude of the rod-cone mediated ERG is, however, larger than the cone mediated ERG. The later difference in amplitude could be explained by the relatively brighter flash intensity in rod-cone mediated ERG because of the absence of a rod desensitizing background. This similarity in morphology between both scotopic mixed and photopic ERGs in mutants could suggest that only cone photoreceptors participate to the genesis of the ERG in our mutants, as previously demonstrated in other animal models (Calvert 2000; Jaissle 2001; Daniele 2005; Wenzel 2007). Furthermore, since the amplitude of the ERG a-wave, which is generated by the photoreceptors, is similar in both rod-cone and cone-mediated ERG, it could also suggest that only cone photoreceptors participate in the genesis of the rod-cone mediated ERG in our mutants. Finally, histology and immunohistochemistry analysis of the retinal structure in mutants confirmed the presence of only one type of photoreceptor, namely the cones.

Interestingly, our results revealed that our mutants do not have rod photoreceptor outer segments from birth and that only cone outer segments are present. However, immunolabeling revealed in our mutants that even if rod cell bodies do not develop rod outer segments, they still produced the visual chromophore rhodopsin, suggesting that rhodopsin needs to be inserted in the rod

outer segments in order to be functional. Then, we can suggest that our night blind guinea pigs are affected with a disorder that affects rod outer segments formation instead of rhodopsin formation.

Our results also revealed that, according to time, retinal function showed signs of degeneration in our mutants when compared to normal. In fact, both, the photopic and the scotopic mixed responses, which are both solely generated by cones in our mutants, revealed signs of degeneration over time. This phenomenon could be explained by the deterioration, with time, of the cone outer segment lamellar structure as revealed by light and electron microscopy. These changes in the organization of the lamellar structure in the cone outer segment could have an impact on the normal phototransduction cascade in our mutants and subsequently affect the ERG potential. The later anomaly seen in the cone outer segment lamellar structure could be explained by the absence of the rod-cone derived survival factor. In fact, it was reported in the literature that a normal rod-cone interaction is necessary for the survival of both types of photoreceptors (rod-cone survival factor) (Leveillard 2004). For example, in the human form of *retinitis pigmentosa*, the affected genes, which are exclusively expressed in rod photoreceptors, cause the death of both rod and cone photoreceptor cells. In their study in 2006, Hartong et al. suggested that the lack of interaction between rods and cones and subsequently the missing factors from rods that promote cone survival (rod-cone survival factor), might be the cause of cone degeneration in RP patients. Thus, in our animal model, the cones, which are functionally normal at birth, could degenerate over time due to the lack of rod photoreceptors and of the rod-cone survival factor.

Even if the ERG deteriorates over time in our mutants, there is a short period of time, just after birth, where the amplitude of the ERG components was larger than normal. In fact, the b-wave of the night blind guinea pigs is of larger amplitude than normal up until P25 in photopic condition and P10 in scotopic mixed condition. The latter finding could be explained by a thicker retina in our

younger mutants as shown at figures 8 and 9. This could suggest that there are more cells participating in the genesis of the ERG in young mutants compared to age matched control, thus explaining the larger responses. With age, the total retinal thickness is decreased in mutants compared to normal; hence lower photopic and scotopic mixed ERG amplitudes in our aging mutants.

Analysis of photopic and scotopic responses of our mutants revealed that the a-wave, OP₂ and OP₃, were the ERG components that showed the most significant age-dependent deterioration, while OP₄, even if there was some changes compared to normal, was the least affected. That finding further supports the previous suggestion of a different origin between the earlier and later OPs (Wachtmeister 1978). Of interest, Kojima et al. (1978) published evidence that the early OPs signaled the activation of the ON-retinal pathway, while the late OPs signaled the activation of the OFF-retinal pathway; thus suggesting that, in our mutants, the ON-retinal pathway and to a lesser extent the OFF-retinal pathway could be impaired. The later is in accordance with our results published earlier on the long flash ERG in mutants where we showed an attenuated OFF-retinal response and ON-ERG post b-wave electronegativity in our mutants (Racine 2003).

The cone-mediated ERGs of our mutants also revealed another abnormal feature, where OP₃ disappeared at around P120, while in normal OP₃ could still be recorded at P450. It was previously reported that the photopic ERG of patients affected with the complete form of Congenital Stationary Night Blindness (cCSNB) was characterized with the loss of early oscillatory potentials and the relative preservation of the late OP₄ (Lachapelle 1983; Miyake 1986). This is a finding similar to that observed in our older mutant guinea pigs aged P120, where OP₂ is nearly abolished, OP₃ extinguished and OP₄ remains almost unaltered. This would suggest that our colony of guinea pigs would be affected with a retinopathy similar to the human complete CSNB. Of interest, the complete form was shown to result from an anomaly of the ON-retinal pathway, as a result of an impaired

NYX gene encoding the nyctalopin protein (Bech-Hansen 2000; Pusch 2000). However, the anomaly previously reported in our mutants not only includes an anomaly of the ON-ERG post b-wave electronegativity, but also of the OFF-retinal response (Racine 2003). Therefore, our animal model of night blindness is not totally similar to the human form of complete CSNB, but could represent a potential model to study the pathological processes of a human-like retinal disorder such as *retinitis pigmentosa*.

Several animal models of retinal degeneration presenting with non-recordable rod mediated ERGs and near normal cone ERGs such as the rhodopsin knockout ($\rho^{-/-}$) mouse (Jaissle et al., 2001; Toda et al., 1999), the RPE 65 $^{-/-}$ mouse (Redmond et al., 1998), the α -transducin $^{-/-}$ knockout mouse (Calvert et al., 2000), the arrestin $^{-/-}$ knockout mouse (Xu et al., 1997) and the NRL $^{-/-}$ (Mears AJ 2001, Daniele 2005; Wenzel 2007) knockout mouse are reported in the literature. However, to our knowledge, our guinea pig is the only animal model presenting with a spontaneous mutation yielding structural and functional anomalies suggestive of a night blinding disorder.

Based on these knockout animals, the phenotype of our mutant guinea pigs is similar to that reported for the α -transducin $^{-/-}$ knockout mouse or the rhodopsin knockout ($\rho^{-/-}$) mouse. In the α -transducin $^{-/-}$ knockout mouse, reports indicated absence of the rod-driven ERGs, while the rod-cone mediated responses were of photopic-like morphology (Calvert 2000). Furthermore, cone-driven ERGs retained normal features, just like in our model (Calvert 2000). Absence of a rod-mediated b-wave indicated a major defect in the rods and in the rod bipolar cells. In the α -transducin $^{-/-}$ knockout mouse, the rod-cone mediated ERG was of positive morphology and closely resemble the cone ERG; supporting the hypothesis that the α -transducin $^{-/-}$ knockout mouse response originated from cone photoreceptors only, similarly to what is seen in our mutant model. Although the gross morphology of the retina was largely unaffected by α -transducin deletion, there was some evidence of degeneration with age (Calvert 2000). However, contrasting

with our results, outer segments of photoreceptors could always be evidenced. On the other hand, thickness of the retinal layer was significantly reduced compared to controls. The rhodopsin knockout mouse, which is viewed as a model of *retinitis pigmentosa*, results from a replacement mutation in exon 2 of the rhodopsin gene. It is characterized by a complete absence of rhodopsin and lack of rod outer segments (Jaissle 2001). It is not clear whether this degeneration is the direct consequence of the absence of regular rods or results from the altered development of the retinal pigment epithelium (RPE) and/or the choroids (Mohand-Said 1998). These animals presented with photopic-like scotopic mixed ERGs and normal photopic ERGs that where, at a young age, of supranormal amplitudes (Toda 1999; Jaissle 2001).

In summary our colony of mutant guinea pigs is affected with a congenital form of night blindness, progressive in nature, which affects not only the retinal function (rod- and cone-mediated vision) but also its structure. Our animal model offers us a unique opportunity to study the cone function in the absence of rods and consequently could help us better characterize the normal (antagonistic) relationship between rods and cones. Finally, our model could also be very helpful in understanding the origin of the unusual dark-adapted negative ERG in normal guinea pigs, a feature also portrayed in several human retinopathies.

7 Acknowledgments

The authors would like to acknowledge Mme Louise Pelletier for her help and assistance with histology and electron microscopy.

8 References

1. Bech-Hansen N.T., Naylor M.J., Maybaum T.A., Sparkes R.L., Koop B., Birch D.G., Bergen A.A., Prinsen C.F., Polomeno R.C., Gal A., Drack A.V. Musarella M.A., Jacobson S.G., Young R.S., Weleber R.G. (2000) Mutations in NYX, encoding the leucine-rich proteoglycan nyctalopin, cause X-linked complete congenital stationary night blindness. *Nat Genet*, 26 (3): 319-323.
2. Calvert P.D., Krasnoperova N.V., Lyubarsky A.L., Isayama T., Nicolo M., Kosaras B., Wong G., Ganon K.S., Margolis R.F., Sidman R.L., Pugh E.N. Makino C.L., Lem J. (2000) Phototransduction in transgenic mice after targeted deletion of the rod transducin α -subunit. *Proc Natl Acad Sci U S A*, 97: 13913-13918.
3. Candille S.I., Pardue M.T., McCall M.A., Peachey N.S., Gregg R.G. (1999) Localization of the mouse nob (no b-wave) gene to the centromeric region of the X chromosome. *Invest Ophthalmol Vis Sci*, 40: 2748-2751.
4. Chader G.J. (2002) Animal models in research on retinal degenerations: past progress and future hope. *Vision Res*, 42 (4): 393-399.
5. Chang G.Q., Hao Y., Wong F. (1993) Apoptosis: final common pathway of photoreceptor death in rd, rds, and rhodopsin mutant mice. *Neuron*, 11: 595-605.
6. D'Cruz P.M., Yasumura D., Weir J., Matthes M.T., Abderrahim H., LaVail M.M., Vollrath D. (2000) Mutation of the receptor tyrosine kinase gene *Mertk* in the retinal dystrophic RCS rat. *Hum Mol Genet*, 9 (4): 645-651.
7. Daniele L.L., Lillo C., Lyubarsky A.L., Nikonov S.S., Philip N., Mears A.J., Swaroop A., Williams D.S., Pugh E.N. (2005) Cone-like morphological, molecular and

electrophysiological features of the photoreceptors of the Nrl knockout mouse. *Invest Ophthalmol Vis Sci*, 46 (6) 2156-2167.

8. Edwards A.O., Malek G. (2007) Molecular genetics of AMD and current animal models. *Angiogenesis*, 10 (2): 119-132.

9. Hartong D.T., Berson E.L., Dryja T.P. (2006) Retinitis pigmentosa. *Lancet*, 368 (9549): 1795-1809.

10. Jaissle GB, May A, Reinhard J, Kohler K, Fauser S, Lütjen-Drecoll E, Zrenner E, Seeliger MW. (2001) Evaluation of the rhodopsin knockout mouse as a model of pure cone function. *Invest Ophthalmol Vis Sci*, 42: 506-513.

11. Kojima M., Zrenner E. (1978) OFF-components in response to brief light flashes in the oscillatory potential of the human electroretinogram. *Albrecht Bon Braefes Arch Klin Exp Ophthalmol*, 206: 107-120.

12. Lachapelle P., Little J.M., Polomeno R.C. (1983) The photopic electroretinogram in congenital stationary night blindness with myopia. *Invest Ophthalmol Vis Sci*, 24: 442-450.

13. Lachapelle P, Blain L (1990a) A new speculum electrode for electroretinography. *J Neurosci Methods*, 32: 245-249.

14. Lachapelle P, Benoit J, Clain L, Guité P, Roy M (1990b) The oscillatory potentials in response to stimuli of photopic intensities delivered in dark adaptation: an explanation of the conditioning effect. *Vision Res*, 30: 503-513.

15. Leveillard T., Mohand-Said S. Lorentz O., Hicks D., Fintz A.C., Clerin E., Simonutti M., Forester V., Cavusoglu N., Chalmel F., Dolle P., Poch O., Lambrou G., Sahel J.A.

(2004) Identification and characterization of rod-derived cone viability factor. *Nat Genet*, 36 (7): 755-759.

16. Mears A.J., Kondo M., Swain P.K., Takada Y., Bush R.A., Saunders T.L., Seiving P.A., Swaroop A. (2001) Nrl is required for rod photoreceptor development. *Nat Genet*, 29 (4): 447-452.

17. Miyake Y., Yagasaki K., Horiguchi M., Kawase Y., Kanda T. (1986) Congenital stationary night blindness with negative electroretinogram: a new classification. *Arch Ophthalmol*, 104: 1013-1020.

18. Mohand-Said S., Deudon-Combe A., Hicks D., Simonutti M., Forster V., Fintz A.C., Leveillard T., Dreyfus H., Sahel J.A. (1998) Normal retina releases a diffusible factor stimulating cone survival in the retinal degeneration mouse. *Proc Natl Acad Sci USA*, 95 (14):8357-8362.

19. Narfstrom K., Wrigstad A., Nilsson S.E. (1989) The briard dog: a new animal model of congenital stationary night blindness. *Br J Ophthalmol*, 73: 750-756.

20. Pak W.L. 1995 *Drosophila* in vision research. *Invest Ophthalmol Vis Sci*, 36: 2340-2357.

21. Pardue M.T., McCall M.A., LaVail M.M., Gregg R.G., Peachey N.S. (1998) A naturally occurring mouse model of X-linked congenital stationary night blindness. *Invest Ophthalmol Vis Sci*, 39: 2443-2449.

22. Peachey N, Alexander R, Fishman G (1987) Rod and cone system contribution to oscillatory potentials: an explanation for the conditioning effect. *Vision Res*, 27: 859-866.

23. Petters R.M., Alexander C.A., Wells K.D., Collins B., Sommer J.R., Blanton M.R., Rojas G., Hao Y., Flowers W.L., Banin E., Cideciyan A.V., Jacobson S.G., Wong F.

(1997) Genetically engineered large animal models for studying cone photoreceptor survival and degeneration in retinitis pigmentosa. *Nat biotech*, 15: 965-970.

24. Portera-Cailliau C., Sung C.H., Nathans J., Adler R. (1994) Apoptotic photoreceptor cell death in mouse models of retinitis pigmentosa. *Proc Natl Acad Sci U S A*, 91:974-978.

25. Pusch C.M., Zeitz C., Brandau O., Pesch K., Achatz H., Feil S., Scarfe C, Maurer J., Jacobi F.K., Pinckers A., Andreasson S., Hardcastle A., Wissinger B., Berger W., Meindl A. (2000) The complete form of X-linked congenital stationary night blindness is caused by mutations in a gene encoding a leucine-rich repeat protein. *Nat Genet*, 26 (3): 324-327.

26. Racine J., Benh D., Simard E., Lachapelle P. (2003) Spontaneous occurrence of a night blinding disorder in guinea pigs. *Doc Ophthalmol*, 107, 59-69.

27. Redmond TM, Yu S, Lee E, Bok D, Hamasaki D, Chen N, Goletz P, Ma JX, Crouch RK, Pfeifer K. (1998) Rpe65 is necessary for production of 11-cis-vitamin A in the retinal visual cycle. *Nat Genet*, 20: 344-351.

28. Toda K, Bush RA, Humphries P, Sieving PA. (1999) The electroretinogram of the rhodopsin knockout mouse. *Vis Neurosci*, 16: 391-398.

29. Travis G.H., Brennan M.B., Danielson P.E., Kozak C.A., Sutcliffe J.G. (1989) Identification of a photoreceptor-specific mRNA encoded by the gene responsible for retinal degeneration slow (rds). *Nature*, 338 (6210): 70-73.

30. Wachtmeister L., Dowling J.E. (1978) The oscillatory potentials of the mudpuppy retina. *Invest Ophthalmol Vis Sci*, 17: 1176-1188.

31. Wenzel A., Von Lintig J., Oberhauser V., Tanimoto N., Grimm C., Seeliger M.W. (2007) RPE65 is essential for the function of cone photoreceptor in NRL-deficient mice. *Invest Ophthalmol Vis Sci*, 48 (2): 534-542.
32. Xu J., Dodd R.L., Makino C.L., Simon M.I., Baylor D.A., Chen J. (1997) Prolonged photoresponses in transgenic mouse rods lacking arrestin. *Nature*, 389 (6650): 505-509.
33. Zhang Z., Gu Y., Li L., Long T., Guo Q., Shi L. (2003) A potential spontaneous rat model of X-linked congenital stationary night blindness. *Doc Ophthalmol*, 107: 53-57.

9 Figures and legends

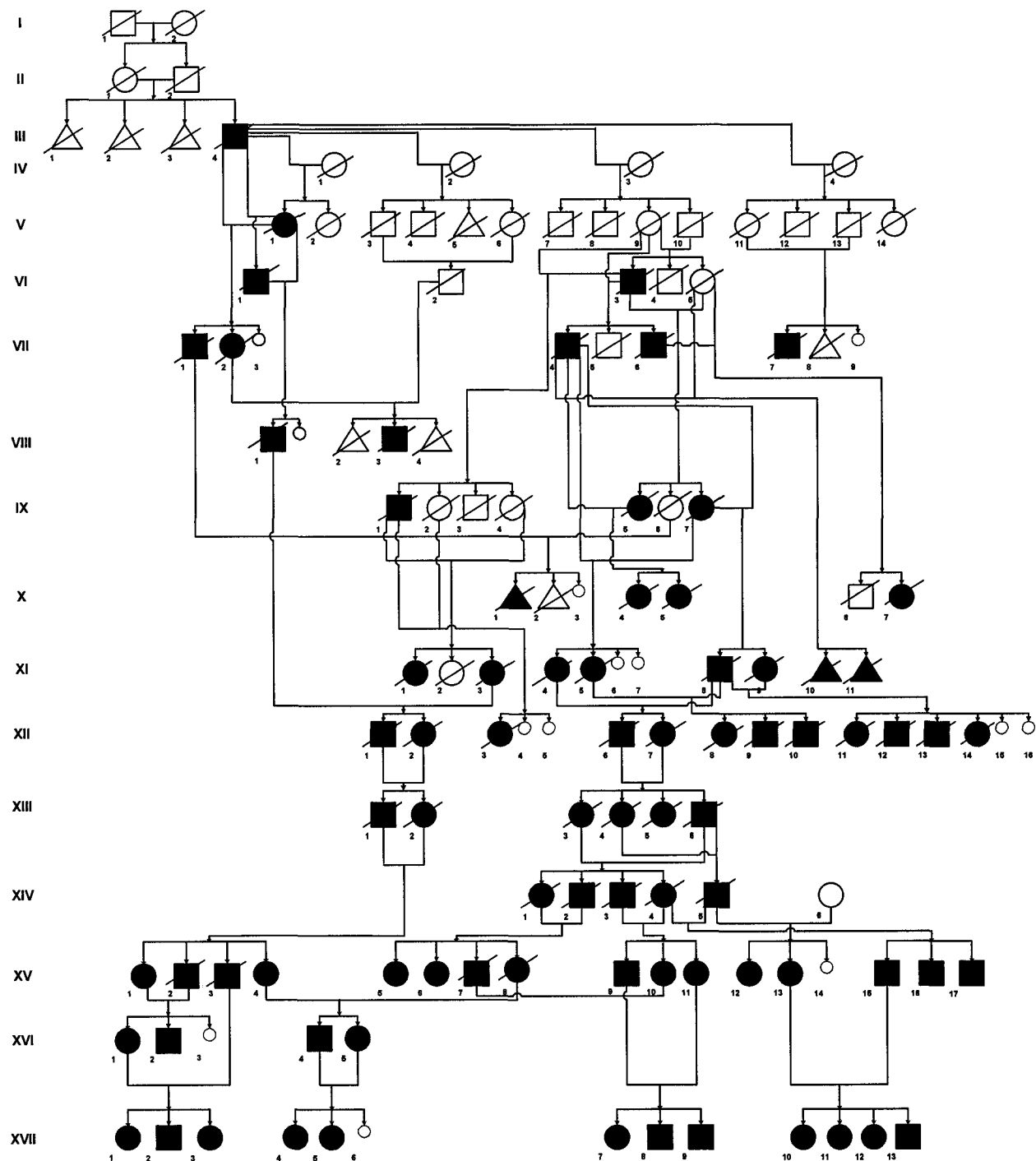


Figure 1: Pedigree of a population of albino Hartley night blind guinea pigs. (○) Normal female, (□) normal male, (●■) night blind female and male, (△) euthanized before sex identification, (○) still born, (∅) dead.

P1 P5 P10 P15 P30 P75 P150 P450

Cone mediated ERG (photopic ERG)



Rod mediated ERG (scotopic ERG)



Rod-Cone mediated ERG (scotopic mixed ERG)

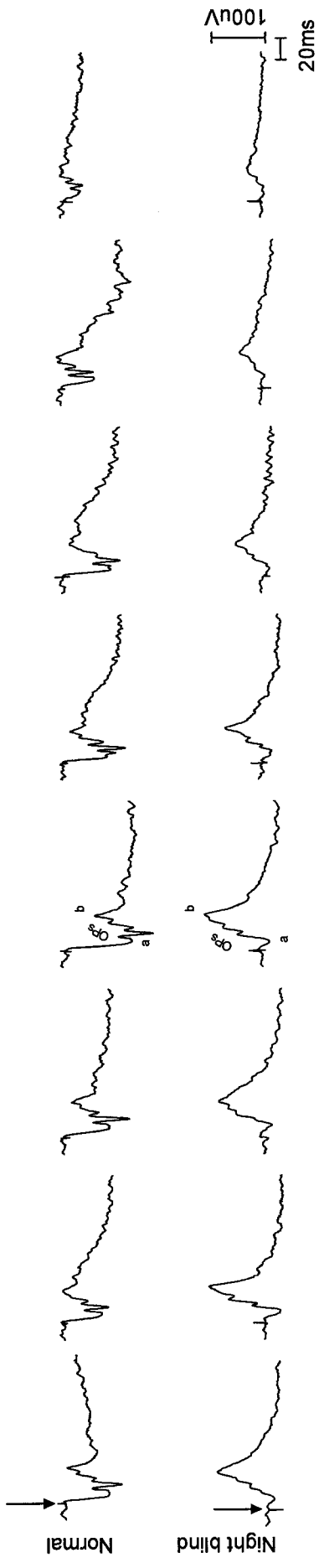


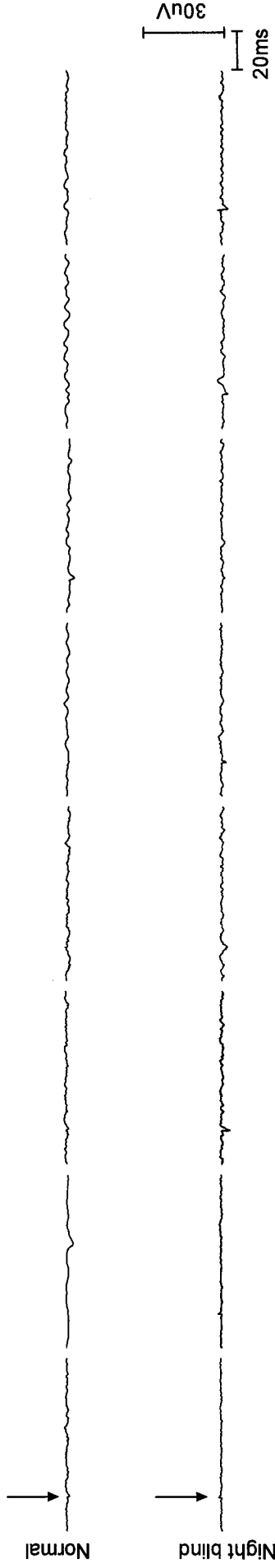
Figure 2: Representative cone (flash intensity: $0.9 \log \text{ cd}\cdot\text{sec}\cdot\text{m}^{-2}$; background: $30 \text{ cd}\cdot\text{m}^{-2}$, average of 20 flashes at ISI of 0.96 seconds), rod (flash intensity: $-2.7 \log \text{ cd}\cdot\text{sec}\cdot\text{m}^{-2}$; average of 3 flashes at ISI of 9.6 seconds) and rod-cone (flash intensity: $0.6 \log \text{ cd}\cdot\text{sec}\cdot\text{m}^{-2}$; average of 3 flashes at ISI of 9.6 seconds) mediated ERGs obtained from normal and night blind guinea pigs aged P1, P5, P10, P15, P30, P75, P150 and P450. Vertical arrows identify flash onset, (a) a-wave, (b) b-wave, (OPs) oscillatory potentials. Horizontal calibrations: 20 ms. Vertical calibrations: $100 \mu\text{V}$.

P1 P5 P10 P15 P30 P75 P150 P450

Cone mediated ERG (photopic ERG)



Rod mediated ERG (scotopic ERG)



Rod-Cone mediated ERG (scotopic mixed ERG)

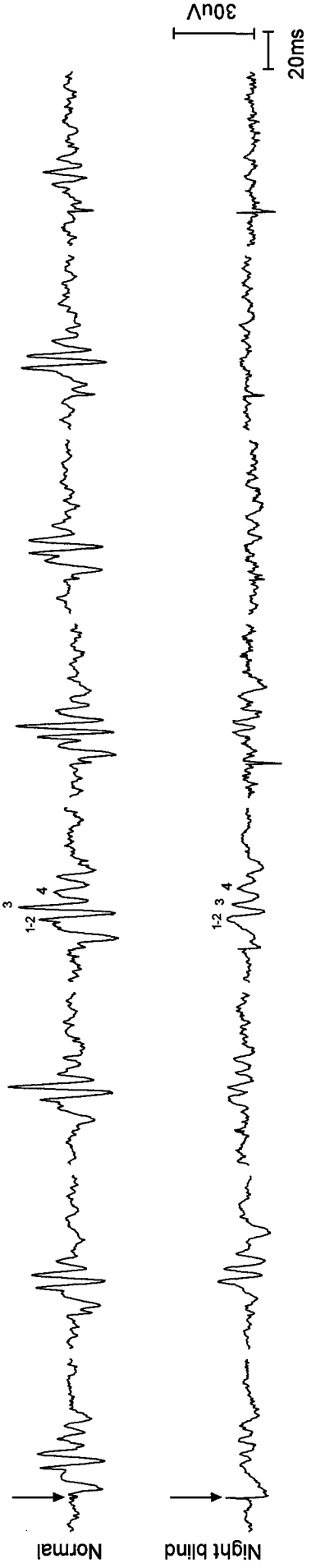


Figure 3: Representative cone (flash intensity: $0.9 \log \text{ cd} \cdot \text{sec} \cdot \text{m}^{-2}$; background: $30 \text{ cd} \cdot \text{m}^{-2}$, average of 20 flashes at ISI of 0.96 seconds), rod (flash intensity: $-2.7 \log \text{ cd} \cdot \text{sec} \cdot \text{m}^{-2}$; average of 3 flashes at ISI of 9.6 seconds) and rod-cone (flash intensity: $0.6 \log \text{ cd} \cdot \text{sec} \cdot \text{m}^{-2}$; average of 3 flashes at ISI of 9.6 seconds) mediated OPs obtained from normal and night blind guinea pigs aged P1, P5, P10, P15, P30, P75, P150 and P450. Vertical arrows identify flash onset, (2) OP₂, (3) OP₃, (4) OP₄. Horizontal calibrations: 20 ms. Vertical calibrations: ERG: $6 \mu\text{V}$; OP: $30 \mu\text{V}$.

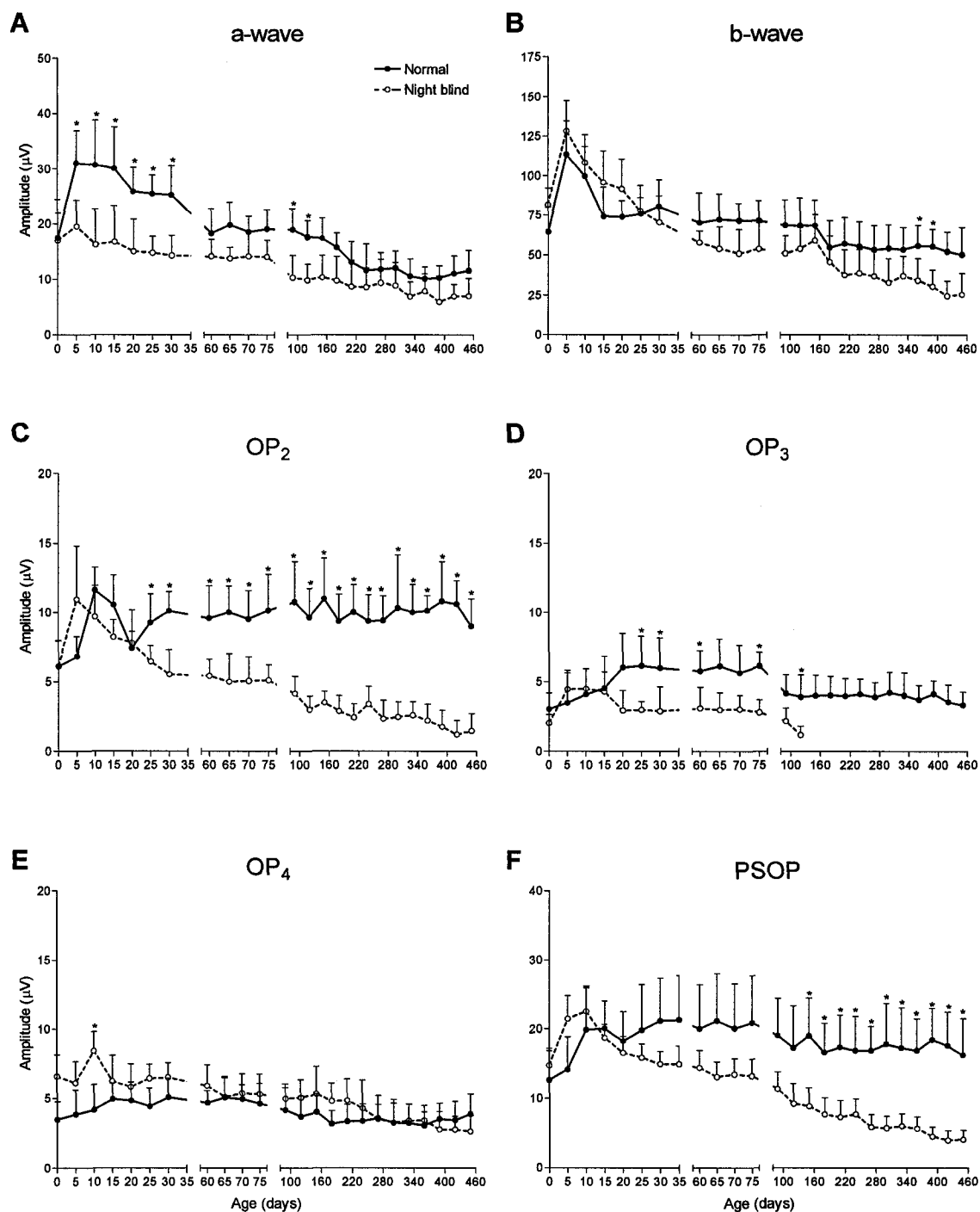


Figure 4: Cone-mediated ERG (flash intensity: $0.9 \log \text{cd} \cdot \text{sec} \cdot \text{m}^{-2}$; background: $30 \text{ cd} \cdot \text{m}^{-2}$) [A] a-wave, [B] b-wave, [C] OP₂, [D] OP₃, [E] OP₄ and [F] PSOP amplitude changes as a function of age (P1 to P450) in normal (full line) and night blind (dashed line) guinea pigs. Each data point represents the mean \pm 1 S.D. * Values are significantly ($p < 0.05$) different between night blind guinea pigs and aged match control.

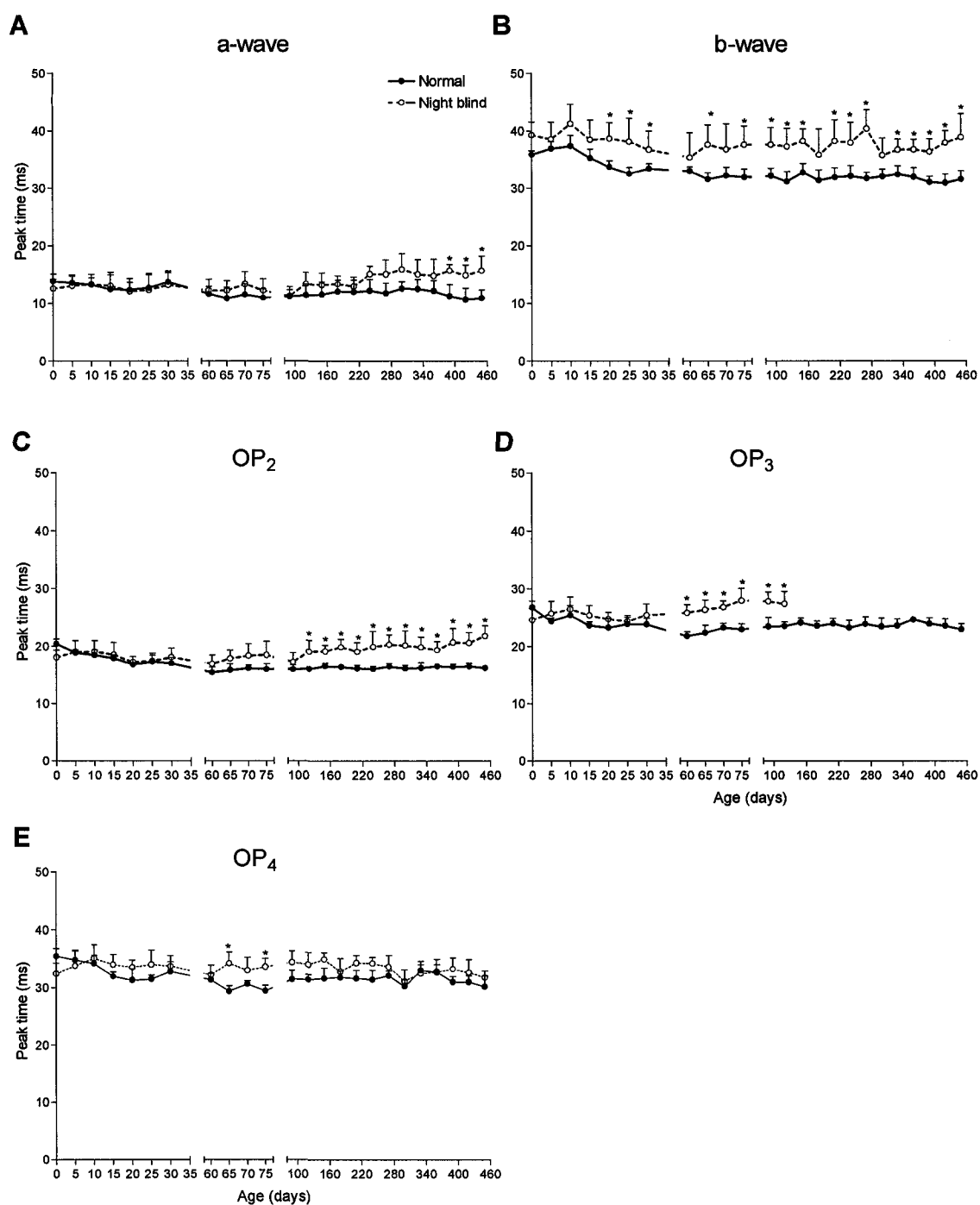


Figure 5: Cone-mediated ERG (flash intensity: $0.9 \log \text{cd} \cdot \text{sec} \cdot \text{m}^{-2}$; background: $30 \text{ cd} \cdot \text{m}^{-2}$) [A] a-wave, [B] b-wave, [C] OP₂, [D] OP₃ and [E] OP₄ peak time changes as a function of age (P1 to P450) in normal (full line) and night blind (dashed line) guinea pigs. Each data point represents the mean ± 1 S.D. * Values are significantly ($p < 0.05$) different between night blind guinea pigs and aged match control.

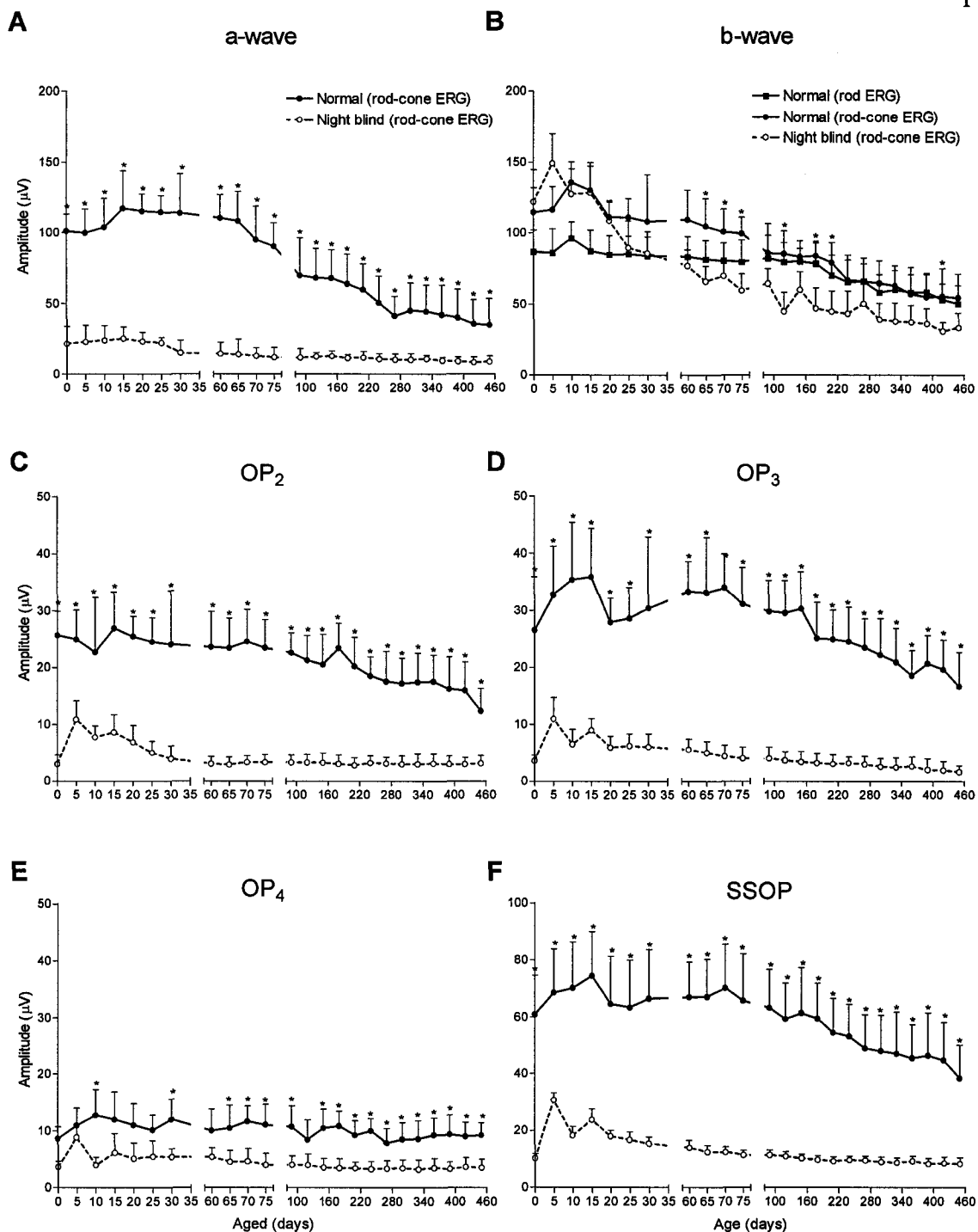


Figure 6: Rod (flash intensity: $-2.7 \log \text{cd} \cdot \text{sec} \cdot \text{m}^{-2}$) and rod-cone (flash intensity: $0.6 \log \text{cd} \cdot \text{sec} \cdot \text{m}^{-2}$) mediated ERG [A] a-wave, [B] b-wave, [C] OP₂, [D] OP₃, [E] OP₄ and [F] SSOP amplitude changes as a function of age (P1 to P450) in normal (full line) and night blind (dashed line) guinea pigs. Each data point represents the mean \pm 1 S.D. * Values are significantly ($p < 0.05$) different between night blind guinea pigs and aged match control.

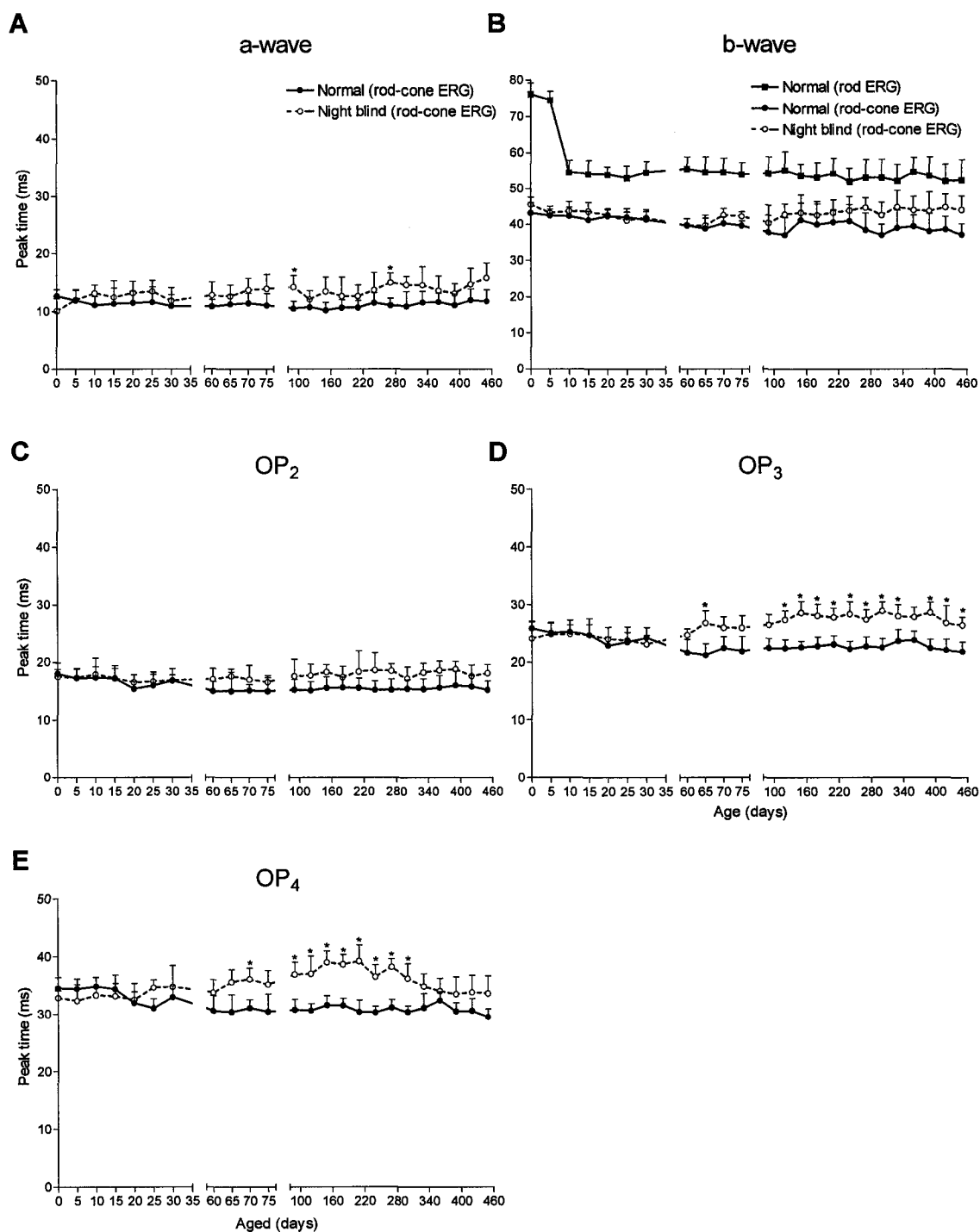


Figure 7: Rod (flash intensity: $-2.7 \log \text{cd}\cdot\text{sec}\cdot\text{m}^{-2}$) and rod-cone mediated ERG (flash intensity: $0.6 \log \text{cd}\cdot\text{sec}\cdot\text{m}^{-2}$) [A] a-wave, [B] b-wave, [C] OP₂, [D] OP₃ and [E] OP₄ peak time changes as a function of age (P1 to P450) in normal (full line) and night blind (dashed line) guinea pigs. Each data point represents the mean ± 1 S.D. * Values are significantly ($p < 0.05$) different between night blind guinea pigs and aged match control.

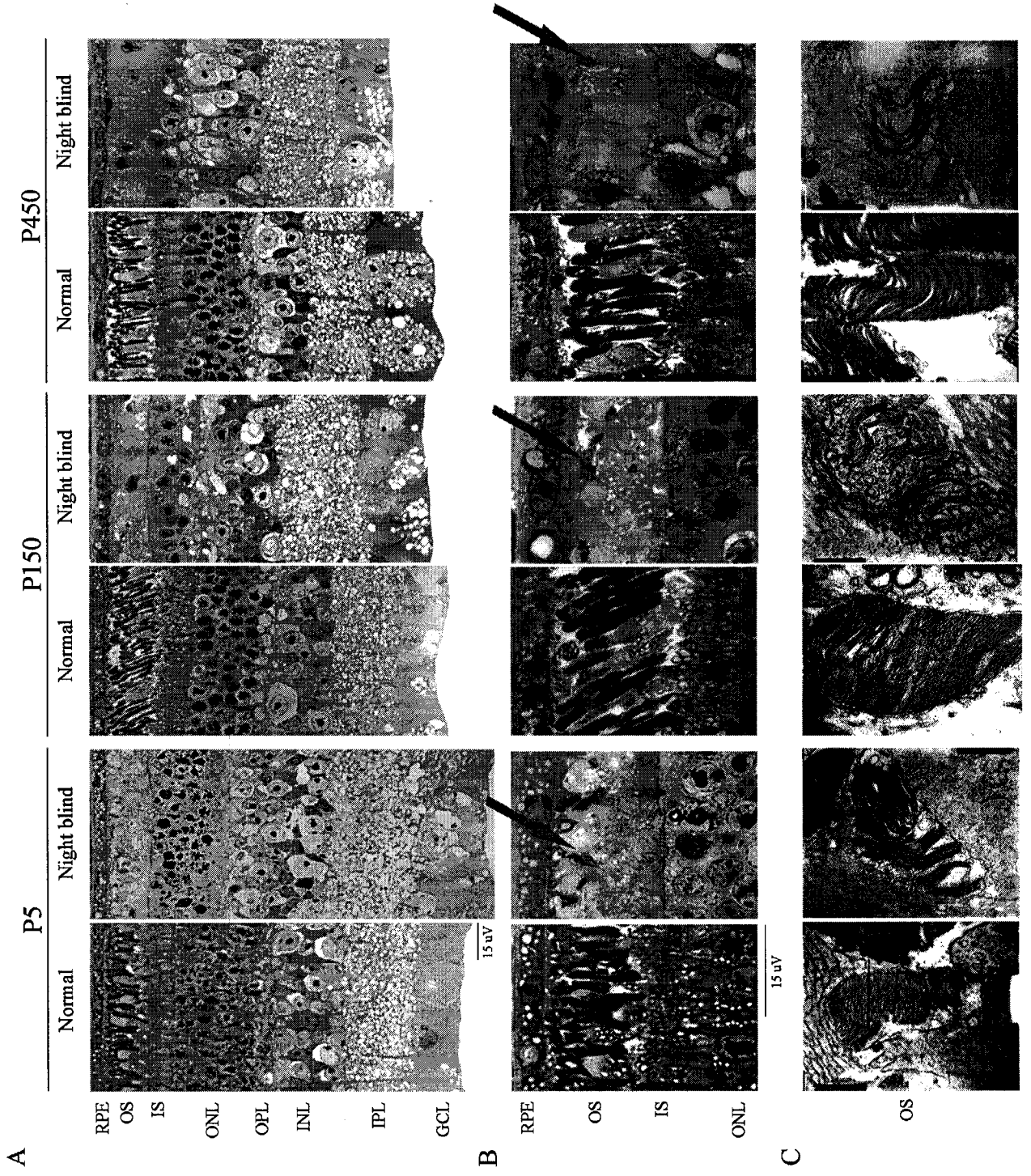


Figure 8: Retinal sections obtained from normal and night blind guinea pigs aged P5, P150 and P450 days. (A) Light microscopy photographs (retinal section thickness: 0.7 μm ; magnification: 40X). (B) Light microscopy photographs (retinal section thickness: 0.7 μm ; magnification: 100X). (C) Electron microscopy photographs (retinal section thickness: 150 nm; magnification: 25 000 X). RPE: retinal pigmented epithelium, OS: outer segment of the photoreceptors, IS: inner segment of the photoreceptors, ONL: outer nuclear layer, OPL: outer plexiform layer, INL: inner nuclear layer, IPL: inner plexiform layer, GCL: ganglion cell layer, Arrows: cone outer segments. Horizontal calibration: 15 μm .

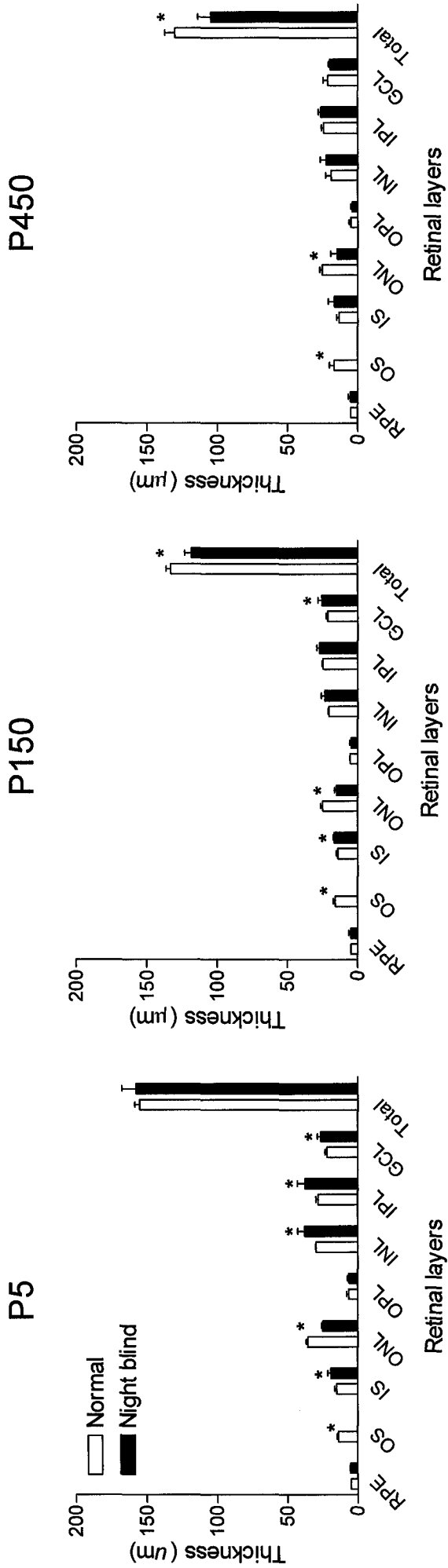


Figure 9: Retinal layer thickness obtained from P5, P150 and P450 days old normal and night blind guinea pigs. RPE: retinal pigmented epithelium, OS: outer segment of the photoreceptors, IS: inner segment of the photoreceptors, ONL: outer nuclear layer, OPL: outer plexiform layer, INL: inner nuclear layer, IPL: inner plexiform layer, GCL: ganglion cell layer. Each bar represents the mean \pm 1 S.D. * Significantly ($p < 0.05$) different from normal.

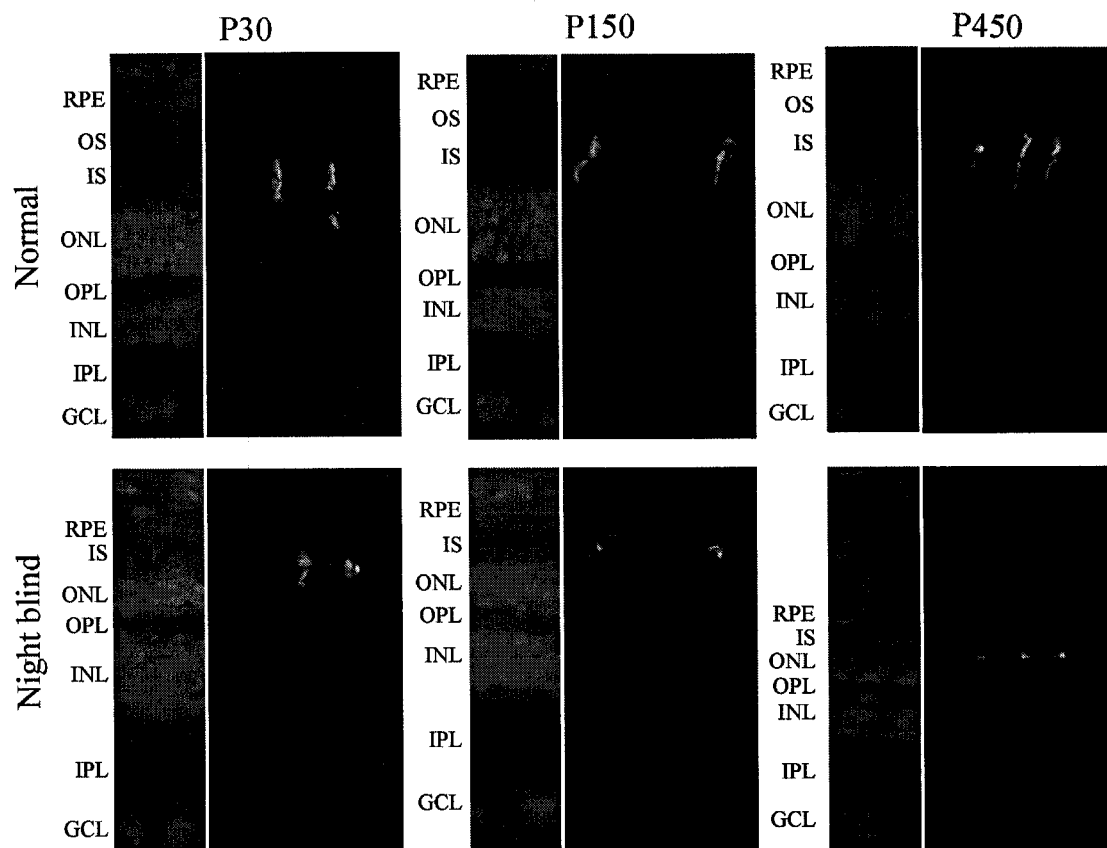


Figure 10: Blue cone opsin (green staining) immunoreactivity obtained from normal and night blind guinea pigs aged 30, 150 and 450 days old. RPE: retinal pigmented epithelium, OS: outer segment of the photoreceptors, IS: inner segment of the photoreceptors, ONL: outer nuclear layer, OPL: outer plexiform layer, INL: inner nuclear layer, IPL: inner plexiform layer, GCL: ganglion cell layer. Red staining (propidium iodide) identifies the retinal cell nuclei.

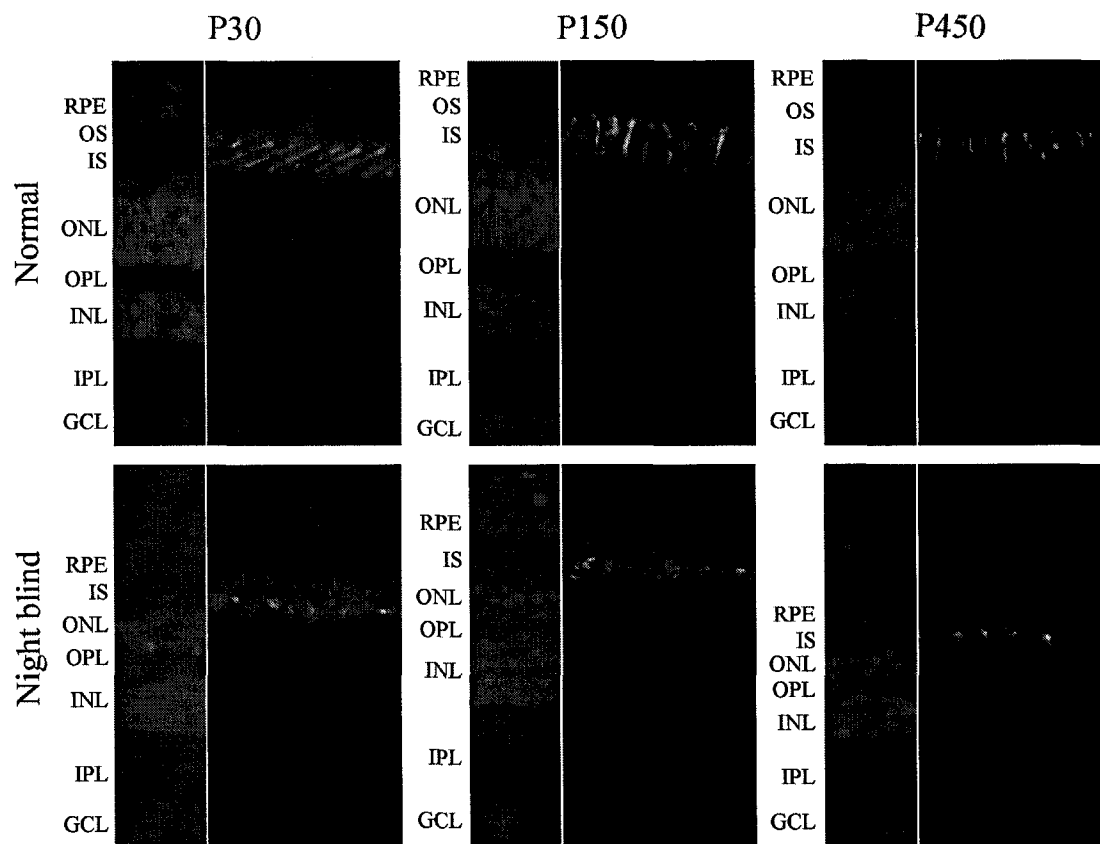


Figure 11: Red/Green cone opsin (green staining) immunoreactivity obtained from normal and night blind guinea pigs aged 30, 150 and 450 days old. RPE: retinal pigmented epithelium, OS: outer segment of the photoreceptors, IS: inner segment of the photoreceptors, ONL: outer nuclear layer, OPL: outer plexiform layer, INL: inner nuclear layer, IPL: inner plexiform layer, GCL: ganglion cell layer. Red staining (propidium iodide) identifies the retinal cell nuclei.

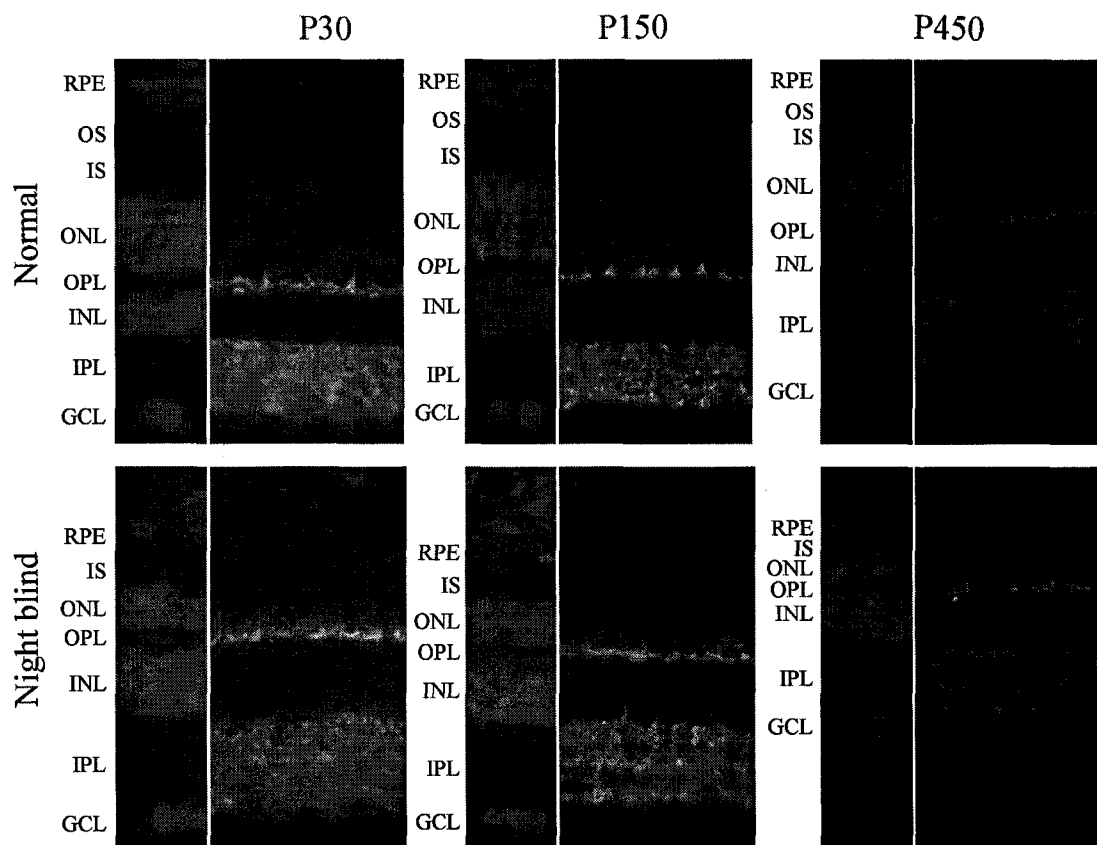


Figure 12: Synaptophysin (green staining) immunoreactivity in normal and night blind guinea pigs aged 30, 150 and 450 days old. RPE: retinal pigmented epithelium, OS: outer segment of the photoreceptors, IS: inner segment of the photoreceptors, ONL: outer nuclear layer, OPL: outer plexiform layer, INL: inner nuclear layer, IPL: inner plexiform layer, GCL: ganglion cell layer. Red staining (propidium iodide) identifies the retinal cell nuclei.

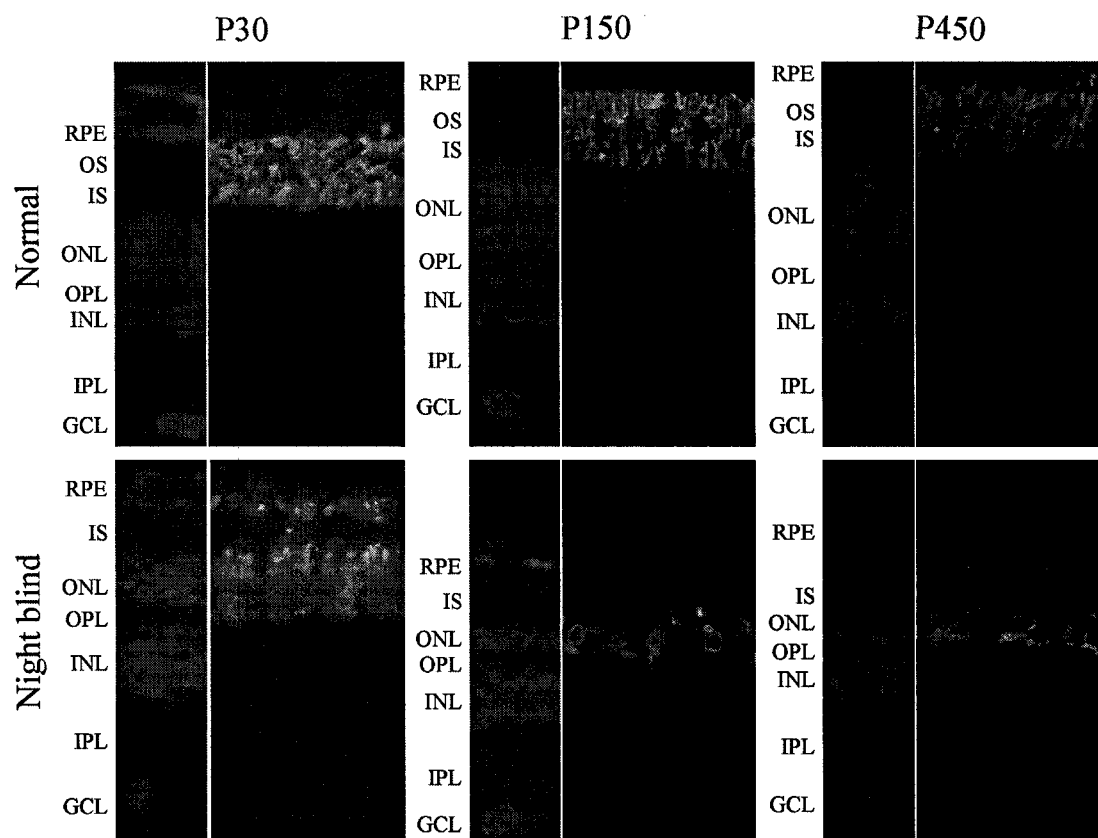


Figure 13: Rhodopsin (green staining) immunoreactivity in normal and night blind guinea pigs aged 30, 150 and 450 days old. RPE: retinal pigmented epithelium, OS: outer segment of the photoreceptors, IS: inner segment of the photoreceptors, ONL: outer nuclear layer, OPL: outer plexiform layer, INL: inner nuclear layer, IPL: inner plexiform layer, GCL: ganglion cell layer. Red staining (propidium iodide) identifies the retinal cell nuclei.

CHAPTER VI: GENERAL DISCUSSION AND CONCLUSION

1 General Discussion

1.1 Summary of findings

The purpose of this thesis was to characterize the maturation and aging of the retinal structure and function of a precocial animal model, namely the albino Hartley guinea pig, and compare our findings with those previously published on altricial animals such as cats (Hamasaki 1985; Jacobson 1987), dogs (Gum 1973; Kirk 1973), rats (Braekevelt 1970; El Azazi 1990, 1991; Kurihara 1977), rabbits (Sanada 1962; Gorfinkel 1988, 1990) and mice (Bonaventure 1968; Gresh 2003). Altricial animals are born with closed eyelids and with an immature retinal circuitry as opposed to precocial animals, which are born with opened eyelids and a more developed retina. Our findings were also compared with those of the night blind guinea pig, a mutant that was developed in our laboratory.

We investigated if the visual system of the guinea pig also undergoes postnatal maturation of its retinal structure and function similar to information previously published for altricial animals (Hamasaki 1985; Braekevelt 1970; El Azazi 1990, 1991; Gresh 2003). We found that despite a relatively more mature visual system at birth compared to altricial animals (rats and mice), the retina of guinea pigs (another rodent) undergoes significant postnatal maturation of its structure and function. We reported that the rod-mediated ERG was more mature at birth than the cone-mediated ERG, since the changes in amplitude in the first few days of life were less important in scotopic condition than in photopic condition. Changes according to time were also accompanied by a subtle reorganization (increase in length of the inner and outer segments of the photoreceptors along with a thinning of all the other cellular layers) of the retinal tissue with age, albeit not to the same extent as was previously documented for altricial animals (Bonaventure 1968; Braekevelt 1970; Kurihara 1977; el Azazi 1990, 1991; Gresh 2003).

While performing the later experiments, an accidental mating between a brother and a sister occurred. Out of this union, one pup presented abnormal ERG recordings consisting of a lack of rod mediated vision and photopic-like scotopic ERG responses when exposed to bright flashes of light. Furthermore, this mutant revealed a significant attenuation of the OFF-retinal response and of the photopic negative response (PhNR) of the ON-ERG. With time, we were able to reproduce this phenotype on several occasions, through selective breeding. In order to further our understanding of this unique retinopathy, we investigated, with long-term follow-up studies, if this retinopathy was stationary or degenerative and also tried to identify the retinal origin of this disorder. Our key findings were as follows; 1- recessive mode of inheritance, 2- retinopathy, which affects rod photoreceptors first (absent from birth) and the secondly cones, 3- no recordable rod mediated ERG from birth, 4- decreased photopic negative response and OFF-retinal response, 5- scotopic rod-cone mediated ERG of photopic-like morphology, 6- loss of photopic OP₃ with age, 7- decreased retinal thickness, 8- no rod photoreceptor outer segments, 8- misplaced rhodopsin staining, 9- normal cone immunostaining and 10- functional deterioration (significant decrease of the ERG components amplitude) with age indicative of a degenerative condition.

Analysis of the cone ERG of the normal guinea pig allowed us to confirm that it is almost identical to that of humans, with a- b- and i-waves of amplitude, peak time and morphology similar to human cone ERG; features not seen in other rodents commonly used in vision research such as rats and mice. In fact, the photopic ERG of rats and mice lacks of recordable a-wave and i-wave while the amplitude of the ERG b-wave is significantly larger than in humans (Nixon 2001; Xu 2003; Gresh 2003, Rosolen 2004). Furthermore, in guinea pigs, similar to humans, we were able to obtain a photopic hill (Wali 1992, Racine 2005). The above led us to suggest that the guinea pig could represent a better animal model (compared to rats and mice) to study the human photopic ERG. We also noticed, while recording intensity response functions in scotopic condition, that ERGs elicited with bright flashes were of negative morphology, a feature never before

reported in other normal animal models. This aspect of the guinea pig ERG is further discussed in section 1.5 of the discussion.

1.2 Maturation of the retinal structure and function in precocial guinea pigs

Maturation and aging of the retinal structure and function of altricial animals, such as rats and mice, have been studied extensively (Gum 1973; Kirk 1973; Kurihara 1977; Hamasaki 1985; Jacobson, 1987; Gorfinkel 1988; El Azazi 1990, 1991; Gorfindel 1990; Gresh 2003). Altricial animals are born with closed eyelids and an immature visual system, where the formation of the outer segment of the photoreceptors precedes the development of synapses. In fact, at birth the retina of altricial animals is not functional since synapses and retinal cells are not fully developed. That is why an ERG cannot be elicited from retina of altricial animals at birth. In general, the first ERG recorded is usually a negative wave, which is present for the first time at the opening of the eye (Bonaventure 1968; Kirk 1973; Fulton 1980; Gorfinkel 1988). The other elements of the ERG (b-wave, OPs) usually develop a few days later. By the end of the first month of life, the retina of altricial animals is functionally mature (Bonaventure 1968; Braekevelt 1970; Jacobson 1987; Gorfinkel 1988)

The genesis of retinal cells in rats and mice starts at around embryony day 10 (E10). At postnatal day one (P1), the retina of rats consists of the nerve fiber layer, the ganglion cell layer, the inner plexiform layer and a single layer of undifferentiated neuroblastic cells (Braekevelt 1970; Weisse 1995). In fact, the degree of development of the rat retina at birth corresponds to the retina of a 4-5 months old human fetus (Weidman 1968). During the first few days after birth, mitosis of the retinal cells increase in frequency and the neuroblastic layer thickens considerably. In rats and mice, maximal retinal cell count will occur at around P12 (Cepko 1996; Rapaport 2004).

In the outer nuclear layer, normal developmental loss of cells begins at P12 and proceeds until approximately P27 (Maslim 1997). Developmental organization of the inner plexiform layer starts from eye opening at P14-P15 through P25-P30. For instance, the terminals of cone bipolar cells in the inner plexiform layer develop mature characteristics starting at P25 (Johansson 2000), and dopaminergic neurons in the inner plexiform layer are not fully light responsive until P25. Furthermore, the spontaneous activity of ganglion cells will start at around P22-P27 in rats (Tian 2001, 2004). By the time the eyes open, which occurs in rats between days 12-14, the visual system becomes functional. In fact, a study published by Molotchnikoff et al. in 1993 showed that the functional development of the retinotectal pathway in neonatal rats begins at the end of the first week after birth, and that much of the functional maturation occurs mainly during the second week of life. Maturation of the retina in rats seems to be completed between postnatal days 30 to 40. In summary, the genesis of retinal cells and synapses in the retina of altricial animals is incomplete at birth, which leads to massive structural and functional changes of the altricial retina during the first month or so of life (figure 5).

In contrast, precocial animals, like humans, primates and guinea pigs, to name a few, are born with opened eyes and a more mature visual system compared to altricial animals where the genesis of synapses precedes the formation of the photoreceptor outer segments (Winkelman 1962; Shipley 1964; Smelser 1974; Spira 1975; Huang 1990). In fact, the entire retinal cell formation and synapses occur *in utero*, so that, by birth, the retina is of almost adult-like architecture. The study of Spira in 1975, which described the maturation and development of the retina in guinea pigs, revealed that differentiation of the neural retina begins at around day 23 of gestation (E23). By E34 the retina reaches its maximum thickness and primitive synapses are already evident in the inner plexiform layer. At E43-E45 synaptic ribbons are fully formed in synaptic layers. Outer plexiform layer develops within the neuroblast layer at E40 simultaneously with the inner segment of the photoreceptors. The formation of the outer segments

is finished by E69. The retina appears mature by E57-E69. Therefore, an electroretinogram can be recorded at birth in newborn guinea pigs. In fact, a study published by Huang et al. in 1990 reported that the retina of precocial guinea pigs is fully responsive electroretinographically by E55 and that a mature-appearing ERG is recordable at approximately 64 days of gestation. Therefore, the ERG recorded in newborn guinea pigs is of adult-like morphology (figure 5) (Huang 1990; Bui 1999; Vingrys 2001; Lei 2003, Racine 2003).

Significant maturational events	Altricial animals	Precocial animals
Days of gestation	21 days	68-69 days
Opening of the eyes	P12/P14	E56
First recordable electroretinogram (ERG)	P12/P14	E55/E56
Genesis of the first retinal cells	E10	E20/E23
Photoreceptor outer segments (OS)	P4-P14	E50-E69
Outer nuclear layer (ONL)	P5-P12	E40-E60
Outer plexiform layer (OPL)	P15-P30	E40-E60
Inner nuclear layer (INL)	P4-P12	E40-E60
Inner plexiform layer (IPL)	P14-P30	E34- E60
Ganglion cell layer (GCL)	E17-E22	E30-E60-
Maximal retinal thickness	P12	E34
Completed retinal maturation	P60	P20-P30

Table 3: Table summarizing the most significant maturational events in retinal development of altricial animals (ie: rats) versus precocial animals (ie: guinea pigs). (E): embryonic day, (P) postnatal day. Data taken from: Altricial animals (Weidman 1968; Braekevelt 1970; Webster 1991; Weisse 1995; Cepko 1996; Maslim 1997; Rapaport 2004; Johansson 2000; Tian 2001, 2004); Precocial animals (Spira 1975; Huang 1990; Loeliger 2005, Racine 2007).

One could wonder, given their relative retinal maturity at birth, if the retina of precocial animals could undergo structural and functional maturation after birth, like altricial animals? Results presented in the literature suggest that it does (Horsten 1960; Ookawa 1971 a, b; Knave 1972; Smelser 1974; Woods 1983; Rodriguez-Saez 1993; Breton 1995; Mets 1995; Westall 1996; Hansen 2005). In fact, studies reporting retinal changes over time in precocial animals suggest that, even if the retinal cells and synapses are mature at birth in these animals, the structure and function can change with time. For example, in their study on the maturation of the pattern electroretinogram and visual evoked potentials, Breceelj (2003) reported that the pattern electroretinogram (PERG) and the pattern visual evoked potentials (PVEP) change persists until adulthood in human. This study also revealed that the macula continues to mature beyond 4 years of age in humans. In 2005, Hansen et al. showed in their study on young infants that the peripheral cone function was relatively more mature compared to that of adjacent rods. Furthermore, they reported that there was also a lack of the photopic hill effect in infants, a finding that could reflect an immaturity in the relative contributions of ON- and OFF-bipolar cell responses to the genesis of the cone ERG b-wave as suggested with the push-pull concept of Sieving et al. (1994). More recently, Moskowitz et al. reported low amplitude oscillatory potentials in infants, indicating that the OPs are also less mature compared to adults. Tian et al. (2004) showed that the synaptic network of the retina continues to mature after eye opening in precocial mammals: the retinal neurogenesis and synaptogenesis started before birth and continued during early postnatal development. In fact, the pruning of RGC dendrites is one of the best examples of the maturational reorganization of neuronal processes in precocial animals (Wong 2002). Consequently, although most of the maturation of the retina occurs *in utero*, giving to the retina an adult-like appearance at birth, it does not preclude that it will not continue to mature after birth.

Is the latter also true for the precocial guinea pig? Bui et al. (1999) and Vingrys et al. (2001), examined the development of the rod mediated

electroretinogram in pigmented and albino guinea pigs, from birth to postnatal day 60. Similarly to us, they reported a significant postnatal maturation, up to postnatal day 12, of the a-wave amplitude that was accompanied by a significant shortening of its peak time. Likely, Vingrys et al. (2001), reported that the b-wave matured soon after birth at around P10-P12, an age comparable to that reported in the present study (P10 for rod and rod-cone mediated ERGs). Additionally, they also reported that the postnatal maturation of the oscillatory potentials is similar to that of the b-wave (e.g. maximal amplitude reached at about P10-P12), an age range again comparable to that reported in this thesis (P10 and P15, depending on whether we are looking at early or late OPs). We believe that the latter discrepancy between our results and that of Vingrys et al. reflects the different approaches used in quantifying the OPs. In our study we measured and reported each OP individually, while in Vingrys' study, the OPs were mathematically extracted from the ERG signal, modeled and then reported collectively, thus preventing comments on individual OPs.

When the rod and the rod-cone ERGs are considered, our results confirm those obtained by Bui et al. and Vingrys et al. Our original contribution to these studies is that we are also showing similar age-related changes to the cone-mediated ERG and compared these functional alterations with maturation-induced modifications to the retinal cytoarchitecture, aspects that were not covered in the previous studies alluded above.

In accordance with the study of Spira et al. (1975) that showed that during the development of the guinea pig retina, the cones matured faster than the rods, we reported that the photopic ERG components (a-wave, b-wave) reached their maximal values before the scotopic ERG components. However, we also reported that following the first few days of life the gain in amplitude of the a- and b-waves was significantly larger for the cone mediated ERG compared to rod mediated responses, suggesting that guinea pigs are born with a more mature rod signal. Similarly, photopic OPs also reached their peak amplitude before the scotopic

OPs. Furthermore, as reported above for the a- and b-wave, the gain in amplitude for the cone SOPs was significantly larger than that measured for the rod SOPs, pointing again to a more mature rod function at birth. Not only does the rod function appear more mature than cone function at birth in guinea pigs, it also demonstrates less amplitude changes within the first month of life or so, compared to the cone function. We noted that, after P5, there was a rapid decline of the cone ERG, a feature not seen for rod function where only small decrease in amplitude are recorded after reaching maximal values. One could wonder why the rod function is more mature than the cone function at birth in guinea pigs. Given that the rods are only connected to the ON-retinal pathway whereas the cones are connected to both the ON- and OFF-retinal pathways, we could suggest that, at birth, the ON-retinal pathway is more mature than the OFF-retinal pathway. The later is supported by the study by Hansen et al. (2005) that showed that in human infants there is an immaturity in the relative contributions of the ON and OFF bipolar cell responses to the ERG (Hansen 2005). The delayed maturation of the OFF-retinal pathway compared to the ON-retinal pathway, could also explain why cone function after P5 yielded a larger ERG amplitude decrease compared to that of rod.

It is interesting to note that the above-mentioned ERG amplitude changes observed in precocial guinea pigs were also noticed in maturing altricial animals although not at the same age. For example, El Azasi and Wachtmeister (1990) reported that scotopic OPs in rats appeared to mature thirteen days earlier than photopic OPs (scotopic: P17; photopic: P30). Similarly, Jacobson and Ikeda (1987) reported that the implicit time of the rod generated b-wave in cats reached adult values between the 6th and 7th week of life, compared to 11th -12th week for the cone b-wave.

In this thesis we report that the retinal function of the albino guinea pig, as evaluated with the electroretinogram, undergoes significant amplitude and peak time changes with age, changes that are also significantly correlated with

concomitant modifications of the retinal ultrastructure. We claim that these changes in structure and function resulted from the normal maturation processes. This is not to say that other factors such as 1- growth of the papillary aperture, 2- axial elongation, 3- size of the eyeball, 4- changes in cardiac rhythm, 5- changes in the resistance of the ocular tissues and the like, that are also age related, could not have contributed to our results, especially those pertaining to retinal function.

Notwithstanding the above, we believe that these factors should have had an equal influence on the maturation of all the ERG components. Given that our results show that the different ERG components do not mature at the same rate, we postulate that these other factors had a negligible (if any) impact on the functional maturation processes and consequently the ERG data reported in this do reflect the functional transformations taking place in the retina as it matures.

Finally, the maturation of the retinal function in guinea pigs was also accompanied by an overall thinning of the retina during maturation. These structural changes could explain the concomitant attenuation of the b-wave of the ERG and corresponding OPs with maturation. Few studies reported similar structural and functional changes in maturing altricial animals. For example, Liu et al. (2006) reported that the maturation of the oscillatory potentials in neonatal rats might be the consequence of the final refinement of the inner retinal circuitry. Similarly, Gum et al. in 1983 reported that the decrease in b-wave latency observed in the neonatal dog occurred between the 3rd and 4th week of life, which corresponds to the retinal maturation of the inner and outer nuclear layer.

Finally, although guinea pigs are born with a mature visual system, retinal structure and function will undergo significant modification as the animal ages, where the functional changes take place simultaneously with the structural changes.

1.3 Aging of the retinal structure and function in precocial guinea pigs

We know that during the first few weeks of life, maturation of the retina in altricial and precocial animals is very different between the two groups, given that the retina of altricial animals is not fully mature at birth whereas it is almost totally developed in precocial animals. Do the retinal structure and function of two animal models (altricial and precocial) also differ in their aging process? In altricial animals, substantial structural changes accompany the aging process, particularly affecting the neuronal cells, the pigment epithelial cells and, to a lesser extent, the retinal blood vessels (Weisse 1995). Between the ages of 1 to 27 months old, there is an overall decline in nuclear density of the outer nuclear layer by 38-50% and of the inner nuclear layer by 27-33% (Weisse 1995). Similarly, over the same period of time, the loss in ganglion cells was comparable to the decline in the inner nuclear layer density (i.e.: 27-33%). As the animals got older there was also, in the retinal pigment epithelium, substantial accumulation of lipofuscin and thickening of the basal membrane accompanied with a shortening of the apical microvilli (Weisse 1995). Using standard electroretinogram, Gresh et al. in 2003 demonstrated that the cone and the rod a- and b-waves in mice also decreased with age up to 17 months. The latter results were in accordance with those published by Cillino et al. (1993) and Li et al. (2001), where they revealed a reduction in ERG amplitudes with age in rats and mice up to 12 months, respectively. Similarly, Aleman et al. (2001) showed that the amplitude of the rod-cone mediated a-wave in older rats (18 months old) was 60%, and that the b-wave was 80% of that recorded in younger animals.

In comparison, our results, reported in the following figure 5, showed that the cone ERG parameters (a-wave + b-wave + PSOP) and the rod-cone mediated ERG parameters (a-wave + b-wave + SSOP) in albino guinea pigs decreased by 40% and 60% respectively, in animals aged from P1 to P450. Of interest, this

decrease in amplitude of the cone and rod-cone ERGs, is also accompanied by a gradual thinning of the retina in albino guinea pigs. Furthermore, from the second month of life or so, the amplitude of the photopic a-wave, b-wave, OP₃ and OP₄ decreased regularly until 450 days while that of OP₂ remained stable, further supporting the claim of a different retinal origin for the early and late OPs (Kojima 1978; Lachapelle 1983, King-Smith 1986). In scotopic ERG it is the a-wave, b-wave, OP₂ and OP₃ that showed progressive amplitude decreased with age while OP₄ remained stable. In general, the amplitude changes after postnatal day 60 (P60), were more pronounced in scotopic compared to photopic conditions. These results are in accord with the study of Gresh et al. in 2003, showing that the cone ultra structure was more resistant to aging than that of the rod. This discrepancy between photopic and scotopic ERG changes with age could also be explained by the fact that, in albino retina, rod apoptosis starts earlier in time compared to cone apoptosis, since in albino animals rods are more susceptible to light damage while cones are more resistant (Shinowara 1982; Semple-Rowland 1987; Weisse 1995).

In fact, our results are in accordance with the latter. As illustrated in figure 5, plotting together the normalized amplitude of the cone ERG parameters (a-wave + b-wave + PSOP) and of the rod-cone ERG parameters (a-wave + b-wave + SSOP) revealed that the scotopic ERG parameters decreased more rapidly than the cone ERG parameters, suggesting that the rods died first followed by the cones in the guinea pig retina. The linear regression equation also informed us about the Y-intercept. The later value indicates that, in the eventuality where no rod-cone mediated ERG are recordable in albino guinea pigs, a 25.67 ± 5.23 uV cone ERG could still be elicited.

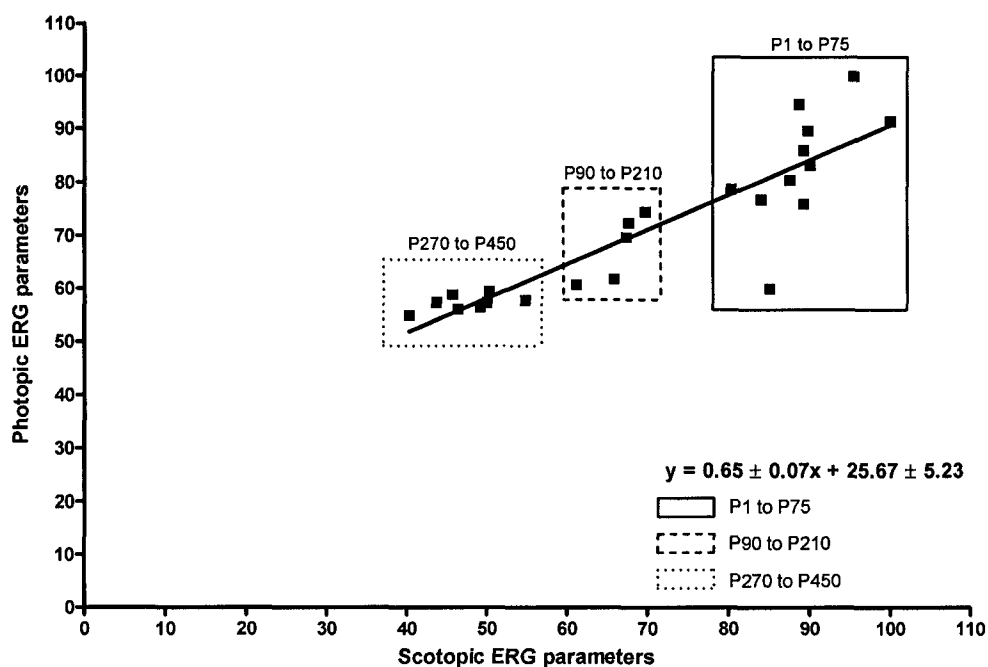


Figure 5: Normalized photopic ERG parameters VS scotopic ERG parameters in normal Hartley albino guinea pigs aged from P1 to P450.

One could also wonder if human retinas also undergo structural and functional changes as they age. A few studies have already reported the effect of age on the ERG and revealed that the amplitude of the human ERG components decreases with age (Karpe 1950; Zeidler 1959; Weleber 1981; Wright et al 1985; Birch 1992). The differences in recording conditions and in methods of analysis make it hard to compare these studies, but they all come to the same conclusion: human ERG decreases according to age. In 1950, Karpe et al. measured the b-wave amplitude in patients over 50 years old and found that the amplitude has a tendency to decrease with age. In fact, patient under 50 years of age revealed ERG amplitude of 0.36 ± 0.06 mV, whereas patient over 50 years old revealed ERG amplitude of 0.32 ± 0.08 mV. Zeidler (1959) also reported a significant difference in b-wave amplitude between young and old human subjects, where the ERG responses reached adult values by 5 years of age and remained relatively unchanged until after 50 years when responses decline gradually. Similarly,

Weleber in 1981, in his study of the effect of age on human cone and rod ERG, revealed significant decrease of the b-wave amplitude of both photopic and scotopic mediated responses with age. However, Weleber (1981) reported that the scotopic mixed a-wave and the implicit times were not age-dependent. In 1985, Wright et al. also described a gradual decrease in amplitude of the scotopic and photopic ERG with age. Finally, Birch et al. (1992) revealed that the b-wave amplitude for both rods and cones declined gradually up to 55 years old. They also suggested that, by 70 years old, the ERG amplitude was one half of that of young adults.

According to Fortune et al. (2002), the decrease in ERG amplitude in human subjects could be the result of a decreased transmission of light through the eye. However, a study published in 1982 by Hemenger et al. revealed that there were no age-related changes in ocular transmission in healthy human patients up to 62 years old. Similarly, Horiguchi et al. in 1998, detected age-related decline in ERG amplitude in pseudoaphakic patients, implying that at least some of the deficits associated with normal aging are not due to decrease lens transmission. Whether the decrease in ERG amplitude is due or not to a decrease in transmission of light through the eye is still a question that remains debated.

1.4 Albino versus pigmented animals

Results presented in this thesis were all obtained using the albino Hartley guinea pigs model. Would we have obtained similar results with a pigmented strain? In their studies, Bui et al. (1999) and Vingrys et al. (2001), reported that the maturation sequence of the rod-mediated ERG was equivalent in both strains. They also showed that, compared to pigmented guinea pigs, the ERG responses of the albino strain were of larger amplitude, of faster peak time and of lower threshold; findings that are compatible with those reported in human albinism. These results are also in accordance with Krill et al. (1963), who proposed that an increase in light penetration that is associated with the hypopigmented albino

irises, results in greater stimulus effectiveness. Notwithstanding the above it is often difficult to distinguish the possible role of the melanin pigment from what could simply reflect a strain difference. For example, Behn et al., in 2003 showed that pigmented Long Evans (LE) rats had a significantly faster rate of dark-adaptation compared to Sprague Dawley (SD) rats; results that probably reflect the increase in bio-availability of calcium associated with melanin. More recently, Dorfman et al. (2004) reported that the retinal structure and function in pigmented rats exposed postnatally to hyperoxia were significantly more affected than in albino animals, suggesting that melanin could act as a pro-oxidant. In contrast, Joly et al. (2005) and Zimak et al. (2007) reported that albino rats exposed postnatally to intense light developed a severe retinopathy (structure and function) while pigmented rats did not, as if melanin protected the retina from the intense light insult.

1.5 The night blind guinea pig

We depend on animal models to further our understanding of acquired and inherited retinal disorders. Many animal models have arisen from spontaneous mutations, while others have been induced by genetic manipulations. During the last 20 years, more than 80 different genes responsible for hereditary retinal degeneration have been cloned and 52 genes have been mapped (Besch 2003, RetNet <http://www.sph.uth.tmc.edu/Retnet/>). On the other hand, the diversity of spontaneously occurring animal models available for research purposes, during the same period, has not increased as fast as for genetically engineered animal models.

Our guinea pig model of night blindness is one of the few naturally occurring animal models reported in the literature. However, to our knowledge, our mutant is the only spontaneously occurring animal model that presents non-recordable rod mediated ERGs at birth with near normal cone function. There are, however, genetically manipulated animal models such as the rhodopsin knockout

(rho^{-/-}) mouse (Toda 1999; Jaissle 2001), the RPE 65^{-/-} mouse (Redmond 1998), the α -transducin^{-/-} knockout mouse (Calvert 2000), the arrestin^{-/-} knockout mouse (Xu 1997) and the NRL^{-/-} knockout mouse (Mears 2001) that present extinguished rod-mediated function and a normal cone ERGs.

Our night blind phenotype resulted from an accidental mating between a brother and a sister. Following selective breeding, we postulated that the retinopathy was inherited as an autosomal recessive trait as described by our pedigree. At first, the pathophysiological processes were almost entirely limited to the impairment of the rod pathway. However, the OFF-retinal response anomalies reported could suggest that there were, although relatively minimal, also some repercussions in the cone pathway since only cone photoreceptors are directly connected to the OFF-retinal pathway. Long-term follow-up studies suggest that the retinopathy could be degenerative. However, although the retinopathy appears to degenerate with time, some key features of the human congenital stationary night blindness (CSNB) are seen in our mutant guinea pigs. First, it is congenital; no rod-mediated ERG could be elicited from birth, and the cone ERGs were of normal amplitude. Furthermore, the loss of the photopic OP₃ in adult guinea pigs (P120) could also be indicative of CSNB, as in humans, short latency photopic OPs also disappears, while long latency OPs remains intact (Lachapelle 1983; Miyake 1986).

From birth, night blind guinea pigs did not generate a pure rod mediated response (e.g.: no rod ERG at threshold intensities) and a positive, almost photopic-like, ERG in scotopic mixed condition, leading us to suggest that only the cones contributed to the dark adapted ERG. Immunostochemistry and histology also revealed the presence of cone opsins and cone outer segments, respectively, in the night blind guinea pig retina. However, the cone outer segments were misplaced in the inner segment layer (ISL). The later would suggest that, in order to be functional, the cone outer segments do not need to be inserted in the outer segment layer of the retina. Furthermore, in young night blind

guinea pigs (prior to P25), the cone-mediated ERG was of larger amplitude than normal. But how to explain this larger than normal cone ERG amplitudes in young night blind guinea pigs and near normal cone ERG in older ones, when the histology reveals abnormal cone outer segment morphology and location? It is as if we do not need intact cone outer segments in order to generate a normal cone ERG. Our results revealed that, as far as the opsin is inserted in the outer segment of the cone, the cone ERG is of normal amplitude. In fact, the larger ERG in the young mutant could be explained by a thicker retina in mutants than normal at young ages. Furthermore, in older night blind guinea pigs, the ERG are of smaller amplitude than normal, which is in line with histology reports which reveal a thinner retina in adult mutants compared to normal. In fact, in a previous study of ours (Racine 2007, submitted) on the maturation of the retinal structure and function in the albino guinea pig, we reported that the decrease in ERG amplitude associated with age occurred at the same time as the decrease in the total retinal thickness in these animals, therefore suggesting that the retinal thickness could have an effect on the ERG amplitude. For example, rats rod ($433.1 \pm 148.8 \mu\text{V}$), rod-cone ($611.2 \pm 194.8 \mu\text{V}$) and cone-mediated ERG ($136.0 \pm 28.0 \mu\text{V}$) b-wave amplitudes measured at P60 are all of larger amplitude than what is measured for guinea pigs at the same age [rod b-wave: $83.13 \pm 14.24 \mu\text{V}$; rod-cone b-wave: $110.26 \pm 16.60 \mu\text{V}$; cone b-wave: $70.20 \pm 18.95 \mu\text{V}$] and also have a thicker retina ($220.0 \pm 10.0 \mu\text{m}$) than guinea pigs ($121.38 \pm 5.99 \mu\text{m}$) (July 2006; Racine 2007, submitted).

This discrepancy in cone ERG amplitude between young normal and mutants could also be explained by the push-pull model (Sieving 1994). Cone photoreceptors synapse to ON-depolarizing (ONDBC) and OFF-hyperpolarizing bipolar cells (OFFHBC), where the ON-DBC pushes the b-wave amplitude up to its maximum while the OFF-HBC pulls it back to baseline in order to limit the overall amplitude of the cone b-wave. It could be that in our young mutants, the cones would be preferentially connected to the ON-DBC rather than to the OFF-HBC cells, thus giving rise to ERGs of larger amplitudes compared to normal.

Another explanation could be that the maturation of the OFF-retinal pathway is delayed in our mutant guinea pigs compared to normal. In fact, this could result, in the first month of life, in ERGs that are mostly produced by the ON-retinal pathway, giving rise to a larger than normal cone ERG in mutants compared to normal.

As previously mentioned, our animal model of a night blinding disorder is not totally similar to the human form of CSNB since, in our animal model, there is and absence from birth of the rod photoreceptor outer segments, and since the retinopathy deteriorates over time. However, the latter characteristics can be associated with the retinal disorder *retinitis pigmentosa*. In the literature, several studies have reported hearing impairments and/or sperm motility anomalies in human patients affected with retinal disorders like retinitis pigmentosa or Usher syndrome (Hunter 1988; Connor 1997; Khanna 2005; Kremer 2006; Malekpour 2007). In their study, Kremer et al. (2006) reported that patients suffering from Usher syndrome, which is the most common form of deaf-blindness, often revealed other anomalies like vestibular dysfunction, reduced odour, and decrease sperm motility. Their study reported that the proteins encoded by the defective genes are part of a dynamic protein complex that is present in hair cells of the inner ear and in photoreceptor cells of the retina. Malekpour et al. (2007) also revealed that tissues of the auditory, ocular and reproductive systems have some similarities in their protein families and structures, often leading to infertility and late onset deafness in patient affected with RP. Moreover, an animal model of retinal degeneration was also described by Ohlemiller et al. (1998), where they reported that mice homozygous for the tub (rd5) mutation exhibit progressive retinal degeneration, sensorineural hearing loss, reduced fertility, and obesity. More recently, Bösl et al. (2001) reported a mouse model (CIC-2 CL⁻ deficient mice) which revealed a severe degeneration of the outer segments of the photoreceptors with severe degeneration of the testes that led to male infertility. Then, one could wonder if the anomaly reported in this thesis could also be associated with other system dysfunction like hearing impairment or sperm

motility? Since impairment of hearing and/or infertility are often related to patients suffering from retinal degeneration of the photoreceptor outer segments, we could suggest that our mutant guinea pigs could also be affected with other systemic problem like hearing loss and sperm motility. Could the decrease in sperm motility explain the difficulty of generating new pups? More work needs to be performed in order to answer this question.

Even though the retinal anomalies found in our guinea pig model of night blindness do not exactly match a specific human retinopathy, our mutant could be used as a model to study the pathophysiological processes of a human like retinal disorder. Furthermore our model also offers the unique opportunity to study cone function in the absence of functional rods.

1.6 Understanding the negative morphology of the mixed scotopic rod-cone ERG in albino guinea pigs

One interesting feature of the dark adapted ERG in guinea pigs is that its morphology becomes negative when elicited to bright stimuli, the amplitude of the a-wave exceeding that of the b-wave. To our knowledge, there are no other reports of a similar ERG morphology in other normal animal models. Negative ERGs were previously reported to characterize some human retinal disorders (Miyake 1986, 1987), such as the X-linked Congenital Stationary Night Blindness (XLCSNB). This recessive, allegedly non progressive night blinding retinopathy, results from a mutation of the gene NYX, which encodes nyctalopin, a small leucine-rich proteoglycan. The nyctalopin protein is thought to be essential to the development of functional ON-retinal pathways, including ON-bipolar cells (Greg 2003). Similarly, X-linked juvenile retinoschisis (XLRS) is characterized by an electronegative ERG (Peachey 1987). In XLRS, the negative ERG most probably results from Muller cell dysfunction since the mutation within the XLRS1 gene, which encodes retinoschisin, presumably leads to the disruption of Muller cells, resulting in the splitting of the inner plexiform layer (Kim 2006). One wonders if

the retinal anomalies found in human retinopathies revealed with negative ERG could help us understand the retinal mechanism at the origin of the negative ERG in guinea pigs. In guinea pigs, the scotopic ERGs elicited to dim flashes are characterized by a small positive wave, the b-wave. As we increase the intensity of the flash, a negative wave, the a-wave, as well as oscillatory potentials (small wavelets on the ascending limb of the b-wave) will be added to the ERG response. Further increase in flash intensity will bring the negative ERG morphology proper to guinea pigs. In order to determine if the electronegative scotopic ERG was dependent or not upon the duration of the dark adaptation period, scotopic ERGs were obtained following 12, 3, 1 or 0 hour of dark adaptation as seen in the following figure 6.

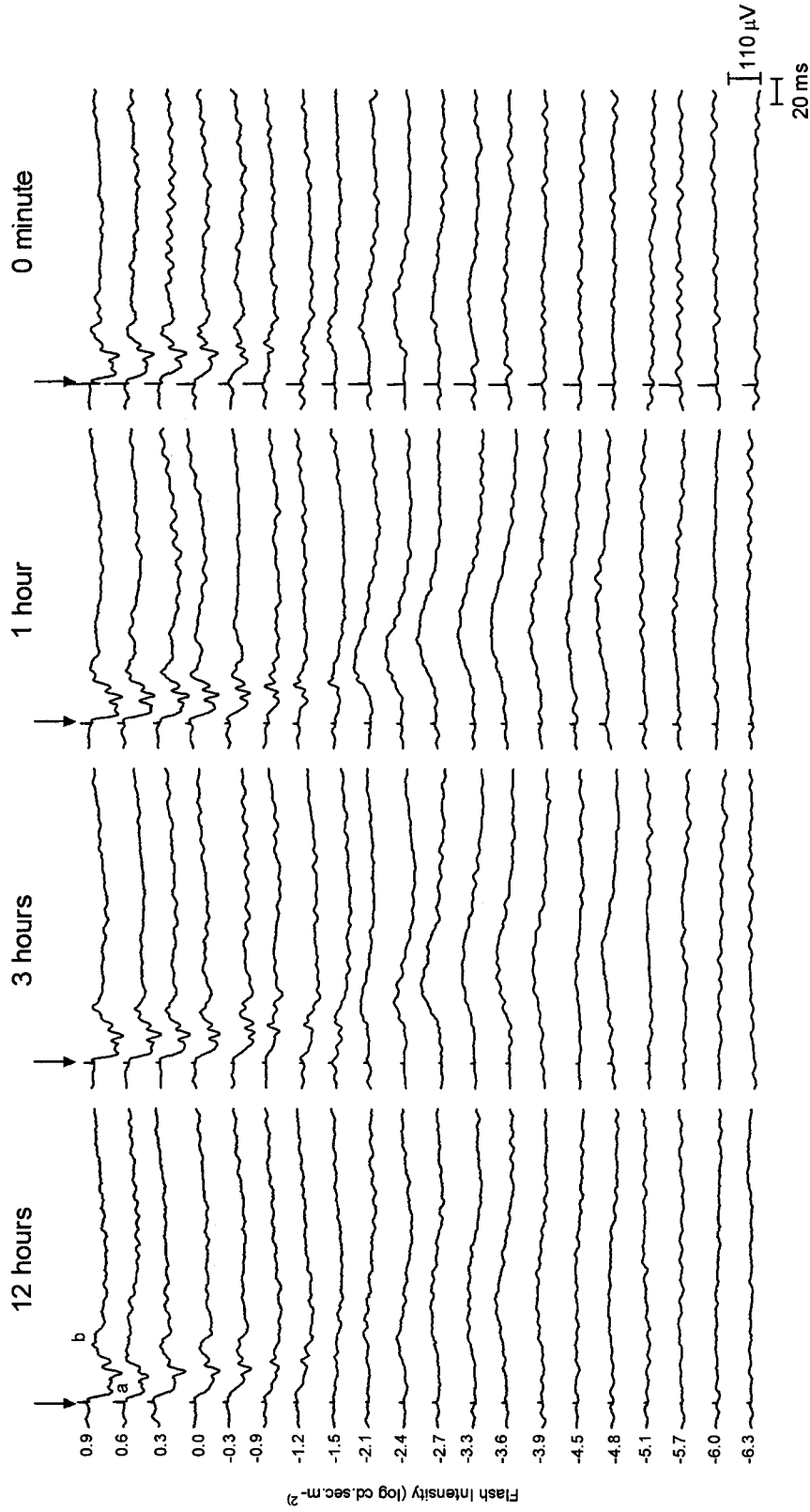


Figure 6: Scotopic ERGs (intensity range from -6.3 to 0.9 log cd.sec.m⁻² as indicated at left of each tracing) recorded in a normal albino Hartley guinea pig following different dark adaptation periods (ISI: 9.6 sec). Vertical arrows identify flash onset, (a) a-wave, (b) b-wave. Horizontal calibration: 20 ms. Vertical calibration: 110 uV.

The results presented in figure 4 suggest that the negative morphology of the dark adapted guinea pig ERG was dependent upon the flash intensity used to evoke the response. In fact, the negative ERG only appeared when brighter flashes were used to elicit the response (e.g.: brighter than $-1.2 \log \text{ cd}\cdot\text{sec}\cdot\text{m}^{-2}$); intensities that solicited both rod and cone contribution. Meanwhile, the duration of the dark adaptation period did not appear to play a key role.

The negative morphology was observed only when the flash intensity used to evoke the response was strong enough to include a cone contribution. Interestingly, in photopic condition, cones did not yield negative-like ERGs except for very bright intensities where a progressive decrease in b-wave amplitude was observed (Racine 2005). In fact, the luminance-response function of the photopic b-wave was previously shown to adopt a unique shape where the amplitude of the b-wave first increases, then saturates briefly, following which it decreases to reach a final plateau where the amplitude of the b-wave is approximately equal to, or slightly lower, than the a-wave: the so-called photopic hill effect. (Peachey 1992; Wali 1992, 1993; Kondo 2000; Lachapelle 2001; Rufiange 2002, 2003, 2005). The decay in b-wave amplitude seen with the photopic hill was previously suggested to result from a decrease in the positive amplitude of the ON bipolar cell response and a delay in the peak of the OFF response (Kondo 2000).

The above claim finds support with our results which showed that inhibition of the OFF-retinal pathway with selective glutamate receptor analogues (agonist or antagonist), yielded positive-like ERG morphologies in scotopic condition (figure 5). Pharmacological blocking of the ON retinal response with L-AP-4 (L-2-amino-4-phosphonobutyric acid) will bring upon the ERG a larger a-wave and subsequently give an even more negative ERG, whereas inhibition of the OFF-retinal response with KYN (kynurenic acid) will reduce the a-wave amplitude resulting in a positive ERG morphology, similar to the cone-mediated ERG (figure 7).

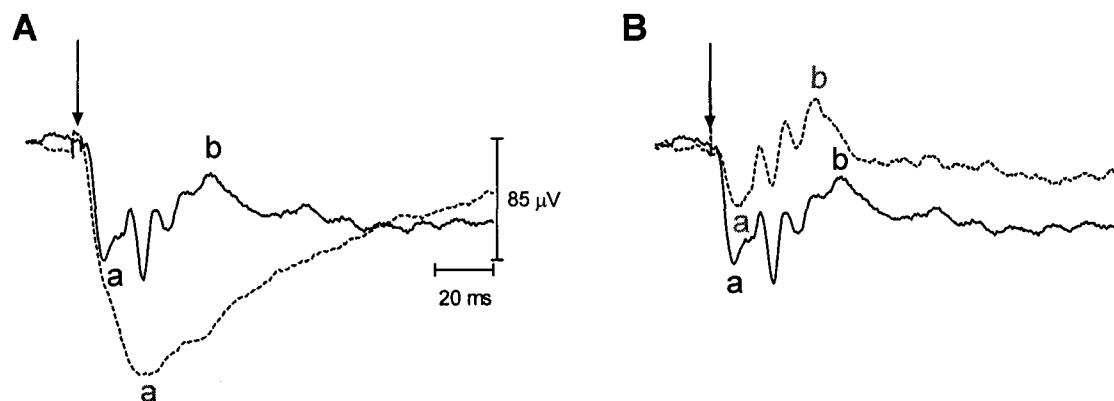


Figure 7: Representative rod-cone mediated ERGs (solid lines) recorded from normal Hartley albino guinea pigs (flash intensity: $0.9 \log \text{ cd} \cdot \text{sec} \cdot \text{m}^{-2}$; ISI: 9.6 sec) and representative rod-cone mediated ERGs (dashed lines) following intravitreal injection of either L-2-amino-4-phosphonobutyric acid ((A); L-AP-4) or kynurenic acid ((B); KYN). Vertical arrows identify flash onset, (a) a-wave, (b) b-wave. Horizontal calibration: 20 ms. Vertical calibration: $85 \mu\text{V}$.

The above suggests that the negative morphology of the bright flash scotopic ERG of guinea pigs would result from a larger than normal contribution of the OFF-retinal pathway compared to the ON-retinal pathway. As previously reported by Sharp et al., (1999), there is evidence for more than one (primary) pathway (rod-ON-bipolar cells) in the routing of the rod signal. Their study revealed that two other pathways (secondary) are also available for the transmission of rod signal to the ganglion cell: one via ON rod bipolar cells-amacrine II cells and OFF cone bipolar cells and a second via rod-cone gap junction and OFF-cone bipolar cells. The fact that the guinea pig's dark adapted ERG, evoked by low flash intensities, only produced a positive b-wave, would suggest that only the rods connected to the ON-retinal pathway are activated. However, when the flash is bright enough, the secondary pathway could be activated and could add the contribution of the OFF-retinal pathway to the ERG. As per Sieving et al. (1994), the ON contribution to the ERG helps the b-wave

reach large amplitude (push) whereas the OFF contribution to the ERG decreases the b-wave amplitude (pull). Since the ON-pathway (primary) is already used by rods when using low flash stimulation, the secondary rod-OFF-retinal pathway could be preferentially used and thus yield the negative ERG morphology reported with bright flashes. A more direct pathway could also explain the negative ERG in rod-cone mediated signal of guinea pigs. Given that guinea pigs have a higher percentage of cones in their retina compared to other species, such as rats (1-2%) and mice (3%) (LaVail 1974; Carter-Dawson 1979; Curcio 1990; Peichl 1994), it could be possible that in guinea pigs there is a larger percentage of cones that connect to the OFF-retinal pathway. In summary, the typical negative shape of the bright flash scotopic ERGs in guinea pigs would result from: A contribution of cone photoreceptors to the dark-adapted responses, combined with an enhancement of the OFF-pathway contribution.

Finally, given the electronegative shape of the rod-cone mediated ERG in guinea pigs, the latter could represent an interesting animal model to study the genesis of negative scotopic electroretinograms similar to those shown to characterize several human retinopathies (Miyake 1986; Peachey 1987; Peachey 1990; Tremblay 1995 Miyake 1996; Kimura 2004).

1.7 Novelty of the results

Some of the results presented in this thesis represent major findings in vision research. I showed that even if the guinea pig, which is a precocial animal, is born with an adult-like mature retina, its retinal function and structure does undergo significant maturational changes, albeit not to the same extent than the changes previously shown for altricial animals. These findings could help us better understand the developmental process of the retina in young precocial infants.

We also reported in our study the aging of the structural and functional retinal changes that occur in the precocial guinea pig. In fact, most studies only

report data on adult animals without showing the changes that occur between birth and adulthood. In fact, only few studies reported the functional and/or structural retinal changes that occur with age in human and animals. Therefore, our findings could help us understand the retinal changes that take place in human retina with age and better understand the normal aging process of the retina.

I also reported the similarities between the cone-mediated electroretinogram between humans and guinea pigs. These ERG parameters recorded in guinea pigs were of similar amplitude and morphology than those previously reported in humans, suggesting that the guinea pig could represent a better alternative to other rodents, such rats and mice, to study the human cone ERG.

Furthermore, not only did I report the unusual negative morphology of the rod-cone ERG in guinea pigs, I also tried to identify the origin of this unique ERG shape. We reported that the negative morphology of the dark adapted ERG in guinea pigs is not the consequence of the dark adaptation period, but of the intensity of the flash used to evoke the response. It also results from the participation of cone photoreceptors to the scotopic ERGs and to an enhancement of the OFF-retinal response in dark conditions.

Finally, I reported a new and naturally occurring guinea pig model of a night blinding disorder. Our precocial animal of a naturally occurring retinopathy was characterized with a non-recordable rod-mediated ERG from birth and normal cone function. There was an absence from birth of rod photoreceptors and abnormal cone outer segments. In addition, we reported that we were able to record normal cone function in the presence of abnormal cone outer segments, a feature which, to our knowledge, was never reported elsewhere. This model could represent a good model to study a human-like retinal disorder and enable us to study the cone function in the absence of rods.

1.8 Future avenues

In this thesis, I presented results on the maturation and aging of the retinal structure and function of the normal and night blind Hartley albino guinea pigs. Techniques such as the electroretinogram (rod, rod-cone and cone mediated ERG), light histology, electron microscopy and immunohistochemistry were used. Even though several different experiments were performed, other analysis could be conducted in order to further our understanding of the visual function in normal Hartley albino guinea pigs. The double-flash electroretinogram technique or chromatic ERG could help us better understand the cone-mediated vision of these animals. Furthermore, multifocal ERG (mfERG) could be very informative on assessing the local ERG evoked from different regions of the retina in order to identify if the retinopathy in our mutant varies with eccentricities. Visual evoked potential (VEP) could help us determine if the pathway from the retina to the visual cortex is intact in our mutant guinea pigs when compared to normal. Finally, immunohistochemistry could be performed in order to better understand the retinal circuitry in young and adult guinea pigs.

Double-flash ERG testing is a technique used to isolate the cone mediated electroretinogram. In the double flash ERG technique, the role of the first flash (conditioning flash) is to transiently saturate rods so that they are rendered unresponsive to the second flash (probe flash). Responses to the probe flash are then taken as reflecting cone-driven activity of the retina (Birch 1995, Pepperberg 1997, Lyubarsky 1996). It provides a measure of the remaining circulating current in the photoreceptors at a particular a time after the conditioning flash. Double-flash ERG would then be another way to test the cone driven responses in guinea pigs.

Chromatic electroretinograms, could also be performed in our colony of normal and abnormal guinea pigs. It would enable us to further our knowledge of the cone ERG function in these precocial animals. The results obtained could then

be compared with the previously published data on the human photopic ERGs evoked to chromatic stimulus (Rufiange 2005). Similar experiments could be performed with our mutant guinea pigs to determine if their color vision is normal.

Multifocal electroretinogram (mfERG), which is a new technique that allows analysis of local retinal function (Ball 2000), could help us determine in more detail the retinal function of the central retina in normal guinea pigs, and even determine if the retinal anomaly in our animal model of night blindness affects the entire retina equally or if it varies with retinal eccentricities.

Visual evoked potentials could also be assessed (Ridder 2006). In our animal model of night blindness, VEP would help us determine how the retinal anomaly, as determined by electroretinography or histology, will affect the visual signal when recorded at the level of the occipital lobe. Also, VEP performed on normal and mutant guinea pigs could help us determine the rod contribution to the VEP. Single or mass cell recording could also be informative on the processing of visual information at the cortical level.

Molecular identification of the gene responsible for the retinal anomaly that affects our colony of guinea pigs could also help us increase our chances of producing more mutant animals. In fact, since the affected pups are all born from consanguineous mating, most of the fetuses are stillborn. Then, knowing the gene defect that affects our mutants could help us reproduce the colony with more chances of survival. The genetic identification of the gene could also help us find an homologous gene in humans. Finally, not only genetic analysis would help us in keeping the colony alive, it would also help us determine the genotype origin of the anomaly and consequently help us find a treatment for this retinopathy in guinea pigs and ultimately find a cure to treat similar retinal disorders in humans.

Immunohistochemistry using antibody against other retinal cells (i.e.: ganglion cells, bipolar cells, Muller cells, amacrine cells...) could also help us to

better identify the structural anomalies present in our colony of night blind guinea pigs and could also be informative on the normal retinal cell changes that occur during the maturation and aging of normal guinea pig retina. Interestingly, an increasing number of papers are documenting the sprouting of dendrites from rod bipolar cells as well as from horizontal cells in ageing mice and human retinas. It would then be interesting to use markers such as anti-PKC antibodies to examine whether sprouting of dendrites also happens in the normal and night blind albino guinea pig retinas. Finally, since in this thesis, we report an age-related decrease retinal function that is accompanied by a gradual thinning of the retina, it would be of interest to examine if this phenomenon is solely the result of normal retinal cell death (e.g. apoptosis) or if other mechanisms, such as cellular compaction or cellular shrinkage could have also contributed.

2 Conclusion

In conclusion, the results presented in this thesis on the maturation and aging of the retinal structure and function of the normal and night blind albino Hartley guinea pigs reveal that even if guinea pigs are precocial animals, their retina does undergo significant postnatal maturation of its structure and function. Additionally, my results also reveal that guinea pigs represent an excellent alternative animal model to study the human retinal structure and function when compared to the more frequently used altricial animals (i.e.: rats, mice, rabbits, cats, to name a few).

Finally, our new and naturally occurring animal model of night blindness could represent a valid model to study the mechanisms involved in generating a functional retinal disorder such as those encountered in humans. It also gives us the opportunity to study the cone retinal function in absence of functional rods and consequently better understand the normal (antagonistic) relationship between rods and cones.

CHAPTER VII: REFERENCES

1 References

Acland G.M., Ray K., Mellersh C.S., Gu W., Langston A.A., Rine J., Ostrander E.A., Aguirre G.D. (1998) Linkage analysis and comparative mapping of canine progressive rod-cone degeneration (*prcd*) establishes potential locus homology with *retinitis pigmentosa* (RP17) in humans. *Proc Natl Acad Sci USA*, 95: 3048–3053.

Acland G.M., Ray K., Mellersh C.S., Langston A.A., Rine J., Ostrander E.A., Aguirre G.D. (1999) A novel retinal degeneration locus identified by linkage and comparative mapping of canine early retinal degeneration. *Genomics*, 59: 134–142.

Aguirre G.D., Rubin L.F. (1975) The electroretinogram in dogs with inherited cone degeneration. *Invest Ophthalmol Vis Sci*, 14: 840–847.

Aguirre G.D., Baldwin V., Pearce-Kelling S., Narfstrom K., Ray K., Acland G.M. (1998) Congenital stationary night blindness in the dog: common mutation in the RPE65 gene indicates founder effect. *Mol Vis*, 4: 23-29.

Aguirre G.D., Baldwin V., Weeks K.M., Acland G.M., Ray K. (1999) Frequency of the codon 807 mutation in the cGMP phosphodiesterase beta-subunit gene in Irish setters and other dog breeds with hereditary retinal degeneration. *J Hered*, 90 (1):143-147.

Aleman T.S., LaVail M.M., Montemayor R., YingG-S., MaguireM.M., Laties A.M., Jacobson S.G., Cideciyan A.V. (2001) Augmented rod bipolar cell function in partial receptor loss: an ERG study P23H rhodopsin transgenic and aging normal rats. *Vis Reseach*, 41: 2779-2797.

Alexander K.R., Fishman G.A., Peachey N.S., Marchese A.L., Tso M.O.M. (1992). ON response defect in paraneoplastic night blindness with cutaneous maligna melanoma. *Invest Ophthalmol Vis Sci*, 33 (3): 477-483.

Arshavsky V.Y., Lamb T.D., Pugh E.N. (2002) G proteins and phototransduction. *Annu Rev Physiol*, 64: 153-187.

Auerbach E., Godel V., Rowe H. (1969). An electrophysiological and psychophysical study of two forms of congenital night blindness. *Invest Ophthalmol*, 8 (3): 332-345.

Ball S.L., Petry H.M. (2000) Noninvasive assessment of retinal function in rats using multifocal electroretinography. *Invest Ophthalmol Vis Sci* 41 (2): 610-617.

Barnett K.C., Curtis R., (1985) Autosomal dominant progressive retinal atrophy in Abyssinian cats. *J Hered*, 76 (3): 168-170.

Bayer A.U., Cook P., Brodie S.E., Maag K.P., Mittag T. (2001) Evaluation of different recording parameters to establish a standard for flash electroretinography in rodents. *Vision Res*, 41 (17): 2173-2185.

Baylor D.A. (1987) Photoreceptor signals and vision : Proctor lecture. *Invest Ophthalmol Vis Sci*, 28: 34-49.

Bech-Hansen N.T., Naylor M.J., Maybaum T.A., Pearce W.G., Koop B., Fishman G.A., Mets M., Musarella M.A., Boycott K.M. (1998) Loss-of-function mutations in a calcium-channel alpha1-subunit gene in Xp11.23 cause incomplete X-linked congenital stationary night blindness. *Nat Genet*, 19 (3): 264-267.

Behn D., Doke A., Racine J., Casanova C., Chemtob S., Lachapelle P. (2003) Dark adaptation is faster in pigmented than albino rats. *Doc Ophthalmol*, 106: 153-159.

Berson D.M. (2003) Strange vision: ganglion cells as circadian photoreceptors. *Trends Neurosci*, 26: 314-320.

Berson E.L. (1993) Retinitis Pigmentosa: The Friedenwald Lecture. *Invest Ophthalmol Vis Sci*, 34 (5): 1659-1676.

Besch D., Zrenner E. (2003) Prevention and therapy in hereditary retinal degenerations. *Doc Ophthalmol*, 106: 31-35.

Bharti K., Nguyen M.T., Skuntz S., Bertuzzi S., Arnheiter H. (2006) The other pigment cell: specification and development of the pigmented epithelium of the vertebrate eye. *Pigment Cell Res*, 19 (5):380-394.

Birch D.G., Anderson J.L. (1992) Standardized full-field electroretinography. Normal values and their variation with age. *Arch Ophthalmol*, 10: 1571-1576.

Birch D.G. Hood D.C., Nusinowitz S., Pepperberg D.R. (1995) Abnormal activation and inactivation mechanisms of rod transduction in patients with autosomal dominant retinitis pigmentosa and the pro-23-his mutation. *Invest Ophthalmol Vis Sci*, 36 (8) : 1603-1614.

Bonaventure N., Karli P. (1968) Maturation des potentials ERG et évoqués visuels chez la souris. *C R Soc Biol (Paris)*, 161 : 553-555.

Bösl M.R., Stein V., Hübner C., Zdebik A.A., Jordt S.E., Mukhopadhyay A.K., Davidoff M.S., Holstein A.F., Jentsch T.J. (2001) Male germ cells and photoreceptors, both dependent on close cell-cell interactions, degenerate upon CIC-2 CL(-) channel disruption. *EMBO J*, 20 (6); 1289-1299.

Bourne M.C., Campbell C.A., Tansley K. (1938) Hereditary degeneration of rat retina. *Brit J of Ophthalmol*, 22: 613-623.

Bowed C., Li T., Danciger M., Baxter L.C., Applebury M.L., Gaber D.B. (1990) Retinal degeneration in the rd mouse is caused by a defect in the beta subunit of rod cGMP-phosphodiesterase. *Nature*, 347 (6294): 677-680.

Braekevelt C., Hollenberg M. (1970) The development of the retina of the albino rat. *Am. J Anat*, 127: 281-302.

Brecelj J. (2003) From immature to mature pattern ERG and VEP. *Doc Ophthalmol*, 107 (3): 215-224.

Breton M.E., Quinn G.E., Schuller A.W. (1995) Development of electroretinogram and rod phototransduction response in human infants. *Invest Ophthalmol Vis Sci*, 36: 1588-1602.

Brockerhoff S.E., Hurley J.F., Janssen-Bienhold U., Neuhauss S.C., Driever W., Dowling J.E. (1995) A behavioural screen for isolating zebrafish mutants with visual system defects. *Proc Natl Acad Sci U S A*, 92: 10545-10549.

Brown K.T., Wiesel T.N. (1961). Localization of origins of electroretinogram components by intraretinal recording in the intact cat eye. *J Physiol (Lond)*, 158: 257–280.

Brown K.T. (1968). The electroretinogram: its components and their origins. *Vision Res*, 8: 633–677.

Brunette J.R., Desrochers R. (1970). Oscillatory potentials: a clinical study in diabetics. *Can J Ophthalmol*, 5: 373–380.

Bui B.V., Vingrys A.J. (1999) Development of receptor responses in pigmented and albino Guinea pigs (*Cavia porcellus*). *Doc Ophthalmol*, 99: 151-170.

Bunker C.H., Berson E.L., Bromley W.C., Hayes R.P., Roderick T.H. (1984) Prevalence of retinitis pigmentosa in Maine. *Am J Ophthalmol*, 97: 357–365.

Bush R.A., Sieving P.A. (1994) A proximal retinal component in the primate ERG a-wave. *Invest Ophthalmol Vis Sci*, 35: 635–645.

Cajal S.R. (1892) *The structure of the retina*. Springfield, Ill., Thomas, 1972.

Calvert P.D., Krasnoperova N.V., Lyubarsky A.L., Isayama T., Nicolo M., Kosaras B., Wong G., Ganon K.S., Margolis R.F., Sidman R.L., Pugh E.N. Makino C.L., Lem J. (2000) Phototransduction in transgenic mice after targeted deletion of the rod transducin α -subunit. *Proc Natl Acad Sci U S A*, 97: 13913-13918.

Candille S.I., Pardue M.T., McCall M.A., Peachey N.S., Gregg R.G. (1999) Localization of the mouse nob (no b-wave) gene to the centromeric region of the X chromosome. *Invest Ophthalmol Vis Sci*; 40: 2748-2751.

Cao Y., Adachi J., Yano T., Hasegawa M. (1994) Phylogenetic place of guinea pigs: no support of the rodent-polyphyly hypothesis from maximum-likelihood analyses of multiple protein sequences. *Mol Biol Evol*, 11:593–604.

Cao Y., Okada N., Hasegawa M. (1997) Phylogenetic of guinea pigs revisited. *Mol Biol Evol*, 14: 461-464.

Carter-Dawson L.D., LaVail M.M. (1979) Rods and cones in the mouse retina. 1-Structural analysis using light and electron microscopy. *J Comp Neurol*, 188: 245-262.

Cepko C.L., Austin C.P., Yang X., Alexiades M., Ezzeddine D. (1996) Cell fate determination in the vertebrate retina. *Proc Natl Acad Sci U S A*, 93: 589-595.

Chader G.J. (2002) Animal models in research on retinal degenerations: past progress and future hope. *Vision Res*, 42 (4): 393-399.

Chang B., Hawes N.L., Hurd R.E., Davisson M.T., Nusinowitz S., Heckenlively J.R. (2002) Retinal degeneration mutants in the mouse. *Vision Res*, 42: 517-527.

Chang B., Hawes N.L., Hurd R.E., Wang J., Howell D., Davisson M.T., Roderick T.H., Nusinowitz S., Heckenlively J.R. (2005) Mouse models of ocular diseases. *Vis Neurosci*, 22 (5): 587-593.

Chang G.Q., Hao Y., Wong F. (1993) Apoptosis: final common pathway of photoreceptor death in rd, rds, and rhodopsin mutant mice. *Neuron*, 11: 595–605.

Chase J. (1982) The evolution of retinal vascularisation in mammals. A comparison of vascular and avascular retinae. *Ophthalmology*, 89 (12): 1518-1525.

Chen C.K. (2005) The vertebrate phototransduction cascade: amplification and termination mechanisms. *Rev Physiol Biochem Pharmacol*, 154:101-21.

Cillino S., Guarneri R., Guarneri P., Pennica C., Chichi G., Piccoli R., Ponte R. (1993). Electroretinographic response in WAG/Rij rats after low-intensity cyclic light exposure. *Ophthalm Res*, 25: 137-144.

Cobb W., Morton H.B. (1954) A new component of the human electroretinogram. *J Physiol*, 123: 36–37.

Colotto A., Falsini B., Salgarello T., Iarossi G., Galan A.E., Scullica L. (2000) Photopic negative response of the human ERG: Losses associated with glaucomatous damage. *Invest Ophthalmol Vis Sci*, 41: 2205-2211.

Connor W.E., Weleber R.G., DeFrancesco C., Lin D.S., Wolf D.P. (1997) Sperm abnormalities in retinitis pigmentosa. *Invest Ophthalmol Vis Sci*, 38 (12): 2619-2628.

Cringle S., Yu D-Y., Alder V., Su E-N., Yu P. (1996) Oxygen consumption in the avascular guinea pig retina. *Am J Physiol*, 271: 1162-1165.

Cunier R. (1838) Historie d'une héméropie, héréditaire depuis siècles dans un famille do la commune de Vendemian, pres Montpellier. *Ann Soc Mes Grand*, 4: 385.

Curcio C.A., Sloan K.R., Kalina R.E., Hendrickson A.E. (1990) Human photoreceptor topography. *J Comp Neurol*, 292: 497-523.

Curcio C.A. (2001) Photoreceptor topography in ageing and age-related maculopathy. *Eye*, 15: 376-383.

D'Cruz P.M., Yasumura D., Weir J., Matthes M.T., Abderrahim H., LaVail M.M., Vollrath D. (2000) Mutation of the receptor tyrosine kinase gene *Mertk* in the retinal dystrophic RCS rat. *Hum Mol Genet*, 9 (4): 645-651.

D'Erchia A.M., Gissi C., Pesole G., Saccone C., Arnason U. (1996) The guinea-pig is not a rodent. *Nature*, 381 (6583): 597-600.

Dacey D.M. (1999) Primate retina: cell types, circuits and color opponency. *Prog Retin Eye Res*, 18: 737-763.

Dalke C., Graw J. (2005) Mouse mutants as models for congenital retinal disorders. *Exp Eye Res*, 81 (5): 503-552.

Dawson W.W., Trick G.L., Litzkow C.A. (1979) Improved electrode for electroretinography. *Invest Ophthalmol Vis Sci*, 18: 988-991.

Dejneka N.S., Rex T.S., Bennett J. (2003) Gene therapy and animal models for retinal disease. *Dev Ophthalmol*, 37: 188-198.

Del Priore L.V., Tezel T.H., Kaplan H.J. (2006) Maculoplasty for age-related macular degeneration: reengineering Gruch's membrane and the human macula. *Prog Retin Eye Res*, 25 (6): 539-562.

Delyfer M.N., Leveillard T., Mohand-Said S., Hicks D., Picau S., Sahel J.A. (2004) Inherited retinal degenerations: therapeutic prospects. *Biol cell*, 96 (4): 261-269.

Deward J. (1877). The physiological action of light. *Nature* 15: 433–435.

Dick E., Miller R.F. (1978) Light evoked potassium activity in the mudpuppy retina: its relationship to the b-wave of the electroretinogram. *Brain Res*, 154 (2): 388–394.

Do-Nascimento J.L., Do-Nascimento R.S., Damasceno B.S., Silveira L.C. (1991) The neurons of the retinal ganglion cell layer of the guinea pigs: quantitative analysis of their distribution and size. *Braz J Med Biol Res*, 24 (2): 199-214.

Dorfman A.L., Joly S., Beauchamp M.H., Checchin D., Sennlaub F., Moukhles H., Chemtob S., Lachapelle P. (2004) Postnatal hyperoxia: Strain comparisons from the retinal blood vessels to the optic nerve. Annual meeting of the Association for Research in Vision and Ophthalmology, Fort Lauderdale, Florida, USA. E-Abstract: www.arvo.org.

Dowling J.E., Sidman R.L. (1962) Inherited retinal dystrophy in the rat. *J Cell Biol*, 14, 73-109.

Dowling J.E., Boycott B.B. (1966) Organization of the primate retina; electron microscopy. *Proc R Soc*, B166: 80-111.

Dowling J.E. (1970) Organization of vertebrate retinas. *Invest Ophthalmol Vis Sci*, 9: 655.

Dowling J.E. (1987) *The retina, an approachable part of the brain*. Cambridge, MA, Harvard University Press.

Dreher Z., Robinson S.R., Distler C. (1992) Müller cells in vascular and avascular retinæ: a survey of seven mammals. *J Comp Neurol*, 323: 59-80.

Dryja T.P., Berson E.L., Rao V.R., Oprian D.D. (1993) Heterozygous missense mutation in the rhodopsin gene as a cause of congenital stationary night blindness. *Nat Genet*, 4 (3): 280-283.

Dryja T.P., Hahn L.B., Reboul T., Arnaud B. (1996) Missense mutation in the gene encoding the alpha subunit of rod transducin in the Nougaret form of congenital stationary night blindness. *Nat Genet*, 13 (3): 358-360.

Einthoven W., Jolly W.A. (1908) The form and magnitude of the electrical response of the eye to stimulation by light at various intensity. *Quat J Exp Physiol*, 1: 373-416.

El Azazi M., Wachtmeister L. (1990) The postnatal development of the oscillatory potentials of the electroretinogram: Basic characteristics. *Acta Ophthalmol*, 68: 401-409.

El Azazi M., Wachtmeister L. (1991) The postnatal development of the oscillatory potentials of the electroretinogram II: photopic characteristics. *Acta Ophthalmol*, 69: 6-10.

Fauser S., Luberichs J., Schuttaur F. (2002) Genetic animal models for retinal degeneration. *Surv Ophthalmol*, 47: 357-367.

Flynn M.F., Bohnert D. (1999) Fundus albipunctatus and other flecked syndromes. *J Am Optom Assoc*, 70 (9): 571-580.

Forrester J.V., Dick A.D., McMenemy P.F., Lee W.R. (2002) Anatomy of the eye and orbit. In: The eye-Basic Sciences in Practice. Saunders, W.B. Edition (Forrester JV, Dick AD, McMenemy PG, Lee WR, eds), pp 1-98. Edinburgh, London, New York, Philadelphia, St. Louis, Sydney, Toronto.

Fortune B., Johnson C.A. (2002) Decline of photopic multifocal electroretinogram responses with age is due primarily to preretinal optical factors. *J Opt Soc Am A*, 19: 173-184.

Frye M.S., Hedges S.B. (1995) Monophyly of the order Rodentia inferred from mitochondrial DNA sequences of the genes for 12S rRNA, 16S rRNA, and tRNA-Valine. *Mol Biol Evol*, 12: 168-176.

Fuchs S., Nakazawa M., Maw M., Tamai M., Oguchi Y., Gal A. (1995) A homozygous 1-base pair deletion in the arrestin gene is a frequent cause of Oguchi disease in Japanese. *Nat Genet*, 10 (3): 360-362.

Fulton A.B., Graves A.L. (1980) Background adaptation in developing rat retina: An electroretinographic study. *Vis Res*, 20: 819-826.

Gal A., Orth U., Baehr W., Schwiger E., Rosenberg T. (1994) Heterozygous missense mutation in the rod cGMP phosphodiesterase beta-subunit gene in autosomal dominant stationary night blindness. *Nat Genet*, 7 (1): 64-68.

Gorfinkel J., Lachapelle P., Molotchinikoff S. (1988) Maturation of the electroretinogram of the neonatal rabbit. *Doc Ophthalmol*, 69: 237-245.

Gorfinkel J., Lachapelle P. (1990) Maturation of the photopic b-wave and oscillatory potentials of the electroretinogram in the neonatal rabbit. *Can J Ophthalmol*, 25: 138-144.

Granit R. (1933). The components of the retinal action potential in mammals and their relation to the discharge in the optic nerve. *J Physiol*, 77: 207–240.

Granit R. (1944) Stimulus intensity in relation to excitation and pre- and post-excitatory inhibition in isolated elements of mammalian retinae. *J Physiol*, 103: 103-118.

Graur D., Hide W.A., Li W-H. (1991) Is the guinea-pig a rodent? *Nature*, 351:649–652.

Gregg R.G., Mukhopadhyay S., Candille S.I., Ball S.L., Pardue M.T., McCall M.A., Peachey N.S. (2003) Identification of the gene and the mutation responsible for the mouse nob phenotype. *Invest Ophthalmol Vis Sci*, 44 (1): 378-384.

Gresh J., Goletz P.W., Crouch R.K., Rohrer B. (2003) Structure-function analysis of rods and cones in juvenile, adult, and age C57BL/6 and Balb/c mice. *Visual Neurosci*, 20: 211-220.

Grondahl J. (1987) Estimation of prognosis and prevalence of retinitis pigmentosa and Usher syndrome in Norway. *Clin Genet*, 31: 255–264.

Gropp K.E., Szel A., Huang J.C., Alcan G.M., Faber D.B., Aguirre G.D. (1996) Selective absence of cone outer segment beta 3-transducin immunoreactivity in hereditary cone degeneration (cd). *Exp Eye Res*, 63:285–296.

Grun G. (1982) The development of the vertebrate retina: a comparative survey. *Adv Anat Embryol Cell Biol*, 78: 1-85.

Gu Y.H., Zhang Z.M., Long T, Li L., Hou B.K., Guo O. (2003) A naturally occurring rat model of X-linked cone dysfunction. *Invest Ophthalmol Vis Sci*, 44 : 5321-5326.

Guité P., Lachapelle P. (1990) The effect of 2-amino-4-phosphonobutyric acid on the oscillatory potentials of the electroretinogram. *Doc Ophtholmol*, 75: 125-133.

Gum G.G., Gelatt K.N., Samuelson D.A. (1973) Maturation of the retina of the canine neonate as determined by electroretinography and histology. *Am J Vet Res*, 45: 1166-1171.

Gurevich L., Slaughter M.M. (1993) Comparison of the waveforms of the ON bipolar neuron and the b-wave of the electroretinogram. *Vis Res*, 33 (17): 2431-2435.

Haim M. (1992) Prevalence of retinitis pigmentosa and allied disorders in Denmark. II. Systemic involvement and age at onset. *Acta Ophthalmol (Copenh)*, 70: 417-426.

Hamasaki D.I., Maguire G.W. (1985) Physiological development of the kitten's retina: An ERG study. *Vision Res*, 25: 1537-1543.

Hanitzsch R., Lichtenberger T.H., Mätting W.U. (1996) The influence of MgCl₂ and APB on the light induced potassium changes and the ERG b-wave of the isolated superfused rat retina. *Vis Res*, 36: 499-507.

Hansen R.M., Fulton A.B. (2005) Development of the cone ERG in infants. *Invest Ophthalmol Vis Sci*, 46: 3458-3462.

Hartong D.T., Berson E.L., Dryja T.P. (2006) Retinitis pigmentosa. *Lancet*, 368 (9549): 1795-1809.

Hattar S., Liao H.W., Takao M., Berson D.M., Yau K.W. (2002) Melanopsin-containing retinal ganglion cells: architecture, projections, and intrinsic photosensitivity. *Science*, 295: 1065-1070.

Hemenger R.P. (1982) Optical density of the crystalline lens. *Ame J Optometry Physiol Optics*, 59: 34-42.

- Heynen H., Van Norren D. (1985) Origin of the electroretinogram in the intact macaque eye – I: Principal component analysis. *Vis Res*, 25: 697–707.
- Hollenberg J.J., Spira A.W. (1972) Early development of the human retina. *Can J Ophthal*, 7: 472-491.
- Hollenberg J.J., Spira A.W. (1973) Human retinal development: Ultrastructure of the outer retina. *Amer J Anat*, Vol 137: 357-386.
- Holmgren F. (1865) En method att objektivera effekten av zjusintryck på retina. *Ups Läkaref Förh.* 1: 177 – 191. Berson E.L. Electrical phenomena in the retina. In: Adler's physiology of the eye. William M. Hart, Jr. 9th ed. p641-645-707.
- Hood D.C., Birch D.G. (1996) Assessing abnormal rod photoreceptor activity with the a-wave of the electroretinogram: applications and methods. *Doc Ophthmol.* 92 (4): 253-267.
- Horsten G.P.M., Winkelman J.E. (1960) Development of the ERG in relation to histological differentiation of the retina in man and animals. *Arch Ophthalmol*, 63: 232-242.
- Huang J., Wyse J., Spira A. (1990) Ontogenesis of the electroretinogram in a precocial mammal, the guinea pig (*Cavia Porcellus*). *Comp Biochem Physiol*, 95A: 149-155.
- Hunter D.G., Fishman G.A., Kretzer F.L. (1988) Abnormal axonemes in X-linked retinitis pigmentosa. *Arch Ophthalmol* 106 (3): 362-368.
- Isenmann S., Kretz A., Cellierino A. (2003) Molecular determinants of retinal ganglion cell development, survival, and regeneration. *Prog Ret Eye Res*, 22: 483-543.

Jacobs G.H., Degan II J.F. (1994) Spectral sensitivity, photopigments, and color vision in the guinea pig (*Cavia porcellus*). *Behav Neurosci*, 108: 339-1004.

Jacobson S.G., Ikeda H., Ruddock K. (1987) Cone-mediated retinal function in cats during development. *Doc Ophthalmol*, 65: 7-14.

Jaissle G.B., May A., Reinhard J., Kohler K., Fauser S., Lütjen-Drecoll E., Zrenner E., Seeliger M.W. (2001) Evaluation of the rhodopsin knockout mouse as a model of pure cone function. *Invest Ophthalmol Vis Sci*, 42: 506-513.

Jindrova H., Detwiler P.B. (1998) Protein kinase C and IP3 in photoresponses of functionally intact rod outer segments: constraints about their role. *Physiol Res*, 47 (4): 285-290.

Johansson K., Brun A., DeVente J., Ehinger G. (2000) Immunohistochemical analysis of the developing inner plexiform layer in postnatal rat retina. *Invest Ophthalmol Vis Sci*, 41 (1): 305-313.

Johnson A.T., Kretzer F.L., Hittner H.M., Glazebrook P.A., Bridges C.D.B., Lam D.M. (1985) Development of the subretinal space in the pattern human eye: Ultra structural and immunocytochemical studies. *J Comp Neurol*, 233: 497-505.

Joly S., Dorfman A.L., Moukhles H., Chemtob S., Lachapelle P. (2005) The kinetic of light-induced retinopathy in adult and juvenile rats. Annual meeting of the Association for Research in Vision and Ophthalmology, Fort Lauderdale, Florida, USA. E-Abstract: www.arvo.org.

Joly S., Dorfman A.L., Chemtob S., Moukhles H., Lachapelle P. (2006) Structural and functional consequences of bright light exposure on the retina of neonatal rats. *Doc Ophthalmol*, 113: 93-103.

Kandori F., Setogawa T., Tamai A. (1966) Electoretinographical studies on fleck retina with congenital nonprogressive night blindness. *Yonago Acta Med*, 10 (2): 98-108.

Kandori F., Tamai A., Kurimoto S., Fukunaga K. (1972) Fleck retina. *Am J Ophthalmol*, 73 (5): 673-685.

Karpe G. (1945) The basis of clinical electoretinography. *Acta Ophthalmol, Suppl.* 24: 1-118.

Karpe B., Rickenbach D., Thomasson S. (1950) The clinical electoretinogram A. The normal electoretinogram above fifty years of age. *Acta Ophthalmol*, 28: 301-305.

Karwoski C.J., Xu X., Yu H. (1996) Current-source density analysis of the electoretinogram of the frog: methodological issues and origin of components. *J Opt Soc Am A Opt Image Sci Vis*, 13 (3): 549-56.

Keeler C.E. (1924) The inheritance of a retinal abnormality in white mice. *Proc Natl Acad Sci U S A*, 10: 329-333.

Keunen J.E.E., VanMeel G.J.V., Norren D.V. (1988) Rod densitometry in congenital stationary night blindness. *Doc Ophthalmol*, 68 (3-4): 375-87.

Khanna H., Hurd T.W., Lillo C., Shu X., Parapuram S.K., He S., Akimoto M., Wright A.F., Margolis B., Williams D.S., Swaroop A. (2005) RPGR-ORF15, which is mutated in retinitis pigmentosa, associates with SMC1, SMC3, and microtubule transport proteins. *J Biol Chem*, 280 (39). 33580-33587.

Khouri G., Mets M.B., Smith V.C., Wendell M., Pass, A.S. (1988) X-linked congenital stationary night blindness. Review and report of family with hyperopia. *Arch Ophthalmol*, 106: 1417-1422.

Kim D.Y., Neely K.A., Sassanj J.W., Vrabec T.R., Tantri A., Frost A., Donoso L.A. (2006) X-linked retinoschisis: novel mutation in the initiation codon of the XLR51gene in a large family. *Retina*, 26 (8): 940-946.

Kimura A., Nemoto H., Nishimiya J., Yuasa T., Hiroko Y. (2004) Spinocerebellar degeneration with negative electroretinogram: dysfunction of the bipolar cells. *Doc Ophthalmol*, 108: 241-247.

King-Smith P.E., Loffing D.H., Jones R. (1986) Rod and cone ERGs and their oscillatory potentials. *Invest Ophthalmol Vis Sci*, 27: 270-273.

Krill A.E., Lee G.B. (1963) The electroretinogram in albinos and carriers of the ocular albinino trait. *Arch Ophthalmol* 69: 66-72.

Kirk G.R., Boyer S.F. (1973) Maturation of the electroretinogram in the dog. *Exp Neurol*, 38: 252-264.

Klein D.C., Weller J.L. (1972) Rapid light-induced decrease in pineal serotonin N-acetyltransferase activity. *Science*, 177 (48), 532-533.

Knave B., Moller A., Persson H.E. (1972) A component analysis of the electroretinogram. *Vis Res*, 12: 1669-1684.

Kojima M., Zrenner E. (1978) OFF-compotents in response to brief light flashes in the oscillatory potential of the human electroretinogram. *Albrecht Bon Braefes Arch Klin Exp Ophthalmol*, 206: 107-120.

Kolb H. (1991a) Anatomical pathways for color vision in the human retina. *Vis Neurosci*, 7 (1-2): 61-74.

- Kolb H., Dekorver L. (1991b) Midget ganglion cells of the parafovea of the human retina: a study by electron microscopy and serial section reconstructions. *J Comp Neurol*, 303 (4): 617-636.
- Kolb H. (1994) The architecture of functional neural circuits in the vertebrate retina. The Proctor Lecture. *Invest Ophthalmol Vis Sci*, 35: 2385-2404.
- Kolb H. (1997) Amacrine cells of the mammalian retina: neurocircuitry and functional roles. *Eye*, 11: 904-23.
- Kolb H., Nelson R., Ahnelt P., Cuenca N. (2001) Cellular organization of the vertebrate retina. *Prog Brain Res*, 131: 3-26.
- Kolb H. (2003) How the retina works. *Am Sci*, 91: 28-35.
- Kondo M., Piao C-H., Tanikawa A., Horiguchi M., Terasaki H., Miyake Y. (2000) Amplitude decrease of photopic ERG b-wave at higher stimulus intensities in humans. *Jpn J Ophthalmol*, 44: 20-28.
- Kremer A., Van Wijk E., Märker T., Wolfrum U., Roepman R. (2006) Usher syndrome: molecular links of pathogenesis, proteins and pathways. *Hum Mol genet*, 15 (2): R262-R270.
- Kurihara H. (1977) Developmental process of ERG of the albino rat. *Jpn J Ophthalmol*, 81: 1313-1320.
- Lachapelle P., Little J.M., Polomeno R.C. (1983) The photopic electroretinogram in congenital stationary night blindness with myopia. *Invest Ophthalmol Vis Sci*, 24: 442-450.

Lachapelle P., Benoit J., Guité P., Tran C.N., Molotchnikoff S. (1990) The effect of iodoacetic acid on the electroretinogram and oscillatory potentials in rabbits. *Doc Ophthalmol*, 75: 7-14.

Lachapelle P., Benoit J., Little J.M., Lachapelle B. (1993) Recording the oscillatory potentials with the DTL electrode. *Doc Ophthalmol*, 83: 119-130.

Lachapelle P., Rousseau S., McKerral M., Benoit J., Polomeno R.C., Koenekoop R.K., Little J.M.. (1998) Evidence supportive of a functional discrimination between photopic oscillatory potentials as revealed with cone and rod mediated retinopathies. *Doc Ophthalmol*, 95: 35-54.

Lachapelle P., Rufiange M., Dembinska O. (2001) A physiological basis for definition of the ISCEV ERG standard flash (SF) based on the photopic hill. *Doc Ophthalmol*, 102: 157-162.

LaVail M.M., Sidman M., Rausin R., Sidman R.L. (1974) Discrimination of light intensity by rats with inherited retinal degeneration: a behavioural and cytological study. *Vis Res*, 14: 693-702.

Lei B. (2003) The ERG of guinea pig (*Cavia porcellus*): comparison with I-type monkey and E-type rat. *Doc Ophthalmol*, 106 (3): 243-249.

Li C., Cheng M., Yang H., Peachey N.S., Naash M.I. (2001) Age-related changes in the mouse outer retina. *Optometry and Vis Sci*, 78: 425-430.

Linberg D., Cuenca N., Ahmelt P., Fisher S., Kolb H. (2001) Comparative anatomy of major retinal pathways in the eyes of nocturnal and diurnal animals. *Prog Brain Res*, 131: 27-52.

- Liu K., Akula J.D., Hansen R.M., Moskowitz A., Kleinman M.S., Fulton A.B. (2006) Development of the electroretinographic oscillatory potentials in normal and ROP rats. *Invest Ophthalmol Vis Sci*, 47: 5447-5452.
- Loeliger M., Rees S., (2005) Immunocytochemical development of the guinea pig retina. *Exp Eye Res*, 80 (1): 9-21.
- Lucas R.J., Douglas R.H., Foster R.G. (2001) Characterization of an ocular photopigment capable of driving pupillary constriction in mice. *Nat Neurosci*, 4 (6):621-626.
- Luckett W.P., Hartenberger J-L. (1993) Monophyly or polyphyly of the order Rodentia: possible conflict between morphological and molecular interpretations. *J Mamm Evol*, 1: 127-147.
- Lyubarsky A.L., Pugh E.N. Jr. (1996) Recovery phase of the murine rod photoresponse reconstructed from electroretinographic recordings. *J Neurosci*, 16 (2) : 563-571.
- Lyubarsky A.L., Falsini B., Pennesi M.E., Valentini P., Pugh E.N. Jr. (1999) UV- and midwave-sensitive cone-driven retinal responses of the mouse : a possible phenotype for coexpression of cone photopigments. *J Neurosci*, 19 (1): 442-455.
- Malekpour M., Shahidi A., Khorsandi Ashtiani M.T., Motasaddi Zarandy M. (2007) Novel syndrome of cataracts, retinitis pigmentosa, late onset deafness and sperm abnormalities: A new Usher syndrome subtype with X-linked inheritance? *Am J Med Genet A*, 143 (14): 1646-1652.
- Marmor M.F., Holder G.E., Seeliger M.W., Yamamoto S. (2004) Standard for clinical electroretinography (2004 update). *Doc Ophthalmol*, 108: 107-114.
- Martignetti J.A., Brosius J. (1993) Neural BC1 RNA as an evolutionary marker: guinea pig remains a rodent. *Proc Natl Acad Sci USA*, 90: 9698-9702.

Maslim J., Valter K., Egensperger R., Hollander H., Stone J. (1997) Tissue oxygen during a critical developmental period controls the death and survival of photoreceptors. *Invest Ophthalmol Vis Sci*, 38: 1667-1677.

Matthews G.P., Crane W.G., Sandberg M.A. (1989) Effects of 2-amino-4-phosphonobutyric acid (APB) and glycine on the oscillatory potentials of the rat electroretinogram. *Exp Eye Res*, 49 (5): 777-87.

Mears A.J., Kondo M., Swain P.K., Takada Y., Bush R.A., Saunders T.L., Seiving P.A., Swaroop A. (2001) Nrl is required for rod photoreceptor development. *Nat Genet*, 29 (4): 447-452.

Mets M.B., Smith V.C., Pokorny J., Pass A. (1995) Postnatal retinal development as measured by the electroretinogram in premature infants. *Doc Ophthalmol*. Vol. 90: 111-127.

Miller R.F., Dowling J.E. (1970) Intracellular responses of the Müller (glial) cells of mudpuppy retina: their relation to b-wave of the electroretinogram. *J Neurophysiol*, 33: 323-341.

Miyake Y., Yagasaki K., Horiguchi M., Kawase Y., Kanda T. (1986) Congenital stationary night blindness with negative electroretinogram: a new classification. *Arch Ophthalmol*, 104: 1013-1020.

Miyake Y., Yagasaki K., Horiguchi M., Kawase Y. (1987) On- and off-responses in photopic electroretinogram in complete and incomplete types of congenital stationary night blindness. *Jpn J Ophthalmol*, 31 (1): 81-87.

Miyake Y., Shiroyama N., Sugita S., Horiguchi M., Yagasaki K. (1992) Fundus albiglutatus associated with cone dystrophy. *Br J Ophthalmol*, 76 (6): 375-379.

Miyake Y., Horiguchi M., Suzuki S., Kondo M., Tanikawa A. (1996) Electrophysiological findings in patients with Oguchi's disease. *Jpn J Ophthalmol*, 40 (4): 511-519.

Molotchnikoff S., Itaya S.K. (1993) Functional development of the neonatal rat retinotectal pathway. *Brain Res Dev Brain Res*, 72 (2): 300-304.

Moskowitz A., Hansen R.M., Fulton A.B. (2005) ERG oscillatory potentials in infants. *Doc Ophthalmol*, 110 (2-3): 265-270.

Murayama K., Seiving P.A. (1992) Different rate of growth of monkey and human photopic a-, b- and d-wave suggest two sites of ERG light adaptation. *Clin Vision Sci*, 7: 385-392.

Nagata M. (1963). Studies on the photopic ERG of the human retina. *Jpn J Ophthalmol*, 7: 96-124.

Naka K.I., Rushton W.A. (1966) S-potentials from colour units in the retina of fish (Cyprinidae). *J Physiol*, 185 (3): 536-55.

Narfstrom K. (1983) Hereditary progressive retinal atrophy in the Abyssinian cat. *J Hered*, 74 (4): 273-276.

Narfstrom K., Weigstad A., Nilsson S.E. (1989) The Briard dog: a new animal model of congenital stationary night blindness. *Brit J Ophthalmol*, 73: 750-756.

Neves G., Lagnado L. (1999) The retina. *Curr Biol*, 9 (18): 674-677.

Newman E.A. (1980) Current source density analysis of the b-wave of the frog retina. *J Neurophysiol*, 43: 1355-1366.

- Newman E.A., Odette L.L. (1984) Model of electroretinogram b-wave generation: a test of the K^+ hypothesis. *J Neurophysiol*, 51: 164–182.
- Newman E.A., Reichenbach A. (1996) The Muller Cell: a functional element of the retina. *Trends Neurosci*, 19: 307-312.
- Nixon P.J., Bui BV., Armitage J.A., Vingrys A.J. (2001) The contribution of cone responses to rat electroretinogram. *Clin Exp Ophthalmol*, 29: 193-196.
- Noell W. (1954). The origin of the electroretinogram. *Am J Ophthalmol*, 38: 78–90.
- Novacek N.J. (1992) Mammalian phylogeny: shaking the tree. *Nature*, 356: 121–125.
- Nowak J.Z. (1996) Age-related macular degeneration (AMD): pathogenesis and therapy. *Pharmacol Rep*, 58 (3): 353-363.
- O'Day K. (1947) Visual cells of the guinea pig. *Nature*, 160: 648.
- Ogden T.E. (1973). The oscillatory waves of the primate electroretinogram. *Vision Res*, 13: 1059–1074.
- Ohlemiller K.K., Mosinger Ogilvie J., Lett J.M., Hughes R.M., LaRegina M.C., Olson L.M. (1998) The murine tub (rd5) mutation is not associated with a primary axonemal defect. *Cell Tissue Res*, 291 (3): 489-495.
- Ookawa T. (1971a) The onset and development of the chick electroretinogram: the a- and b-waves. *Poult Sci*, 50: 601-608.
- Ookawa T. (1971b) Further studies on the ontogenetic development of the chick electroretinogram. *Poult Sci*, 50: 1185-1190.

- Pak W.L. (1995) *Drosophila* in vision research. *Invest Ophthalmol Vis Sci*, 36: 2340-2357.
- Pardue M.T., LaVail M.M., Gregg R.G., Peachey N.S. (1998) A naturally occurring mouse model of X-linked congenital stationary night blindness. *Invest Ophthalmol Vis Sci*, 39 (12): 2443-2449.
- Parry J.W.L., Bowmaker J.K. (2002) Visual pigment coexpression in guinea pig cones: a microspectrophotometric study. *Invest Ophthalmol Vis Sci*, 43: 1662-1665.
- Peachey N.S., Fishman G.A., Derlacki D.J., Brigell M.G. (1987) Psychophysical and electroretinographic findings in X-linked juvenile retinoschisis. *Arch Ophthalmol*, 105: 513-516.
- Peachey N.S., Alexander K.R., Fishman G.A. (1989) The Luminance-response function of the dark-adapted human electroretinogram. *Vision Res*, 29 (3): 263-270.
- Peachey N.S., Fishman G.A., Kilbride P.E., Alexander K.R., Keehan K.M., Derlacki D.J. (1990) A form of congenital stationary night blindness with apparent defect of rod phototransduction. *Invest Ophthalmol Vis Sci*, 31: 237-246.
- Peachey N.S., Alexander K.R., Derlacki D.J., Fishman G.A. (1992) Light adaptation and the luminance-response function of the cone electroretinogram. *Doc Ophthalmol*, 79: 363-369.
- Peichl L., Gonzalez-Suriano J. (1994) Morphological types of horizontal cells in rodent retinae: A comparison of rat, mouse, gerbil, and guinea pig. *Vis Neurosci*, 11: 501-517.
- Peirson S., Foster R.G. (2006) Melanopsin: another way of signaling light. *Neuron*, 49 (3): 331-339.

Penn R.D., Hagins W.A. (1969) Signal transmission along retinal rods and the origin of the electroretinographic a-wave. *Nature*, 223: 201-205.

Pepperberg D.R., Birch D.G., Hood D.C. (1997) Photoresponses of human rods in vivo derived from paired-flash electroretinogram. *Vis Neurosci*, 14 (1): 73-82.

Petersen-Jones S.M., Entz D.D., Sargan D.R.: (1999) cGMP phosphodiesterase- alpha mutation causes progressive retinal atrophy in the Cardigan Welsh corgi dog. *Invest Ophthalmol Vis Sci*, 40: 1637-44.

Petters R.M., Alexander C.A., Wells K.D., Collins B., Sommer J.R., Blanton M.R., Rojas G., Hao Y., Flowers W.L., Banin E., Cideciyan A.V., Jacobson S.G., Wong F. (1997) Genetically engineered large animal model for studying cone photoreceptor survival and degeneration in retinitis pigmentosa. *Nat biotech*, 15: 965-970.

Phelan J.K., Bok D. (2000) A brief review of retinitis pigmentosa and the identified retinitis pigmentosa genes. *Mol Vis*, 6: 116-124.

Portera-Cailliau C., Sung C.H., Nathans J., Adler R. (1994) Apoptotic photoreceptor cell death in mouse models of retinitis pigmentosa. *Proc Natl Acad Sci U S A*, 91:974-978.

Provis J.M., Sandercoe T., Hendrickson A.E. (2000) Astrocytes and blood vessels define the foveal rim during primate retinal development. *Invest Ophthalmol Vis Sci*, 41: 2827-2836.

Pusch C.M., Zeitz C., Brandau O., Pesch K., Achatz H., Feil S., Scarfe C, Maurer J., Jacobi F.K., Pinckers A., Andreasson S., Hardcastle A., Wissinger B., Berger W., Meindl A. (2000) The complete form of X-linked congenital stationary night blindness is caused by mutations in a gene encoding a leucine-rich repeat protein. *Nat Genet*, 26 (3): 324-327.

Quigley M., Roy M-S., Barsoum-Homsy M., Chevrette L., Jacob J-L., Milot J. (1996) ON and OFF-responses in the photopic electroretinogram in complete-type congenital stationary night blindness. *Doc Ophthalmol*, 92: 159-165.

Racine J., Behn D., Simard E., Lachapelle P. (2003) Spontaneous occurrence of a potentially night blinding disorder in guinea pigs. *Doc Ophthalmol*, 107: 59-69.

Racine J., Joly S., Rufiange M., Rosolen S., Lachapelle P. (2005) The photopic ERG of the albino guinea pig (*Cavia porcellus*): A model of the human photopic ERG. *Doc Ophthalmol*, 110: 67-77.

Racine J., Behn D., Lachapelle P. (2007) Structural and functional maturation of the retina of the albino Hartley guinea pig. *Doc Ophthalmol*, accepted with revisions.

Rapaport D.H., Wong L.L., Wood E.D., Yasumura D., LaVail M.M. (2004) Timing and topography of cell genesis in the rat retina. *J Comp Neurol*, 474 (2); 304-324.

Ray K., Tejero M.D., Baldwin V.J., Aguirre G.D. (1996) An improved diagnostic test for rod cone dysplasia 1 (*rcd1*) using allele-specific polymerase chain reaction. *Curr Eye Res*, 15 (5): 583-587.

Redmond T.M., Yu S., Lee E., Bok D., Hamasaki D., Chen N., Goletz P., Ma J.X., Crouch R.K., Pfeifer K. (1998) *Rpe65* is necessary for production of 11-cis-vitamin A in the retinal visual cycle. *Nat Genet*, 20: 344-351.

Rees S., Bainbridge A. (1992) The structural and neurochemical development of the fetal guinea pig retina and optic nerve in experimental growth retardation. *Int J Dev Neurosci*, 10 (1): 93-108

Ridder III W.H., Nusinowitz S. (2006) The visual evoked potential in the mouse-Origins and response characteristics. *Vis Res*, 46: 902-913.

Riggs L.A. (1941) Continuous and reproducible records of the electrical activity of the human retina. *Proc Soc Exp Biol Med*, 48: 204–207.

Riggs L.A. (1954) Electroretinography in cases of night blindness. *Am J Ophthalmol*, 38: 70.

Riggs L.A. (1986) Electroretinography. *Vision Res*, 26 (9):1443-1459.

Ripps H. (1982) Night blindness revised: From man to molecules. *Invest Ophthalmol Vis Sci*, 23: 588–611.

Rizzolo L.J. (1997) Polarity and the development of the outer blood-retinal barrier. *Histol Histopathol*, 12: 1057–1067.

Rodieck R.W. (1998) Retinas. In: *The first steps in seeing* (Rodieck R.W., ed): 37-55. USA: Sinauer Associates Inc.

Röhlich P., Van Veen T.H., Szél A. (1994) Two different visual pigments in one retinal cone cell. *Neuron*, 13 (5): 1159-1166.

Rosolen S.G., Rigaudiere F., Legargasson J-F., Chalier C., Rufiange M., Racine J., Joly S., Lachapelle P. (2004) Comparing the photopic ERG i-wave in different species. *Vet Ophthalmol*, 7: 189-192.

Rodriguez-Saez E., Otero-Costas J., Moreno-Montanes J., Relova J.L. (1993) Electroretinographic changes during childhood and adolescence. *European J Ophthalmol*, 3: 6-12.

Rousseau S., McKerral M., Lachapelle P. (1996) The i-wave: Bridging flash and pattern electroretinohgraphy. *Electroencephalogr Clin Neurophysiol, Suppl.* 46:165-171.

Rufiange M., Rousseau S., Dembinska O., Lachapelle P. Cone-dominated ERG luminance-response function: the Photopic Hill revisited. (2002) *Doc Ophthalmol*, 104: 231-248.

Rufiange R., Dassa J., Dembinska O., Koenekoop R.K., Little J.M., Polomeno R.C., Dumont M, Chemtob S., Lachapelle P. (2003) The photopic ERG luminance-response function (photopic hill): method of analysis and clinical application. *Vis Res*, 43: 1405-1412.

Rufiange M., Dumont M., Lachapelle P. (2005) Modulation of the human photopic ERG luminance-response function with the use of chromatic stimuli. *Vis Res*, 45: 2321-2330.

Sanada T. (1962) Study on the ERG on suckling rabbits. Report I. Development of the ERG (in dark adaptation). *Jpn J Ophthalmology*, 66: 1430-1436.

Schiller P.H. (1992) The ON and OFF channels of the visual system. *Trends Neurosci*, 15 (3): 86-92.

Schubert G.V., Bornschein H. (1952). Beitrag zur analyse des menschliches elektroretinogramms. *Ophthalmologica*, 123: 396.

Semple-Roland S., Dawson W. (1987) Retinal cyclic light damage threshold for albino rats. *Lab ani Sci*, 37: 289-298.

Semple-Rowland S.L., Lee N.R., Van Hooser J.P., Palczewski K., Baehr W. (1998) A null mutation in the photoreceptor guanylate cyclase gene causes the retinal degeneration chicken phenotype. *Proc Natl Acad Sci USA*, 95:1271–1276.

Semple-Rowland S.L., Lee N.R. (2000) Avian models of inherited retinal disease. *Methods in Enzymol*, 316: 526-536.

- Sharpe L.T., Stockman A. (1999) Rod pathways: the importance of seeing nothing. *Trends Neurosci*, 22: 497-504.
- Shinowara N.L. (1982) Changes in retinal morphology and glucose utilization in aging albino rats. *Exp Eye Res*, 3: 517-530.
- Shipley T., Anton M. (1964) The human electroretinogram in the first day of life. *J Ped*, 65: 733-739.
- Sieving P.A., Murayama K., Naarendorp F. (1994) Push-pull model of the primate photopic electroretinogram: a role for hyperpolarizing neurons in shaping the b-wave. *Vis Neurosci*, 11: 519-532.
- Silveira L.C., Saito C.A., Lee B.B., Kremers J., Da Silva Filho M., Kilavik B.E., Yamada E.S., Perry V.H. (2004) Morphology and physiology of primate M- and P-cells. *Prog Brain Res*, 144: 21-46.
- Sjostrand F.S. (1965) The synaptology of the retina. In A.V.S. De Reuck & Knight (Eds.) *Colour vision: Physiology and experimental psychology* (pp:110-150). Boston: Little, Brown.
- Smelser G.K., Ozanics V., Fayborn M., Sagun D. (1974) Retinal synaptogenesis in the primate. *Invest Ophthalm*, 13: 340-361.
- Speros P., Price J. (1981) Oscillatory potentials: History, techniques and potential use in the evaluation of disturbances of retinal circulation. *Surv Ophthalmol*, 25: 237-252.
- Spira A.W., Hollenberg M.J. (1973) Human retinal development: Ultrastructure of the inner retinal layers. *Develop Biol*, 31: 1-21.

Spira A.W. (1975) In utero development and maturation of the retina of a non-primate mammal: a light and electron microscopic study of the Guinea pig. *Anat Embryol*, 14: 279-300.

Spira A.W. (1976) The localization of cholinesterase in the retina of the fetal and newborn guinea pigs. *J Comp Neurol*, 169: 393-408.

Spira A.W., Shimizu Y., Rorstad O.P. (1984) Localization, chromatographic characterization and development of somatostatin-like immunoreactivity in the guinea pigs retina. *J Neurosci*, 4: 3069-3079.

Steinbert R.H., Schmidt R., Brown K.T. (1970) Intracellular responses to light from cat pigment epithelium: origin of the electroretinogram c-wave. *Nature*, 227: 728-730.

Steinbert R.H., Oakley B., Niemeyer G. (1980) Light-evoked changes in potassium in the retina of the intact cat eye. *J Neurophysiol*, 44: 897-921.

Steinberg R.H. (1985) Interactions between the retinal pigment epithelium and the neural retina. *Doc Ophthalmol*, 60: 327-346.

Stockton R.A., Slaughter M.M. (1989) B-wave of the electroretinogram. A reflection of ON bipolar cell activity. *J Gen Physiol*, 93 (1): 101-122.

Strauss O. (2005) The retinal pigment epithelium in visual function. *Physiol Rev*, 85 (3): 845-881.

Suber M.L., Pittler S.J., Qin N., Wright G.C., Holcombe V., Lee R.H., Craft C.M., Lolley R.N., Baehr W., Hurwitz R.L. (1993) Irish setter dogs affected with rod/cone dysplasia contain a nonsense mutation in the rod cGMP phosphodiesterase beta-subunit gene. *Proc Natl Acad Sci U S A*, 90 (9): 3968-3972.

Szikra T., Witkovsky P. (2001) Contributions of AMPA- and kainate-sensitive receptors to the photopic electroretinogram of the *Xenopus* retina. *Vis Neurosci*, 18 (2): 187-196.

Takahashi Y., Onoe S., Yoshimura Y., Asamizu N., Tazawa Y. (1987) Congenital stationary night blindness, incomplete type (Miyake) – Case report, with special reference on clinical findings on sensory-motor system abnormalities. *Folia Ophthalmol Jpn*, 38: 109–113.

Tessier-Lavigne M. (2000) Visual Processing by the retina. In: Principles of neural science (Kandel ER, Schwartz JH, Jessel RM, eds), pp 507-522: McGraw-Hill companies.

Tian N., Slaughter M.M. (1994) Correlation of dynamic responses in the ON bipolar neuron and the b-wave of the electroretinogram. *Vision Res*, 35: 1359-1364.

Tian N., Copenhagen D.R. (2001) Visual deprivation alters development of synaptic function in innerretina after eye opening. *Neuron*, 32 (3): 439-449.

Tian N. (2004) Visual experience and maturation of retinal synaptic pathways. *Vis Res*, 44: 3307-3316.

Toda K., Bush R.A., Humphries P., Sieving P.A. (1999) The electroretinogram of the rhodopsin knockout mouse. *Vis Neurosci*, 16: 391-398.

Tomita T. (1950) Studies on the intraretinal action potential. I: Relation between the localization of micropipette in the retina and the shape of the intraretinal action potential. *Jpn J physiol*, 1: 110–117.

Travis G.H., Brennan M.B., Danielson P.E., Kozak C.A., Sutcliffe J.G. (1989) Identification of a photoreceptor-specific mRNA encoded by the gene responsible for retinal degeneration slow (rds). *Nature*, 338 (6210): 70-73.

Travis G.H. (1998) Mechanisms of cell death in the inherited retinal degenerations. *Am J Hum Genet*, 62: 503-508.

Tremblay F., Laroche R.G., Becker I. (1995) The electroretinographic diagnosis of the incomplete form of congenital stationary night blindness. *Vision Res*, 35: 2383-2393.

Ueno S., Kondo M., Niwa Y., Rerasaki H., Miyake Y. (2004) Luminance dependence of neural components that underlies the primate photopic electroretinogram. *Invest Ophthalmol Vis Sci*, 45: 1033-1040.

Ueno S., Kondo M., Ueno M., Miyata K., Terasaki H., Miyake Y. (2006) Contribution of retinal neurons to d-wave of primate photopic electroretinograms. *Vision Res*, 46: 658-664.

Ulshafer R.J., Allen C., Dawson W.W., Wolf E.D. (1984) Hereditary retinal degeneration in the Rhode Island Red chicken. I. Histology and ERG. *Exp Eye Res*, 39: 125-135.

Van Nie R., Ivanyi D., Demant P. (1978) A new H-2-linked mutation, *rds*, causing retinal degeneration in the mouse. *Tissue Antigens*, 12: 106-108.

Vingrys A.J., Bui B.V. (2001) Development of postreceptoral function in pigmented and albino guinea pigs. *Visual Neurosci*, 18: 605-613.

Viswanathan S., Frishman L.J., Robson J.G., Harwerth R.S., Smith III E.L. (1999) The photopic negative response of the macaque electroretinogram: Reduction by experimental glaucoma. *Invest Ophthalmol Vis Sci*, 40: 1124-1136.

Viswanathan S., Frishman L.J., Robson J.G., Walters J.W. (2001) The photopic negative response of the flash electroretinogram in primary open angle glaucoma. *Invest Ophthalmol Vis Sci*, 42: 514-522.

Wachtmeister L., Dowling J.E. (1978) The oscillatory potentials of the mudpuppy retina. *Invest Ophthalmol Vis Sci*, 17: 1176–1188.

Wali N., Leguire L.E. (1992) The photopic Hill: A new phenomenon of the light adapted electroretinogram. *Doc Ophthalmol*, 80: 335-345.

Wali N., Leguire L.E. (1993) Fundus pigmentation and the electroretinographic luminance-response function. *Doc Ophthalmol*, 84: 61-69.

Weleber R. (1981) The effect of age on human cone and rod ganzfeld electroretinograms. *Invest Ophthalmol Vis Sci*, 20: 392-399.

Webster M.J., Rowe M.H. (1991) Disruption of developmental timing in the albino rat retina. *J comp Neurol*, 307: 160-174.

Weidman T.A., Kuwabara T. (1968) Postnatal development of the rat retina. *Arch Ophthalmol*, 79: 470-484.

Weisse I. (1995) Changes in the aging rat retina. *Ophthalmic Res*, 27: 154-163.

Westall C.A., Panton C.M., Levin A.V. (1996) Time courses for maturation of electroretinogram responses from infancy to adulthood. *Doc Ophthalmol*, 96: 355-379.

Wilder H. (1953) Oguchi's disease. *Am J Ophthalmol*, 36 (5): 718-719.

Winkelman J., Horsten G. (1962) The ERG of premature and full term born infants during their first days of life. *Ophthalmologica*, 143: 92-101.

Witzel D.A., Smith E.L., Wilson R.D., Aguirre G.D. (1978) Congenital stationary night blindness: an animal model. *Invest Ophthalmol Vis Sci*, 17: 788 –795.

Woods J.R., Parisi V., Coppes V., Brooks D.E. (1983) Maturation sequence of the visual system: Serial measurements of visual evoked potential and electroretinogram in the healthy neonatal lamb. *J Obstet Gynecol*, 145: 738-743.

Wong R.O., Ghosh A. (2002) Activity-dependent regulation of dendritic growth and patterning. *Nat Rev Neurosci*, 3 (10): 803-812.

Wright C.E., Williams D.E., Drasdo N., Harding G.F.A. (1985) The influence of age on the electroretinogram and visual evoked potential. *Doc Ophthalmol*, 59: 365-384.

Xu X., Karwoski C.J. (1994a) Current source density analysis of retinal field potentials. II. Pharmacological analysis of the b-wave and M-wave. *J Neurophysiol*, 72: 96-120.

Xu X., Karwoski C.J. (1994b) Current source density (CSD) analysis of retinal field potentials. I. Methodological considerations and depth profiles. *J Neurophysiol*, 72 (1): 84-95.

Xu J., Dodd R.L., Makino C.L., Simon M.I., Baylor D.A., Chen J. (1997) Prolonged photoresponses in transgenic mouse rods lacking arrestin. *Nature*, 389 (6650): 505-509.

Xu L., Ball S.L., Alexander K.R., Peachey N.S. (2003) Pharmacological analysis of the rat cone electroretinogram. *Vis Neurosci*, 20: 297-306.

Yamamoto S., Sippel K.C., Berson E.L., Dryja T.P. (1997) Defects in the rhodopsin kinase gene in the Oguchi form of stationary night blindness. *Nat Genet*, 15 (2): 175-178.

Yanagida T., Koshimizu M., Kawasaki K., Yonemura D. (1988) Microelectrode depth study of the electroretinographic oscillatory potentials in the frog retina. *Doc Ophthalmol*, 67: 355-361.

Yonemura D., Aoki T., Tsuzuki K. (1962) Electroretinogram in diabetic retinopathy. *Arch Ophthalmol*, 68: 19–24.

Yonemura D., Hatta M. (1966) Studies of the minor components of the frog's electroretinogram. *Jpn J Physiol*, 16: 11-22.

Young R.S.L., Price J., Harisson J. (1986) Psychophysical study of rod adaptation in patients with congenital stationary night blindness. *Clin Vis Sci*, 1: 137.

Yu D-Y., Cringle S.J. (2001) Oxygen distribution and consumption within the retina in vascularized and avascular retinas in animal models of retinal disease. *Prog Retin Eye Res*, 20 (2): 175-208.

Zeidler I. (1959) The electroretinogram IX. The normal ERG values of the b-potential in different age groups and its difference in men and women. *Acta Ophthalmol*, 37: 294-301.

Zeiss C.J., Acland G.M., Aguirre G.D. (1999) Retinal pathology of canine X-linked progressive retinal atrophy, the locus homologue of RP3. *Invest Ophthalmol Vis Sci*, 40: 3292–3304.

Zhang Z., Gu Y., Li L., Long T., Guo Q., Shi L. (2003) A potential spontaneous rat model of X-linked congenital stationary night blindness. *Doc Ophthalmol*, 107: 53-57.

Zimak E., Joly S., Dorfman A.L., Polosa A., Nguyen B-A., Racine J, Chemtob S., Lachapelle P. (2007) Irreversible increases in ERG amplitude and retinal thickness following postnatal exposure of Long Evans rats to bright lights. Annual meeting of the Association for Research in Vision and Ophthalmology, Fort Lauderdale, Florida, USA. E-Abstract: www.arvo.org.

CHAPTER VIII: APPENDIX

1 Permission to published manuscript 1, 2 and manuscript 3 letters.

2 Signed waiver from the publishers for published manuscripts 1, 2 and 3.

Date: Thu, 16 Feb 2006 09:14:19 +0100 [02/16/2006 03:14:19 AM EST]
 From: "Essenpreis, Alice, Springer DE" <Alice.Essenpreis@springer.com>
 To: julie.racine@mail.mcgill.ca
 Cc: Doc_Oph@di-ep.com
 Subject: WG: AW: Information
 Priority: 1
 Part(s): 2 Letter to Documenta (permission to publish).doc [application/msword] 27 KB
 1 unnamed [text/plain] 3.99 KB

Dear Ms. Racine,

With reference to your request (copy herewith) to re-use material on which Springer controls the copyright, our permission is granted free of charge, on the following conditions:

- * it concerns original material which does not carry references to other sources,
- * if material in question appears with credit to another source, authorization from and reference to that source is required as well, and permission is also obtained from the author (address is given on the imprint page or with the article);
- * allows you non-exclusive reproduction rights throughout the world,
- * permission includes use in an electronic form, on the condition that content is
 - password protected,
 - at Intranet or
 - in CD-ROM/E-book;
- * full credit (book/journal title, volume, year of publication, page, chapter/article title, name(s) of author(s), figure number(s), original copyright notice) is given to the publication in which the material was originally published by adding:
 With kind permission of Springer Science and Business Media.

Permission free of charge does not prejudice any rights we might have to charge for reproduction of our copyrighted material in the future.

With best regards,

-
 Alice Essenpreis
 Springer
 Rights and Permissions

-
 Tiergartenstrasse 17 | 69121 Heidelberg GERMANY
 FAX: +49 6221 487 8223
 Alice.Essenpreis@springer.com
 www.springeronline.com/rights

-----Ursprüngliche Nachricht-----
 Von: DOOP [mailto:Doc_Oph@di-ep.com]
 Gesendet: Montag, 13. Februar 2006 22:00
 An: Sturm, Rosita, Springer DE
 Cc: Permissions Heidelberg
 Betreff: WG: AW: Information
 Wichtigkeit: Hoch

Dear Rosita,

Dear Permissions Department,

Please contact and advise the authors as soon as possible. The names of the papers can be found in the attachment.

Kind regards,

Diana

Diana Epstein
Di-Ep Biomedical Editorial Services
10 Sandyford Place
Glasgow G3-7NB
Scotland
U.K.
Tel/Fax: (+44) 141 616 9095
Website: <http://www.di-ep.com>

-----Ursprüngliche Nachricht-----

Von: Julie Racine [mailto:julie.racine@mail.mcgill.ca]
Gesendet: Freitag, 10. Februar 2006 18:14
An: Doc_Oph@di-ep.com
Betreff: Re: AW: Information

Hi,

Attached you will find a copy of the lettre written by my supervisor Dr. Pierre Lachapelle including the authors and publishing date of the two papers that I wish to include in my thesis.

Thank you very much for your help,

Julie Racine
Research Institute of the Montreal Children's Hospital 4060 Ste-Catherine West Place Toulon room 208
Montreal, Quebec H3Z 2Z3 Canada
Phone: 514-412-4400 ext. 23890
Fax: 514-412-4331
e-mail: julie.racine@mail.mcgill.ca

Quoting DOOP <Doc_Oph@di-ep.com>:

> Dear Julie,

>

> Since the journal has moved publishers would you be able to advise by return

Hide Quoted Text]

> as soon as possible the title, names of all authors and publishing
> date of each of the papers-I will then forward this to the permissions department.

>

>

> Kind regards,

>

> Diana

>

> Diana Epstein

> Di-Ep Biomedical Editorial Services

> 10 Sandyford Place

> Glasgow G3-7NB

> Scotland

3 Ethic certificates

3.1 Animal use protocol-Research (4164).

3.2 Animal use protocol-Research (3267).

3.3 Theory training course on animal use for research and teaching (advanced level) certificate.

3.4 Guinea pig methodology workshop certificate.

3.5 Mouse methodology workshop certificate.

3.6 Rats methodology workshop certificate.

3.7 Environmental health and safety certificates.

3.7.1 Chemical laboratory safety.

3.7.2 Biosafety.